Investigation into mechanisms for antifungal resistance in *Aspergillus fumigatus*

INVESTIGATION INTO MECHANISMS FOR ANTIFUNGAL RESISTANCE IN ASPERGILLUS FUMIGATUS

By YU YING FAN, M.Sc.

A Thesis Submitted to the School of Graduate Studies in Partial Fulfilment of the Requirements for the Degree Master of Science

McMaster University

Master of Science (2021)

Hamilton, Ontario (Department of Biology)

TITLE: Investigation into mechanisms for antifungal resistance in *Aspergillus fumigatus*

AUTHOR: Yu Ying Fan (McMaster University)

SUPERVISOR: Dr. Jianping Xu

NUMBER OF PAGES: vii, 141

Lay Abstract

Aspergillus fumigatus is a common fungal mold that can be found throughout the environment, both indoors and outdoors. Inhalations of the spores can cause infections in humans, which is referred to as aspergillosis, and severe invasive infections primarily affect the immunocompromised. For treatment, antifungal drugs such as triazoles (voriconazole and itraconazole) and amphotericin B are used. However, rising reports of triazole resistance and the emergence of amphotericin B resistant *A. fumigatus* strains has become a major public health concern. My thesis aims to investigate mechanisms associated with triazole and amphotericin B resistance by analyzing the relationships between genome-wide single nucleotide polymorphisms and antifungal drug susceptibilities of environmental and clinical *A. fumigatus* isolates. By identifying candidate genes and mutations associated with resistance, our findings will contribute to developing quick and effective diagnostic markers for clinical screening of antifungal resistance in *A. fumigatus* strains.

Abstract

Aspergillus fumigatus is a filamentous saprophytic mold that is found abundantly in the biosphere. *A. fumigatus* is also an airborne human pathogen and is considered the major cause of aspergillosis, infections caused by inhalation of conidia. In immunocompetent individuals, the spores rarely cause any harm as they are cleared by innate pulmonary defences; however, in immunocompromised patients, the host immune system can fail to clear the inhaled conidia and aspergillosis may develop. Indeed, aspergillosis represents a major cause of morbidity and mortality in these populations. Aspergillosis is commonly treated using triazole and amphotericin B (AMB) antifungal agents. However, the increasing prevalence of triazole resistant strains and emergence of AMB resistance has become a challenge in treatment. To further expand our knowledge on the mechanisms of antifungal resistance in the species, we tested previously known or associated genes for antifungal resistance as well as investigated novel mechanisms via multiple genome-wide association studies (GWAS), which used a total of 211 genomes from *A. fumigatus* strains in 12 countries. Our results identified many novel mutations related to triazole and AMB resistance. Specifically, using stepwise GWAS analyses, we identified 6 and 18 missense variants to be significantly associated with itraconazole and voriconazole resistance, respectively. A linkage disequilibrium analysis identified six additional missense variants associated with triazole resistance, with two of these six being consistently associated with pan-azole resistance across subsets of samples. Furthermore, examination of known mutation sites and genes overexpressed with triazole exposure found a total of 65 SNPs implicated in triazole resistance. For the AMB study, we identified a total of 34 mutations associated with AMB tolerance using a GWAS. Subsequent analysis with 143 progeny strains, generated from a laboratory cross and genotyped with PCR-RFLP, identified epistatic interactions between five of these SNP sites that impacted growth in different concentrations of AMB. With the expanding immunocompromised population and increasing frequency of antifungal resistance, our results will help in investigating novel resistance mechanisms in *A. fumigatus* and in expanding the molecular diagnostic toolset in resistance screening, to enable rapid and accurate diagnosis and treatment decision-making.

Acknowledgments

I would like to begin by thanking my supervisor, Dr. Jianping Xu, who has provided a great deal of support throughout my thesis project and whose expertise & knowledge has been invaluable. I've gained so much during my time in the Xu lab, learning new skills and working with various equipment, and I am very grateful for all the opportunities. I would also like to thank my supervisory committee, Dr. Ben Evans and Dr. Deborah Yamamura, for their feedback during my supervisory committee meeting and inputs from their bioinformatic and medical microbiology perspectives.

This work would also not have been completed without the help of Xu lab members. I was fortunate to work with Himeshi Samarasinghe, Man You (Sally), Greg Korfanty, Yue Wang, Meagan Archer, and Heather Yoell, as well as past lab members, Adrian Forsythe and Sarah Sandor. It's been a lot of fun being a part of the lab and I will greatly miss everyone. Although with the COVID quarantine there were less opportunities to meet up, I've really enjoyed our game nights and the potlucks hosted by JP & Heather.

Finally, a big thank you to my family for all their love and support. To my mother whose been accompanying me throughout my academic career and done so much for me, thank you for all your encouragement and support. To my sister whose always willing to drive down to Hamilton just to hang, thank you for dealing with me and calming me down when I get concerned about the smallest of things. To my grandparents who've been concerned about me getting enough food & sleep and not being stressed more than anything else, thank you for all your love and the advices. And thank you to my pup Teddy, for the companionship and mostly just sitting there looking cute.

Table of Contents

List of Figures

List of Tables

Abbreviations

ABC	ATP-binding cassette
AMB	Amphotericin B
ATU	Area of technical uncertainty
CFU	Colony forming unit
CLSI	Clinical and Laboratory Standards Institute
EUCAST	European Committee on Antimicrobial Susceptibility Testing
GWAS	Genome-wide association study
IBS	Identity by state
INDEL	Insertion-Deletion
MIC	Minimum inhibitory concentration
MFS	Major facilitator superfamily
ROS	Reactive oxygen species
PCR	Polymerase chain reaction
QQ	Quantile-Quantile
RFLP	Restriction fragment length polymorphism
SDA	Sabouraud dextrose agar
SDB	Sabouraud dextrose broth
SNP	Single nucleotide polymorphism
TR	Tandem repeat
VIF	Variance inflation factor

Chapter 1

General Introduction

1.1. Fungal Infections

Fungi are among the oldest known causes for infection in humans and are highly prevalent in human populations. Their impact on both plant and animal life is widely recognized; being involved in topics including food security, plant disease epidemics, and biodiversity loss (Fisher et al., 2012). However, fungal disease in humans is generally a neglected topic and often overlooked by public health authorities, research funding bodies, and governments. Until the second half of the 20th century, systematic fungal infections were not seen as a major medical problem and were relatively rare (Casadevall, 2018). However, medical advancement in the mid-20th century led to an expanding immunocompromised population. In combination with factors such as the HIV epidemic in 1980s, travel, and commerce, fungal diseases in humans have increased dramatically (Casadevall, 2018). Although currently fungal infections contribute substantially to human mortality and global burden of fungal diseases is increasing, their impact on human health is not widely appreciated. On the other hand, bacterial, viral, and protozoan diseases have been accepted as important public health threats for centuries (Rodrigues and Nosanchuk, 2020). In the past decade, the Canadian Institutes for Health Research (CIHR) has invested around $50 million towards total funding in fungal research, meanwhile approximately $500 million had been provided for bacterial research (Horianopoulos et al., 2021). In addition, no licensed vaccine exists yet against any fungal disease and the World Health Organization conducted their first meeting for determining fungal pathogens of public health importance only recently in 2020.

Superficial dermatophytic fungal infections affect about 20 to 25% of the global population, with incidence rates continuing to increase (Kalita et al., 2019). Over 300 million people are affected by serious fungal infections and an annual estimation of 1.6 million

deaths are caused by fungal diseases (Jermy, 2017). Furthermore, over 90% of deaths caused by fungal infections are caused by species belonging to four genera: *Candida*, *Pneumocystis*, *Cryptococcus*, and *Aspergillus* (Brown et al., 2012).

Among species in the *Aspergillus* genus, *Aspergillus fumigatus* is the predominant cause of human *Aspergillus* infections, being responsible for ~60% of infections, and is the most common airborne opportunistic fungal pathogen (Brandres et al., 2021; Mousavi et al., 2016).

1.2. *Aspergillus fumigatus* and Aspergillosis

Aspergillus fumigatus is a ubiquitous saprophytic mold that plays a major role in recycling carbon and nitrogen. The mold is commonly found in soil and decaying vegetation, but can also be found throughout the environment as they adapt well to a broad range of environmental conditions (Dagenais & Keller, 2020). The widespread nature of *A. fumigatus* has been attributed to multiple factors. *A. fumigatus* is known for its thermotolerance, being able to grow at temperatures of 55°C and survive even at a high temperature of 75°C (Abad et al., 2010). On the opposite spectrum, the mold can grow at a low temperature of 12°C and its conidia can tolerate trauma from prolonged freezing, surviving liquid nitrogen storage for at least 18 years (Kwon-Chung & Sugui, 2013). The conidia also have a highly hydrophobic layer of rodlets on the cell wall surface, which facilitates high air dispersibility (Valsecchi et al., 2017). *A. fumigatus* conidia are also much more hydrophobic than other *Aspergillus* spp. and disperses in the atmosphere more efficiently that most other molds (Kwon-Chung & Sugui, 2013; Van De Veerdonk et al., 2017). This contributes to *A. fumigatus* conidia being the dominant fungal component found through air sampling (Van De Veerdonk et al., 2017). The cell wall of *A. fumigatus* conidia also contains melanin, which provide protection against various environmental and have also been implicated with pathogenicity. Melanin in the conidial wall is involved in protection against stressors including UV irradiation, high temperatures, reactive oxygen species (ROS) as well as lysis by host cells (Kwon-Chung & Sugui, 2013).

With the ubiquitous atmospheric presence of *A. fumigatus*, humans are estimated to inhale hundreds of conidia daily (Van De Veerdonk et al. 2017). Inhalation of *A. fumigatus* spores can cause a broad range of diseases, depending on the immunological status of the

human host, and can extend from allergic reactions to severe invasive mycoses. The group of diseases is defined together under the umbrella term "aspergillosis". In terms of non-invasive manifestations, *A. fumigatus* is a major aeroallergen, possessing 21 known and 25 predicted allergenic proteins (Mousavi et al., 2016). Moreover, *A. fumigatus* is the most prevalent cause of severe pulmonary allergic diseases (Chaudhary & Marr, 2011). Allergic bronchopulmonary aspergillosis (ABPA) is the most severe allergic pulmonary complication cause by *A. fumigatus* and is more common in patients with underlying lung conditions such as asthma and cystic fibrosis (Latgé, 1999). ABPA is estimated to affect over 4 million people worldwide, with prevalence rates of 1-40% in chronic asthma patients, ~38% in acute severe asthma patients, and 7-15% in cystic fibrosis patients (Brown et al., 2012; Chaudhary & Marr, 2011). On the other end of the spectrum, invasive aspergillosis is the most severe form of aspergillosis and primarily affects immunocompromised hosts. *A. fumigatus* is considered the primary cause of invasive aspergillosis and over 300,000 cases of invasive aspergillosis occur globally each year (Bongomin et al., 2017). However, this global estimate is most likely an underestimation, representing only about 50 to 65% of actual cases (Brown et al., 2012).

1.3. Triazoles and Amphotericin B

For treatment, triazole antifungals such as voriconazole and itraconazole are used in first-line therapy against aspergillosis. These agents inhibit the biosynthesis of ergosterol, a major sterol of the fungal cell membrane and essential in fungal growth and maintenance. Triazoles work by inhibiting the enzyme 14α-lanosterol demethylase (Cyp51) that converts lanosterol to ergosterol (Sharpe et al., 2017). The antifungal binds to the heme iron atom of Cyp51 using one of its nitrogen atoms, thereby inhibiting enzyme activity (Sandhu et al., 2014). This inhibition prevents the production of ergosterol and leads to an accumulation of toxic sterol intermediates in the fungal cell membrane (Sandhu et al., 2014). These composition changes ultimately interfere with the cell membrane function, disrupts the structure, and alters the activity of membrane bound enzymes, including those associated with nutrient transport, chitin synthesis, fungal cell growth and proliferation (Mazu et al., 2017).

The polyene antifungal amphotericin B (AMB) is also often used in the treatment of severe fungal infections such as invasive aspergillosis. AMB is a fungicidal agent that has the broadest spectrum of activity, being effective against most clinically relevant fungi (Mazu et al., 2017). Unlike many antifungal classes that target vital enzymes, AMB targets ergosterol and alters the fungal membrane permeability (Carolus et al., 2020). Although the process of sterol sequestration has not been fully elucidated, multiple models of action for AMB have been proposed over the years (Carolus et al., 2020). These are grouped into four models: ion-channel model, surface absorption model, sterol sponge model, and oxidative damage model (Carolus et al., 2020). Three of these models propose that the binding and/or sequestering of ergosterol by AMB results in disruption of the cell membrane and impacts various ergosterol-dependent cellular processes (Carolus et al., 2020). Meanwhile, the oxidative damage model suggests an additional mode of action involving ROS accumulation and oxidative stress (Carolus et al., 2020).

1.4. Mechanisms of Resistance to Triazoles

Mechanisms for triazole resistance in *A. fumigatus* can be broadly grouped into two categories which are Cyp51A-mediated and non Cyp51A-mediated. *A. fumigatus* contains two *cyp51*-related genes, which produce two isoforms of the enzyme: *cyp51A* and *cyp51B*. However, studies suggest that *cyp51A* plays the dominant role in regulation of 14α-lanosterol demethylase activity, while *cyp51B* is either a redundant gene that functions when *cyp51A* is absent or has functions under unknown conditions (Nash and Rhodes, 2018; Garcia-Rubio et al., 2017). Recently, a mutation in *cyp51B* has been found in an azole-resistant strain to be potentially associated with triazole resistance, however, the majority of known mutations related to triazole resistance are found in the *cyp51A* gene (Gonzalez-Jimenez et al., 2020).

Studies have shown that the main mechanism of triazole resistance in *A. fumigatus* can be attributed to point mutations in *cyp51A*. Depending on the position and amino acid change, mutations in Cyp51A can result in reduced susceptibility to all or a subset of triazoles. Although numerous *cyp51A* mutations conferring resistance have been documented in *A. fumigatus*, there are four commonly reported mutation sites (Sharma et al., 2020). The four most frequently noted mutations are hot spot amino acid substitutions at glycine-54

(G54), glycine-138 (G138), methionine-220 (M220), and glycine-448 (G448) (Sharma et al., 2020). These mutations have also been confirmed to directly confer triazole resistance in *A. fumigatus* in studies that replaced the wild-type *cyp51A* gene with alleles containing the amino acid substitutions (Sharma et al., 2020). These studies determined that the amino acid substitutions each by itself were sufficient to confer reduced triazole susceptibility (Diaz-Guerra et al., 2003; Mann et al., 2003; Mellado et al., 2004; Natesan et al., 2012; Albarrag et al., 2011). Overall, the mutations in *cyp51A* are believed to either decrease the binding affinity of triazole drugs to Cyp51A, thus allowing replacement by the native sterol substrate, or impact the structure of Cyp51A, resulting in conformational changes that favor the native substrate (Chen et al., 2020; Liu et al., 2016). The second major Cyp51A-mediated mechanism for triazole resistance is overexpression. The expression of *cyp51A* is regulated through interactions between transcription factors and environmental conditions (Rybak et al., 2019). There is evidence for positive *cyp51A* regulation in *A. fumigatus* by the sterol element binding protein SrbA (Hagiwara et al., 2016). This relationship has been noted by decreased *cyp51A* expression level in *srbA* deletion mutants (Hagiwara et al., 2016). SrbA binds to the promoter region of *cyp51A* at two binding sites as a homodimer (Rybak et al., 2019). One of these sites is negatively regulated by the heterotrimeric CCAAT-binding complex (CBC) and the transcription factor HapX (Rybak et al., 2019). It is thought that under conditions favoring ergosterol biosynthesis repression and thus decreased *cyp51A* expression, CBC and HapX will both bind directly downstream of the single SrbA binding site to decrease positive regulation of *cyp51A* by SrbA (Rybak et al., 2019). However, two separate mechanisms for *cyp51A* overexpression have been found in triazole resistant clinical *A. fumigatus* strains. The first and most prevalent one is tandem repeats in the *cyp51A* promoter region (Rybak et al., 2019). There have been reports of three common tandem repeat versions, which are a 34, 46 and 53 base-pair tandem repeat or TR_{34}, TR_{46} and TR_{53} (Rybak et al., 2019). Although these repeats differ in length, they all produce two additional SrbA binding sites that aren't effectively regulated by CBC and HapX (Rybak et al., 2019). Strains with these tandem repeats have a reported 2-fold or greater increase in *cyp51A* expression and about a 4-fold increase in triazole minimum inhibitory concentration (MIC) (Rybak et al., 2019). The TR_{34} and TR_{46} variations are also almost always found accompanied

by non-synonymous mutations in *cyp51A* (Rybak et al., 2019). For TR_{34}, this is a single amino acid substitution from lysine to histidine at codon 98 (Rybak et al., 2019). This combination, known as TR_{34}/L98H, induces up to an 8-fold increase in the expression of *cyp51A* (Berger et al., 2017). The second combination is known as TR_{46}/Y121F/T289A, a 46 base-pair tandem repeat along with two amino acid substitutions, which are tyrosine to phenylalanine at codon 121 and threonine to alanine at codon 289 (Rybak et al., 2019). The second mechanism leading to *cyp51A* overexpression are mutations in the *hapE* gene. CBC is a heterotrimeric protein, comprised of HapB, HapC and HapE subunits and a P88L amino acid substitution in *hapE* has been shown to directly increase *cyp51A* expression levels (Rybak et al., 2019). This mutation significantly impairs CBC's binding affinity to its target site, which is the promoter region of *cyp51A* (Gsaller et al., 2016). With CBC being a negative regulator for *cyp51A* expression, this mutation results in a 2-fold or greater increase in *cyp51A* expression (Rybak et al., 2019).

The second major group of triazole resistance mechanisms is non-Cyp51A mediated, which mostly includes overexpression of drug efflux pumps and other mutations outside of *cyp51A*. Overexpression of drug efflux pumps reduces the intracellular accumulation of triazoles by pumping them out of the cell. Compared to susceptible strains, resistant *A. fumigatus* strains show over 5 to 30-fold increase in certain efflux transporters (Chen et al., 2020). Many important transporters related to azole resistance belong to the ATP-binding cassette (ABC) transporters or major facilitator superfamily (MFS) transporters. Overall, numerous *in vitro* studies have proven that overexpression of drug efflux pumps is tightly associated with triazole resistance. In the past decade, multiple mutations outside of *cyp51A* have also been found linked to resistance. For example, mutations in *hmg1* and *cox10* have been reported to confer triazole resistance (Rybak et al., 2019). The gene *hmg1* encodes a 3-hydroxy-3-methyl-glutaryl (HMG) coenzyme A (CoA) reductase and is a key enzyme involved with the start of the ergosterol biosynthesis pathway, catalyzing HMG-CoA to mevalonate. Meanwhile, the *cox10* gene in yeast is involved in the heme biosynthetic pathway, catalyzing heme B to heme O through farnesylation (Wei et al., 2017). Although the role and function of these genes in triazole resistance are currently unknown, the emergence of non-canonical resistance mechanisms may prove to be a problem in resistance screening

and thus treatment. Furthermore, the prevalence of non-Cyp51A mediated mechanisms for triazole resistance in *A. fumigatus* strains throughout the world is increasing. Although these rates vary depending on the study, there have been reported rates of 6.5% in the United Kingdom, 25% in the United States, and 44% in Germany for resistant *A. fumigatus* strains with no *cyp51A* mutations (Macedo et al., 2021).

1.5. Mechanisms of Resistance to Amphotericin B

In addition to triazole resistance, recently amphotericin B (AMB) resistance in *A. fumigatus* has also been reported. However, little is known about the mechanisms for AMB resistance in *A. fumigatus* and they remain largely unexplored. Routes for AMB resistance have been proposed in related *Aspergillus* species as well as other pathogenic yeasts, and these proposed mechanisms seem to be species dependent.

A common AMB resistance mechanism found in *Candida* spp. is alterations to sterol composition of the fungal cell membrane and specifically, mutations in the genes *erg2*, *erg3*, *erg6* and *erg11* (Ruiz-Baca et al., 2021). In *Candida albicans*, AMB resistance stemmed from loss of function in both *erg3* and *erg11* genes, which encode for a C-5 sterol desaturase and lanosterol 14α-demethylase, respectively (Ruiz-Baca et al., 2021). AMB resistance in *Candida lusitaniae* seemed to involve deletion of *erg6* and in *Candida glabrata*, was associated with mutations in *erg2* and *erg6* – encoding a C-8 sterol isomerase and C-24 methyltransferase, respectively (Ahmad et al., 2019; Young et al., 2003). The *erg* mutations are associated with changes to the sterol composition of the cell membrane, with an accumulation of sterol intermediates – which are not targets of AMB – in exchange for ergosterol. Members of the *Candida haemulonii* species complex – *C. haemulonii, C. haemulonii* var. *vulnera* and *C. duobushemulonii* – that are known for AMB tolerance, also have been shown to have altered cell membrane sterol profiles that are similar to those seen in resistant strains with *erg2*, *erg3*, *erg6*, and *erg11* mutations (Carolus et al., 2020).

The second AMB resistance mechanism is related to protection against oxidative stress induced by AMB. In comparison to susceptible *A. fumigatus* strains, intrinsically resistant *A. terreus* had comparable levels of ergosterol membrane content but had significantly higher catalase activity (Blum et al., 2008). Furthermore, this mechanism may

play a role in AMB resistant *C. albicans* strains as they showed reduced susceptibility to H_2O_2 and increased catalase activity (Mesa-Arango et al., 2012). The mitochondrial respiratory chain also plays a key role in ROS production as well as ergosterol biosynthesis, providing NADPH for squalene dimerization as well as the fact that in the ergosterol biosynthesis pathway, conversion of squalene to 2,3-oxidosqualene pathway is an oxygen-dependent step (Silva et al., 2020). Therefore, mitochondrial involvement may also play a role in many of the mechanisms for AMB resistance. For example, the disruption of mitochondrial respiratory function resulted in reduced ergosterol levels and increased AMB tolerance in *C. albicans* (Mesa-Arango et al., 2012). This pattern was also seen in the *C. haemulonii* species complex as disruption of mitochondrial function increased AMB tolerance and was also linked to decreased ergosterol content (Silva et al., 2020).

Additional mechanisms through alterations to the cell wall and the involvement of molecular chaperones have also been frequently described in other fungal species. In *Aspergillus flavus*, a highly AMB resistant strain derived from subcultures of increasing AMB concentration had similar ergosterol content to its susceptible progenitor but showed an altered cell wall composition (Posch et al., 2018). The mutant showed growth up to 100 mg/L AMB but lost its tolerance as a protoplast. Focusing on cell wall composition, the strain had a significantly higher ß-1-3 glucan content (Posch et al., 2018). This resistance mechanism was also found in *Candida tropicalis* and *Candida albicans*. In *C. tropicalis*, AMB resistant isolates had increased ß-1-3 glucan content as well as thicker cell walls (Posch et al., 2018). However, the strains also exhibited changes in mitochondrial potential and respiration defects which may have played a role in the observed resistance (Posch et al., 2018). A study conducted on *C. albicans* also found the removal of ß-1-3 glucan to increase AMB susceptibility (Posch et al., 2018). However, this pattern was not seen in the intrinsically resistant *A. terreus* as cell wall-free protoplasts were equally resistant (Blum et al., 2008). In terms of molecular chaperons, the heat shock protein 90 (Hsp90) and heat shock protein 70 (Hsp70) have been implicated with AMB resistance. In *C. albicans*, inhibition of Hsp90 prevented growth of AMB resistant strains both in the presence and in the absence of AMB exposure (Vincent et al., 2013). Hsp90 facilitates maturation of numerous substrate proteins involved in stress response pathways (Vincent et al., 2013). It was hypothesized that

mutations in the ergosterol biosynthetic enzymes associated with resistance in these strains depended on Hsp90 function to survive (Vincent et al., 2013). Hsp90 was also found to be involved with resistance in *A. terreus*. Hsp90 inhibitors decreased AMB minimum inhibitory concentration (MIC) values in AMB resistant isolates, with a decrease from 32 mg/L to 0.38 mg/L (Blum et al., 2013). Furthermore, a higher basal level of Hsp90 in both resistant and susceptible *A. terreus* strains was seen in comparison to susceptible *A. fumigatus* strains (Blum et al., 2013). However, results in vivo, through a murine model, determined that Hsp90 inhibitors did not reduce fungal burden nor improve survival (Blum et al., 2013). This outcome was suggested as being related to the immunosuppressive side effects of these drugs and most likely led to reduced immune response (Blum et al., 2013). Furthermore, when comparing susceptible and resistant *A. terreus* strains, use of Hsp70 inhibitors increased AMB susceptibility in vitro and was more pronounced in resistant strains (Blatzer et al., 2015). Similarly, the Hsp70 inhibitors did not improve the in vivo outcome in a murine infection model, which again could have been related to the immunosuppressive drug side effects (Blatzer et al., 2015). A majority of Hsp70 genes were also immediately expressed at the transcriptional level in the resistant *A. terreus* strains when exposed to AMB while susceptible strains showed delayed responses (Blatzer et al., 2015).

1.6. Genome-Wide Association Studies

Genome-wide association studies (GWAS) are used to examine the genome of multiple individuals and identify genotype-phenotype associations. In the past decade, GWAS analyses have facilitated numerous discoveries in determining the genetic basis for a wide variety of complex diseases and other phenotypic traits. In terms of antifungal resistance, microbial GWAS is a new field of research that focuses on examining microbial genome variability to identify genetic variations impacting traits such as drug resistance, virulence, host specificity, and patient outcome (San et al., 2020). GWAS have already been used to identify mutations associated with antifungal tolerance or sensitivity in multiple fungal species, including *Rhynchosporium commune* (Mohd-Assaad et al., 2016), *Fusarium graminearum* (Talas et al., 2016), and *Parastagonospora nodorum* (Pereira et al., 2020). Furthermore, a recent GWAS conducted by Zhao and colleagues investigated mutations

associated with itraconazole sensitivity in *A. fumigatus* clinical strains from Japan. The study identified a SNP in the *Afu2g02220* gene to be significantly associated with itraconazole sensitivity. They were also able to functionally validate the gene's involvement using the CRISPR-Cas9 system – with knockout strains showing a minor and consistent reduction in growth at an itraconazole concentration of 0.15 mg/L (Zhao et al., 2021).

Overall, these studies demonstrate the promising use of GWAS in understanding underlying mechanisms for antifungal resistance in a variety of fungi, including our species of interest *A. fumigatus*.

1.7. Objectives

The objective of my thesis was to examine resistance mechanisms for triazole drugs, specifically itraconazole and voriconazole, and AMB antifungal in *A. fumigatus*. This work has been separated into two chapters: The first chapter, Chapter 2, will focus on studying mutations associated with itraconazole and voriconazole resistance through the use of a genome-wide association study (GWAS) and 195 *A. fumigatus* whole-genome sequences. Despite the known mutations conferring triazole resistance, we want to confirm the significance and extent these mutations play in triazole resistance at a population level. In addition, with the increasing prevalence of non-Cyp51A mediated resistance, the second objective was to identify novel mutations by focusing on resistant *A. fumigatus* strains that did not contain *cyp51A* mutations. The second chapter, Chapter 3, will focus on the topic of AMB resistance in *A. fumigatus*. To facilitate identification of potential genes of interest, we will investigate mutations associated with AMB resistance through a GWAS using 98 *A. fumigatus* sequences. In addition, variant genotyping at select mutation sites of interest was conducted on 143 progeny strains, obtained from a laboratory cross.

1.8. References

Abad, A., Fernández-Molina, J. V., Bikandi, J., Ramírez, A., Margareto, J., Sendino, J., ... & Rementeria, A. (2010). What makes *Aspergillus fumigatus* a successful pathogen? Genes and molecules involved in invasive aspergillosis. *Revista Iberoamericana de Micologia*, *27*(4), 155-182.

Ahmad, S., Joseph, L., Parker, J. E., Asadzadeh, M., Kelly, S. L., Meis, J. F., & Khan, Z. (2019). ERG6 and ERG2 are major targets conferring reduced susceptibility to amphotericin B in clinical *Candida glabrata* isolates in Kuwait. *Antimicrobial Agents and Chemotherapy*, *63*(2), e01900-18.

Albarrag, A. M., Anderson, M. J., Howard, S. J., Robson, G. D., Warn, P. A., Sanglard, D., & Denning, D. W. (2011). Interrogation of related clinical pan-azole-resistant *Aspergillus fumigatus* strains: G138C, Y431C, and G434C single nucleotide polymorphisms in *cyp51A*, upregulation of *cyp51A*, and integration and activation of transposon Atf1 in the *cyp51A* promoter. *Antimicrobial Agents and Chemotherapy*, *55*(11), 5113-5121.

Bandres, M. V., Modi, P., & Sharma, S. (2020). *Aspergillus fumigatus*. *StatPearls [Internet]*.

Bauer, I., Misslinger, M., Shadkchan, Y., Dietl, A. M., Petzer, V., Orasch, T., ... & Haas, H. (2019). The lysine deacetylase RpdA is essential for virulence in *Aspergillus fumigatus*. *Frontiers in Microbiology*, *10*, 2773.

Berger, S., El Chazli, Y., Babu, A. F., & Coste, A. T. (2017). Azole resistance in *Aspergillus fumigatus*: a consequence of antifungal use in agriculture?. *Frontiers in Microbiology*, *8*, 1024.

Bongomin, F., Gago, S., Oladele, R. O., & Denning, D. W. (2017). Global and multi-national prevalence of fungal diseases—estimate precision. *Journal of Fungi*, *3*(4), 57.

Blatzer, M., Blum, G., Jukic, E., Posch, W., Gruber, P., Nagl, M., ... & Wilflingseder, D. (2015). Blocking Hsp70 enhances the efficiency of amphotericin B treatment against resistant *Aspergillus terreus* strains. *Antimicrobial Agents and Chemotherapy*, *59*(7), 3778-3788.

Blum, G., Perkhofer, S., Haas, H., Schrettl, M., Würzner, R., Dierich, M. P., & Lass-Flörl, C. (2008). Potential basis for amphotericin B resistance in *Aspergillus terreus*. *Antimicrobial Agents and Chemotherapy*, *52*(4), 1553-1555.

Brown, G. D., Denning, D. W., Gow, N. A., Levitz, S. M., Netea, M. G., & White, T. C. (2012). Hidden killers: human fungal infections. *Science Translational Medicine*, *4*(165), 165rv13-165rv13.

Carolus, H., Pierson, S., Lagrou, K., & Van Dijck, P. (2020). Amphotericin B and other polyenes—discovery, clinical use, mode of action and drug resistance. *Journal of Fungi*, *6*(4), 321.

Casadevall, A. (2018). Fungal diseases in the 21st century: the near and far horizons. *Pathogens and Immunity*, *3*(2), 183.

Chaudhary, N., & Marr, K. A. (2011). Impact of *Aspergillus fumigatus* in allergic airway diseases. *Clinical and Translational Allergy*, *1*(1), 1-7.

Chen, P., Liu, J., Zeng, M., & Sang, H. (2020). Exploring the molecular mechanism of azole resistance in *Aspergillus fumigatus*. *Journal de Mycologie Medicale*, *30*(1), 100915.

Dagenais, T. R., & Keller, N. P. (2009). Pathogenesis of *Aspergillus fumigatus* in invasive aspergillosis. *Clinical Microbiology Reviews*, *22*(3), 447-465.

Diaz-Guerra, T. M., Mellado, E., Cuenca-Estrella, M., & Rodriguez-Tudela, J. L. (2003). A point mutation in the 14α-sterol demethylase gene *cyp51A* contributes to itraconazole resistance in *Aspergillus fumigatus*. *Antimicrobial Agents and Chemotherapy*, *47*(3), 1120-1124.

Fisher, M. C., Henk, D. A., Briggs, C. J., Brownstein, J. S., Madoff, L. C., McCraw, S. L., & Gurr, S. J. (2012). Emerging fungal threats to animal, plant and ecosystem health. *Nature*, *484*(7393), 186-194.

Garcia-Rubio, R., Cuenca-Estrella, M., & Mellado, E. (2017). Triazole resistance in *Aspergillus* species: an emerging problem. *Drugs*, *77*(6), 599-613.

Gonzalez-Jimenez, I., Lucio, J., Amich, J., Cuesta, I., Sanchez Arroyo, R., Alcazar-Fuoli, L., & Mellado, E. (2020). A Cyp51B mutation contributes to azole resistance in *Aspergillus fumigatus*. *Journal of Fungi*, *6*(4), 315.

Gsaller, F., Hortschansky, P., Furukawa, T., Carr, P. D., Rash, B., Capilla, J., ... & Bromley, M. J. (2016). Sterol biosynthesis and azole tolerance is governed by the opposing actions of SrbA and the CCAAT binding complex. *PLoS Pathogens*, *12*(7), e1005775.

Hagiwara, D., Watanabe, A., & Kamei, K. (2016). Sensitisation of an azole-resistant *Aspergillus fumigatus* strain containing the Cyp51A-related mutation by deleting the SrbA gene. *Scientific Reports*, *6*(1), 1-8.

Horianopoulos, L. C., Gluck-Thaler, E., Benoit Gelber, I., Cowen, L. E., Geddes-McAlister, J., Landry, C. R., ... & Gerstein, A. C. (2021). The Canadian Fungal Research Network: current challenges and future opportunities. *Canadian Journal of Microbiology*, *67*(1), 13-22.

Jermy, A. (2017). Stop neglecting fungi. *Nature Microbiology*, *2*, 17120.

Kalita, J. M., Sharma, A., Bhardwaj, A., & Nag, V. L. (2019). Dermatophytoses and spectrum of dermatophytes in patients attending a teaching hospital in Western Rajasthan, India. *Journal of Family Medicine and Primary Care*, *8*(4), 1418.

Kwon-Chung, K. J., & Sugui, J. A. (2013). *Aspergillus fumigatus*—what makes the species a ubiquitous human fungal pathogen?. *PLoS Pathogens*, *9*(12), e1003743.

Latgé, J. P. (1999). *Aspergillus fumigatus* and aspergillosis. *Clinical Microbiology Reviews*, *12*(2), 310-350.

Liu, M., Zheng, N., Li, D., Zheng, H., Zhang, L., Ge, H., & Liu, W. (2016). *cyp51A*-based mechanism of azole resistance in *Aspergillus fumigatus*: illustration by a new 3D structural model of *Aspergillus fumigatus* CYP51A protein. *Sabouraudia*, *54*(4), 400-408.

Macedo, D., Leonardelli, F., Gamarra, S., & Garcia-Effron, G. (2021). Emergence of triazole resistance in *Aspergillus* spp. in Latin America. *Current Fungal Infection Reports*, 1-11.

Mann, P. A., Parmegiani, R. M., Wei, S. Q., Mendrick, C. A., Li, X., Loebenberg, D., ... & McNicholas, P. M. (2003). Mutations in *Aspergillus fumigatus* resulting in reduced susceptibility to posaconazole appear to be restricted to a single amino acid in the cytochrome P450 14α-demethylase. *Antimicrobial Agents and Chemotherapy*, *47*(2), 577-581.

Mazu, T. K, Bricker, B. A, Flores-Rozas, H., & Ablordeppey, S. Y. (2016). The mechanistic targets of antifungal agents: an overview. *Mini Reviews in Medicinal Chemistry*, *16*(7), 555-578.

Mesa-Arango, A. C., Scorzoni, L., & Zaragoza, O. (2012). It only takes one to do many jobs: amphotericin B as antifungal and immunomodulatory drug. *Frontiers in Microbiology*, *3*, 286.

Mellado, E., Garcia-Effron, G., Alcazar-Fuoli, L., Cuenca-Estrella, M., & Rodriguez-Tudela, J. L. (2004). Substitutions at methionine 220 in the 14α-sterol demethylase (Cyp51A) of *Aspergillus fumigatus* are responsible for resistance in vitro to azole antifungal drugs. *Antimicrobial Agents and Chemotherapy*, *48*(7), 2747-2750.

Mohd-Assaad, N., McDonald, B. A., & Croll, D. (2016). Multilocus resistance evolution to azole fungicides in fungal plant pathogen populations. *Molecular Ecology*, 25(24), 6124-6142.

Mousavi, B., Hedayati, M. T., Hedayati, N., Ilkit, M., & Syedmousavi, S. (2016). *Aspergillus* species in indoor environments and their possible occupational and public health hazards. *Current Medical Mycology*, *2*(1), 36.

Nash, A., & Rhodes, J. (2018). Simulations of CYP51A from *Aspergillus fumigatus* in a model bilayer provide insights into triazole drug resistance. *Medical Mycology*, *56*(3), 361-373.

Natesan, S. K., Wu, W., Cutright, J. L., & Chandrasekar, P. H. (2012). In vitro–in vivo correlation of voriconazole resistance due to G448S mutation (*cyp51A* gene) in *Aspergillus fumigatus*. *Diagnostic Microbiology and Infectious Disease*, *74*(3), 272-277.

Pereira, D., McDonald, B. A., & Croll, D. (2020). The genetic architecture of emerging fungicide resistance in populations of a global wheat pathogen. *Genome Biology and Evolution*, *12*(12), 2231-2244.

Posch, W., Blatzer, M., Wilflingseder, D., & Lass-Flörl, C. (2018). *Aspergillus terreus*: Novel lessons learned on amphotericin B resistance. *Medical Mycology*, *56*(suppl_1), S73-S82.

Resendiz Sharpe, A., Lagrou, K., Meis, J. F., Chowdhary, A., Lockhart, S. R., Verweij, P. E., & ISHAM/ECMM Aspergillus Resistance Surveillance Working Group. (2018). Triazole resistance surveillance in *Aspergillus fumigatus*. *Medical Mycology*, *56*(suppl_1), S83-S92.

Rodrigues, M. L., & Nosanchuk, J. D. (2020). Fungal diseases as neglected pathogens: a wake-up call to public health officials. *PLoS Neglected Tropical Diseases*, *14*(2), e0007964.

Ruiz-Baca, E., Arredondo-Sánchez, R. I., Corral-Pérez, K., López-Rodríguez, A., Meneses-Morales, I., Ayala-García, V. M., & Martínez-Rocha, A. L. (2021). Molecular mechanisms of resistance to antifungals in *Candida albicans*. In *Candida albicans*. IntechOpen.

Rybak, J. M., Fortwendel, J. R., & Rogers, P. D. (2019). Emerging threat of triazole-resistant *Aspergillus fumigatus*. *Journal of Antimicrobial Chemotherapy*, *74*(4), 835-842.

San, J. E., Baichoo, S., Kanzi, A., Moosa, Y., Lessells, R., Fonseca, V., ... & de Oliveira, T. (2020). Current affairs of microbial genome-wide association studies: approaches, bottlenecks and analytical pitfalls. *Frontiers in Microbiology*, *10*, 3119.

Sandhu, S. S, Shukla, H., P Aharwal, R., Kumar, S., & Shukla, S. (2014). Antifungal azole derivatives and their pharmacological potential: prospects & retrospects. *The Natural Products Journal*, *4*(2), 140-152.

Sharma, C., Hagen, F., Moroti, R., Meis, J. F., & Chowdhary, A. (2015). Triazole-resistant *Aspergillus fumigatus* harbouring G54 mutation: is it de novo or environmentally acquired?. *Journal of Global Antimicrobial Resistance*, *3*(2), 69-74.

Silva, L. N., Oliveira, S. S., Magalhães, L. B., Andrade Neto, V. V., Torres-Santos, E. C., Carvalho, M. D., ... & Santos, A. L. (2020). Unmasking the amphotericin B resistance mechanisms in *Candida haemulonii* species complex. *ACS Infectious Diseases*, *6*(5), 1273-1282.

Talas, F., Kalih, R., Miedaner, T., & McDonald, B. A. (2016). Genome-wide association study identifies novel candidate genes for aggressiveness, deoxynivalenol production, and azole sensitivity in natural field populations of *Fusarium graminearum*. *Molecular Plant-Microbe Interactions*, *29*(5), 417-430.

Valsecchi, I., Dupres, V., Stephen-Victor, E., Guijarro, J. I., Gibbons, J., Beau, R., ... & Beauvais, A. (2018). Role of hydrophobins in *Aspergillus fumigatus*. *Journal of Fungi*, *4*(1), 2.

Van De Veerdonk, F. L., Gresnigt, M. S., Romani, L., Netea, M. G., & Latge, J. P. (2017). *Aspergillus fumigatus* morphology and dynamic host interactions. *Nature Reviews Microbiology*, *15*(11), 661-674.

Vincent, B. M., Lancaster, A. K., Scherz-Shouval, R., Whitesell, L., & Lindquist, S. (2013). Fitness trade-offs restrict the evolution of resistance to amphotericin B. *PLoS Biology*, *11*(10), e1001692.

Wei, X., Chen, P., Gao, R., Li, Y., Zhang, A., Liu, F., & Lu, L. (2017). Screening and characterization of a non-*cyp51A* mutation in an *Aspergillus fumigatus cox10* strain conferring azole resistance. *Antimicrobial Agents and Chemotherapy*, *61*(1), e02101-16.

Young, L. Y., Hull, C. M., & Heitman, J. (2003). Disruption of ergosterol biosynthesis confers resistance to amphotericin B in *Candida lusitaniae*. *Antimicrobial Agents and Chemotherapy*, *47*(9), 2717-2724.

Zhao, S., Ge, W., Watanabe, A., Fortwendel, J. R., & Gibbons, J. G. (2021). Genome-wide association for itraconazole sensitivity in non-resistant clinical isolates of *Aspergillus fumigatus*. *Frontiers in Fungal Biology*, *1*.

Chapter 2

Genome-wide association analysis for triazole resistance in *Aspergillus fumigatus*

2.1. Preface

This study has been published in the journal "Pathogens" on June 4, 2021. The authors of this paper are: YuYing Fan, Yue Wang, Gregory Korfanty, Meagan Archer, and Jianping Xu. I am a co-first author with Yue Wang in this publication. Yue Wang provided the scripts for the initial data preparation steps, which comprised of quality control of raw reads, trimming, alignment & mapping, variant calling, and annotation; while variant filtering, association analysis and linkage disequilibrium analysis were conducted by me. Yue Wang conducted the phylogenetic tree, clade identification and strain distribution sections of this study. The genome-wide association analysis, linkage disequilibrium analysis, and Fisher's exact test sections were conducted by myself. Writing of the manuscript was predominantly completed by me, with great help from Yue Wang, Gregory Korfanty, Meagan Archer, and Jianping Xu. Jianping Xu also designed the experiments, supervised the work, and edited the manuscript.

The journal link for the supplementary files in Chapter 2 can also be found and downloaded from "https://www.mdpi.com/2076-0817/10/6/701".

2.2. Abstract

Aspergillus fumigatus is a ubiquitous fungus and the main agent of aspergillosis, a common fungal infection in the immunocompromised population. Triazoles such as itraconazole and voriconazole are the common first-line drugs for treating aspergillosis. However, triazole resistance in *A. fumigatus* has been reported in an increasing number of countries. While most studies of triazole resistance have focused on mutations in the triazole target gene *cyp51A*,

>70% of triazole-resistant strains in certain populations showed no mutations in *cyp51A*. To identify potential non-*cyp51A* mutations associated with triazole resistance in *A. fumigatus*, we analyzed the whole genome sequences and triazole susceptibilities of 195 strains from 12 countries. These strains belonged to three distinct clades. Our genome-wide association study (GWAS) identified a total of six missense mutations significantly associated with itraconazole resistance and 18 missense mutations with voriconazole resistance. In addition, to investigate itraconazole and pan-azole resistance, Fisher's exact tests revealed 26 additional missense variants tightly linked to the top 20 SNPs obtained by GWAS, of which two were consistently associated with triazole resistance. The large number of novel mutations related to triazole resistance should help further investigations into their molecular mechanisms, their clinical importance, and the development of a comprehensive molecular diagnosis toolbox for triazole resistance in *A. fumigatus*.

2.3. Introduction

Aspergillus fumigatus is an opportunistic human fungal pathogen that is found in a broad range of substrates and is capable of surviving and growing in numerous environmental conditions. *A. fumigatus* is the primary cause of invasive aspergillosis, a life-threatening mold infection with high morbidity and mortality rates in immunocompromised patients. Its high sporulating capacity contributes to the environmental prevalence of *A. fumigatus*, leading to the high likelihood of infection in at-risk populations [1]. Globally, it is estimated that over 200,000 cases of invasive aspergillosis occur annually [2]. However, this number may represent only one-half of actual cases due to under- and mis-diagnoses [2]. Depending on factors such as population of patients, site of infection and antifungal management, mortality rates associated with invasive aspergillosis range from 60 to 90% [3].

Currently, there are four main classes of antifungals for aspergillosis treatment: azoles, polyenes, echinocandins, and allylamines. Among all antifungal agents, aspergillosis is commonly treated with triazole antifungals as the first choice because their use has been associated with better clinical response, less infusion-related toxicity, less nephrotoxicity and increased survival [4]. For aspergillosis treatment, itraconazole and voriconazole are among

some of the commonly used triazole antifungals. Triazole antifungals work by inhibiting a vital enzymatic step in the synthesis of ergosterol, a major sterol and crucial part of the fungal cellular membrane [5]. Ergosterol plays a key role in membrane fluidity, membrane permeability, the activity of membrane proteins, and cell growth [5]. The triazoles work by inhibiting the demethylation of precursor sterols by binding to 14α-lanosterol demethylase (also known as Cyp51), a crucial enzyme involved in the ergosterol biosynthesis pathway. Triazoles act as competitive Cyp51 inhibitors through the binding of the N4 in their azole ring with the heme iron atom at the center of Cyp51 [5]. This binding prevents access of precursor sterols to the active site where demethylation occurs. Disruption of this enzymatic step causes significant damage to the cell membrane and results in the accumulation of toxic sterol intermediates, eventually leading to cell lysis and death [6]. However, the emergence of triazole-resistant *A. fumigatus* strains throughout the world has been a growing public health concern and a problem in the treatment of patients with aspergillosis.

Triazole-resistant strains have been extensively documented and characterized within multiple countries around the world. The majority of these studies have focused on the prevalence of resistant strains in a clinical setting. Furthermore, most analyses of the mechanisms of triazole resistance have focused on mutations in *cyp51A,* the gene coding for the triazole target enzyme [7]. The most common mutations in *cyp51A* among clinical-resistant strains, that develop during aspergillosis treatment, occur in amino acid sites G54, G138, M220, and G448 [7,8,9,10]. Meanwhile, the most common triazole drug resistant mutations in the global *A. fumigatus* population are TR_{34}/L98H and TR_{46}/Y121F/T289A, with many of these resistant strains originating from the environment [11,12].

The global population structure of *A. fumigatus* is shaped by high levels of gene flow between different populations [13,14]. Triazole-resistant *A. fumigatus* genotypes can rise and spread as a result of local selection due to elevated antifungal pressure within the environment. Clonal expansion of these highly fit triazole-resistant genotypes has been suggested to have led to their high abundance across the world [15,16]. Two main factors could have facilitated the spread of *A. fumigatus* genotypes and drug-resistant genes among geographic populations: the high dispersal ability of its asexual spores by wind and

contemporary anthropogenic influences such as travel and trade [1]. Additionally, as aspergillosis is one of the leading causes of fungal deaths in avian species, bird migration may also be a factor in *A. fumigatus* dispersal [17,18]. The study by Ashu and colleagues further noted a large number of triazole-resistant genotypes and determined certain resistance genotypes were more commonly found in certain population genetic clusters than others [13]. Specifically, their analyses of 2026 *A. fumigatus* strains from 13 countries revealed that certain-resistant genotypes were mostly clustered into one genetic population and it was suggested that clonal expansion might have contributed to such a distribution.

Many research laboratories and hospitals around the world have been tracking the distribution of triazole-resistant clinical and environmental strains [19]. When examining prior epidemiological data, an increasing trend of triazole-resistant strains and infections has been reported. For example, within the Netherlands, the number of triazole-resistant infections has increased from 7.6% in 2013 to 14.7% in 2018 [20]. Another study in the Netherlands has also reported an increasing resistance rate in Radboud University Medical Center, from 0.79% between 1996 and 2001 to 7.04% between 2012 and 2016 [21]. These upward trends have also been reported in Iran (3.3% in 2013 to 6.6% in 2015), the United Kingdom (0.43% between 1998–2011 to 2.2% between 2015–2017), and in Texas, United States (7.2% between 1999–2002 to 22.6% between 2003–2015) [22,23,24]. The increasing prevalence of triazole-resistant *A. fumigatus* strains has become a major burden to many health institutions.

Triazole resistance in *A. fumigatus* is typically separated into two main categories, Cyp51A-mediated and non-Cyp51A-mediated mechanisms of resistance. In addition, studies on triazole resistance have mainly focused on three molecular mechanisms: (i) mutations in the Cyp51A protein, (ii) overexpression of the Cyp51A protein, and (iii) upregulation of drug efflux pumps. Alterations in Cyp51A are the most commonly studied mechanism for triazole resistance. Until 2008, all reported triazole resistance focused on the context of mutations in *cyp51A*. However, from 2008 onwards, the frequency of resistant strains with no mutations in *cyp51A* was increasing [25,26]. At present, most epidemiological studies of

triazole resistance in *A. fumigatus* only investigate mutations at the *cyp51A* gene. Consequently, mutations in other genes remain largely uncharacterized.

Microbial genome-wide association studies (GWAS) are a relatively new but powerful tool in understanding the relationships between genetic variations and microbial phenotypes. There have been several successful GWAS applications in identifying novel genomic markers responsible for antifungal drug resistance, with several studies focused on examining azole resistance in plant fungal pathogens [27,28]. In *A. fumigatus*, Zhao and colleagues recently conducted a genome-wide association study for itraconazole sensitivity in non-resistant clinical isolates from Japan [29]. In the current study, a GWAS was performed for itraconazole and voriconazole resistance in *A. fumigatus* based on a global population of published genomes. The aim of the study was to determine the genetic variants associated with triazole resistance using genome-wide SNP data, with the focus placed on novel *non-cyp51A* related mutations, as well as conduct a phylogenetic analysis with 195 strains to examine the phylogenetic distributions of itraconazole and voriconazole resistance in *A. fumigatus*.

2.4. Results

2.4.1. Phylogenetic Tree

Phylogenetic analysis of the whole-genome SNPs grouped the 195 samples and the reference strain Af293 into three large clades based on pairwise SNP differences between all 196 strains (Figure 2.1). Within each clade, whole-genome SNP differences were identified as ≤35,112 in Clade I, ≤45,160 in Clade II, and ≤48,670 in Clade III. Among the analyzed strains, 15 were in Clade I, 134 strains and the reference Af293 were in Clade II, and 46 strains were in Clade III. Geographically, the Clade II strains were from 10 countries, with 16 strains found in Canada, 4 in India, 1 in Ireland, 27 in Japan, 16 in Netherlands, 7 in Portugal, 1 in Singapore, 14 in Spain, 9 in the United Kingdom, and 37 in the United States. Furthermore, two strains were collected from the International Space Station. Clade III strains were obtained from the following seven countries: Canada (n = 1), India (n = 8),

Netherlands (n = 8), Spain (n = 6), the United Kingdom (n = 16), Germany (n = 1), and the United States (n = 6). Finally, the 15 Clade I strains were from four countries: Canada (n = 1), Peru (n = 1), Portugal (n = 1), and Spain (n = 12). Within each clade, the samples were predominantly from infected patients, with 93.33% (14/15) in Clade I, 82.84% (111/134) in Clade II, and 82.61% (38/46) in Clade III of the analyzed samples were from clinical sources. The overall percentage of isolates from patients in the whole sample-set was 83.59%. According to the European Committee on Antimicrobial Susceptibility Testing (EUCAST), the MIC breakpoints for susceptible strains was set at ≤1 mg/L and the area of technical uncertainty (ATU) was set at 2 mg/L for both itraconazole and voriconazole antifungals. Among the samples with available MIC information and using an MIC ≥ 2 mg/L as the resistance cut-off value for both antifungals, 61.48% (75/122) were itraconazole resistant and 43.90% (54/123) were voriconazole resistant. At a clade-level, the percentages of itraconazole-resistant strains were as follows: 0% in Clade I, 57.75% in Clade II, and 82.93% in Clade III. For voriconazole, the percentage of resistant strains were 0% in Clade I, 37.50% in Clade II, and 65.85% in Clade III. Using MICs ≥ 4 mg/L as the resistance cut-off value for both antifungals, the itraconazole-resistant rate remained the same in our sample set, at 61.48% (75/122). However, the voriconazole-resistant rate dropped to 34.96% (43/123). The percentages of itraconazole-resistant strains in each clade remained the same while the voriconazole-resistant rates were as follows: 0% in Clade I, 27.78% in Clade II, and 56.10% in Clade III. Information on the 195 strains and clade divisions can be found in Appendix A.

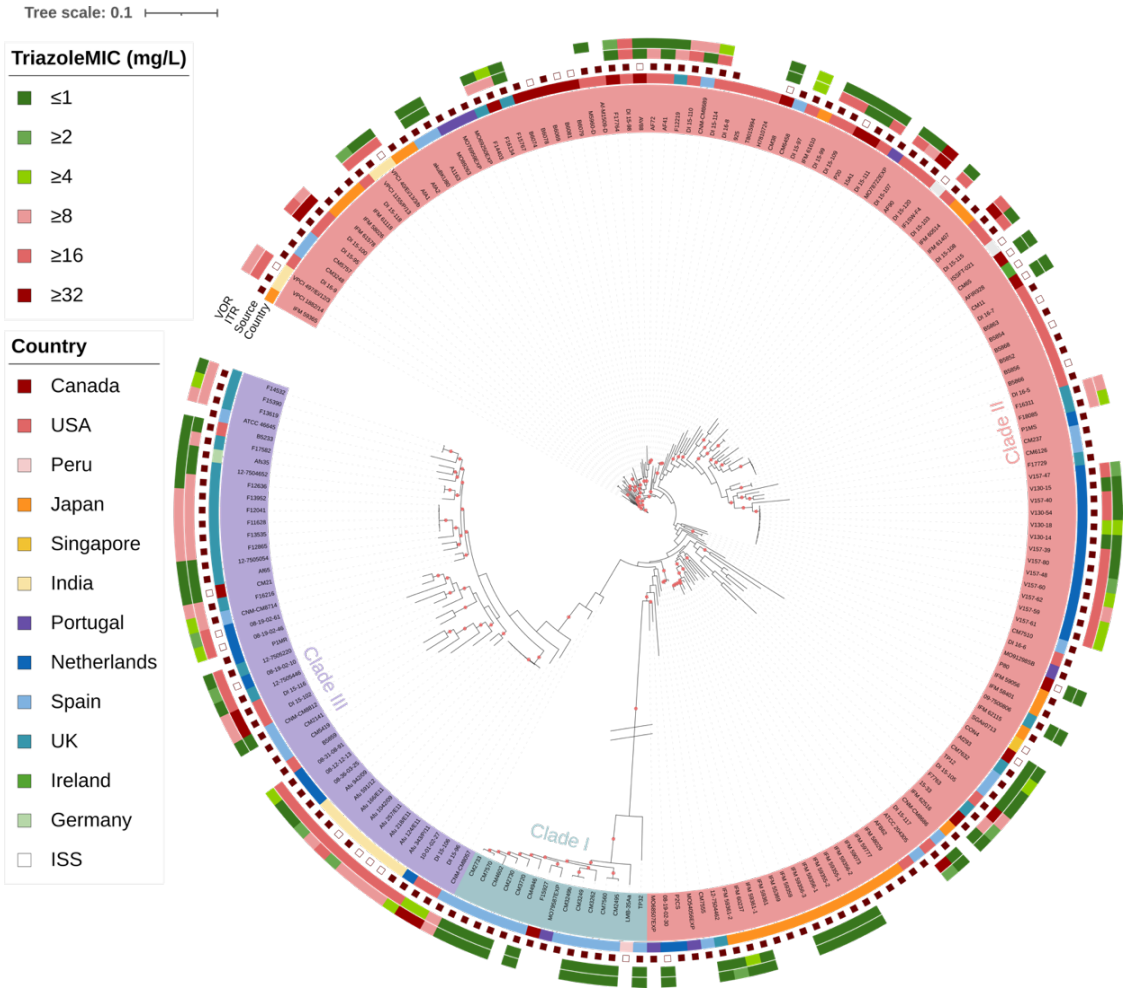

Figure 2.1. Maximum likelihood phylogenetic tree detailing the strain characteristics. Branches with a red dot represent those with over 75% bootstrap support, based on 500 bootstrap iterations. The inner-most circle denotes the clade affiliation of strains with strain names corresponding to those in Supplementary Table S2.1. The second inner-most circle represents country of origin for individual strains with different colors representing different countries as shown in the left "Country" panel. The third circle from the inside denotes strain ecological niche, with hollow squares representing strains from the natural environment, solid red squares representing strains from the clinical environment, and the source for the remaining strains (unmarked) were unknown. The itraconazole and voriconazole minimum inhibitory concentrations (MIC) were represented in the two outer circles with different colors representing different MIC values as shown in the left "TriazoleMIC" panel. The white boxes in the two outer circles represent strains with no MIC data. The branch length separating Clade I from the two other clades was manually truncated to make relationships in the other two clades more visible.

2.4.2. Known Mutations Associated with Triazole Resistance

The MIC data for triazole drugs in this population identified 122 and 123 strains with known itraconazole and voriconazole MIC values respectively. We first examined the statistical association between mutations at 44 amino acid sites that had been previously found to be related to triazole resistance in *A. fumigatus*. The 44 known sites were mainly identified based on epidemiological surveys and are listed in Table 2.1.

Table 2.1. The 44 known mutation sites previously reported to be associated with triazole resistance and results of the Fisher's Exact tests using 122 *A. fumigatus* strains with known itraconazole and voriconazole MICs.

Gene	Codon	Amino Acid Change	Chromosome - Position (bp)	Fisher's Exact Test (p-values), MIC ≥ 2 mg/L		Fisher's Exact Test (p-values), MIC ≥ 4 mg/L		Reference
				Itraconazole	Pan-Azole	Itraconazole	Pan-Azole	
cyp51A (AFUA_4G06890)	N22			NA[1]				[30]
	*F46	Y	CHR 4-1,781,686	4.50×10^{-3}	3.54×10^{-2}	4.50×10^{-3}	2.96×10^{-2}	[30]
	S52			NA[1]				[31]
	G54	V, E	CHR 4 - 1,781,662	1.55×10^{-1}	1.00	1.55×10^{-1}	1.00	[30]
		W, R	CHR 4 - 1,781,663	8.16×10^{-2}	2.72×10^{-2}	8.16×10^{-2}	8.90×10^{-3}	
	Q88			NA[1]				[31]
	L98	H	CHR 4 - 1,781,459	1.19×10^{-5}	3.33×10^{-6}	1.19×10^{-5}	1.47×10^{-5}	[30]
	V101			NA[1]				[31]
	Y121	F	CHR 4 - 1,781,390	2.81×10^{-1}	2.42×10^{-1}	2.81×10^{-1}	9.71×10^{-2}	[30]
	N125			NA[1]				[31]
	G138	C	CHR 4 - 1,781,340	8.09×10^{-2}	1.00	8.09×10^{-2}	1.00	[31]
	Q141			NA[1]				[31]
	H147	Y	CHR 4 - 1,781,313	1.00	1.00	1.00	1.00	[31]
	F165			NA[1]				[30]
	*M172			NA[1]				[30]
	P216	L	CHR 4 - 1,781,105	5.23×10^{-1}	4.95×10^{-1}	5.23×10^{-1}	2.19×10^{-1}	[30]
	F219	S	CHR 4 - 1,781,096	2.91×10^{-1}	2.44×10^{-1}	2.91×10^{-1}	1.04×10^{-1}	[30]
	M220	I	CHR 4 - 1,781,092	1.00	1.00	1.00	1.00	[30]
		V	CHR 4 - 1,781,094	2.87×10^{-1}	1.00	2.87×10^{-1}	1.00	
	M236			NA[1]				[31]
	*N248			NA[1]				[30]
	*D255	E	CHR 4 - 1,780,987	6.30×10^{-1}	1.00	6.30×10^{-1}	1.00	[30]
	D262			NA[1]				[30]
	A284			NA[1]				[30]
	T289	A	CHR 4 - 1,780,887	2.91×10^{-1}	2.44×10^{-1}	2.91×10^{-1}	1.04×10^{-1}	[30]

	S297	T	CHR 4 - 1,780,863	5.26×10^{-1}	1.00	5.26×10^{-1}	1.00	[31]
	P394			NA[1]				[31]
	*E427	K	CHR 4 - 1,780,473	5.00×10^{-3}	3.69×10^{-2}	5.00×10^{-3}	3.11×10^{-2}	[30]
	Y431			NA[1]				[30]
	G432			NA[1]				[30]
	G434			NA[1]				[30]
	T440			NA[1]				[30]
	G448	S	CHR 4 - 1,780,410	1.00	1.00	1.00	4.71×10^{-1}	[30]
	N479			NA[1]				[30]
	Y491			NA[1]				[30]
	F495	I	CHR 4 - 1,780,269	5.22×10^{-1}	1.00	5.22×10^{-1}	1.00	[31]
cyp51B (AFUA_7G03740)	G457			NA[1]				[32]
hapE (AFUA_6G05300)	P88			NA[1]				[30]
hmg1 (AFUA_2G03700)	F262			NA[1]				[33]
	S305	P	CHR 2 - 985,959	5.22×10^{-1}	4.95×10^{-1}	5.22×10^{-1}	2.14×10^{-1}	[33]
	P309	L	CHR 2 - 985,972	1.00	1.00	1.00	1.00	[33]
	I412	T, S	CHR 2 - 986,281	1.56×10^{-1}	1.17×10^{-1}	1.56×10^{-1}	4.34×10^{-2}	[33]
erg6 (AFUA_4G03630)	A350			NA[1]				[34]
cox10 (AFUA_4G08340)	R243			NA[1]				[35]
AFUA_7G01960	L167	Stop Gained	CHR 7 - 531,582	1.00	1.00	1.00	4.66×10^{-1}	[36]
AFUA_2G10600	E180	D	CHR 2 - 2,714,188	6.39×10^{-2}	2.33×10^{-2}	6.39×10^{-2}	8.79×10^{-3}	[37]

* The reference strain Af293 contains the *cyp51A* mutations F46Y, M172V, N248T, D255E, and E427K.
[1] The mutation sites were not found in the soft filtered genotype file, prior to multiallelic site removal.

Among these 44 known amino acid sites, 22 SNPs at 20 amino acid positions were found in our sample-set using the filtered vcf file, prior to multiallelic site removal (Table 2.1). Fisher's Exact tests were conducted on these sites to determine their statistical associations with triazole resistance (Table 2.1). For these tests, using the 122 strains with known MIC values for both antifungals, we identified SNPs significantly associated with itraconazole and pan-azole resistance (Table 2.1).

According to EUCAST guidelines, MIC breakpoints for susceptible strains are set at ≤1 mg/L with an ATU of 2 mg/L for both itraconazole and voriconazole. To accommodate this buffer region, two resistance criteria were used and tested in this study. The first test defined resistant strains as having MIC values ≥ 2 mg/L and the second test set the

resistance values at MIC ≥ 4 mg/L. A Bonferroni-corrected *p*-value threshold of 4.07×10^{-4} (0.05/122) was used to evaluate associations between the 22 SNPs and triazole resistance. Of the 22 known SNPs tested, only one in the Lysine-98 amino acid site, located in the gene *cyp51A*, was found to be significantly associated with itraconazole and pan-azole resistance in both Fisher's Exact tests (Table 2.1).

We further sought to conduct Fisher's Exact tests using subgroups consisting of solely itraconazole resistant (i.e., resistant to itraconazole but susceptible to voriconazole) or solely voriconazole resistant (i.e., resistant to voriconazole but susceptible to itraconazole) strains groups. However, the sample sizes of these subgroups were all below the requirement needed to achieve the desired Bonferroni-corrected *p*-value threshold. Thus, these subgroups were omitted from testing.

To unmask the effect of all these listed known mutation sites in *cyp51A* associated with triazole resistance, our study conducted a stepwise analysis of these sites using Fisher's Exact tests. First, additional Fisher's Exact tests were conducted after strains with the well-documented L98H mutation in *cyp51A*, which alone with its accompanying tandem repeat TR_{34} can confer triazole resistance, were removed. From the 122 strains with known MIC values, 21 strains contained the TR_{34}/L98H mutation (Table S2.1). Using both MIC resistance thresholds and a Bonferroni-corrected threshold of 4.95×10^{-4} (0.05/101), the additional Fisher's Exact tests identified no SNPs significantly associated with itraconazole and/or pan-azole resistance among these 22 known mutations.

To unmask the effect of other known *cyp51A* mutations associated with triazole resistance, additional Fisher's Exact tests were also conducted after removal of strains containing any of these known mutations (Table S2.1). From the strains with known MIC values, 64 strains contained the known mutations in these *cyp51A* sites (Table S2.1). After removal of the 64 strains and using a Bonferroni-corrected threshold of 8.62×10^{-4} (0.05/58), the additional Fisher's Exact tests identified no SNPs significantly associated with itraconazole and/or pan-azole resistance among these 22 mutation sites.

A final set of Fisher's Exact tests were conducted focusing on a clade-level. Clade II was chosen for these additional analyses as the cluster contained the greatest number of strains and none of the Clade II strains contained the L98H mutation in *cyp51A*. The strains from Clade II with both itraconazole and voriconazole MIC values (n = 71) were used in this final set of the Fisher's Exact tests. Using a Bonferroni-corrected threshold of 7.04×10^{-4} (0.05/71), no SNPs were found to be significantly associated with itraconazole and/or pan-azole resistance from these 22 mutations sites.

Together, the stepwise analyses results revealed that these well-characterized mutation sites do not account for the observed triazole resistance in our sample sets. Therefore, additional modes of action and uncharacterized novel mutations should be investigated for their possible involvement with triazole susceptibility in *A. fumigatus*.

2.4.3. Genes Overexpressed with Triazole Exposure

We further examined the potential overlap between the genome-wide population level SNPs identified here with previously identified genes not listed in Table 2.1 but were related with triazole resistance in *A. fumigatus*. Specifically, we extracted information about specific genes that were overexpressed in *A. fumigatus* during exposure to itraconazole and/or voriconazole. Table 2.2 summarizes the genes that were overexpressed upon exposure to each antifungal. The overexpression of these genes under triazole stress were determined using RT-qPCR and RNA-seq information [25,38,39]. Supplementary Table S2.2 describes the details on the experimental conditions and setup associated with each gene listed in Table 2.2. Specifically, previous work demonstrated that ten ATP-binding cassette (ABC) transporters (*abcA-1*, *abcA-2*, *abcB*, *abcC*, *abcD*, *abcE, atrF*, *mdr1*, *mdr4*, and *AFUA_5G02260*), four major facilitator superfamily (MFS) transporters (*AFUA_2G11580*, *mfs56*, *mfsA* and *mfsC*), the 14-alpha sterol demethylase *cyp51A,* and 16 transcription factors (*ace1, AFUA_1G02870, AFUA_1G04140, AFUA_1G16460, AFUA_2G01190, AFUA_3G09130, AFUA_4G06170, AFUA_4G13600, AFUA_5G02655, AFUA_5G06350, AFUA_5G07510, AFUA_6G01960, AFUA_6G03430, AFUA_7G03910, AFUA_8G07360*, and *fumR*) were overexpressed following itraconazole exposure [21,35]. Similarly, five ABC transporters (*mdr1*, *abcB*, *abcC*, *abcD* and *abcE*), three

MFS multidrug transporters (*mfsA*, *mfsB* and *mfsC*), a F-box domain protein (*fbpA*), an AAA-family ATPase (*aaaA*), a C6 zinc finger domain protein (*finA*), a BZIP transcription factor (*cpcA*), and a putative C2H2 zinc-finger transcription factor (*zfpA)* were overexpressed with voriconazole exposure [38].

Table 2.2. Overexpressed genes associated with triazole exposure in *A. fumigatus* from previous RT-qPCR and RNA-seq studies.

Overexpressed Gene Name	Encoded Protein	Fold Change When Exposed to Itraconazole	Fold Change When Exposed to Voriconazole	Reference
abcA-1 (AFUA_1G17440)	ABC multidrug transporter	7.1	NA	[25]
abcA-2 (AFUA_2G15130)		~6.50	NA	[25]
abcB (AFUA_1G10390)		~4.50	~5.00 – 13.00	[25,38]
abcC (AFUA_1G14330)		~5.50	~5.00 – >20.00	[25,38]
abcD (AFUA_6G03470)		~4.50	~2.00 – >20.00	[25,38]
abcE (AFUA_7G00480)		~1.00	~2.00 – >20.00	[25,38]
atrF (AFUA_6G04360)		31.7	NA	[25]
mdr1 (AFUA_5G06070)		~5.00	~2.00 – 5.00	[25,38]
mdr4 (AFUA_1G12690)		~4.70	NA	[25]
AFUA_5G02260	ABC multidrug transporter, putative	~4.90	NA	[25]
AFUA_2G11580	MFS multidrug transporter, putative	14.2	NA	[25]
mfs56 (AFUA_1G05010)		~4.50–700.00	NA	[25]
mfsA (AFUA_8G05710)	MFS multidrug transporter	~4.70	~1.50 – 11.00	[25,38]
mfsB (AFUA_1G15490)		NA	~4.00 – 18.00	[38]
mfsC (AFUA_1G03200)		~7.90	~2.50 – 30.00	[25,38]
cyp51A (AFUA_4G06890)	14-alpha sterol demethylase	21.00–550.90	NA	[25]
fbpA (AFUA_1G14050)	F-box domain protein	NA	~ >50.00 – 600.00	[38]
aaaA (AFUA_7G06680)	AAA-family ATPase, putative	NA	~2.00 – 90.00	[38]
finA (AFUA_8G05800)	C6 zinc finger domain protein	NA	~4.00 – 40.00	[38]
AFUA_1G02870	Transcription factor involved in oxidative stress response, putative	2.48–2.61	NA	[39]
AFUA_1G04140	C6 finger domain protein, putative	2.04–2.94	NA	[39]
AFUA_6G01960		2.01–3.02	NA	[39]

AFUA_6G03430		2.78–2.93	NA	[39]
fumR *(AFUA_8G00420)*	C6 zinc finger transcription factor	4.00–4.70	NA	[39]
AFUA_5G07510		2.39–3.50	NA	[39]
AFUA_3G09130	C6 transcription factor, putative	1.73–2.22	NA	[39]
AFUA_8G07360		1.90–1.92	NA	[39]
cpcA *(AFUA_4G12470)*	BZIP transcription factor	NA	>1.50 – ~5.50	[38]
AFUA_1G16460	BZIP transcription factor (LziP), putative	1.75–2.12	NA	[39]
AFUA_7G03910	C2H2 zinc finger protein	2.50–2.86	NA	[39]
ace1 *(AFUA_3G08010)*	C2H2 zinc-finger transcription factor, putative	1.66–2.32	NA	[39]
AFUA_4G13600		2.30–2.71	NA	[39]
zfpA *(AFUA_8G05010)*		NA	~1.50 – 60.00	[38]
AFUA_2G01190	Cu-dependent DNA-binding protein, putative	1.30–2.10	NA	[39]
AFUA_4G06170	Predicted DNA-binding transcription factor	3.79–3.89	NA	[39]
AFUA_5G02655		2.75–3.84	NA	[39]
ada *(AFUA_5G06350)*	DNA repair and transcription factor, putative	1.23–2.05	NA	[39]

A summary of the overexpressed genes and specific fold changes, revealed in previous studies by RT-qPCR and RNA-seq during triazole exposure, are detailed in Table 2.2. Using these studies, a total of 37 overexpressed genes with triazole exposure were identified for further investigation. However, subsequent analysis excluded *cyp51A*-related mutations as they have already been extensively searched and discussed in Section 2.4.2.

We identified SNPs in these 37 overexpressed genes and their neighbouring intergenic regions using the soft-filtered vcf file. A total of 3230 SNP sites were identified in these overexpressed genes from our dataset. Using the same procedure as that used for the 22 known mutation sites, we identified SNPs significantly associated with itraconazole-resistance and pan-azole resistance in these 36 overexpressed genes. Multiple Fisher's Exact tests, with a Bonferroni-corrected threshold of 1.55×10^{-5} (0.05/3230), were conducted on these sites.

Using a MIC threshold of 2 mg/L and all 122 strains, we found 57 SNPs and 11 SNPs to be significantly associated with itraconazole and pan-azole resistance, respectively (Table S2.3). For itraconazole, these SNPs were located in or beside 14 genes: *abcC* (n = 9), *abcD* (n = 1), *abcE* (n = 8), *fbpA* (n = 1), *fum*R (n = 1), *mfsA* (n = 5), *mfsB* (n = 1), *mfsC* (n = 1),

AFUA_1G16460 (n = 6), *AFUA_2G01190* (n = 1), *AFUA_4G13600* (n = 3), *AFUA_5G02655* (n = 5), *AFUA_6G01960* (n = 9), and *AFUA_6G03430* (n = 6). Among these 57 SNPs, 46 were found in intergenic or intronic regions, two were non-coding transcript variants, eight were synonymous variants, and one was a missense variant (Table S2.3). For pan-azole resistance, the 11 associated SNPs were located in or beside six genes: *mfsA* (n = 1), *mfsB* (n = 1), *AFUA_2G01190* (n = 1), *AFUA_4G06170* (n = 1), *AFUA_4G13600* (n = 3), and *AFUA_6G03430* (n = 4). The 11 SNPs comprised of 10 intergenic variants and one missense variant. Next, using the MIC threshold of 4 mg/L as the resistance cut-off, we found 57 SNPs and 10 SNPs to be significantly associated with itraconazole and pan-azole resistance, respectively (Table S2.3). When compared to the previous results obtained using a MIC threshold of 2 mg/L, two variants were no longer significantly associated with pan-azole resistance: a missense variant in *mfsA* and an intergenic variant in *mfsB*. Furthermore, a newly found synonymous variant in *AFUA_1G04140* was significantly associated with pan-azole resistance using the MIC threshold of 4 mg/L (Table S2.3).

Fisher's Exact tests were also conducted after removal of the 21 strains containing the L98H mutation in *cyp51A*. Using both MIC resistance thresholds of 2 mg/L and 4 mg/L, three SNPs were found to be significantly associated with itraconazole resistance (Table S2.3). The three SNPs consisted of the previously found intergenic variant in *mfsB,* and two novel intergenic variants—one in *AFUA_6G01960* and the second in *AFUA_6G01960* (Table S2.3). No SNPs were found to be significantly associated with pan-azole resistance.

A third set of Fisher's Exact tests were conducted after removal of the 64 strains containing the mutations in *cyp51A* and using both MIC thresholds. Using the MIC resistance thresholds of 4 mg/L, one SNP was found to be significantly associated with pan-azole resistance. This SNP was found in the intergenic region of *abcA* (Table S2.3).

A final set of Fisher's Exact tests was completed and focused solely on strains from Clade II (n = 71). Using both MIC resistance thresholds, 2 mg/L and 4 mg/L, no SNPs were found to be significantly associated with itraconazole and/or pan-azole resistance in this sample set.

2.4.4. Genome-Wide Association Study

In addition to examining known triazole resistance mutations and SNPs in genes overexpressed during triazole exposure, a genome-wide association study (GWAS) was performed on the 122 and 123 strains with known itraconazole and voriconazole MIC values to investigate potential novel mutations associated with triazole sensitivity. The results of our analyses are summarized in Figure 2.2. Specifically, the itraconazole GWAS Manhattan plot can be found in Figure 2.2A and for voriconazole, in Figure 2.2B. The generated quantile–quantile plots for the GWAS results displayed no systematic inflation in our samples (Figure S2.1A,B).

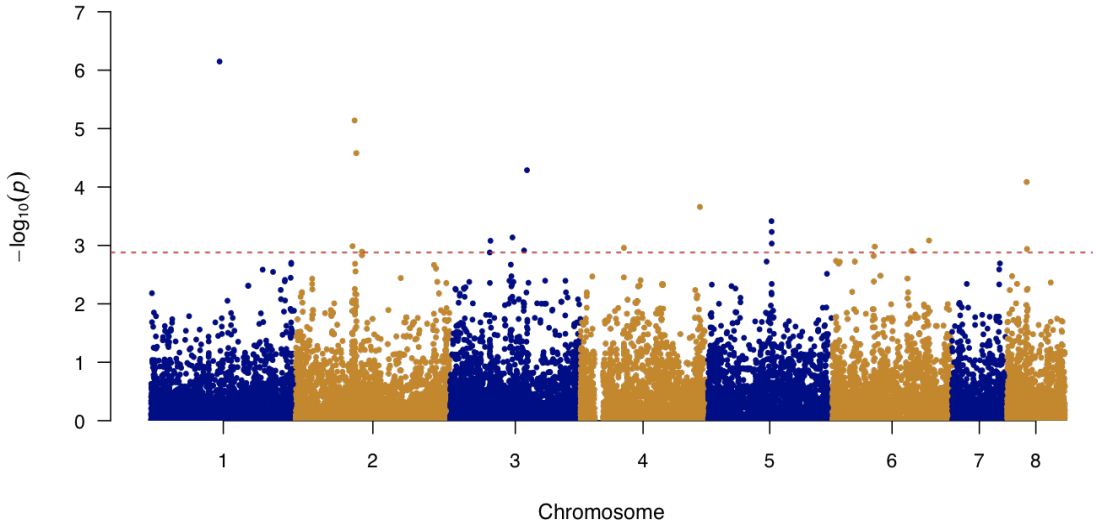

(**A**)

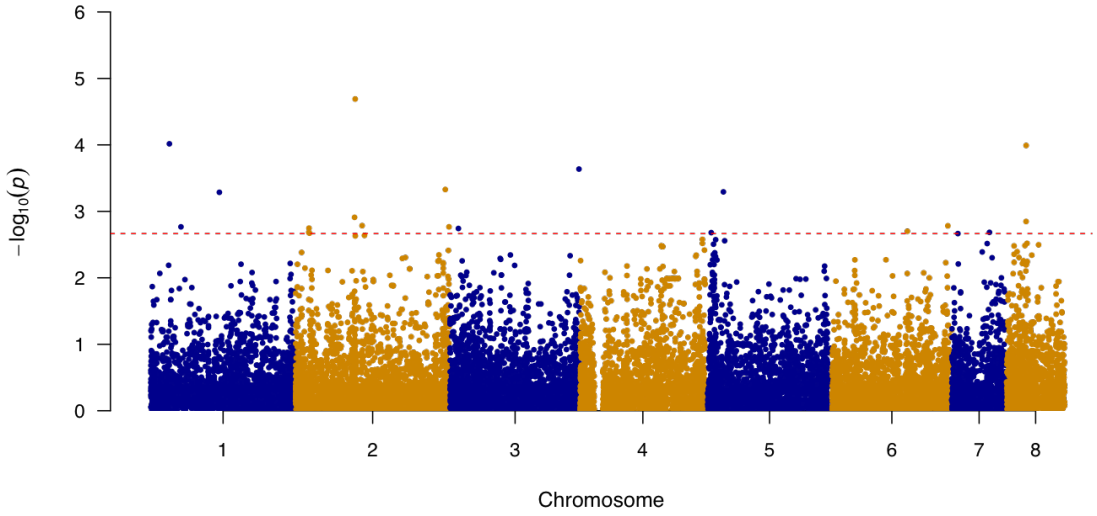

(**B**)

Figure 2.2. The Manhattan plot showing genome-wide SNPs associated with triazole resistance in *A. fumigatus*. (**A**) SNPs associated with itraconazole resistance in *A. fumigatus* isolates (n=122) and (**B**) SNPs associated with voriconazole resistance in *A. fumigatus* isolates (n=123). The top 20 SNPs in each analysis are separated out by the red dashed line. The plot is depicted with chromosome position on the X-axis and the $-\log_{10}$(p-value) on the Y-axis.

We further examined the top 20 significant SNPs identified by the GWAS analysis. Among the 20 SNPs obtained from the itraconazole GWAS, 13 (65%) were located in intergenic regions and 7 (35%) within protein-coding regions (Table 2.3). These seven SNPs consisted

of five missense variants, one synonymous variant, and one non-coding transcript variant (Table 2.3). In terms of the top 20 SNPs found from the voriconazole GWAS, 10 (50%) were found in intergenic regions and the remaining 10 in coding regions (Table 2.4). These 10 coding-region SNPs consist of four missense variants, five synonymous variants, and one non-coding transcript variant (Table 2.4). Among the top 20 SNPs associated with each of the two drugs, only one was shared. This variant was a missense A to C mutation at the position 2,538,614 on chromosome 1, in the gene AFUA_1G09780. The remaining 38 SNPs were unique to each of the two triazole drugs.

Table 2.3. Top 20 significant SNPs obtained from the GWAS that were associated with itraconazole resistance, arranged based on their -$\log_{10}$(p-values) from the highest to lowest.

Chromosome	Position (bp)	Change	$-\log_{10}$(*p*-value)	Gene ID	Annotation	Predicted Effect
1	2,538,614	A to C	6.15	*AFUA_1G09780*	Stomatin family protein	Missense Variant (Asp418Ala)
2	1,845,323	C to T	5.14	*AFUA_2G06330 - AFUA_2G07340*	Ubiquitin C-terminal hydrolase, putative—COP9 subunit 3, putative	Intergenic Region
2	1,899,353	C to T	4.58	*AFUA_2G07430 - AFUA_2G07440*	DDHD domain protein—Thioesterase family protein	Intergenic Region
3	2,408,041	T to C	4.29	*AFUA_3G09400 - AFUA_3G09450*	MFS transporter (Hol1), putative—Alpha/beta fold family hydrolase, putative	Intergenic Region
8	623,331	G to T	4.09	*AFUA_8G02330*	Endoglucanase, putative	Non-coding Transcript Variant
4	3,737,973	C to T	3.66	*AFUA_4G14300 - AFUA_4G14310*	Dynamin family GTPase, putative—APH domain-containing protein	Intergenic Region
5	2,063,521	C to A	3.42	*AFUA_5G08150*	ABC bile acid transporter, putative	Missense Variant (His105Gln)
5	2,069,483	G to A	3.23	*AFUA_5G08160 - AFUA_5G08170*	Cyclin, putative—Autophagy-related protein 3 (Atg3)	Intergenic Region
3	1,953,910	G to A	3.14	*AFUA_3G07730 - AFUA_3G07740*	Uncharacterized protein—Uncharacterized protein	Intergenic Region
6	3,054,001	C to G	3.08	*AFUA_6G12145 - AFUA_6G12150*	Uncharacterized protein—BZIP transcription factor (Atf7), putative	Intergenic Region
3	1,266,358	A to G	3.08	*AFUA_3G04310 - AFUA_3G05320*	SnoRNA binding protein, putative—C2H2 finger domain protein, putative	Intergenic Region
5	2,069,698	A to G	3.03	*AFUA_5G08160 - AFUA_5G08170*	Cyclin, putative—Autophagy-related protein 3 (Atg3)	Intergenic Region
2	1,781,938	G to A	2.99	*AFUA_2G06205 - AFUA_2G06220*	Yippee family protein—Zinc knuckle domain protein	Intergenic Region
6	1,353,971	T to C	2.98	*AFUA_6G06350 - AFUA_6G06360*	Proteasome subunit alpha type 3, putative—Mating alpha-pheromone (PpgA)	Intergenic Region
4	1,363,615	T to C	2.96	*AFUA_4G04820 - AFUA_4G05830*	C-4 methyl sterol oxidase (Erg25), putative—Methylthioribose-1-phosphate isomerase (Mri1)	Intergenic Region

8	635,137	A to G	2.94	*AFUA_8G02350*	Polyketide synthase, putative	Missense Variant (Thr1206Ala)
3	2,316,978	A to G	2.91	*AFUA_3G09090*	RING finger domain protein	Missense Variant (Glu298Gly)
6	2,508,121	A to G	2.91	*AFUA_6G10140 - AFUA_6G10150*	C6 transcription factor, putative—Uncharacterized protein	Intergenic Region
2	2,074,852	A to C	2.89	*AFUA_2G08060*	Involucrin repeat protein	Missense Variant (Lys779Thr)
2	2,080,579	T to C	2.89	*AFUA_2G08060*	Involucrin repeat protein	Synonymous Variant (His2640His)

Table 2.4. Top 20 significant SNPs obtained from the GWAS that were associated with voriconazole resistance.

Chromosome	Position (bp)	Change	$-\log_{10}(p\text{-value})$	Gene ID	Annotation	Predicted Effect
2	1,870,902	G to A	4.69	*AFUA_2G06330 - AFUA_2G07340*	Ubiquitin carboxyl-terminal hydrolase—COP9 subunit 3, putative	Intergenic Region
1	975,914	G to A	4.02	*AFUA_1G03370*	Uncharacterized protein	Missense Variant (Ser174Asn)
8	613,458	G to A	3.99	*AFUA_8G02290 - AFUA_8G02300*	Uncharacterized protein—FMN-dependent dehydrogenase family protein	Intergenic Region
3	4,040,199	T to C	3.64	*AFUA_3G15350 - AFUA_3G15380*	Short chain dehydrogenase family protein, putative—MFS multidrug transporter, putative	Intergenic Region
2	4,689,008	C to T	3.33	*AFUA_2G17600*	Conidial pigment polyketide synthase (Alb1)	Synonymous Variant (Val357Val)
5	564,519	A to C	3.29	*AFUA_5G02210*	Uncharacterized protein	Missense Variant (Met287Arg)
1	2,538,614	A to C	3.29	*AFUA_1G09780*	Stomatin family protein	Missense Variant (Asp418Ala)
2	1,851,010	G to A	2.91	*AFUA_2G06330 - AFUA_2G07340*	Ubiquitin carboxyl-terminal hydrolase—COP9 subunit 3, putative	Intergenic Region
8	611,467	C to A	2.85	*AFUA_8G02280*	C6 transcription factor, putative	Missense Variant (Glu79Asp)
2	2,087,757	C to A	2.79	*AFUA_2G08060*	Involucrin repeat protein	Non-coding Transcript Variant
6	3,648,516	T to C	2.78	*AFUA_6G14330*	5-oxo-L-prolinase, putative	Synonymous Variant (Glu131Glu)
1	1,337,273	A to G	2.77	*AFUA_1G04700 - AFUA_1G04710*	Ras guanyl-nucleotide exchange factor (RasGEF), putative—Cytoplasmic tRNA 2-thiolation protein 1	Intergenic Region
2	4,805,099	C to T	2.77	*AFUA_2G18070 - AFUA_2G18100*	Neutral protease 2—Telomere-associated RecQ helicase, putative	Intergenic Region
2	426,803	C to T	2.75	*AFUA_2G01740*	Sulfate transporter, putative	Synonymous Variant (Ala141Ala)

3	269,388	G to T	2.74	*AFUA_3G01150 - AFUA_3G01160*	GPI anchored cell wall protein, putative—Choline monooxygenase, chloroplastic	Intergenic Region
6	2,383,015	C to T	2.70	*AFUA_6G09745 - AFUA_6G09760*	Uncharacterized protein—Cytochrome P450 monooxygenase, putative	Intergenic Region
2	420,712	T to C	2.68	*AFUA_2G01710*	GPI anchored protein, putative	Synonymous Variant (Ile294Ile)
7	1,182,007	A to C	2.68	*AFUA_7G05020 - AFUA_7G05030*	Uncharacterized protein—Pectin lyase B	Intergenic Region
5	184,363	G to A	2.68	*AFUA_5G00650 - AFUA_5G00660*	Uncharacterized protein—Uncharacterized protein	Intergenic Region
2	441,695	C to T	2.67	*AFUA_2G01780*	Small nucleolar ribonucleoprotein complex subunit (Utp15), putative	Synonymous Variant (Val184Val)

Additional GWAS analyses were conducted in the same stepwise manner seen in the previous Fisher's Exact tests. Firstly, to alleviate any potential masking effect caused by the L98H mutation in *cyp51A*, the 21 strains with the L98H mutation were removed. A second GWAS, using the same previous pipeline, was then conducted. The results of the second GWAS are summarized in Figure 2.3A,B as Manhattan plots for itraconazole and voriconazole, respectively. The generated quantile–quantile plots for both GWAS results displayed no genomic inflation (Figure S2.2A,B).

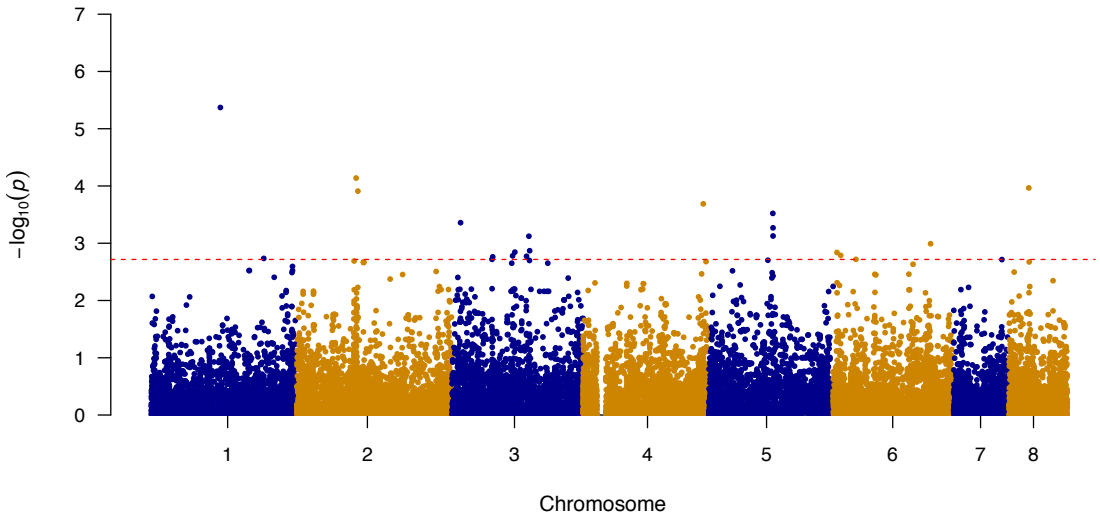

(**A**)

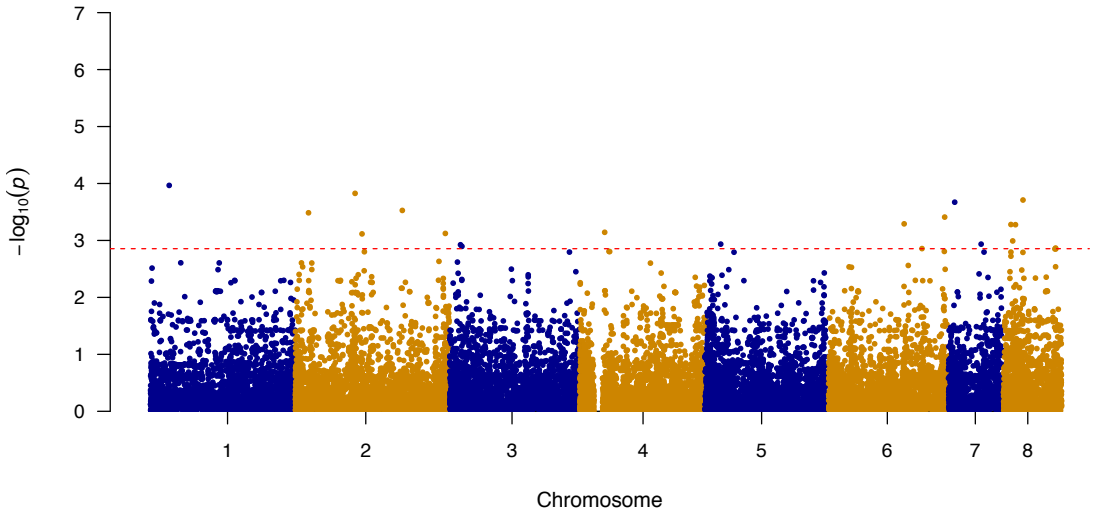

(**B**)

Figure 2.3. The Manhattan plot showing genome-wide SNPs associated with triazole resistance in *A. fumigatus* after removal of strains containing the L98H mutation in *cyp51A*. (**A**) SNPs associated with itraconazole resistance in *A. fumigatus* isolates (n=101) and (**B**) SNPs associated with voriconazole resistance in *A. fumigatus* isolates (n=102). The top 20 SNPs in each analysis are separated out by the red dashed line. The plot is depicted with chromosome position on the X-axis and the $-\log_{10}$(p-value) on the Y-axis.

The top 20 significant SNPs identified by the second GWAS analyses were examined.

Among the 20 SNPs obtained from the itraconazole GWAS, 13 (65%) were located in

intergenic regions and 7 (35%) within protein-coding regions (Table 2.5). These seven SNPs comprised of four missense variants, one synonymous variant, and two non-coding transcript variants (Table 2.5). In terms of the top 20 SNPs obtained from the second voriconazole GWAS, 10 (50%) were found in intergenic regions and the remaining 10 in coding regions (Table 2.6). These 10 coding-region SNPs consist of 5 missense variants, 3 synonymous variants, and 2 non-coding transcript variants (Table 2.6). Among the top 20 SNPs associated with each of the two drugs, none were shared between the two triazole drugs.

Table 2.5. Top 20 significant SNPs obtained from the second GWAS associated with itraconazole resistance, arranged based on their -$\log_{10}$(p-values) from the highest to lowest.

Chromosome	Position (bp)	Change	$-\log_{10}$(*p*-value)	Gene ID	Annotation	Predicted Effect
1	2,538,614	A to C	5.37	*AFUA_1G09780*	Stomatin family protein	Missense Variant (Asp418Ala)
2	1,845,323	C to T	4.14	*AFUA_2G06330-AFUA_2G07340*	Ubiquitin C-terminal hydrolase, putative – COP9 subunit 3, putative	Intergenic Region
8	623,331	G to T	3.96	*AFUA_8G02330*	Endoglucanase, putative	Non-coding Transcript Variant
2	1,899,353	C to T	3.91	*AFUA_2G07430-AFUA_2G07440*	DDHD domain protein – Thioesterase family protein	Intergenic Region
4	3,737,973	C to T	3.69	*AFUA_4G14300-AFUA_4G14310*	Dynamin family GTPase, putative – APH domain-containing protein	Intergenic Region
5	2,063,521	C to A	3.52	*AFUA_5G08150*	ABC bile acid transporter, putative	Missense Variant (His105Gln)
*3	267,884	T to G	3.36	*AFUA_3G01140-AFUA_3G01150*	Uncharacterized protein – GPI anchored cell wall protein, putative	Intergenic Region
5	2,069,483	G to A	3.27	*AFUA_5G08160-AFUA_5G08170*	Cyclin, putative – Autophagy-related protein 3 (Atg3)	Intergenic Region
5	2,069,698	A to G	3.13	*AFUA_5G08160-AFUA_5G08170*	Cyclin, putative – Autophagy-related protein 3 (Atg3)	Intergenic Region
*3	2,389,222	G to A	3.12	*AFUA_3G09400-AFUA_3G09450*	MFS transporter (Hol1), putative – Alpha/beta fold family hydrolase, putative	Intergenic Region
6	3,054,001	C to G	2.99	*AFUA_6G12145-AFUA_6G12150*	Uncharacterized protein – BZIP transcription factor (Atf7), putative	Intergenic Region
*3	2,414,011	A to G	2.87	*AFUA_3G09480*	15-hydroxyprostaglandin dehydrogenase (NAD(+))	Synonymous Variant (Ser60Ser)
3	1,953,910	G to A	2.84	*AFUA_3G07730-AFUA_3G07740*	Uncharacterized protein – Uncharacterized protein	Intergenic Region
*6	145,947	T to C	2.84	*AFUA_6G00570-AFUA_6G00580*	Uncharacterized protein – Ankyrin repeat protein	Intergenic Region
*6	262,795	G to A	2.79	*AFUA_6G01860*	MFS lactose permease, putative	Missense Variant (Val106Met)

*3	1,883,390	C to A	2.78	*AFUA_3G07510-AFUA_3G07520*	Uncharacterized protein – Exo-beta-1,3-glucanase, putative	Intergenic Region
3	2,316,978	A to G	2.77	*AFUA_3G09090*	RING finger domain protein	Missense Variant (Glu298Gly)
3	1,266,358	A to G	2.76	*AFUA_3G04310-AFUA_3G05320*	SnoRNA binding protein, putative – C2H2 finger domain protein, putative	Intergenic Region
*1	3,885,980	G to A	2.74	*AFUA_1G14540*	Oxidoreductase, short-chain dehydrogenase/reductase family	Non-coding Transcript Variant
*6	734,136	G to T	2.72	*AFUA_6G03400-AFUA_6G03430*	Uncharacterized protein – C6 finger transcription factor (FsqA)	Intergenic Region

Unique SNP sites are denoted by asterisks "*" (n = 8).

Table 2.6. Top 20 significant SNPs obtained from the second GWAS associated with voriconazole resistance, arranged based on their -$\log_{10}$(p-values) from the highest to lowest.

Chromosome	Position (bp)	Change	$-\log_{10}$(*p*-value)	Gene ID	Annotation	Predicted Effect
1	975,914	G to A	3.97	*AFUA_1G03370*	Uncharacterized protein	Missense Variant (Ser174Asn)
2	1,870,902	G to A	3.83	*AFUA_2G06330-AFUA_2G07340*	Ubiquitin carboxyl-terminal hydrolase – COP9 subunit 3, putative	Intergenic Region
8	613,458	G to A	3.71	*AFUA_8G02290-AFUA_8G02300*	Uncharacterized protein – FMN-dependent dehydrogenase family protein	Intergenic Region
*7	195,144	A to G	3.67	*AFUA_7G00740*	Protein kinase, putative	Missense Variant (Ile188Val)
*2	3,345,583	A to G	3.53	*AFUA_2G13030*	Phenylalanyl-tRNA synthetase	Missense Variant (Asp343Gly)
*2	416,242	C to T	3.49	*AFUA_2G01700*	Carbon catabolite derepressing protein kinase (Snf1), putative	Non-coding Transcript Variant
6	3,648,516	T to C	3.41	*AFUA_6G14330*	5-oxo-L-prolinase, putative	Synonymous Variant (Glu131Glu)
6	2,383,015	C to T	3.29	*AFUA_6G09745-AFUA_6G09760*	Uncharacterized protein – Cytochrome P450 monooxygenase, putative	Intergenic Region
*8	237,297	T to G	3.28	*AFUA_8G01030-AFUA_8G01050*	Uncharacterized protein – Lipase/esterase, putative	Intergenic Region
*8	379,123	C to T	3.28	*AFUA_8G01480-AFUA_8G01490*	Potassium channel, putative – Endoglucanase, putative	Intergenic Region
*4	776,628	A to G	3.14	*AFUA_4G02800-AFUA_4G02805*	Haemolysin-III family protein – Asp hemolysin-like protein	Intergenic Region
2	4,689,008	C to T	3.12	*AFUA_2G17600*	Conidial pigment polyketide synthase (Alb1)	Synonymous Variant (Val357Val)
2	2,087,757	C to A	3.12	*AFUA_2G08060*	Involucrin repeat protein	Non-coding Transcript Variant
*8	292,607	C to T	2.99	*AFUA_8G01250*	GNAT family acetyltransferase, putative	Missense Variant (Arg134Cys)
5	564,519	A to C	2.94	*AFUA_5G02210*	Uncharacterized protein	Missense Variant (Met287Arg)
*7	1,019,801	A to G	2.94	*AFUA_7G04470-AFUA_7G04480*	Uncharacterized protein – DNA mismatch repair protein (Msh3)	Intergenic Region

*3	341,035	T to A	2.92	*AFUA_3G01370-AFUA_3G01400*	MFS transporter, putative – ABC multidrug transporter, putative	Intergenic Region
*3	386,560	T to C	2.90	*AFUA_3G01520*	MFS multidrug transporter, putative	Synonymous Variant (Val170Val)
*8	1,631,284	G to A	2.87	*AFUA_8G06690-AFUA_8G06700*	Cytochrome P450 alkane hydroxylase – Annexin	Intergenic Region
*6	2,940,890	T to C	2.86	*AFUA_6G11780-AFUA_6G11790*	Uncharacterized protein – Uncharacterized protein	Intergenic Region

Unique SNP sites are denoted by asterisks "*" (n = 12).

A third set of GWAS analyses was also done to alleviate any potential masking effect caused by the known mutations in *cyp51A,* previously listed in Table 2.1. The 64 strains with *cyp51A* mutations were removed and the third GWAS, using the same previous pipeline, was then conducted. The results of the third GWAS are summarized in Figure 2.4A,B as Manhattan plots for itraconazole and voriconazole, respectively. The generated quantile–quantile plots for both GWAS results displayed no genomic inflation (Figure S2.3A,B).

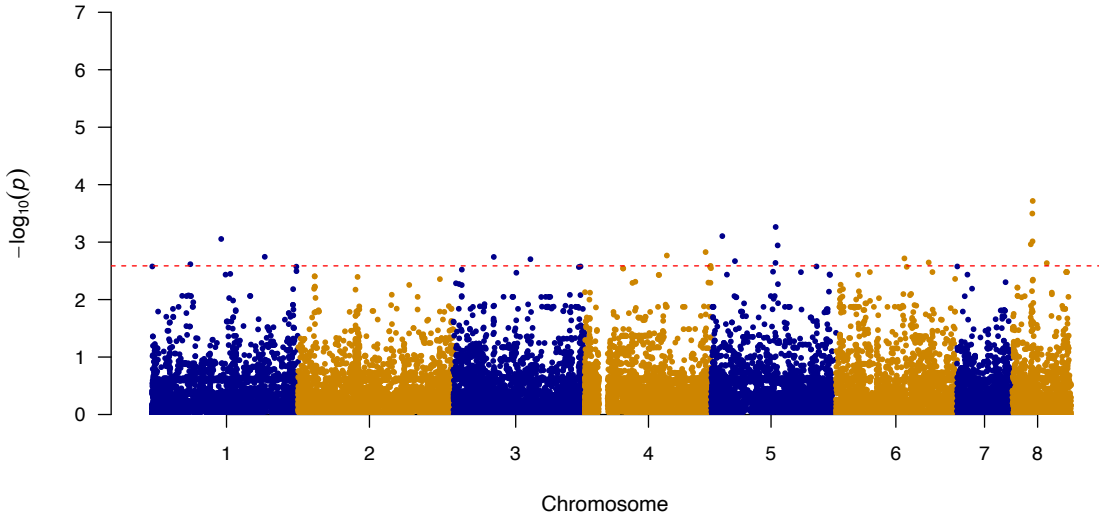

(**A**)

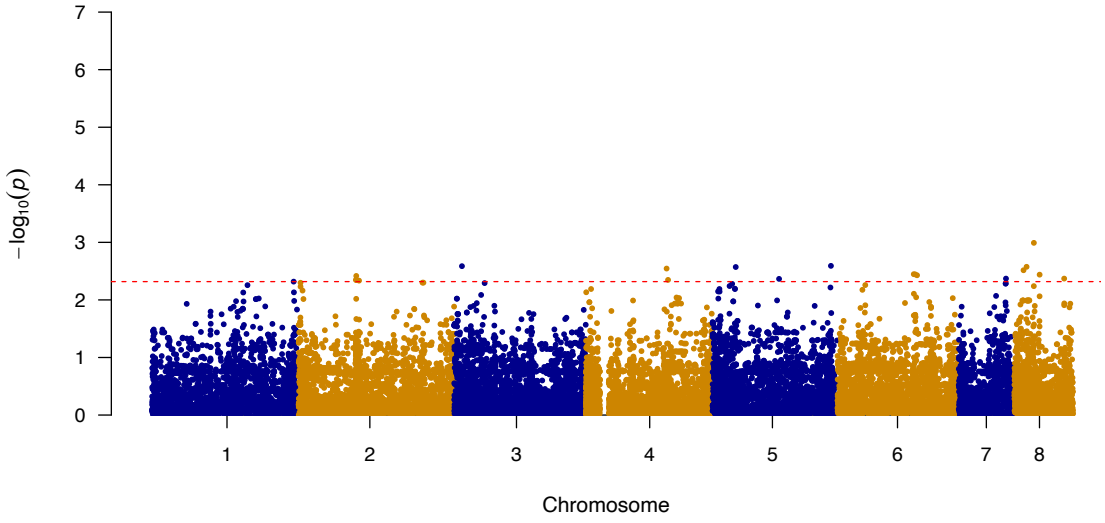

(**B**)

Figure 2.4. The Manhattan plot showing genome-wide SNPs associated with triazole resistance in *A. fumigatus* after removal of strains containing the mutations in *cyp51A*. (**A**) SNPs associated with itraconazole resistance in *A. fumigatus* isolates (n=58) and (**B**) SNPs associated with voriconazole resistance in *A. fumigatus* isolates (n=59). The top 20 SNPs in each analysis are separated out by the red dashed line. The plot is depicted with chromosome position on the X-axis and the $-\log_{10}$(p-value) on the Y-axis.

The top 20 significant SNPs identified by the third GWAS analyses were examined. Among the top 20 SNPs obtained from the itraconazole GWAS, 11 (55%) were located in intergenic

regions and 9 (45%) within protein-coding regions (Table 2.7). These nine SNPs comprised of three missense variants, two synonymous variants, three non-coding transcript variants and one intragenic variant (Table 2.7). In terms of the top 20 SNPs obtained from the third voriconazole GWAS, 10 (50%) were found in intergenic regions and the remaining 10 in coding regions (Table 2.8). These 10 coding-region SNPs consist of six missense variants and four synonymous variants (Table 2.8). Among the top 20 SNPs associated with each of the two drugs, two SNPS were shared between the two triazole drugs. The first variant was a synonymous C to A mutation at the position 2,539,714 on chromosome 4, in the gene *AFUA_4G09770*. The second mutation was a synonymous T to C mutation at position 2,131,740 of chromosome 5, in the gene *AFUA_5G08390*.

Table 2.7. Top 20 significant SNPs obtained from the third GWAS associated with itraconazole resistance, arranged based on their -$\log_{10}$(p-values) from the highest to lowest.

Chromosome	Position (bp)	Change	$-\log_{10}$(*p*-value)	Gene ID	Annotation	Predicted Effect
8	635,137	A to G	3.72	*AFUA_8G02350*	Polyketide synthase (PKS), putative	Missense Variant (Thr1206Ala)
8	623,331	G to T	3.50	*AFUA_8G02330*	Endoglucanase, putative	Non-coding Transcript Variant
5	2,069,698	A to G	3.26	*AFUA_5G08160-AFUA_5G08170*	Cyclin, putative—Autophagy-related protein 3 (Atg3)	Intergenic Region
*5	419,750	A to G	3.11	*AFUA_5G01640-AFUA_5G01650*	Ankyrin repeat protein—bZIP transcription factor (JlbA), putative	Intergenic Region
1	2,538,614	A to C	3.06	*AFUA_1G09780*	Stomatin family protein	Missense Variant (Asp418Ala)
*8	629,524	G to T	3.01	*AFUA_8G02340-AFUA_8G02350*	Uncharacterized protein—Polyketide synthase, putative	Intergenic Region
*8	576,158	T to C	2.96	*AFUA_8G02210-AFUA_8G02220*	Alpha-ketoglutarate-dependent taurine dioxygenase—Uncharacterized protein	Intergenic Region
*5	2,131,740	T to C	2.94	*AFUA_5G08390*	Response regulator, putative (Ssk1)	Synonymous Variant (Lys532Lys)
4	3,737,973	C to T	2.83	*AFUA_4G14300-AFUA_4G14310*	Dynamin family GTPase, putative—APH domain-containing protein	Intergenic Region
*4	2,539,714	C to A	2.77	*AFUA_4G09770*	Velvet domain-containing protein	Synonymous Variant (Leu193Leu)
1	3,885,980	G to A	2.74	*AFUA_1G14540*	Oxidoreductase, short-chain dehydrogenase/reductase family	Non-coding Transcript Variant
*3	1,256,445	T to A	2.74	*AFUA_3G04310-AFUA_3G05320*	SnoRNA binding protein, putative—C2H2 finger domain protein, putative	Intergenic Region

*6	2,141,290	T to C	2.72	*AFUA_6G09000-AFUA_6G09010*	PHD finger domain protein, putative—U1 snRNP splicing complex subunit (Luc7), putative	Intergenic Region
3	2,389,222	G to A	2.70	*AFUA_3G09400-AFUA_3G09450*	MFS transporter (Hol1), putative—Alpha/beta fold family hydrolase, putative	Intergenic Region
*5	810,835	T to C	2.67	*AFUA_5G03020-AFUA_5G03030*	6 0S ribosomal protein L4, putative—C6 transcription factor, putative	Intergenic Region
*6	2,891,637	A to G	2.65	*AFUA_6G11620-AFUA_6G11630*	Formyltetrahydrofolate deformylase, putative—FAD-dependent isoamyl alcohol oxidase, putative	Intergenic Region
5	2,063,521	C to A	2.64	*AFUA_5G08150*	ABC bile acid transporter, putative	Missense Variant (His105Gln)
*8	1,069,676	A to G	2.63	*AFUA_8G04680*	Oxidoreductase, short-chain dehydrogenase/reductase family, putative	Non-coding Transcript Variant
*1	1,585,001	C to T	2.62	*AFUA_1G00410*	C6 transcription factor, putative	Intragenic Variant
*4	3,891,318	A to C	2.59	*AFUA_4G14751-AFUA_4G14770*	Uncharacterized protein—Protostadienol synthase (HelA)	Intergenic Region

Unique SNP sites compared to the previous two GWAS analyses are denoted by asterisks "*" (n = 12).

Table 2.8. Top 20 significant SNPs obtained from the third GWAS associated with voriconazole resistance, arranged based on their -$\log_{10}$(p-values) from the highest to lowest.

Chromosome	Position (bp)	Change	$-\log_{10}$(*p*-value)	Gene ID	Annotation	Predicted Effect
8	613,458	G to A	2.99	*AFUA_8G02290-AFUA_8G02300*	Uncharacterized protein—FMN-dependent dehydrogenase family protein	Intergenic Region
*5	3,732,385	G to A	2.59	*AFUA_5G14315*	Uncharacterized protein	Synonymous Variant (Phe212Phe)
*3	246,050	C to A	2.59	*AFUA_3G01060-AFUA_3G01070*	Uncharacterized protein—Tyrosinase, putative	Intergenic Region
*8	388,274	G to A	2.58	*AFUA_8G01510-AFUA_8G01520*	Uncharacterized protein—Pectinesterase	Intergenic Region
*5	794,519	G to T	2.57	*AFUA_5G02970*	LCCL domain protein	Synonymous Variant (Thr24Thr)
*4	2,494,977	G to C	2.55	*AFUA_4G09580*	Major allergen (Aspf2)	Missense Variant (Gly276Ala)
*8	293,836	G to A	2.52	*AFUA_8G01260*	Uncharacterized protein	Synonymous Variant (Pro383Pro)
*6	2,379,483	T to C	2.45	*AFUA_6G09745-AFUA_6G09760*	Uncharacterized protein—Cytochrome P450 monooxygenase, putative	Intergenic Region
*6	2,424,223	C to A	2.44	*AFUA_6G09870*	C6 transcription factor, putative	Missense Variant (Val360Phe)
*8	791,268	A to G	2.44	*AFUA_8G02870-AFUA_8G03870*	Uncharacterized protein—Uncharacterized protein	Intergenic Region

*6	2,480,554	C to T	2.43	*AFUA_6G10050-AFUA_6G10060*	Small oligopeptide transporter, OPT family—F-actin-capping protein subunit alpha	Intergenic Region
*2	1,785,216	G to A	2.42	*AFUA_2G06205-AFUA_2G06220*	Yippee family protein—Zinc knuckle domain protein	Intergenic Region
*7	1,458,738	C to G	2.37	*AFUA_7G05960*	C2H2 finger domain protein, putative	Missense Variant (Arg759Pro)
*8	1,548,514	C to T	2.37	*AFUA_8G06410*	MFS multidrug transporter, putative	Synonymous Variant (Arg17Arg)
*5	2,131,740	T to C	2.37	*AFUA_5G08390*	Response regulator, putative (Ssk1)	Synonymous Variant (Lys532Lys)
*2	1,774,354	T to C	2.35	*AFUA_2G06205-AFUA_2G06220*	Yippee family protein—Zinc knuckle domain protein	Intergenic Region
*4	2,539,714	C to A	2.35	*AFUA_4G09770*	Velvet domain-containing protein	Synonymous Variant (Leu193Leu)
*2	1,787,001	C to T	2.35	*AFUA_2G06205-AFUA_2G06220*	Yippee family protein—Zinc knuckle domain protein	Intergenic Region
2	1,870,902	G to A	2.34	*AFUA_2G06330-AFUA_2G07340*	Ubiquitin carboxyl-terminal hydrolase—COP9 subunit 3, putative	Intergenic Region
*1	4,762,609	A to G	2.32	*AFUA_1G17410*	Beta-glucosidase, putative	Missense Variant (Val287Ala)

Unique SNP sites compared to the previous two GWAS analyses are denoted by asterisks "*" (n = 18).

A final set of GWAS was completed to focus our analysis on a clade-level, using strains from Clade II. The strains from Clade II with itraconazole (n = 71) and voriconazole (n = 72) MIC values were used for the fourth GWAS, using the same previous pipelines. The results of this GWAS are summarized in Figure 2.5A,B as Manhattan plots for itraconazole and voriconazole, respectively. The generated quantile–quantile plots for both GWAS results displayed no genomic inflation (Figure S2.4A,B).

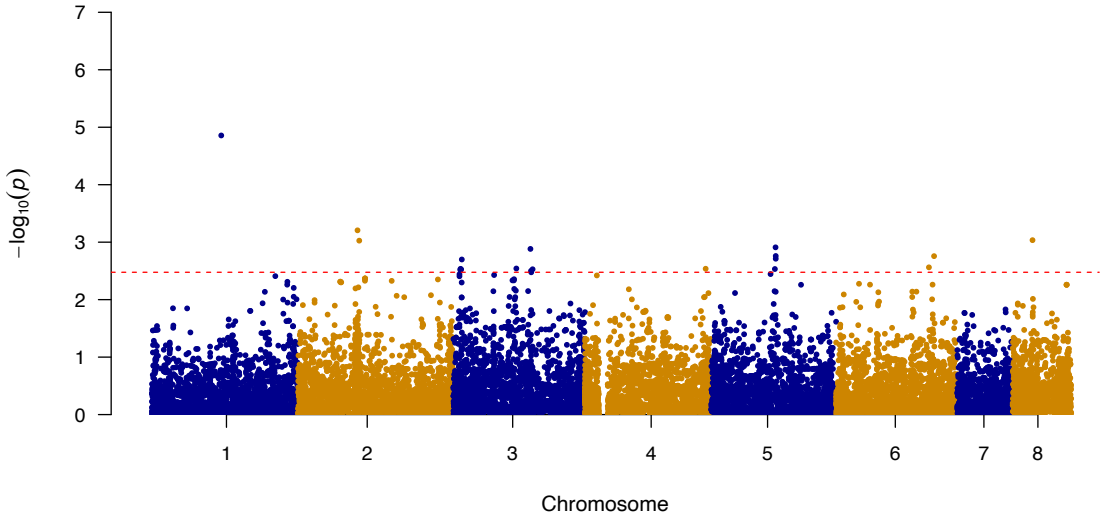

(**A**)

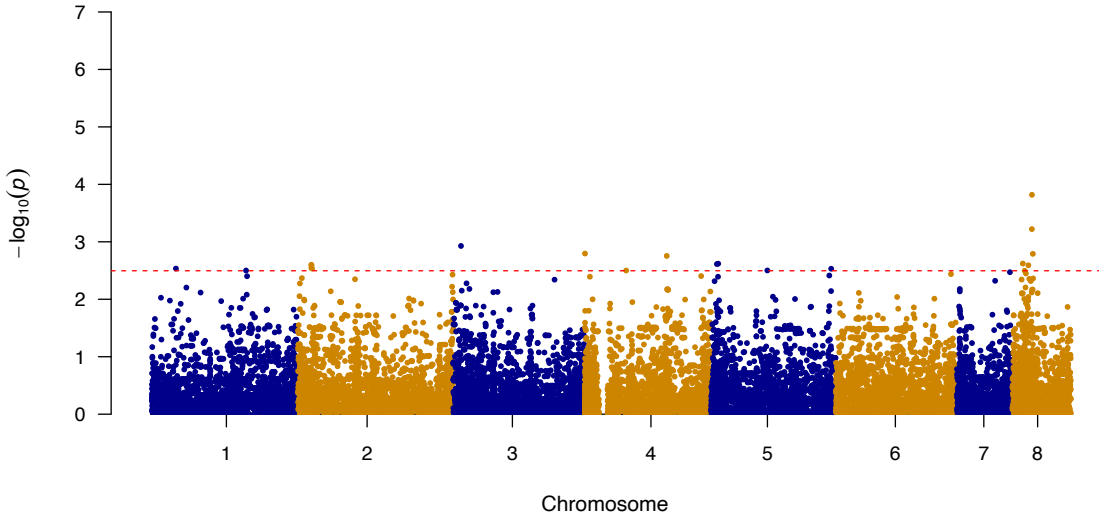

(**B**)

Figure 2.5. The Manhattan plot showing genome-wide SNPs associated with triazole resistance in *A. fumigatus* in Clade II (**A**) SNPs associated with itraconazole resistance in *A. fumigatus* isolates (n=71) and (**B**) SNPs associated with voriconazole resistance in *A. fumigatus* isolates (n=72). The top 20 SNPs in each analysis are separated out by the red dashed line. The plot is depicted with chromosome position on the X-axis and the $-\log_{10}$(p-value) on the Y-axis.

The top 20 significant SNPs identified by the GWAS analyses on strains from Clade II were examined. Among the top 20 SNPs obtained from the itraconazole GWAS, 15 (75%) were

located in intergenic regions and 5 (25%) within protein-coding regions (Table 2.9). These five SNPs comprised of two missense variants, two synonymous variants, and one non-coding transcript variant (Table 2.9). In terms of the top 20 SNPs obtained from the voriconazole GWAS, 6 (30%) were found in intergenic regions and the remaining 14 in coding regions (Table 2.10). These 14 coding-region SNPs consist of seven missense variants, five synonymous variants, one non-coding transcript variant and one intragenic variant (Table 2.10). Among the top 20 SNPs associated with each of the two drugs, no mutation sites were shared between the two triazole drugs.

Table 2.9. Top 20 significant SNPs obtained from the fourth GWAS associated with itraconazole resistance, arranged based on their -$\log_{10}$(p-values) from the highest to lowest.

Chromosome	Position (bp)	Change	$-\log_{10}$(*p*-value)	Gene ID	Annotation	Predicted Effect
1	2,538,614	A to C	4.86	*AFUA_1G09780*	Stomatin family protein	Missense Variant (Asp418Ala)
2	1,845,323	C to T	3.21	*AFUA_2G06330 - AFUA_2G07340*	Ubiquitin C-terminal hydrolase, putative—COP9 subunit 3, putative	Intergenic Region
8	623,331	G to T	3.04	*AFUA_8G02330*	Endoglucanase, putative	Non-coding Transcript Variant
2	1,899,353	C to T	3.03	*AFUA_2G07430 - AFUA_2G07440*	DDHD domain protein—Thioesterase family protein	Intergenic Region
5	2,063,521	C to A	2.91	*AFUA_5G08150*	ABC bile acid transporter, putative	Missense Variant (His105Gln)
3	2,389,222	G to A	2.88	*AFUA_3G09400- AFUA_3G09450*	MFS transporter (Hol1), putative—Alpha/beta fold family hydrolase, putative	Intergenic Region
5	2,069,483	G to A	2.76	*AFUA_5G08160 - AFUA_5G08170*	Cyclin, putative—Autophagy-related protein 3 (Atg3)	Intergenic Region
6	3,054,001	C to G	2.76	*AFUA_6G12145 - AFUA_6G12150*	Uncharacterized protein—BZIP transcription factor (Atf7), putative	Intergenic Region
5	2,069,698	A to G	2.71	*AFUA_5G08160 - AFUA_5G08170*	Cyclin, putative—Autophagy-related protein 3 (Atg3)	Intergenic Region
3	267,884	T to G	2.70	*AFUA_3G01140- AFUA_3G01150*	Uncharacterized protein—GPI anchored cell wall protein, putative	Intergenic Region
*6	2,895,225	T to C	2.56	*AFUA_6G11620- AFUA_6G11630*	Formyltetrahydrofolate deformylase, putative—FAD-dependent isoamyl alcohol oxidase, putative	Intergenic Region
3	1,953,910	G to A	2.54	*AFUA_3G07730 - AFUA_3G07740*	Uncharacterized protein—Uncharacterized protein	Intergenic Region
4	3,737,973	C to T	2.54	*AFUA_4G14300 - AFUA_4G14310*	Dynamin family GTPase, putative—APH domain-containing protein	Intergenic Region
*3	228,628	C to T	2.54	*AFUA_3G00970- AFUA_3G00980*	Uncharacterized protein—MFS transporter Liz1/Seo1, putative	Intergenic Region
*5	2,042,856	G to A	2.53	*AFUA_5G08050- AFUA_5G08060*	Aminopeptidase P, putative—Importin 13, putative	Intergenic Region

*3	2,456,111	A to G	2.53	*AFUA_3G09630-AFUA_3G09640*	Asparaginyl-tRNA synthetase Slm5, putative—Camp independent regulatory protein	Intergenic Region
*3	247,848	G to A	2.53	*AFUA_3G01060-AFUA_3G01070*	Uncharacterized protein—Tyrosinase, putative	Intergenic Region
*3	220,452	G to A	2.52	*AFUA_3G00930*	C6 transcription factor, putative	Synonymous Variant (Ile259Ile)
3	2,408,041	T to C	2.50	*AFUA_3G09400 - AFUA_3G09450*	MFS transporter (Hol1), putative—Alpha/beta fold family hydrolase, putative	Intergenic Region
3	2,414,011	A to G	2.48	*AFUA_3G09480*	15-hydroxyprostaglandin dehydrogenase (NAD(+))	Synonymous Variant (Ser60Ser)

Unique SNP sites compared to the previous three GWAS analyses are denoted by asterisks "*" (n = 6).

Table 2.10. Top 20 significant SNPs obtained from the fourth GWAS associated with voriconazole resistance, arranged based on their -$\log_{10}$(p-values) from the highest to lowest.

Chromosome	Position (bp)	Change	$-\log_{10}(p\text{-value})$	Gene ID	Annotation	Predicted Effect
8	613,458	G to A	3.82	*AFUA_8G02290-AFUA_8G02300*	Uncharacterized protein—FMN-dependent dehydrogenase family protein	Intergenic Region
8	611,467	C to A	3.22	*AFUA_8G02280*	C6 transcription factor, putative	Missense Variant (Glu79Asp)
3	246,050	C to A	2.93	*AFUA_3G01060-AFUA_3G01070*	Uncharacterized protein—Tyrosinase, putative	Intergenic Region
*4	12,352	G to A	2.80	Chr Start - *AFUA_4G00100*	Rhamnogalacturonase, putative	Intergenic Region
*8	641,537	T to C	2.79	*AFUA_8G02380-AFUA_8G02390*	FAD-dependent monooxygenase, putative—Uncharacterized protein	Intergenic Region
4	2,539,714	C to A	2.75	*AFUA_4G09770*	Velvet domain-containing protein	Synonymous Variant (Leu193Leu)
*8	331,435	C to A	2.62	*AFUA_8G01340*	MFS sugar transporter, putative	Missense Variant (Leu239Met)
*5	295,677	C to T	2.62	*AFUA_5G01180*	RAN small monomeric GTPase (Ran), putative	Synonymous Variant (Ser74Ser)
*5	256,650	T to C	2.61	*AFUA_5G01000*	Oxidoreductase, 2OG-Fe(II) oxygenase family, putative	Missense Variant (Ser110Pro)
*2	417,623	C to T	2.60	*AFUA_2G01700*	Carbon catabolite derepressing protein kinase (Snf1), putative	Missense Variant (Arg188Gln)
2	426,803	C to T	2.59	*AFUA_2G01740*	Sulfate transporter, putative	Synonymous Variant (Ala141Ala)
*8	503,790	C to G	2.59	*AFUA_8G01940*	C6 finger domain protein, putative	Missense Variant (Pro261Arg)
2	420,712	T to C	2.55	*AFUA_2G01710*	GPI anchored protein, putative	Synonymous Variant (Ile294Ile)

*1	1,138,713	A to G	2.53	*AFUA_1G00410*	C6 transcription factor, putative	Intragenic Variant
2	441,695	C to T	2.53	*AFUA_2G01780*	Small nucleolar ribonucleoprotein complex subunit (Utp15), putative	Synonymous Variant (Val184Val)
*5	3,788,892	C to T	2.53	*AFUA_5G14610*	Carboxypeptidase Y, putative	Missense Variant (Val254Met)
*5	1,815,994	A to G	2.50	*AFUA_5G07300-AFUA_5G07310*	Electron transfer flavoprotein, beta subunit—DUF500 domain protein	Intergenic Region
*1	3,306,670	A to C	2.50	*AFUA_1G12540*	TMEM1 family protein, putative	Missense Variant (Phe879Cys)
*4	1,285,247	G to A	2.50	*AFUA_4G04570*	Uncharacterized protein	Non-coding Transcript Variant
8	388,274	G to A	2.50	*AFUA_8G01510-AFUA_8G01520*	Uncharacterized protein—Pectinesterase	Intergenic Region

Unique SNP sites compared to the previous three GWAS analyses are denoted by asterisks "*" (n = 12).

2.4.5. Linkage Disequilibrium Analysis

Linkage disequilibrium analyses were conducted using the top 20 SNPs obtained by the four GWAS analyses and all 314,999 SNPs in the soft-filtered vcf file to search for SNPs highly linked ($R^2 > 0.85$) to these significantly associated SNPs. Specifically, we focused on highly linked non-synonymous mutations. The results of this association analysis are presented in Table 2.11 for itraconazole and in Table 2.12 for voriconazole. In total, for itraconazole resistance, we identified 15 additional highly linked missense variants located in 13 (putative) protein-coding genes (Table 2.11). For voriconazole resistance, this analysis revealed 11 additional missense SNPs located in 11 different (putative) protein coding genes (Table 2.12). None of these additional missense SNPs were shared between the two drugs.

Table 2.11. Additional non-synonymous SNPs found to be highly linked to the 46 SNP sites obtained by GWAS analyses for itraconazole.

Chromosome	Position	Gene ID	Predicted Effect (Amino Acid Substitution)	Description
2	2,079,605	*AFUA_2G08060*	Missense Variant (Ala2316Ser)	Involucrin repeat protein
2	2,083,296	*AFUA_2G08060*	Missense Variant (Asn3546Ser)	Involucrin repeat protein
2	2,086,695	*AFUA_2G08060*	Missense Variant (Val4679Ala)	Involucrin repeat protein
3	587,378	*AFUA_3G02360*	Missense Variant (Leu413Gln)	Carboxylic ester hydrolase

3	1,604,491	*AFUA_3G06490*	Missense Variant (Gln531Arg)	Uncharacterized protein
3	1,629,278	*AFUA_3G06570*	Missense Variant (Gln77Pro)	Uncharacterized protein
3	1,693,467	*AFUA_3G06800*	Missense Variant (Arg615Thr)	Uncharacterized protein
3	1,700,605	*AFUA_3G06820*	Missense Variant (Lys540Arg)	Oxidoreductase, FAD-binding
3	2,132,951	*AFUA_3G08280*	Missense Variant (Glu28Lys)	Cell cycle regulatory protein (Srw1), putative
3	2,155,356	*AFUA_3G08400*	Missense Variant (Glu393Lys)	SNF2 family helicase/ATPase, putative
3	2,304,691	*AFUA_3G09040*	Missense Variant (Ser13Leu)	Uncharacterized protein
3	2,311,362	*AFUA_3G09070*	Missense Variant (Ile406Thr)	Carboxylesterase, putative
3	2,409,306	*AFUA_3G09450*	Missense Variant (Pro220Leu)	Alpha/beta fold family hydrolase, putative
4	3,875,753	*AFUA_4G14712*	Missense Variant (Pro208Ser)	C6 transcription factor, putative
6	2,583,985	*AFUA_6G10420*	Missense Variant (Gln309Glu)	Uncharacterized protein

Table 2.12. Additional non-synonymous SNPs found to be highly linked to the 62 SNP sites obtained by GWAS analyses for voriconazole.

Chromosome	Position	Gene ID	Predicted Effect (Amino Acid Substitution)	Description
1	976,070	*AFUA_1G03370*	Missense Variant (Ser226Leu)	Uncharacterized protein
1	4,754,138	*AFUA_1G17380*	Missense Variant (Leu226Pro)	3-oxoacyl-(Acyl-carrier-protein) reductase, putative
2	437,241	*AFUA_2G01760*	Missense Variant (Thr1812Ala)	NACHT domain protein
2	541,777	*AFUA_2G02170*	Missense Variant (Ser67Pro)	Nuclear condensin complex subunit (Smc4), putative

5	205,924	*AFUA_5G00730*	Missense Variant (Val814Phe)	H /K ATPase alpha subunit, putative
5	3,290,025	*AFUA_5G12670*	Missense Variant (Phe390Ser)	Nucleoporin (Nup192), putative
6	3,252,789	*AFUA_6G12890*	Missense Variant (Arg878Gly)	Vacuole-associated enzyme activator complex component (Vac14), putative
6	3,330,314	*AFUA_6G13180*	Missense Variant (Ala529Thr)	CECR1 family adenosine deaminase, putative
7	1,457,904	*AFUA_7G05960*	Missense Variant (Arg1037Gln)	C2H2 finger domain protein, putative
7	1,541,519	*AFUA_7G06290*	Missense Variant (Gln666Leu)	NACHT domain protein, putative
8	332,292	*AFUA_8G01340*	Missense Variant (Met524Ile)	MFS sugar transporter, putative

Fisher's Exact tests, with a Bonferroni-corrected *p*-value threshold of 4.07×10^{-4} (0.05/122), were conducted to examine associations among these highly linked mutations to itraconazole and pan-azole resistance (Table 2.13). MIC resistance thresholds of 2 mg/L and 4 mg/L were both tested for these 26 sites and using all 122 strains. Both MIC thresholds identified four SNPs to be significantly associated with itraconazole resistance as well as two of these SNPs also being associated with pan-azole resistance (Table 2.13).

Table 2.13. Highly linked significant SNP sites associated with triazole resistance determined using Fisher's Exact tests (n=122).

Chromosome	Position (bp)	Gene ID	Predicted Effect (Amino Acid Substitution)	Fisher's Exact Test (p-values), MIC ≥ 2 mg/L		Fisher's Exact Test (p-values), MIC ≥ 4 mg/L	
				Itraconazole	Pan-azole	Itraconazole	Pan-azole
1	976,070	*AFUA_1G03370*	Missense Variant (Ser226Leu)	2.37×10^{-5} *	8.10×10^{-6} *	2.37×10^{-5} *	5.48×10^{-6} *
1	4,754,138	*AFUA_1G17380*	Missense Variant (Leu226Pro)	8.40×10^{-6} *	5.57×10^{-5} *	8.40×10^{-6} *	9.21×10^{-5} *
3	2,304,691	*AFUA_3G09040*	Missense Variant (Ser13Leu)	3.92×10^{-4} *	3.82×10^{-3}	3.92×10^{-4} *	2.41×10^{-3}
3	2,311,362	*AFUA_3G09070*	Missense Variant (Ile406Thr)	3.74×10^{-4} *	1.99×10^{-3}	3.74×10^{-4} *	2.41×10^{-3}
3	2,409,306	*AFUA_3G09450*	Missense Variant (Pro220Leu)	2.79×10^{-4} *	7.05×10^{-5} *	2.79×10^{-4} *	1.64×10^{-4} *

* Statistically significant association between SNP and antifungal resistance.

Additional Fisher's Exact tests were also conducted after the removal of the 21 strains with the L98H mutation in *cyp51A* and using a Bonferroni-corrected *p*-value threshold of 4.95×10^{-4} (0.05/101) (Table 2.14). For both MIC resistance thresholds, the results showed that the three previously noted SNPs, in *AFUA_1G17380, AFUA_3G09040* and *AFUA_3G09070,* were again significantly associated with itraconazole resistance. After removal of the 21 strains and using both MIC thresholds, two of these SNPs, *AFUA_3G09040* and *AFUA_3G09070,* were now also significantly associated with pan-azole resistance. Another shared SNP with the previous analysis is the missense variant in *AFUA_1G03370,* which was found to be significantly associated with pan-azole resistance at both MIC resistance thresholds. Furthermore, using the MIC threshold of 2 mg/L, a novel missense variant in *AFUA_7G06290* was found to be associated with pan-azole resistance (Table 2.14).

Table 2.14. Highly linked significant SNP sites associated with triazole resistance determined using Fisher's Exact tests after removing the 21 strains with the L98H mutation in *cyp51A* (n=101).

Chromosome	Position (bp)	Gene ID	Predicted Effect (Amino Acid Substitution)	Fisher's Exact Test (p-values), MIC ≥ 2 mg/L		Fisher's Exact Test (p-values), MIC ≥ 4 mg/L	
				Itraconazole	Pan-azole	Itraconazole	Pan-azole
1	976,070	*AFUA_1G03370*	Missense Variant (Ser226Leu)	3.20×10^{-3}	4.79×10^{-4} *	3.20×10^{-3}	1.84×10^{-4} *
1	4,754,138	*AFUA_1G17380*	Missense Variant (Leu226Pro)	3.15×10^{-4} *	2.12×10^{-3}	3.15×10^{-4} *	1.41×10^{-3}
3	2,304,691	*AFUA_3G09040*	Missense Variant (Ser13Leu)	1.06×10^{-5} *	7.39×10^{-5} *	1.06×10^{-5} *	6.19×10^{-5} *
3	2,311,362	*AFUA_3G09070*	Missense Variant (Ile406Thr)	5.07×10^{-6} *	3.47×10^{-5} *	5.07×10^{-6} *	6.19×10^{-5} *
7	1,541,519	*AFUA_7G06290*	Missense Variant (Gln666Leu)	1.08×10^{-3}	4.35×10^{-4} *	1.08×10^{-3}	1.29×10^{-3}

* Statistically significant association between SNP and antifungal resistance.

A third set of Fisher's exact tests were conducted after removal of the 64 strains containing known *cyp51A* mutations and using a Bonferroni-corrected *p*-value threshold of 8.62×10^{-4} (0.05/58) (Table 2.15). For both MIC resistance thresholds, the tests determined three previously identified SNPs to be significantly associated with both itraconazole and pan-azole resistance. These three SNPs were a missense variant in *AFUA_1G17380, AFUA_3G09040,* and *AFUA_3G09070.* Using both MIC

thresholds, the tests also identified the previous *AFUA_7G06290* missense variant to be significantly associated with pan-azole resistance.

Table 2.15. Highly linked significant SNP sites associated with triazole resistance determined using Fisher's Exact tests after removing the 64 strains with the mutations in *cyp51A* (n=58).

Chromosome	Position (bp)	Gene ID	Predicted Effect (Amino Acid Substitution)	Fisher's Exact Test (p-values), MIC ≥ 2 mg/L		Fisher's Exact Test (p-values), MIC ≥ 4 mg/L	
				Itraconazole	Pan-azole	Itraconazole	Pan-azole
1	4,754,138	*AFUA_1G17380*	Missense Variant (Leu226Pro)	1.87×10^{-5} *	1.25×10^{-4} *	1.87×10^{-5} *	2.91×10^{-4} *
3	2,304,691	*AFUA_3G09040*	Missense Variant (Ser13Leu)	8.33×10^{-5} *	2.33×10^{-5} *	8.33×10^{-5} *	3.10×10^{-5} *
3	2,311,362	*AFUA_3G09070*	Missense Variant (Ile406Thr)	8.33×10^{-5} *	2.33×10^{-5} *	8.33×10^{-5} *	3.10×10^{-5} *
7	1,541,519	*AFUA_7G06290*	Missense Variant (Gln666Leu)	1.18×10^{-3}	3.64×10^{-4} *	1.18×10^{-3}	5.03×10^{-4} *

* Statistically significant association between SNP and antifungal resistance.

Lastly, another set of Fisher's Exact test was conducted to focus solely on strains from Clade II and used a Bonferroni-corrected threshold of 7.04×10^{-4} (0.05/71) (Table 2.16). For both MIC resistance thresholds, the tests determined three previously identified SNPs to be significantly associated with both itraconazole and pan-azole resistance. These SNPs were a missense variant in *AFUA_1G17380, AFUA_3G09040* and *AFUA_3G09070*. Furthermore, using both MIC thresholds, the tests also identified the previously noted missense variant in *AFUA_7G06290* to be significantly associated with pan−azole resistance (Table 2.16).

Table 2.16. Highly linked significant SNP sites associated with triazole resistance determined using Fisher's Exact tests and strains in Clade II (n=71).

Chromosome	Position (bp)	Gene ID	Predicted Effect (Amino Acid Substitution)	Fisher's Exact Test (p-values), MIC ≥ 2 mg/L		Fisher's Exact Test (p-values), MIC ≥ 4 mg/L	
				Itraconazole	Pan-azole	Itraconazole	Pan-azole
1	4,754,138	*AFUA_1G17380*	Missense Variant (Leu226Pro)	1.68×10^{-6} *	4.81×10^{-5} *	1.68×10^{-6} *	4.83×10^{-5} *
3	2,304,691	*AFUA_3G09040*	Missense Variant (Ser13Leu)	2.59×10^{-5} *	8.51×10^{-5} *	2.59×10^{-5} *	1.73×10^{-5} *
3	2,311,362	*AFUA_3G09070*	Missense Variant (Ile406Thr)	1.17×10^{-5} *	3.48×10^{-5} *	1.17×10^{-5} *	1.73×10^{-5} *
7	1,541,519	*AFUA_7G06290*	Missense Variant (Gln666Leu)	3.21×10^{-3}	5.88×10^{-4}*	3.21×10^{-3}	2.85×10^{-4}*

* Statistically significant association between SNP and antifungal resistance.

2.5. Discussion

In this study, we analyzed the genomic polymorphisms among 195 *A. fumigatus* isolates collected from 12 countries as well as the International Space Station to investigate the potential associations between genomic SNPs and triazole resistance. Phylogenetic analyses of the whole-genome SNPs identified three main clades in this sample, with Clade I being very divergent from the other two clades. Most strains in this clade were from Spain and they likely represent a cryptic species within *A. fumigatus sensu stricto*. Among these 195 strains, the minimum inhibitory concentrations of two triazoles, itraconazole and voriconazole, were reported for 122 and 123 strains, respectively. Over the past two decades, an increasing number of studies have been conducted to investigate the genetic diversity and population structure of *A. fumigatus* using different molecular markers [14,40,41,42,43]. A previous study exploring global population genetic variation by Ashu et al. identified 8 genetic clusters by examining nine short tandem repeats in 2026 *A. fumigatus* isolates from 13 countries [13]. However, a more recent study analyzing the same short tandem repeats of 4049 *A. fumigatus* isolates identified two broad genetic clusters [14]. The whole-genome SNP analyses here revealed three divergent clades and within both Clades II and III, several sub-clades with significant bootstrap supports were also found. Therefore, the true number and composition of the genetic clusters in the global *A. fumigatus* population remain uncertain and depend on how clades and genetic clusters are defined. However, based on previous studies, most genetic clusters and clades contain geographically and ecologically diverse strains, consistent with frequent gene flow and great adaptability of *A. fumigatus* genotypes [14,26].

Among geographic and ecological populations, different frequencies of triazole resistance have been reported, likely reflecting their variations in strain source, clinical antifungal usage, agricultural fungicide usage, and surveillance techniques [44,45,46,47,48,49,50,51]. In 2017, Garcia-Rubio et al. reviewed previously published literature and reported that the global triazole-resistant rate ranged from 0.55% to 30% [30]. In the samples analyzed here and using an MIC threshold of 2 mg/L, 61.48% of all isolates with available MIC data were itraconazole resistant and 43.90% were voriconazole resistant.

Furthermore, 63.46% and 43.81% of the clinical isolates were itraconazole and voriconazole resistant, respectively. Similarly, there was a high frequency of environmental isolates resistant to itraconazole and voriconazole, at 50.00% and 44.44%, respectively. Using the MIC threshold of 4 mg/L, resistance frequencies for itraconazole remained the same, however, these values changed for voriconazole. The resistance rate for voriconazole in clinical strains decreased to 35.24% and for environmental strains, it changed to 33.33%. The high rates of resistance among strains analyzed here could be attributed to the biases among research groups in preferentially submitting drug-resistant strains for whole-genome sequencing. However, the broad range of triazole MIC values among the large number of sequenced strains allowed us to infer potential novel genetic variants not identified in previous studies.

Indeed, in this study, GWAS for both itraconazole and voriconazole resistance identified novel genes and mutations linked to triazole resistance. We conducted four GWAS analyses. The first analysis used all strains with known MIC values for itraconazole (n = 122) and voriconazole (n = 123). Meanwhile, the following two analyses investigated novel mutations associated with itraconazole and voriconazole resistance at other SNP loci, unrelated to *cyp51A*. Specifically, the second GWAS removed the 21 strains containing the L98H mutation in *cyp51A* and the third GWAS removed the 64 strains containing known mutations in *cyp51A* related to triazole resistance. The last GWAS was done on a clade-level, focusing the analysis on strains from Clade II with known triazole MIC values (n = 71). For each GWAS, we focused our investigation on the top 20 SNPs obtained via the GWAS analyses for each of the two drugs. We identified a total of six missense variants to be putatively associated with itraconazole resistance. These six missense variants were located in six genes: *AFUA_1G09780, AFUA_2G08060, AFUA_3G09090, AFUA_5G08150, AFUA_6G01860,* and *AFUA_8G02350*. The first mutation was in *AFUA_1G09780*, which encodes for a stomatin family protein. The stomatin proteins belong to a highly conserved family of integral membrane proteins. In humans, stomatin interacts with various ion channels and modulates their activity. The proteins are also thought to perform specific scaffolding functions in membranes. However, the functional information of stomatin proteins in fungi is scarce. The ortholog of *AFUA_1G09780* in the closely related *Aspergillus*

nidulans species is *AN1287* (*stoB*). The AN1287 protein is located in the inner mitochondrial membrane [52]. In addition to targeting ergosterol biosynthesis, triazole exposure also causes production of deleterious mitochondrial reactive oxygen species (ROS). Therefore, since triazoles promote ROS accumulation, the mitochondrial membrane complexes represent another group of targets when studying resistance [53]. Of note, this mutation in *AFUA_1G09780*, was found to be significantly associated with itraconazole resistance in all four GWAS analyses. The second mutation was in *AFUA_5G08150*, which encodes for a putative ABC bile acid transporter. Although this specific gene has not been previously linked to triazole resistance, other ABC transporter members are known to modulate triazole extrusion. Previous studies have found multiple ABC transporter members to be overexpressed with triazole exposure and that expression levels of various ABC transporter members were higher among triazole-resistant isolates [23,37,54]. In most cases, overexpression in this family of transporters seems to prevent intracellular drug concentrations from reaching levels needed to be effective at impacting ergosterol biosynthesis. The next variant was found in *AFUA_8G02350*, encoding a putative polyketide synthase. The polyketide synthases are involved in the biosynthesis of polyketides, which are a large and structurally diverse group of secondary metabolites [55]. These compounds have a wide range of biological activities that are important for ecological and evolutionary adaptation in fungi [55]. Furthermore, the gene *AFUA_8G02350* is within a terpene hybrid cluster [56]. The fourth gene, *AFUA_3G09090*, encodes for an uncharacterized protein. The fifth missense mutation related to itraconazole resistance was found in *AFUA_2G08060*, which encodes an involucrin repeat protein. This protein has been found to be involved in tethering Woronin bodies to septal pores [57]. In multicellular fungi such as *A. fumigatus*, cells are connected to each other via intercellular bridges called septal pores and Woronin bodies plug these pores upon injury to avoid excessive loss of cell content. Deletion mutants with impaired Woronin bodies have shown to have impaired stress resistance and delayed hyphal wounding response [57]. The missense mutation identified here may enhance the strains' ability to respond quickly to triazole drugs. The last missense mutation was in *AFUA_6G01860*, which encodes a putative MFS lactose permease. This class of protein plays a role in transmembrane transport and is an MFS family

member, a superfamily of transport proteins that are mainly responsible for antifungal resistance development through drug efflux activity.

Interestingly, our itraconazole GWAS analysis results differ from those in a GWAS conducted by Zhao and colleagues who examined SNPs associated with itraconazole sensitivity [29]. They completed a GWAS using 76 clinical *A. fumigatus* isolates collected from Japan. Our comparisons revealed no overlap between our top 20 SNPs and the SNPs they found to be highly associated with itraconazole sensitivity. Two factors might have contributed to the different observations. In the first, the study by Zhao et al. focused on itraconazole sensitivity in non-resistant clinical isolates of *A. fumigatus*, with itraconazole MIC ranging from 0.125 to 1 mg/L among their 76 isolates [29]. In contrast, the itraconazole MICs for our 122 strains with itraconazole MICs ranged from 0.13 to 32 mg/L. Secondly, all the strains analyzed by Zhao et al. were from one country, Japan [29]. In contrast, our itraconazole GWAS included 122 strains from eight countries, Canada (n = 12), India (n = 12), Japan (n = 8), Netherlands (n = 21), Spain (n = 19), Germany (n = 1), the United Kingdom (n = 24), and the United States (n = 25). Together, these results suggest that additional novel SNPs associated with itraconazole sensitivity or resistance will likely be present in other geographic and/or ecological populations of *A. fumigatus*. Another recent preprint by Rhodes and colleagues also conducted a GWAS on itraconazole resistance using treeWAS, a phylogenetic tree-based GWAS approach [58]. A comparison between the top 20 SNPs from our GWAS analyses and their significantly associated SNPs to itraconazole resistance found no overlap in SNP sites. This difference in results is most likely related to sample selection, as their sample set focused on strains obtained from the United Kingdom and Republic of Ireland. Another potential reason for the discrepancy is that our study used a quantitative phenotype, based on MIC values, for our GWAS while Rhodes and colleagues used a binary phenotype, separating strains into susceptible and resistant strains by defining resistance as MIC ≥ 2 mg/L. However, their results are consistent with our general conclusion that a large number of additional novel mutations, un-related to *cyp51A*, are significantly associated with triazole resistance in *A. fumigatus*.

The voriconazole GWAS analyses identified a total of 17 missense variants to be putatively associated with resistance. These variants were found in 17 different genes: *AFUA_1G03370, AFUA_1G09780, AFUA_1G12540, AFUA_1G17410, AFUA_2G01700*, *AFUA_2G13030, AFUA_4G09580*, *AFUA_5G01000*, *AFUA_5G02210, AFUA_5G14610*, *AFUA_6G09870*, *AFUA_7G00740, AFUA_7G05960, AFUA_8G01250, AFUA_8G01340, AFUA_8G01940,* and *AFUA_8G02280*. Two of these missense variants were found in *AFUA_1G03370* and *AFUA_5G02210*, which encodes for putative proteins of unknown functions. A third gene, *AFUA_1G12540*, encodes a putative TMEM1 family protein with uncharacterized function. The next seven variants were found in members of enzyme families with roles across a large number of biological processes, which comprised of the genes *AFUA_1G17410* that encodes a putative beta-glucosidase, *AFUA_2G01700* that encodes a putative serine/threonine protein kinase, *AFUA_2G13030* that encodes a phenylalanyl-tRNA synthetase, *AFUA_5G01000* that encodes a putative oxidoreductase of the 2-oxoglutarate (2OG)-Fe(II) oxygenase superfamily, *AFUA_5G14610* that encodes a putative carboxypeptidase Y, *AFUA_7G00740* that encodes a putative protein kinase, and *AFUA_8G01250* that encodes a putative GNAT family acetyltransferase. The next variant was found in *AFUA_7G05960*, which encodes a putative C2H2 finger domain protein. Three significantly associated missense variants also encoded for putative C6 zinc cluster transcription factors, which were found in *AFUA_6G09870*, *AFUA_8G01940* and *AFUA_8G02280*. Other members of this transcription factor family have been linked to triazole resistance. For example, a previous transcriptome study had found *finA*, a C6 zinc finger domain protein, displayed increased mRNA levels during adaptation to voriconazole exposure [38]. In addition, another C6 zinc-cluster transcription factor, AtrR, had been found to be associated with triazole resistance by regulating expression of genes related to ergosterol biosynthesis [59]. However, the Zn cluster family is the largest family of transcription factors known in eukaryotes and thus additional testing is required [60]. Interestingly, a missense mutation in *AFUA_1G09780* was also found significantly associated to voriconazole and was the same SNP found to be associated with itraconazole resistance. The remaining two genes were *AFUA_8G01340* that encodes a putative MFS

sugar transporter and *AFUA_4G09580,* which encodes the major allergen Aspf2. Although our study focused on examining missense variants, significantly associated SNPs obtained by GWAS also included synonymous, intergenic and intronic variants. These variants can have biological consequences and contribute to functional changes in the protein. For example, synonymous mutations can affect critical cis-regulatory sequences, alter mRNA structure, and impact translational speed [61]. Furthermore, non-coding variants can be found within potential regulatory sequences such as enhancers, promoters, and 5' and 3' UTRs [62]. Through these regulatory roles, non-coding variants can influence processes such as transcription, translation and splicing.

The results of the itraconazole and voriconazole GWAS showed few overlaps between significant SNPs; the first GWAS having one SNP overlap in the gene *AFUA_1G09780* and the third GWAS having two shared SNPs, a synonymous mutation in *AFUA_4G09770* and a synonymous mutation in *AFUA_5G08390*. The remaining two GWAS found no overlapping SNPs between the two antifungal drugs. Several reasons could have contributed to the low number of shared SNPs. Although all azoles operate using the same common mode of action, decreasing ergosterol synthesis by inhibiting the fungal enzyme 14α-sterol demethylase, there are differences between itraconazole and voriconazole in terms of their mechanisms of action. Voriconazole also inhibits 24-methylene dihydrolanasterol demethylation in *Aspergillus* and its antifungal activity is likely a result of a combination of effects in addition to inhibition of ergosterol synthesis [63]. Secondly, our sample set consisted of a large number of strains that had different susceptibilities to the two drugs and were only resistant to one of the two antifungals. Finally, our sample set was not a natural randomly mating population but were selected strains sequenced by different laboratories based on their own specific objective and purpose. As a result of the diversity of strains and their originating populations, some of the shared azole-resistance related mutations may have been less frequent in our studied sample set and were, thus, likely filtered out during quality control.

Linkage disequilibrium was also evaluated using the top 20 SNPs obtained by each of the four GWAS analyses to identify additional highly linked missense SNPs. Four sets of

Fisher's Exact tests were conducted: using all 122 strains, after removal of the 21 strains with the L98H mutation, after removal of the 64 strains with the *cyp51A* mutations, and using only the 71 Clade II strains. Interestingly, the last three tests identified two SNPs, missense variants in *AFUA_3G09040* and *AFUA_3G09070,* to be significantly associated with itraconazole as well as pan-azole resistance using both MIC thresholds (Table 2.14, Table 2.15 and Table 2.16). In the first test, conducted using all 122 strains and at both MIC thresholds, these two missense variants were also found to be significantly associated with itraconazole resistance (Table 2.13). Another SNP in *AFUA_1G17380* was also found in three tests to be significantly associated with itraconazole and pan-azole resistance using both MIC thresholds (Table 2.13, Table 2.15, and Table 2.16). Furthermore, in the remaining test, the SNP site was significantly associated with itraconazole resistance (Table 2.14). In terms of the function of these three genes, *AFUA_1G17380* encodes a putative 3-oxoacyl-(acyl-carrier-protein) reductase, *AFUA_3G0904* encodes for an uncharacterized protein and *AFUA_3G09070* encodes a putative carboxylesterase.

In addition, our study examined 20 previously known amino acid sites associated with triazole resistance. Fifteen of these known amino acid sites were in the *cyp51A* gene. Of these 15 sites, several have been functionally validated in previous studies and found to directly contribute to triazole resistance. These validated mutation sites consisted of G54, L98, Y121, G138, M220, T289 and G448 [8,64]. However, hot-spot SNP sites that confer triazole resistance by itself only include five of the seven sites, at G54, Y121, G138, M220 and G448. Meanwhile, for L98 and T289, a combination with a tandem repeat is required for triazole resistance, specifically TR_{34}/L98H and TR_{46}/Y121F/T289A [65]. Mutations in the G138 site has also been validated to cause multi-azole resistance [66]. Lastly, SNP sites P216 and F219 both confer resistance to itraconazole when mutated [67]. Specifically, there have been two amino acid substitutions in F219 in triazole-resistant strains, F219I and F219L [67]. However, interestingly, we have instead identified a different substitution F219S in our sample set; although it was not significantly associated with resistance (Table 2.1). We have also included the amino acid sites F46, M172, N248, D255, and E427; although only 3 of these sites could be found in our filtered genotype file, specifically F46, D255, and E427. Strains with a combination of these five mutations, as F46Y/M172V/D255E or

F46Y/M172V/D255E/N248T/E427K, have shown higher triazole MICs than the wild-type strains [30]. The three remaining *cyp51A* mutation sites, H147, S297 and F495, have been identified to be associated with resistant isolates but have not been functionally validated. Mutations in H147 were found to coincide with isolates with G448 mutations and were not found to be associated with resistance by itself and is thought to only increase protein stability [9,68]. Similarly, S297 and F495 mutations are found in some TR_{34}/L98H mutant *A. fumigatus* strains but have not been proven to be sufficient for triazole resistance by themselves [12,69]. However, these two amino acid positions, S297 and F495, are located near the triazole binding pocket of Cyp51A [70]. The remaining five known amino acid sites associated with triazole resistance are non-*cyp51A* mutations. Three of these SNP sites (I412, P309, and S305) are in *hmg1*, which encodes a 3-hydroxy-3-methyl-glutaryl-coenzyme A (HMG-CoA) reductase. Mutation at these three sites have been identified in triazole-resistant isolates and their association with triazole resistance has been functionally validated by inserting each SNP into the *hmg1* gene of the laboratory strain $akuB^{KU80}$ [33]. These three sites, I412, P309, and S305, are predicted to be within the conserved sterol-sensing domain of *hmg1* [33]. Furthermore, $akuB^{KU80}$ mutants with the substitution I412S and S305P possessed significantly different cellular sterol profiles compared to the unaltered $akuB^{KU80}$ strain; independent of *cyp51A* and *cyp51B* expression [33]. Another known mutation site is L167 in the uncharacterized *AFUA_7G01960* gene. The nonsense mutation L167* was first identified in the multi-azole-resistant clinical isolate V157-62, and subsequently functionally validated by inserting the specific SNP into an azole-susceptible clinical isolate, V130-15 [36]. At this amino acid position, a nonsense mutation was generated, which increased resistance to itraconazole [36]. Furthermore, this SNP was also associated with decreased ergosterol in the fungal membrane [36]. Interestingly, overexpression of the *AFUA_7G01960* gene itself has also been correlated with increased voriconazole resistance [38]. Taken together with bioinformatic analysis, *AFUA_7G01960* is predicted to be a putative transcription factor involved in ergosterol biosynthesis and mutation at L167 likely prevents its activity, thus leading to increased resistance [36]. The last known SNP site we investigated was E180 in *AFUA_2G10600*, a gene encoding the mitochondrial 29.9 KD NADH oxidoreductase subunit of respiratory complex I. The amino acid substitution E180D is present in

itraconazole-resistant clinical isolates of *A. fumigatus* [37]. Furthermore, restriction enzyme-mediated insertion of this mutation in the *AFUA_2G10600* gene led to increased itraconazole resistance [71]. This insertion was at a XhoI site, 534 bp from the start codon of the gene. This increase in resistance indicates that intact *AFUA_2G10600* may confer azole susceptibility through mitochondrial NADH metabolism or NAD/NADH redox stress [71]. Complete deletion of the coding region for this 29.9KD subunit was also found to result in itraconazole resistance in the laboratory strain A1163 KU80, increasing from an MIC of 0.25 mg/L to >8 mg/L, which further supports its contribution to itraconazole resistance [37].

Using a Fisher's Exact test on these 22 mutations, with all 122 strains and using both MIC resistance thresholds (2 mg/L and 4 mg/L), we found only one mutation, L98H in *cyp51A,* to be highly associated with itraconazole and pan-azole resistance (Table 2.1). Examining all samples with known triazole MIC data, this L98H mutation was found in 21 strains. We also determined using coverage data across the promoter region of *cyp51A* that all 21 strains with the L98H mutation were accompanied with the common 34-bp tandem repeat (Figure S2.5). A subsequent Fisher's Exact test was, thus, done after removing strains with the L98H mutation in *cyp51A* (n = 21). Additional Fisher's exact tests were also conducted after removal of all strains containing the *cyp51A* mutations (n = 64) and conducted again with only Clade II strains (n = 71). However, these additional tests identified no SNPs significantly associated with itraconazole and/or pan-azole resistance. A potential reason why the previously functionally validated sites were not highly associated with triazole resistance in our study is that strain counts for mutation genotypes at these sites were low in our 122-strain sample set and only ranged between 1 and 6 strains, making them unable to meet our criteria (>5% frequency in the population) for inclusion (Table S2.4).

We further examined the distribution of mutation phenotypes in these functionally validated sites in our three clades, using all 195 strains. Interestingly, for *cyp51A*, the mutation L98H was only present in strains of Clade III (n = 22). For the T289 site, three strains had the mutation T289A and this mutation always accompanied with the substitution Y121F. Furthermore, these three strains were all from Clade III. Mutations in the site G54, specifically G54V (n = 5), G54E (n = 1), G54W (n = 3) and G54R (n = 2), were found

mostly in Clade II strains with a rate of 90.91% (10/11). Mutations M220I (n = 2), M220V (n = 1), P216L (n = 4), and F219S (n = 1) were also only found in Clade II strains. For the gene *hmg1*, mutations in this gene were only seen in Clade II strains (n = 7).

Fisher's Exact tests were also conducted on 37 genes previously found to be overexpressed with triazole exposure using 3230 SNP sites (Table S2.3). The tests were conducted using both MIC resistance thresholds, 2 mg/L and 4 mg/L. The test conducted with all 122 strains and the MIC threshold set at 2 mg/L found 57 SNPs in or beside 14 genes to be associated with itraconazole resistance. For pan-azole resistance, 11 significantly associated SNPs were found. These SNPs were located in or beside six genes. The test conducted with the MIC threshold of 4 mg/L found the same 57 SNPs in or beside 14 genes to be significantly associated with itraconazole resistance. However, there were slight changes in the SNPs significantly associated with pan-azole resistance when using the 4 mg/L MIC threshold. The 4 mg/L MIC threshold determined 10 SNPs in or beside five genes to be associated with pan-azole resistance. Furthermore, to focus on novel mutations associated with triazole resistance not linked to *cyp51A*, two additional Fisher's Exact tests were also completed after removing the 21 strains containing the L98H mutation and again after removing the 64 strains with well-known mutations in *cyp51A* (Table S2.3). Using both MIC thresholds, the results after removal of the 21 strains found three SNPs to be significantly associated with itraconazole resistance. One SNP had already been noted as associated with itraconazole resistance by the first set of Fisher's Exact test, done prior to the 21-strain removal, which was an intergenic variant in *mfsB*. However, two novel intergenic variants, one in *AFUA_6G01960* and the second in *AFUA_1G16460*, were found to be significantly associated with itraconazole resistance as well. Furthermore, after removal of the 21 strains, no SNPs were found to be significantly associated with pan-azole resistance (Table S2.3). In terms of the results after removal of the 64 strains, one novel SNP site was found to be significantly associated with triazole differences. Using the MIC threshold of 2 mg/L, the test identified an intergenic variant in *abcA* to be associated with itraconazole resistance (Table S2.3). A final set of Fisher's Exact tests were conducted on a clade-level, using only strains in Clade II (n = 71). However, no SNPs sites were significantly associated with triazole resistance using this sample set. The result differences between tests could be due to

genetic hitchhiking alongside the resistance polymorphism L98H in *cyp51A* as well as to the reduced sample size, thus decreasing the sample count of certain SNPs and making them unable to meet the Bonferroni-corrected critical *p*-value threshold criteria in these tests.

In about 20% to 70% of triazole-resistant clinical *A. fumigatus* strains, no mutations related to *cyp51A* were observed [29,72]. Molecular assays for the detection of *A. fumigatus* and its *cyp51A* alterations have been produced to provide rapid detection of *cyp51A*-mediated triazole resistance in clinical samples of *A. fumigatus* [72]. However, as shown in our analyses, in many of the triazole-resistant strains, relying on assays targeting only the *cyp51A* mutations would lead to misidentification of these strains as triazole susceptible and cause inappropriate treatment strategies. Indeed, over the last decade, novel triazole resistance mechanisms have been increasingly reported including mutations in *hapE*, *hmg1, yap1,* and *cox10* genes [10,34,35,73]. The wide and growing range of resistance mechanisms seen in *A. fumigatus* demonstrates the high potential this fungus has for stress adaptation, including adaptation to antifungal drug resistance. Delays in the initiation of appropriate antifungal therapy are associated with overall increased mortality. Thus, tools enabling direct detection of resistance using rapid molecular methods can greatly facilitate optimal therapy for individual patients. Together, the putative variants found in this study represent promising candidates for future studies to investigate emerging mechanisms of triazole resistance in *A. fumigatus*. Moreover, these candidate SNPs hold great potential for developing additional diagnostic markers for accurate and rapid identification of triazole resistance in a clinical setting.

2.6. Materials and Methods

2.6.1. Whole Genome Sequences and Strains

Whole-genome sequences for 195 *A. fumigatus* isolates were used in this study. This sample set comprised of 184 whole-genome sequences obtained from the National Center for Biotechnology Information (NCBI) Sequence Read Archive and an additional 12 isolates that were sequenced from our previous study [63]. This strain collection spans 12 countries, across four continents consisting of 61 strains from North America, 1 from South America, 91 from Europe, 40 from Asia, as well as two strains from the International Space Station. In

total, 163 of the 195 strains were isolated from a clinical environment, 29 from the natural environment and 3 of unknown sources. Among them, 122 and 123 samples had antifungal susceptibility profiles to itraconazole and voriconazole, respectively. These profiles are recorded as the minimum inhibitory concentrations (MICs) and are presented in Table S2.1.

2.6.2. Variant Calling

For genome sequence analysis, a modified pipeline from our previous study was used [74]. In brief, FastQC v0.11.5 was used to check for read quality and low-quality sequences were trimmed using Trimmomatic v0.36 [75,76]. The reads were then mapped to the reference *A. fumigatus* strain Af293 (GenBank accession GCA_000002655.1) using the BWA-MEM algorithm v0.7.17 [77]. Duplicate reads were removed using MarkDuplicates in the Picard tool and variants were called using FreeBayes v0.9.21-19 [78,79]. The initial variant filtering was done via vcftools to remove indels, variants with a quality score below 15, and variants with a call rate less than 0.90 [80]. A second filtering step removing multiallelic sites was also conducted using vcftools and this resulting vcf file was named the "soft-filtered" file, which contained 314,999 SNP sites.

2.6.3. Phylogenetic Analysis

To infer evolutionary relationships among the 195 samples, nucleotides of SNP sites were concatenated for each sample and the invariant sites of sequence alignment were removed using RAxML ascertainment bias correction [81]. The maximum likelihood phylogenetic tree was constructed based on 314,999 SNP sites, using the ASC_GTRCAT nucleotide substitution model and 500 bootstrap replicates in RAxML v8.0.25 [81]. The phylogeny was then visualized using iTOL [82]. Strains were assigned into clades based on pairwise SNP comparisons, with a threshold set at 50,000 SNPs.

2.6.4. Genome-Wide Association Study and Linkage Disequilibrium

Variants were annotated with SnpEff v5.0 using the Af293 reference genome annotation to determine functional effects of genetic variants [83]. Highly linked (VIF > 2) SNP markers were removed using PLINK 1.90 beta to ensure uniform sampling of the genome [84].

Association analysis via a mixed linear model was done in TASSEL 5 using two parameters: a population structure defined by 5 principal component vectors, determined based on the scree plot, and a kinship matrix calculated using the Identity by State method (Centered IBS) [85]. To avoid biases due to imbalanced allele frequencies, the minimum allele frequency was also set to 0.05 using TASSEL 5. A total of 21,432 SNP sites remained for conducting the itraconazole GWAS and a total of 21,226 SNP sites for the voriconazole GWAS. A second GWAS was conducted after the removal of strains that contained the L98H mutation in *cyp51A* (n = 21). For the second association analysis, a total of 22,411 and 21,214 SNP sites remained for conducting the itraconazole and voriconazole GWAS, respectively. A third GWAS was also conducted after the removal of strains that contained well-known mutations associated with in *cyp51A* (n = 64). For the third association analysis, a total of 20,176 and 20,278 SNP sites remained for conducting the itraconazole and voriconazole GWAS, respectively. Lastly, we conducted a GWAS examining only the strains from Clade II for itraconazole (n = 71) and voriconazole (n = 72). For the analysis focusing solely on strains from Clade II, a total of 16,702 SNP sites remained for conducting the itraconazole GWAS and a total of 16,782 SNP sites remained for the voriconazole GWAS. Using the results of the GWAS, further association mapping between the top 20 SNPs and all SNPs in the soft-filtered vcf file was conducted using TASSEL 5 to determine additional highly linked SNPs of interest.

2.7. References

1. Kwon-Chung, K.J.; Sugui, J.A. Aspergillus Fumigatus—What Makes the Species a Ubiquitous Human Fungal Pathogen? *PLoS Pathog.* **2013**, *9*, e1003743, doi:10.1371/journal.ppat.1003743.
2. Brown, G.D.; Denning, D.W.; Gow, N.A.R.; Levitz, S.M.; Netea, M.G.; White, T.C. Hidden Killers: Human Fungal Infections. *Sci. Transl. Med.* **2012**, *4*, 165rv13–165rv13, doi:10.1126/scitranslmed.3004404.
3. Tekaia, F.; Latgé, J.-P. Aspergillus Fumigatus: Saprophyte or Pathogen? *Curr. Opin. Microbiol.* **2005**, *8*, 385–392, doi:10.1016/j.mib.2005.06.017.

4. Latgé, J.-P.; Chamilos, G. *Aspergillus Fumigatus* and Aspergillosis in 2019. *Clin. Microbiol. Rev.* **2019**, *33*, e00140-18, doi:10.1128/CMR.00140-18.
5. Cowen, L.E.; Sanglard, D.; Howard, S.J.; Rogers, P.D.; Perlin, D.S. Mechanisms of Antifungal Drug Resistance. *Cold Spring Harb. Perspect. Med.* **2015**, *5*, doi:10.1101/cshperspect.a019752.
6. Alcazar-Fuoli, L.; Mellado, E. Ergosterol Biosynthesis in Aspergillus Fumigatus: Its Relevance as an Antifungal Target and Role in Antifungal Drug Resistance. *Front. Microbiol.* **2012**, *3*, 439, doi:10.3389/fmicb.2012.00439.
7. Verweij, P.E.; Zhang, J.; Debets, A.J.M.; Meis, J.F.; van de Veerdonk, F.L.; Schoustra, S.E.; Zwaan, B.J.; Melchers, W.J.G. In-Host Adaptation and Acquired Triazole Resistance in Aspergillus Fumigatus: A Dilemma for Clinical Management. *Lancet Infect. Dis.* **2016**, *16*, e251–e260, doi:10.1016/S1473-3099(16)30138-4.
8. Lestrade, P.P.A.; Meis, J.F.; Melchers, W.J.G.; Verweij, P.E. Triazole Resistance in Aspergillus Fumigatus: Recent Insights and Challenges for Patient Management. *Clin. Microbiol. Infect.* **2019**, *25*, 799–806, doi:10.1016/j.cmi.2018.11.027.
9. Howard, S.J.; Cerar, D.; Anderson, M.J.; Albarrag, A.; Fisher, M.C.; Pasqualotto, A.C.; Laverdiere, M.; Arendrup, M.C.; Perlin, D.S.; Denning, D.W. Frequency and Evolution of Azole Resistance in Aspergillus Fumigatus Associated with Treatment Failure1. *Emerg. Infect. Dis.* **2009**, *15*, 1068–1076, doi:10.3201/eid1507.090043.
10. Camps, S.M.T.; Dutilh, B.E.; Arendrup, M.C.; Rijs, A.J.M.M.; Snelders, E.; Huynen, M.A.; Verweij, P.E.; Melchers, W.J.G. Discovery of a HapE Mutation That Causes Azole Resistance in Aspergillus Fumigatus through Whole Genome Sequencing and Sexual Crossing. *PLoS ONE* **2012**, *7*, e50034, doi:10.1371/journal.pone.0050034.
11. Chowdhary, A.; Kathuria, S.; Xu, J.; Meis, J.F. Emergence of Azole-Resistant Aspergillus Fumigatus Strains Due to Agricultural Azole Use Creates an Increasing Threat to Human Health. *PLoS Pathog.* **2013**, *9*, e1003633, doi:10.1371/journal.ppat.1003633.
12. Snelders, E.; van der Lee, H.A.L.; Kuijpers, J.; Rijs, A.J.M.M.; Varga, J.; Samson, R.A.; Mellado, E.; Donders, A.R.T.; Melchers, W.J.G.; Verweij, P.E. Emergence of Azole Resistance in Aspergillus Fumigatus and Spread of a Single Resistance Mechanism. *PLoS Med.* **2008**, *5*, e219, doi:10.1371/journal.pmed.0050219.

13. Ashu, E.E.; Hagen, F.; Chowdhary, A.; Meis, J.F.; Xu, J. Global Population Genetic Analysis of Aspergillus Fumigatus. *mSphere* **2017**, *2*, e00019-17, doi:10.1128/mSphere.00019-17.
14. Sewell, T.R.; Zhu, J.; Rhodes, J.; Hagen, F.; Meis, J.F.; Fisher, M.C.; Jombart, T. Nonrandom Distribution of Azole Resistance across the Global Population of Aspergillus Fumigatus. *mBio* **2019**, *10*, doi:10.1128/mBio.00392-19.
15. Chowdhary, A.; Kathuria, S.; Xu, J.; Sharma, C.; Sundar, G.; Singh, P.K.; Gaur, S.N.; Hagen, F.; Klaassen, C.H.; Meis, J.F. Clonal Expansion and Emergence of Environmental Multiple-Triazole-Resistant Aspergillus Fumigatus Strains Carrying the TR34/L98H Mutations in the Cyp51A Gene in India. *PLoS ONE* **2012**, *7*, e52871, doi:10.1371/journal.pone.0052871.
16. Ahangarkani, F.; Badali, H.; Abbasi, K.; Nabili, M.; Khodavaisy, S.; de Groot, T.; Meis, J.F. Clonal Expansion of Environmental Triazole Resistant Aspergillus Fumigatus in Iran. *J. Fungi* **2020**, *6*, 199, doi:10.3390/jof6040199.
17. Melo, A.M.; Stevens, D.A.; Tell, L.A.; Veríssimo, C.; Sabino, R.; Xavier, M.O. Aspergillosis, Avian Species and the One Health Perspective: The Possible Importance of Birds in Azole Resistance. *Microorganisms* **2020**, *8*, doi:10.3390/microorganisms8122037.
18. Cacciuttolo, E.; Rossi, G.; Nardoni, S.; Legrottaglie, R.; Mani, P. Anatomopathological Aspects of Avian Aspergillosis. *Vet. Res. Commun.* **2009**, *33*, 521–527, doi:10.1007/s11259-008-9199-7.
19. Resendiz Sharpe, A.; Lagrou, K.; Meis, J.F.; Chowdhary, A.; Lockhart, S.R.; Verweij, P.E.; ISHAM/ECMM Aspergillus Resistance Surveillance working group. Triazole Resistance Surveillance in Aspergillus Fumigatus. *Med. Mycol.* **2018**, *56*, 83–92, doi:10.1093/mmy/myx144.
20. Lestrade, P.P.A.; Buil, J.B.; van der Beek, M.T.; Kuijper, E.J.; van Dijk, K.; Kampinga, G.A.; Rijnders, B.J.A.; Vonk, A.G.; de Greeff, S.C.; Schoffelen, A.F.; et al. Paradoxal Trends in Azole-Resistant Aspergillus Fumigatus in a National Multicenter Surveillance Program, the Netherlands, 2013–2018. *Emerg. Infect. Dis.* **2020**, *26*, 1447–1455, doi:10.3201/eid2607.200088.

21. Buil, J.B.; Snelders, E.; Denardi, L.B.; Melchers, W.J.G.; Verweij, P.E. Trends in Azole Resistance in Aspergillus Fumigatus, the Netherlands, 1994–2016. *Emerg. Infect. Dis.* **2019**, *25*, 176–178, doi:10.3201/eid2501.171925.
22. Nabili, M.; Shokohi, T.; Moazeni, M.; Khodavaisy, S.; Aliyali, M.; Badiee, P.; Zarrinfar, H.; Hagen, F.; Badali, H. High Prevalence of Clinical and Environmental Triazole-Resistant Aspergillus Fumigatus in Iran: Is It a Challenging Issue? *J. Med. Microbiol.* **2016**, *65*, 468–475, doi:10.1099/jmm.0.000255.
23. Heo, S.T.; Tatara, A.M.; Jiménez-Ortigosa, C.; Jiang, Y.; Lewis, R.E.; Tarrand, J.; Tverdek, F.; Albert, N.D.; Verweij, P.E.; Meis, J.F.; et al. Changes in In Vitro Susceptibility Patterns of Aspergillus to Triazoles and Correlation With Aspergillosis Outcome in a Tertiary Care Cancer Center, 1999–2015. *Clin. Infect. Dis.* **2017**, *65*, 216–225, doi:10.1093/cid/cix297.
24. Abdolrasouli, A.; Petrou, M.A.; Park, H.; Rhodes, J.L.; Rawson, T.M.; Moore, L.S.P.; Donaldson, H.; Holmes, A.H.; Fisher, M.C.; Armstrong-James, D. Surveillance for Azole-Resistant Aspergillus Fumigatus in a Centralized Diagnostic Mycology Service, London, United Kingdom, 1998–2017. *Front. Microbiol.* **2018**, *9*, doi:10.3389/fmicb.2018.02234.
25. Fraczek, M.G.; Bromley, M.; Buied, A.; Moore, C.B.; Rajendran, R.; Rautemaa, R.; Ramage, G.; Denning, D.W.; Bowyer, P. The Cdr1B Efflux Transporter Is Associated with Non-Cyp51a-Mediated Itraconazole Resistance in Aspergillus Fumigatus. *J. Antimicrob. Chemother.* **2013**, *68*, 1486–1496, doi:10.1093/jac/dkt075.
26. Zhou, D.; Korfanty, G.A.; Mo, M.; Wang, R.; Li, X.; Li, H.; Li, S.; Wu, J.-Y.; Zhang, K.-Q.; Zhang, Y.; et al. Extensive Genetic Diversity and Widespread Azole Resistance in Greenhouse Populations of Aspergillus Fumigatus in Yunnan, China. *mSphere* **2021**, *6*, doi:10.1128/mSphere.00066-21.
27. Mohd-Assaad, N.; McDonald, B.A.; Croll, D. Multilocus Resistance Evolution to Azole Fungicides in Fungal Plant Pathogen Populations. *Mol. Ecol.* **2016**, *25*, 6124–6142, doi:10.1111/mec.13916.
28. Talas, F.; Kalih, R.; Miedaner, T.; McDonald, B.A. Genome-Wide Association Study Identifies Novel Candidate Genes for Aggressiveness, Deoxynivalenol Production, and

Azole Sensitivity in Natural Field Populations of Fusarium Graminearum. *Mol. Plant. Microbe Interact.* **2016**, *29*, 417–430, doi:10.1094/MPMI-09-15-0218-R.

29. Zhao, S.; Ge, W.; Watanabe, A.; Fortwendel, J.R.; Gibbons, J.G. Genome-Wide Association for Itraconazole Sensitivity in Non-Resistant Clinical Isolates of Aspergillus Fumigatus. *Front. Fungal. Biol.* **2021**, *1*, doi:10.3389/ffunb.2020.617338.
30. Garcia-Rubio, R.; Cuenca-Estrella, M.; Mellado, E. Triazole Resistance in Aspergillus Species: An Emerging Problem. *Drugs* **2017**, *77*, 599–613, doi:10.1007/s40265-017-0714-4.
31. Wei, X.; Zhang, Y.; Lu, L. The Molecular Mechanism of Azole Resistance in Aspergillus Fumigatus: From Bedside to Bench and Back. *J. Microbiol.* **2015**, *53*, 91–99, doi:10.1007/s12275-015-5014-7.
32. Gonzalez-Jimenez, I.; Lucio, J.; Amich, J.; Cuesta, I.; Sanchez Arroyo, R.; Alcazar-Fuoli, L.; Mellado, E. A Cyp51B Mutation Contributes to Azole Resistance in Aspergillus Fumigatus. *J. Fungi* **2020**, *6*, 315, doi:10.3390/jof6040315.
33. Rybak, J.M.; Ge, W.; Wiederhold, N.P.; Parker, J.E.; Kelly, S.L.; Rogers, P.D.; Fortwendel, J.R. Mutations in Hmg1, Challenging the Paradigm of Clinical Triazole Resistance in Aspergillus Fumigatus. *mBio* **2019**, *10*, doi:10.1128/mBio.00437-19.
34. Hagiwara, D.; Arai, T.; Takahashi, H.; Kusuya, Y.; Watanabe, A.; Kamei, K. Non-Cyp51A Azole-Resistant Aspergillus Fumigatus Isolates with Mutation in HMG-CoA Reductase. *Emerg. Infect. Dis.* **2018**, *24*, 1889–1897, doi:10.3201/eid2410.180730.
35. Wei, X.; Chen, P.; Gao, R.; Li, Y.; Zhang, A.; Liu, F.; Lu, L. Screening and Characterization of a Non-Cyp51A Mutation in an Aspergillus Fumigatus Cox10 Strain Conferring Azole Resistance. *Antimicrob. Agents Chemother.* **2017**, *61*, doi:10.1128/AAC.02101-16.
36. Ballard, E.; Weber, J.; Melchers, W.J.G.; Tammireddy, S.; Whitfield, P.D.; Brakhage, A.A.; Brown, A.J.P.; Verweij, P.E.; Warris, A. Recreation of In-Host Acquired Single Nucleotide Polymorphisms by CRISPR-Cas9 Reveals an Uncharacterised Gene Playing a Role in Aspergillus Fumigatus Azole Resistance via a Non-Cyp51A Mediated Resistance Mechanism. *Fungal Genet. Biol.* **2019**, *130*, 98–106, doi:10.1016/j.fgb.2019.05.005.

37. Bromley, M.; Johns, A.; Davies, E.; Fraczek, M.; Mabey Gilsenan, J.; Kurbatova, N.; Keays, M.; Kapushesky, M.; Gut, M.; Gut, I.; et al. Mitochondrial Complex I Is a Global Regulator of Secondary Metabolism, Virulence and Azole Sensitivity in Fungi. *PLoS ONE* **2016**, *11*, e0158724, doi:10.1371/journal.pone.0158724.
38. Da Silva Ferreira, M.E.; Malavazi, I.; Savoldi, M.; Brakhage, A.A.; Goldman, M.H.S.; Kim, H.S.; Nierman, W.C.; Goldman, G.H. Transcriptome Analysis of Aspergillus Fumigatus Exposed to Voriconazole. *Curr. Genet.* **2006**, *50*, 32–44, doi:10.1007/s00294-006-0073-2.
39. Du, W.; Zhai, P.; Wang, T.; Bromley, M.J.; Zhang, Y.; Lu, L. The C $_2$ H $_2$ Transcription Factor SltA Contributes to Azole Resistance by Coregulating the Expression of the Drug Target Erg11A and the Drug Efflux Pump Mdr1 in *Aspergillus Fumigatus*. *Antimicrob. Agents Chemother.* **2021**, *65*, e01839-20, doi:10.1128/AAC.01839-20.
40. Meis, J.F.; Chowdhary, A.; Rhodes, J.L.; Fisher, M.C.; Verweij, P.E. Clinical Implications of Globally Emerging Azole Resistance in Aspergillus Fumigatus. *Philos. Trans. R Soc. Lond B Biol. Sci.* **2016**, *371*, doi:10.1098/rstb.2015.0460.
41. Klaassen, C.H.W.; Gibbons, J.G.; Fedorova, N.D.; Meis, J.F.; Rokas, A. Evidence for Genetic Differentiation and Variable Recombination Rates among Dutch Populations of the Opportunistic Human Pathogen Aspergillus Fumigatus. *Mol. Ecol.* **2012**, *21*, 57–70, doi:10.1111/j.1365-294X.2011.05364.x.
42. Molecular Epidemiology of Aspergillus Fumigatus Isolates Recovered from Water, Air, and Patients Shows Two Clusters of Genetically Distinct Strains. Available online: https://www.ncbi.nlm.nih.gov/pmc/articles/PMC193792/ (accessed on 31 March 2021).
43. Bain, J.M.; Tavanti, A.; Davidson, A.D.; Jacobsen, M.D.; Shaw, D.; Gow, N.A.R.; Odds, F.C. Multilocus Sequence Typing of the Pathogenic Fungus Aspergillus Fumigatus. *J. Clin. Microbiol.* **2007**, *45*, 1469–1477, doi:10.1128/JCM.00064-07.
44. Seufert, R.; Sedlacek, L.; Kahl, B.; Hogardt, M.; Hamprecht, A.; Haase, G.; Gunzer, F.; Haas, A.; Grauling-Halama, S.; MacKenzie, C.R.; et al. Prevalence and Characterization of Azole-Resistant Aspergillus Fumigatus in Patients with Cystic Fibrosis: A Prospective Multicentre Study in Germany. *J. Antimicrob. Chemother.* **2018**, *73*, 2047–2053, doi:10.1093/jac/dky147.

45. Romero, M.; Messina, F.; Marin, E.; Arechavala, A.; Depardo, R.; Walker, L.; Negroni, R.; Santiso, G. Antifungal Resistance in Clinical Isolates of Aspergillus Spp.: When Local Epidemiology Breaks the Norm. *J. Fungi* **2019**, *5*, 41, doi:10.3390/jof5020041.
46. Verweij, P.E.; van de Sande-Bruisma, N.; Kema, G.H.J.; Melchers, W.J.G. Azole resistance in Aspergillus fumigatus in the Netherlands--increase due to environmental fungicides? *Ned. Tijdschr. Geneeskd* **2012**, *156*, A4458.
47. Özmerdiven, G.E.; Ak, S.; Ener, B.; Ağca, H.; Cilo, B.D.; Tunca, B.; Akalın, H. First Determination of Azole Resistance in Aspergillus Fumigatus Strains Carrying the TR34/L98H Mutations in Turkey. *J. Infect. Chemother.* **2015**, *21*, 581–586, doi:10.1016/j.jiac.2015.04.012.
48. Vermeulen, E.; Maertens, J.; De Bel, A.; Nulens, E.; Boelens, J.; Surmont, I.; Mertens, A.; Boel, A.; Lagrou, K. Nationwide Surveillance of Azole Resistance in Aspergillus Diseases. *Antimicrob. Agents Chemother.* **2015**, *59*, 4569–4576, doi:10.1128/AAC.00233-15.
49. Sewell, T.R.; Zhang, Y.; Brackin, A.P.; Shelton, J.M.G.; Rhodes, J.; Fisher, M.C. Elevated Prevalence of Azole-Resistant Aspergillus Fumigatus in Urban versus Rural Environments in the United Kingdom. *Antimicrob. Agents Chemother.* **2019**, *63*, doi:10.1128/AAC.00548-19.
50. Van der Linden, J.W.M.; Arendrup, M.C.; Warris, A.; Lagrou, K.; Pelloux, H.; Hauser, P.M.; Chryssanthou, E.; Mellado, E.; Kidd, S.E.; Tortorano, A.M.; et al. Prospective Multicenter International Surveillance of Azole Resistance in Aspergillus Fumigatus. *Emerg. Infect. Dis.* **2015**, *21*, 1041–1044, doi:10.3201/eid2106.140717.
51. Chowdhary, A.; Sharma, C.; Meis, J.F. Azole-Resistant Aspergillosis: Epidemiology, Molecular Mechanisms, and Treatment. *J. Infect. Dis* **2017**, *216*, S436–S444, doi:10.1093/infdis/jix210.
52. Takeshita, N.; Diallinas, G.; Fischer, R. The Role of Flotillin FloA and Stomatin StoA in the Maintenance of Apical Sterol-Rich Membrane Domains and Polarity in the Filamentous Fungus Aspergillus Nidulans. *Mol. Microbiol.* **2012**, *83*, 1136–1152, doi:10.1111/j.1365-2958.2012.07996.x.
53. Shekhova, E.; Kniemeyer, O.; Brakhage, A.A. Induction of Mitochondrial Reactive Oxygen Species Production by Itraconazole, Terbinafine, and Amphotericin B as a

Mode of Action against Aspergillus Fumigatus. *Antimicrob. Agents Chemother.* **2017**, *61*, doi:10.1128/AAC.00978-17.

54. Esquivel, B.D.; Rybak, J.M.; Barker, K.S.; Fortwendel, J.R.; Rogers, P.D.; White, T.C. Characterization of the Efflux Capability and Substrate Specificity of *Aspergillus Fumigatus* PDR5-like ABC Transporters Expressed in *Saccharomyces Cerevisiae*. *mBio* **2020**, *11*, e00338-20, doi:10.1128/mBio.00338-20.
55. Fatema, U.; Broberg, A.; Jensen, D.F.; Karlsson, M.; Dubey, M. Functional Analysis of Polyketide Synthase Genes in the Biocontrol Fungus Clonostachys Rosea. *Sci. Rep.* **2018**, *8*, 15009, doi:10.1038/s41598-018-33391-1.
56. Bignell, E.; Cairns, T.C.; Throckmorton, K.; Nierman, W.C.; Keller, N.P. Secondary Metabolite Arsenal of an Opportunistic Pathogenic Fungus. *Philos. Trans. R Soc. Lond. B Biol. Sci.* **2016**, *371*, doi:10.1098/rstb.2016.0023.
57. Beck, J.; Echtenacher, B.; Ebel, F. Woronin Bodies, Their Impact on Stress Resistance and Virulence of the Pathogenic Mould Aspergillus Fumigatus and Their Anchoring at the Septal Pore of Filamentous Ascomycota. *Mol. Microbiol.* **2013**, *89*, 857–871, doi:10.1111/mmi.12316.
58. Rhodes, J.; Abdolrasouli, A.; Dunne, K.; Sewell, T.R.; Zhang, Y.; Ballard, E.; Brackin, A.P.; van Rhijn, N.; Tsitsopoulou, A.; Posso, R.B.; et al. Tracing Patterns of Evolution and Acquisition of Drug Resistant Aspergillus Fumigatus Infection from the Environment Using Population Genomics. *bioRxiv* **2021**, doi:10.1101/2021.04.07.438821.
59. Paul, S.; Stamnes, M.; Thomas, G.H.; Liu, H.; Hagiwara, D.; Gomi, K.; Filler, S.G.; Moye-Rowley, W.S. AtrR Is an Essential Determinant of Azole Resistance in Aspergillus Fumigatus. *mBio* **2019**, *10*, doi:10.1128/mBio.02563-18.
60. Shelest, E. Transcription Factors in Fungi: TFome Dynamics, Three Major Families, and Dual-Specificity TFs. *Front. Genet.* **2017**, *8*, doi:10.3389/fgene.2017.00053.
61. Hunt, R.C.; Simhadri, V.L.; Iandoli, M.; Sauna, Z.E.; Kimchi-Sarfaty, C. Exposing Synonymous Mutations. *Trends Genet.* **2014**, *30*, 308–321, doi:10.1016/j.tig.2014.04.006.

62. Barrett, L.W.; Fletcher, S.; Wilton, S.D. Regulation of Eukaryotic Gene Expression by the Untranslated Gene Regions and Other Non-Coding Elements. *Cell Mol. Life Sci.* **2012**, *69*, 3613–3634, doi:10.1007/s00018-012-0990-9.
63. Pemán, J.; Salavert, M.; Cantón, E.; Jarque, I.; Romá, E.; Zaragoza, R.; Viudes, Á.; Gobernado, M. Voriconazole in the Management of Nosocomial Invasive Fungal Infections. *Ther. Clin. Risk Manag.* **2006**, *2*, 129–158.
64. Chen, P.; Liu, M.; Zeng, Q.; Zhang, Z.; Liu, W.; Sang, H.; Lu, L. Uncovering New Mutations Conferring Azole Resistance in the Aspergillus Fumigatus Cyp51A Gene. *Front. Microbiol.* **2020**, *10*, doi:10.3389/fmicb.2019.03127.
65. Bernal-Martínez, L.; Gil, H.; Rivero-Menéndez, O.; Gago, S.; Cuenca-Estrella, M.; Mellado, E.; Alastruey-Izquierdo, A. Development and Validation of a High-Resolution Melting Assay To Detect Azole Resistance in Aspergillus Fumigatus. *Antimicrob. Agents Chemother.* **2017**, *61*, doi:10.1128/AAC.01083-17.
66. Snelders, E.; Karawajczyk, A.; Schaftenaar, G.; Verweij, P.E.; Melchers, W.J.G. Azole Resistance Profile of Amino Acid Changes in Aspergillus Fumigatus CYP51A Based on Protein Homology Modeling. *Antimicrob. Agents Chemother.* **2010**, *54*, 2425–2430, doi:10.1128/AAC.01599-09.
67. Camps, S.M.T.; van der Linden, J.W.M.; Li, Y.; Kuijper, E.J.; van Dissel, J.T.; Verweij, P.E.; Melchers, W.J.G. Rapid Induction of Multiple Resistance Mechanisms in Aspergillus Fumigatus during Azole Therapy: A Case Study and Review of the Literature. *Antimicrob. Agents Chemother.* **2012**, *56*, 10–16, doi:10.1128/AAC.05088-11.
68. Chowdhary, A.; Sharma, C.; Hagen, F.; Meis, J.F. Exploring Azole Antifungal Drug Resistance in Aspergillus Fumigatus with Special Reference to Resistance Mechanisms. *Future Microbiol.* **2014**, *9*, 697–711, doi:10.2217/fmb.14.27.
69. Liu, M.; Zeng, R.; Zhang, L.; Li, D.; Lv, G.; Shen, Y.; Zheng, H.; Zhang, Q.; Zhao, J.; Zheng, N.; et al. Multiple Cyp51A-Based Mechanisms Identified in Azole-Resistant Isolates of Aspergillus Fumigatus from China. *Antimicrob. Agents Chemother.* **2015**, *59*, 4321–4325, doi:10.1128/AAC.00003-15.
70. Liu, M.; Zheng, N.; Li, D.; Zheng, H.; Zhang, L.; Ge, H.; Liu, W. Cyp51A -Based Mechanism of Azole Resistance in Aspergillus Fumigatus: Illustration by a New 3D

Structural Model of Aspergillus Fumigatus CYP51A Protein. *Med. Mycol.* **2016**, *54*, 400–408, doi:10.1093/mmy/myv102.

71. Bowyer, P.; Mosquera, J.; Anderson, M.; Birch, M.; Bromley, M.; Denning, D.W. Identification of Novel Genes Conferring Altered Azole Susceptibility in Aspergillus Fumigatus. *FEMS Microbiol. Lett.* **2012**, *332*, 10–19, doi:10.1111/j.1574-6968.2012.02575.x.
72. Dudakova, A.; Spiess, B.; Tangwattanachuleeporn, M.; Sasse, C.; Buchheidt, D.; Weig, M.; Groß, U.; Bader, O. Molecular Tools for the Detection and Deduction of Azole Antifungal Drug Resistance Phenotypes in Aspergillus Species. *Clin. Microbiol. Rev.* **2017**, *30*, 1065–1091, doi:10.1128/CMR.00095-16.
73. Qiao, J.; Liu, W.; Li, R. Truncated Afyap1 Attenuates Antifungal Susceptibility of Aspergillus Fumigatus to Voriconazole and Confers Adaptation of the Fungus to Oxidative Stress. *Mycopathologia* **2010**, *170*, 155–160, doi:10.1007/s11046-010-9309-2.
74. Fan, Y.; Wang, Y.; Xu, J. Comparative Genome Sequence Analyses of Geographic Samples of Aspergillus Fumigatus-Relevance for Amphotericin B Resistance. *Microorganisms* **2020**, *8*, 1673, doi:10.3390/microorganisms8111673.
75. Babraham Bioinformatics—FastQC A Quality Control Tool for High Throughput Sequence Data. Available online: https://www.bioinformatics.babraham.ac.uk/projects/fastqc/ (accessed on 31 March 2021).
76. Bolger, A.M.; Lohse, M.; Usadel, B. Trimmomatic: A Flexible Trimmer for Illumina Sequence Data. *Bioinformatics* **2014**, *30*, 2114–2120, doi:10.1093/bioinformatics/btu170.
77. Li, H. Aligning Sequence Reads, Clone Sequences and Assembly Contigs with BWA-MEM. *arXiv* **2013**, arXiv:1303.3997.
78. Picard Tools—By Broad Institute. Available online: https://broadinstitute.github.io/picard/ (accessed on 31 March 2021).
79. Garrison, E.; Marth, G. Haplotype-Based Variant Detection from Short-Read Sequencing. *arXiv* **2012**, arXiv:1207.3907.

80. Danecek, P.; Auton, A.; Abecasis, G.; Albers, C.A.; Banks, E.; DePristo, M.A.; Handsaker, R.E.; Lunter, G.; Marth, G.T.; Sherry, S.T.; et al. The Variant Call Format and VCFtools. *Bioinformatics* **2011**, *27*, 2156–2158, doi:10.1093/bioinformatics/btr330.
81. Stamatakis, A. RAxML Version 8: A Tool for Phylogenetic Analysis and Post-Analysis of Large Phylogenies. *Bioinformatics* **2014**, *30*, 1312–1313, doi:10.1093/bioinformatics/btu033.
82. Letunic, I.; Bork, P. Interactive Tree of Life (ITOL) v4: Recent Updates and New Developments. *Nucleic Acids Res.* **2019**, *47*, W256–W259, doi:10.1093/nar/gkz239.
83. Cingolani, P.; Platts, A.; Wang, L.L.; Coon, M.; Nguyen, T.; Wang, L.; Land, S.J.; Lu, X.; Ruden, D.M. A Program for Annotating and Predicting the Effects of Single Nucleotide Polymorphisms, SnpEff: SNPs in the Genome of Drosophila Melanogaster Strain W1118; Iso-2; Iso-3. *Fly* **2012**, *6*, 80–92, doi:10.4161/fly.19695.
84. Purcell, S.; Neale, B.; Todd-Brown, K.; Thomas, L.; Ferreira, M.A.R.; Bender, D.; Maller, J.; Sklar, P.; de Bakker, P.I.W.; Daly, M.J.; et al. PLINK: A Tool Set for Whole-Genome Association and Population-Based Linkage Analyses. *Am. J. Hum. Genet.* **2007**, *81*, 559–575, doi:10.1086/519795.
85. TASSEL: Software for Association Mapping of Complex Traits in Diverse Samples | Bioinformatics | Oxford Academic. Available online: https://academic.oup.com/bioinformatics/article/23/19/2633/185151 (accessed on 31 March 2021).

2.8. Supplemental Materials

Table S2.1. Additional information on the total 195 *Aspergillus fumigatus* genomes.

Alias	Run	Project	Collection Date	Country	Type	Lineages	itR MIC (mg/L)	VOR MIC (mg/L)	Sources For MIC Data	Antifungal Susceptibility Testing	Hmg1			Cyp51A												AFUA_7G01960
											S305P	P309L	I412	G448S	T289A	M220I	M220V	F219S	P216L	G138C	Y121F	I381I	G54V,E	G54R,W	K427E	E255D	Y46F	L367* (Stop Gained)
A63S	DRR146814	PRJDB7240	2006 (a mutant of strain D141 originally isolated in Germany in 1980)	Germany	Clinical	Clade III	0.5	0.094	https://doi.org/10.1371/journal.ppat.1006096	CLSI M38-A2	0	0	0	0	0	0	0	0	0	0	0	0	0	0	K427E	E255D	Y46F	0
B5233	ERR2863830	PRJEB28819	1985	United States	Clinical	Clade III	0.5	0.5	DOI: 10.1128/AAC.00129-19	CLSI M38-A2	0	0	0	0	0	0	0	0	0	0	0	0	0	0	K427E	E255D	Y46F	0
P1MR	ERR2864483		2016	Netherlands	Clinical	Clade III	NA	NA	NA	NA	0	0	0	0	0	0	0	0	0	0	0	I381I	0	0	K427E	E255D	Y46F	0
P1MS	ERR2864484		2016	Netherlands	Clinical	Clade II	NA	NA			0	0	0	0	0	0	0	0	0	0	0	0	0	0	K427E	E255D	Y46F	0
P2CS	ERR2864485		2018	Netherlands	Clinical	Clade II	NA	NA			0	0	0	0	0	0	0	0	0	0	0	0	0	0	K427E	E255D	Y46F	0
Af65	ERR769499	PRJEB8623	1997	United Kingdom, Manchester, England	Clinical	Clade III	0.5	0.125	https://mbio.asm.org/content/6/3/e00536-15#T2	CLSI M38-A2	0	0	0	0	0	0	0	0	0	0	0	0	0	0	K427E	E255D	Y46F	0
12-7505446	ERR769500		2012	United Kingdom, Leeds	Clinical	Clade III	>16	1			0	0	0	0	0	0	0	0	0	0	0	I381I	0	0	K427E	E255D	Y46F	0
12-7505220	ERR769501		2012	United Kingdom, Leeds	Clinical	Clade III	>16	1			0	0	0	0	0	0	0	0	0	0	0	I381I	0	0	K427E	E255D	Y46F	0
09-7500806	ERR769502		2009	United Kingdom, Leeds	Clinical	Clade II	1	0.25			0	0	0	0	0	0	0	0	0	0	0	0	0	0	K427E	E255D	Y46F	0
12-7504652	ERR769503		2012	United Kingdom, Leeds	Clinical	Clade III	1	0.5			0	0	0	0	0	0	0	0	0	0	0	0	0	0	K427E	E255D	Y46F	0
12-7504462	ERR769504		2012	United Kingdom, Leeds	Clinical	Clade II	0.5	0.125			0	0	0	0	0	0	0	0	0	0	0	0	0	0	K427E	E255D	Y46F	0
12-7505054	ERR769505		2012	United Kingdom, Leeds	Clinical	Clade III	0.5	0.5			0	0	0	0	0	0	0	0	0	0	0	0	0	0	K427E	E255D	Y46F	0
08-12-12-13	ERR769506		2003	Netherlands, Nijmegen	Clinical	Clade III	>16	1			0	0	0	0	0	0	0	0	0	0	0	I381I	0	0	K427E	E255D	Y46F	0
08-36-03-25	ERR769507		2005	Netherlands, Nijmegen	Clinical	Clade III	>16	1			0	0	0	0	0	0	0	0	0	0	0	I381I	0	0	K427E	E255D	Y46F	0
08-31-08-91	ERR769508		2004	Netherlands, Nijmegen	Clinical	Clade III	>16	4			0	0	0	0	0	0	0	0	0	0	0	I381I	0	0	K427E	E255D	Y46F	0
08-19-02-61	ERR769509		2008	Netherlands, Nijmegen	Environmental	Clade III	>16	2			0	0	0	0	0	0	0	0	0	0	0	I381I	0	0	K427E	E255D	Y46F	0
08-19-02-30	ERR769510		2008	Netherlands, Nijmegen	Environmental	Clade II	0.25	0.5			0	0	0	0	0	0	0	0	0	0	0	0	0	0	K427E	E255D	Y46F	0
10-01-02-27	ERR769511		2010	Netherlands, Nijmegen	Clinical	Clade III	>16	4			0	0	0	0	0	0	0	0	0	0	0	I381I	0	0	K427E	E255D	Y46F	0
08-19-02-46	ERR769512		2008	Netherlands, Nijmegen	Environmental	Clade III	>16	4			0	0	0	0	0	0	0	0	0	0	0	I381I	0	0	K427E	E255D	Y46F	0
08-19-02-10	ERR769513		2008	Netherlands, Nijmegen	Environmental	Clade III	>16	2			0	0	0	0	0	0	0	0	0	0	0	I381I	0	0	K427E	E255D	Y46F	0
Afu 942/09	ERR769514		2009	India, Delhi	Clinical	Clade III	>16	2			0	0	0	0	0	0	0	0	0	0	0	I381I	0	0	K427E	E255D	Y46F	0
Afu 1042/09	ERR769515		2009	India, Delhi	Clinical	Clade III	>16	2			0	0	0	0	0	0	0	0	0	0	0	I381I	0	0	K427E	E255D	Y46F	0
Afu 343/P/11	ERR769516		2011	India, Delhi	Clinical	Clade III	>16	8			0	0	0	0	0	0	0	0	0	0	0	I381I	0	0	K427E	E255D	Y46F	0
Afu 591/12	ERR769517		2012	India, Delhi	Clinical	Clade III	>16	8			0	0	0	0	0	0	0	0	0	0	0	I381I	0	0	K427E	E255D	Y46F	0
Afu 124/E11	ERR769518		2011	India, Delhi	Environmental	Clade III	>16	8			0	0	0	0	0	0	0	0	0	0	0	I381I	0	0	K427E	E255D	Y46F	0
Afu 166/E11	ERR769519		2011	India, Delhi	Environmental	Clade III	16	16			0	0	0	0	0	0	0	0	0	0	0	I381I	0	0	K427E	E255D	Y46F	0
Afu 257/E11	ERR769520		2011	India, Delhi	Environmental	Clade III	>16	8			0	0	0	0	0	0	0	0	0	0	0	I381I	0	0	K427E	E255D	Y46F	0
Afu 218/E11	ERR769521		2011	India, Delhi	Environmental	Clade III	>16	8			0	0	0	0	0	0	0	0	0	0	0	I381I	0	0	K427E	E255D	Y46F	0
CM3262	SRR7418922	PRJNA477519	2005	Spain, Madrid	Clinical	Clade I	1.000/1.0	0.500/0.5	https://aac.asm.org/content/62/6/e00241-18#fn-2	EUCAST	0	0	0	0	0	0	0	0	0	0	0	0	0	0	E255D	0	0
CM2733	SRR7418923		2004	Spain, Madrid	Clinical	Clade I	0.354/0.25-0.5	0.707/0.5-1.0			0	0	0	0	0	0	0	0	0	0	0	0	0	0	E255D	0	0
CM2730	SRR7418924		2004	Spain, Madrid	Clinical	Clade I	0.354/0.25-0.5	0.707/0.5-1.0			0	0	0	0	0	0	0	0	0	0	0	0	0	0	E255D	0	0
CM7560	SRR7418925		2014	Spain, Madrid	Clinical	Clade I	0.707/0.5-1.0	0.707/0.5-1.0			0	0	0	0	0	0	0	0	0	0	0	0	0	0	E255D	0	0
CM3249	SRR7418926		2005	Spain, Madrid	Clinical	Clade I	0.707/0.5-1.0	1.000/0.5-2.0			0	0	0	0	0	0	0	0	0	0	0	0	0	0	E255D	0	0
TP32	SRR7418946		2010	Spain, Madrid	Clinical	Clade I	0.630/0.25-1.0	0.397/0.25-1.0			0	0	0	0	0	0	0	0	0	0	0	0	0	0	E255D	0	0
CM4602	SRR7418928		2006	Spain, Madrid	Clinical	Clade I	0.250/0.25	0.500/0.5			0	0	0	0	0	0	0	0	0	0	0	0	0	0	E255D	0	0
CM4946	SRR7418948		2007	Spain, Madrid	Clinical	Clade I	0.397/0.125–1.0	0.794/0.5–1.0			0	0	0	0	0	0	0	0	0	0	0	0	0	0	E255D	0	0
CM2495	SRR7418930		2002	Spain, Madrid	Clinical	Clade I	0.250/0.25	0.500/0.5			0	0	0	0	0	0	0	0	0	0	0	0	0	0	E255D	0	0
ΔakuBKU80	SRR7418932		2003	Spain, Madrid	Clinical	Clade II	0.175/0.06-0.25	0.297/0.25-0.5			0	0	0	0	0	0	0	0	0	0	0	0	0	0	K427E	E255D	Y46F	0
CM7570	SRR7418933		2014	Spain, Madrid	Clinical	Clade I	0.630/0.5–1.0	0.500/0.5			0	0	0	0	0	0	0	0	0	0	0	0	0	0	E255D	0	0
CBS144.89/A1163	SRR7418934		2008	Spain, Madrid	Clinical	Clade II	0.210/0.125–0.25	0.500/0.5			0	0	0	0	0	0	0	0	0	0	0	0	0	0	K427E	E255D	Y46F	0
TP12	SRR7418940		2001	Spain, Madrid	Clinical	Clade II	0.500/0.5	1.000/1.0			0	0	0	0	0	0	0	0	0	0	0	0	0	0	0	0	0	0
CM7632	SRR7418941		2015	Spain, Madrid	Clinical	Clade II	0.794/0.5–1.0	1.000/1.0			0	0	0	0	0	0	0	0	0	0	0	0	0	0	0	0	0	0
CM237	SRR7418942	PRJNA390160	1996	Spain, Madrid	Clinical	Clade II	NA	NA	NA	NA	0	0	0	0	0	0	0	0	0	0	0	0	0	0	K427E	E255D	Y46F	0
ATCC 204305	SRR7418943		1995	Spain, Madrid	Clinical	Clade II	NA	NA			0	0	0	0	0	0	0	0	0	0	0	0	0	0	K427E	E255D	Y46F	0
CM5419	SRR7418944		2008	Spain, Madrid	Clinical	Clade III	NA	NA			0	0	0	0	0	0	0	0	0	0	0	0	0	0	K427E	E255D	Y46F	0
CM3248	SRR7418945		2005	Spain, Madrid	Clinical	Clade II	NA	NA			0	0	0	0	0	0	0	0	0	0	0	0	0	0	K427E	E255D	Y46F	0
CM2141	SRR7418947		1998	Spain, Madrid	Clinical	Clade III	NA	NA			0	0	0	0	0	0	0	0	0	0	0	0	0	0	K427E	E255D	Y46F	0
CM5757	SRR7418949		2009	Spain, Madrid	Clinical	Clade II	NA	NA			0	0	0	0	0	0	0	0	0	0	0	0	0	0	K427E	E255D	Y46F	0
CM3720	SRR7418927		2005	Spain, Madrid	Clinical	Clade I	NA	NA	NA	NA	0	0	0	0	0	0	0	0	0	0	0	0	0	0	0	E255D	0	0
CM3249b	SRR7418929		2005	Spain, Madrid	Clinical	Clade I	NA	NA			0	0	0	0	0	0	0	0	0	0	0	0	0	0	0	E255D	0	0
ATCC 46645	SRR7418935		2008	Spain, Madrid	Clinical	Clade III	NA	NA			0	0	0	0	0	0	0	0	0	0	0	0	0	0	K427E	E255D	Y46F	0
CM6458	SRR7418936		2011	Spain, Madrid	Clinical	Clade II	NA	NA			0	0	0	0	0	0	0	0	0	0	0	0	0	0	K427E	E255D	Y46F	0
CM6126	SRR7418937		2010	Spain, Madrid	Clinical	Clade II	NA	NA			0	0	0	0	0	0	0	0	0	0	0	0	0	0	K427E	E255D	Y46F	0
CM7555	SRR7418938		2014	Spain, Madrid	Clinical	Clade II	NA	NA			0	0	0	0	0	0	0	0	0	0	0	0	0	0	K427E	E255D	Y46F	0
CM7510	SRR7418939		2014	Spain, Madrid	Clinical	Clade II	NA	NA			0	P309L	0	0	0	0	0	0	0	0	0	0	0	0	K427E	E255D	Y46F	0
Af-M1509-D	SRR6434917	PRJNA427336	2004	United States, North Carolina	Clinical	Clade II	NA	0.25	NA	NA	0	0	0	0	0	0	0	0	0	0	0	0	0	0	K427E	E255D	Y46F	0
M5960-D	SRR6434918		2014	United States, North Carolina	Clinical	Clade II	NA	0.25	https://www.ncbi.nlm.nih.gov/pmc/articles/PMC6175610/	NA	0	0	0	0	0	0	0	0	0	0	0	0	0	0	K427E	E255D	Y46F	0
MO8507EXP	SRR5676586	PRJNA390160	2012	Portugal, Porto	Clinical	Clade II	NA	NA	NA	NA	0	0	0	0	0	0	0	0	0	0	0	0	0	0	K427E	E255D	Y46F	0
MO5405EXP	SRR5676587		2011	Portugal, Porto	Clinical	Clade II	NA	NA			0	0	0	0	0	0	0	0	0	0	0	0	0	0	K427E	E255D	Y46F	0
MO7695EXP	SRR5676588		2013	Portugal, Porto	Clinical	Clade II	NA	NA			0	0	0	0	0	0	0	0	0	0	0	0	0	0	K427E	E255D	Y46F	0
MO6925DEXP	SRR5676589		2013	Portugal, Porto	Clinical	Clade II	NA	NA			0	0	0	0	0	0	0	0	0	0	0	0	0	0	K427E	E255D	Y46F	0
MO7958?EXP	SRR5676590		2013	Portugal, Porto	Clinical	Clade I	NA	NA			0	0	0	0	0	0	0	0	0	0	0	0	0	0	0	E255D	0	0
MO8722EXP	SRR5676591		2013	Portugal, Porto	Clinical	Clade II	NA	NA			0	0	0	0	0	0	0	0	0	0	0	0	0	0	K427E	E255D	Y46F	0
MO91298SB	SRR5676592		2014	Portugal, Porto	Clinical	Clade II	NA	NA			0	0	0	0	0	0	0	0	0	0	0	0	0	0	K427E	E255D	Y46F	0
MO8926?3	SRR5676593		2014	Portugal, Porto	Clinical	Clade II	NA	NA			0	0	0	0	0	0	0	0	0	0	0	0	0	0	K427E	E255D	Y46F	0
IFM 59355-1	DRR022916	PRJDB3064	2009	Japan, Chiba University Hospital	Clinical	Clade II	0.5	1	https://jcm.asm.org/content/52/12/4202/figures-only	CLSI M38-A2	0	0	0	0	0	0	0	0	0	0	0	0	0	0	K427E	E255D	Y46F	0
IFM 59355-2	DRR022917		2009	Japan, Chiba University Hospital	Clinical	Clade II	0.5	0.5			0	0	0	0	NA	0	0	0	0	0	0	0	0	0	K427E	NA	Y46F	0
IFM 59356-1	DRR022919		2009	Japan, Chiba University Hospital	Clinical	Clade II	0.5	0.5			0	0	0	0	0	0	0	0	0	0	0	0	0	0	K427E	E255D	Y46F	0
IFM 59356-2	DRR022922		2009	Japan, Chiba University Hospital	Clinical	Clade II	0.5	0.5			0	0	0	NA	NA	NA	NA	NA	NA	NA	0	0	0	0	K427E	NA	NA	0
IFM 59356-3	DRR022924		2009	Japan, Chiba University Hospital	Clinical	Clade II	1	0.5			0	0	0	0	0	0	0	0	0	0	0	0	0	0	K427E	E255D	Y46F	0
IFM 59361-1	DRR022925		2009	Japan, Chiba University Hospital	Clinical	Clade II	1	1			0	0	0	0	0	0	0	0	0	0	0	0	0	0	K427E	E255D	Y46F	0
IFM 59361-2	DRR022926		2009	Japan, Chiba University Hospital	Clinical	Clade II	1	2			0	0	0	0	0	0	0	0	0	0	0	0	0	0	K427E	E255D	Y46F	0
IFM 60237	DRR022927		2011	Japan, Chiba University Hospital	Clinical	Clade II	4	1			0	0	0	0	0	0	0	0	P216L	0	0	0	0	0	K427E	E255D	Y46F	0
IFM 55369	DRR015087	PRJDB1541	2009	Japan, Ishikawa	Clinical	Clade II	NA	NA	NA	NA	0	0	0	0	0	0	0	0	0	0	0	0	0	0	K427E	E255D	Y46F	0
IFM 59056	DRR015093		2009	Japan, Chiba	Clinical	Clade II	NA	NA			0	0	0	0	0	0	0	0	0	0	0	0	0	0	K427E	E255D	Y46F	0
IFM 59359	DRR015096		2007	Japan, Chiba	Clinical	Clade II	NA	NA			0	0	0	0	0	0	0	0	0	0	0	0	0	0	K427E	E255D	Y46F	0
IFM 59361	DRR015099		2009	Japan, Chiba	Clinical	Clade II	NA	NA			0	0	0	0	0	0	0	0	0	0	0	0	0	0	K427E	E255D	Y46F	0
IFM 60514	DRR015102		2011	Japan, Chiba	Clinical	Clade II	NA	NA			0	0	0	0	0	0	0	0	0	0	0	0	0	0	K427E	E255D	Y46F	0
IFM 59073	DRR015106		2009	Japan, Chiba	Clinical	Clade II	NA	NA			0	0	0	0	0	0	0	0	0	0	0	0	0	0	K427E	E255D	Y46F	0
IFM 61407	DRR015109		2012	Japan, Chiba	Clinical	Clade II	NA	NA			0	0	0	0	0	0	0	0	0	0	0	0	0	0	K427E	E255D	Y46F	0
IFM 61610	DRR015112		2012	Japan, Tokyo	Clinical	Clade II	NA	NA			0	0	0	0	0	0	0	0	0	0	0	0	0	0	K427E	E255D	Y46F	0
IFM 58026	DRR017537		2009	Japan, Tottori	Clinical	Clade II	NA	NA			0	0	0	0	0	0	0	0	0	0	0	0	0	0	K427E	E255D	Y46F	0
IFM 58029	DRR017540		2009	Japan, Nagasaki	Clinical	Clade II	NA	NA			0	0	0	0	0	0	0	0	0	0	0	0	0	0	K427E	E255D	Y46F	0
IFM 58401	DRR017543		2009	Japan, Chiba	Clinical	Clade II	NA	NA			NA	0	0	0	0	0	0	0	0	0	0	0	0	0	K427E	E255D	Y46F	0
IFM 59365	DRR017546		2010	Japan, Chiba	Clinical	Clade II	NA	NA			0	0	0	0	0	0	0	0	0	0	0	0	0	0	K427E	E255D	Y46F	0
IFM 59777	DRR017549		2010	Japan, Okayama	Clinical	Clade II	NA	NA			NA	NA	0	0	0	0	0	0	0	0	0	0	NA	NA	K427E	E255D	NA	0
IFM 61118	DRR017552		2012	Japan, Chiba	Clinical	Clade II	NA	NA			0	0	0	0	0	0	0	0	0	0	0	0	0	0	K427E	E255D	Y46F	0
IFM 61578	DRR017555		2012	Japan, Osaka	Clinical	Clade II	NA	NA			0	0	0	0	0	0	0	0	P216L	0	0	0	0	0	K427E	E255D	Y46F	0
IFM 62115	DRR017558		2013	Japan, Aichi	Clinical	Clade II	NA	NA			0	0	0	0	0	0	0	0	0	0	0	0	NA	NA	NA	E255D	Y46F	0
IFM 62516	DRR017559		2014	Japan, Tokyo	Clinical	Clade II	NA	NA			0	0	0	0	0	0	0	0	0	0	0	0	0	0	K427E	E255D	Y46F	0

CNM-CM8689	SRR10592629	PRJNA592352	NA	Spain, Madrid	Clinical	Clade II	1	8	https://doi.org/10.3389/fgene.2020.00459	EUCAST	0	0	0	0	0	0	0	0	0	0	0	0	0	0	K427E	E255D	Y46F	0
CNM-CM8686	SRR10592630		NA	Spain, Madrid	Clinical	Clade II	0.25	0.25			0	0	0	0	0	0	0	0	0	0	0	0	0	0	K427E	E255D	Y46F	0
CNM-CM8812	SRR10592631		NA	Spain, Madrid	Clinical	Clade III	0.25	0.5			0	0	0	0	0	0	0	0	0	0	0	0	0	0	K427E	E255D	Y46F	0
CNM-CM8714	SRR10592632		NA	Spain, Madrid	Clinical	Clade III	>8	4			0	0	0	0	0	0	0	0	0	0	0	L98H	0	0	K427E	E255D	Y46F	0
CNM-CM8057	SRR10592633		NA	Spain, Madrid	Clinical	Clade III	>8	>8			0	0	0	0	T289A	0	0	0	0	0	Y121F	0	0	0	K427E	E255D	Y46F	0
LMB-35Aa	SRR2954803	PRJNA298653	2005	Remote Tingo Maria forest, Huanuco, Peru	Environmental	Clade I	NA	NA	NA	NA	0	0	0	0	0	0	0	0	0	0	0	0	0	0	0	E255D	0	0
ISSFT-021	SRR4002443	PRJNA319359	2015	ISS (International Space Station)	Environmental	Clade II	NA	NA	NA	NA	0	0	0	0	0	0	0	0	0	0	0	0	0	0	K427E	E255D	Y46F	0
IF1SW-F4	SRR4002444		2015	ISS (International Space Station)	Environmental	Clade II	NA	NA			0	0	0	0	0	0	0	0	0	0	0	0	0	0	K427E	E255D	Y46F	0
DI 15-111	SRR7841976	PRJNA491253	2013	United States	Clinical	Clade II	>16	0.25	DOI: 10.1128/JCM.02478-15	CLSI M38-A2	0	0	0	0	0	0	0	0	0	0	0	0	0	G54R	K427E	E255D	Y46F	0
DI 15-110	SRR7841977		2013	United States, Connecticut	Clinical	Clade II	>16	8			0	0	0	0	0	0	0	0	0	0	0	0	0	0	K427E	E255D	Y46F	0
DI 15-105	SRR7841980		2012	United States	Clinical	Clade II	32	8			0	0	0	0	0	0	0	0	0	0	0	0	0	0	0	0	0	0
DI 15-103	SRR7841981		2010	United States, Ohio	Clinical	Clade II	>16	0.5			0	0	0	0	0	M220I	0	0	0	0	0	0	0	0	K427E	E255D	Y46F	0
DI 15-107	SRR7841982		2012	United States, California	Clinical	Clade II	16	0.5			0	0	0	0	0	0	0	0	0	0	0	0	0	0	K427E	E255D	Y46F	0
DI 15-109	SRR7841984		2012	United States, Washington	Clinical	Clade II	>16	0.25			0	0	0	0	0	0	0	0	0	0	0	0	G54V	0	K427E	E255D	Y46F	0
DI 15-99	SRR7841986		2008	United States, Maryland	Clinical	Clade II	>16	0.5			0	0	0	0	0	0	0	0	0	0	0	0	0	G54W	K427E	E255D	Y46F	0
DI 15-98	SRR7841987		2008	United States	Clinical	Clade II	16	16			S305P	0	0	0	0	0	0	0	0	0	0	0	0	0	K427E	E255D	Y46F	0
DI 15-97	SRR7841992		2008	United States, North Carolina	Clinical	Clade II	4	4			S305P	0	0	0	0	0	0	0	0	0	0	0	0	0	K427E	E255D	Y46F	0
DI 15-118	SRR7841996		2014	United States	Clinical	Clade II	>16	2			0	0	0	0	0	0	0	0	0	0	0	0	0	0	K427E	E255D	Y46F	0
DI 15-114	SRR7841998		2014	United States, California	Clinical	Clade II	>16	4			0	0	0	0	0	0	0	0	0	0	0	0	0	G54R	K427E	E255D	Y46F	0
DI 15-115	SRR7841999		2014	United States	Clinical	Clade II	>16	0.5			0	0	0	0	0	M220I	0	0	0	0	0	0	0	0	K427E	E255D	Y46F	0
DI 15-102	SRR7841978		2010	United States, Pennsylvania	Clinical	Clade III	>32	8	https://dc.uthsc.edu/cgi/viewcontent.cgi?article=1494&context=dissertations	CLSI M38-A2	0	0	0	0	0	0	0	0	0	0	0	L98H	0	0	K427E	E255D	Y46F	0
DI 15-100	SRR7841979		2008	United States	Clinical	Clade II	>32	8			0	0	I412S	0	0	0	0	0	0	0	0	0	0	0	K427E	E255D	Y46F	0
DI 15-106	SRR7841983		2012	United States	Clinical	Clade III	4	>32			0	0	0	0	T289A	0	0	0	0	0	Y121F	0	0	0	K427E	E255D	Y46F	0
DI 15-108	SRR7841985		2012	United States, California	Clinical	Clade II	>32	16			0	0	0	0	0	0	0	0	0	G138C	0	0	0	0	K427E	E255D	Y46F	0
DI 15-96	SRR7841993		2008	United States, Arizona	Clinical	Clade III	4	>32			0	0	0	0	T289A	0	0	0	0	0	Y121F	0	0	0	K427E	E255D	Y46F	0
DI 15-95	SRR7841994		2007	United States, Connecticut	Clinical	Clade II	>32	16			0	0	I412S	0	0	0	0	0	0	0	0	0	0	0	K427E	E255D	Y46F	0
DI 15-120	SRR7841997		2015	United States, Ohio	Clinical	Clade II	>32	>32			0	0	0	G448S	0	0	0	0	0	0	0	0	0	0	K427E	E255D	Y46F	0
DI 15-116	SRR7842000		2014	United States, Pennsylvania	Clinical	Clade III	>32	8			0	0	0	0	0	0	0	0	0	0	0	L98H	0	0	K427E	E255D	Y46F	0
DI 15-117	SRR7842001		2014	United States, Maryland	Clinical	Clade II	>32	2			0	0	0	0	0	0	0	F219S	0	0	0	0	0	0	K427E	E255D	Y46F	0
DI 16-8	SRR7841988		NA	United States	Clinical	Clade II	NA	NA	NA	NA	0	0	0	0	0	0	0	0	0	0	0	0	0	0	K427E	E255D	Y46F	0
DI 16-7	SRR7841989		NA	United States	Clinical	Clade II	NA	NA			0	0	0	0	0	0	0	0	0	0	0	0	0	0	K427E	E255D	Y46F	0
DI 16-6	SRR7841990		NA	United States	Clinical	Clade II	NA	NA			0	0	0	0	0	0	0	0	0	0	0	0	0	0	K427E	E255D	Y46F	0
DI 16-5	SRR7841991		NA	United States	Clinical	Clade II	NA	NA			0	0	0	0	0	0	0	0	0	0	0	0	0	0	K427E	E255D	Y46F	0
DI 16-9	SRR7841995		NA	United States	Clinical	Clade II	NA	NA			0	0	0	0	0	0	0	0	0	0	0	0	0	0	K427E	E255D	Y46F	0
B5852	SRR343134	PRJNA67101	1998	United States, California	Clinical	Clade II	NA	NA	NA	NA	0	0	0	0	0	0	0	0	0	0	0	0	0	0	K427E	E255D	Y46F	0
B5854	SRR343135		1998	United States, California	Clinical	Clade II	NA	NA			0	0	0	0	0	0	0	0	0	0	0	0	0	0	K427E	E255D	Y46F	0
B5856	SRR343136		1998	United States, California	Clinical	Clade II	NA	NA			0	0	0	0	0	0	0	0	0	0	0	0	0	0	K427E	E255D	Y46F	0
B5859	SRR343137		1998	United States, California	Clinical	Clade III	NA	NA			0	0	0	0	0	0	0	0	0	0	0	0	0	0	K427E	E255D	Y46F	0
B5863	SRR343138		1998	United States, California	Environmental	Clade II	NA	NA			0	0	0	0	0	0	0	0	0	0	0	0	0	0	K427E	E255D	Y46F	0
B5866	SRR343139		1998	United States, California	Environmental	Clade II	NA	NA			0	0	0	0	0	0	0	0	0	0	0	0	0	0	K427E	E255D	Y46F	0
B5868	SRR343140		1998	United States, California	Environmental	Clade II	NA	NA			0	0	0	0	0	0	0	0	0	0	0	0	0	0	K427E	E255D	Y46F	0
B6069	SRR343141		2002	Canada	Clinical	Clade II	NA	NA			0	0	0	0	0	0	0	0	0	0	0	0	0	0	K427E	E255D	Y46F	0
B6074	SRR343142		2002	Canada	Clinical	Clade II	NA	NA			0	0	0	0	0	0	0	0	0	0	0	0	0	0	K427E	E255D	Y46F	0
B6078	SRR343143		2002	Canada	Environmental	Clade II	NA	NA			0	0	0	0	0	0	0	0	0	0	0	0	0	0	K427E	E255D	Y46F	0
B6079	SRR343145		2002	Canada	Environmental	Clade II	NA	NA			0	0	0	0	0	0	0	0	0	0	0	0	0	0	K427E	E255D	Y46F	0
B6081	SRR343146		2002	Canada	Environmental	Clade II	NA	NA			0	0	0	0	0	0	0	0	0	0	0	0	0	0	K427E	E255D	Y46F	0
F17729	SRR617739		NA	United Kingdom	Clinical	Clade II	NA	NA			0	0	0	0	0	0	0	0	0	0	0	0	0	0	K427E	E255D	Y46F	0
F15927	SRR617734		NA	Canada	Clinical	Clade I	NA	NA			0	0	0	0	0	0	0	0	0	0	0	0	0	0	0	E255D	0	0
F11628	SRR343149		2004	United Kingdom	Clinical	Clade III	>8	>8	DOI: 10.1128/AAC.00517-11	EUCAST	0	0	0	0	0	0	0	0	0	G138C	0	0	0	0	K427E	E255D	Y46F	0
F12865	SRR343150		2004	United Kingdom	Clinical	Clade III	>8	8			0	0	0	0	0	0	0	0	0	G138C	0	0	0	0	K427E	E255D	Y46F	0
F12041	SRR617723		2004	United Kingdom	Clinical	Clade III	>8	>8			0	0	0	0	0	0	0	0	0	G138C	0	0	0	0	K427E	E255D	Y46F	0
F13535	SRR617726		2005	United Kingdom	Clinical	Clade III	>8	8			0	0	0	0	0	0	0	0	0	G138C	0	0	0	0	K427E	E255D	Y46F	0
F15767	SRR343152		NA	United Kingdom	Clinical	Clade II	0.25	0.5	https://doi.org/10.1111/j.1469-0691.2009.02911.x	EUCAST	0	0	0	0	0	0	0	0	0	0	0	0	0	0	K427E	E255D	Y46F	0
AF41	SRR617720		1988	United States	Clinical	Clade II	0.13	0.5	doi:10.1371/journal.pone.0158724	NA	0	0	0	0	0	0	0	0	0	0	0	0	0	0	K427E	E255D	Y46F	0
AF72	SRR617721		1989	United States	Clinical	Clade II	8	0.5			0	0	0	0	0	0	0	0	0	0	0	0	G54V	0	K427E	E255D	Y46F	0
AF90	SRR617722		1989	United States	Clinical	Clade II	8	1			0	0	0	0	0	0	M220V	0	0	0	0	0	0	0	K427E	E255D	Y46F	0
F12219	SRR617724		NA	United Kingdom	Clinical	Clade II	>8	0.125	DOI: 10.3201/eid1507.090043	EUCAST	0	0	0	0	0	0	0	0	0	0	0	0	0	0	K427E	E255D	Y46F	0
F12636	SRR617725		NA	United Kingdom	Clinical	Clade III	>8	0.125			0	0	0	0	0	0	0	0	0	0	0	0	G54V	0	K427E	E255D	Y46F	0
F13619	SRR617727		NA	United Kingdom	Clinical	Clade III	>8	>8			0	0	0	G448S	0	0	0	0	0	0	0	0	0	0	K427E	E255D	Y46F	0
F13952	SRR617728		NA	United Kingdom	Clinical	Clade III	>8	>8			0	0	0	0	0	0	0	0	0	G138C	0	0	0	0	K427E	E255D	Y46F	0
F14403	SRR617729		NA	United Kingdom	Clinical	Clade II	>8	0.5			0	0	0	0	0	0	0	0	0	0	0	0	0	G54W	K427E	E255D	Y46F	0
F14532	SRR617731		NA	United Kingdom	Clinical	Clade III	>8	1			0	0	0	0	0	0	0	0	0	0	0	0	0	0	K427E	E255D	Y46F	0
F15390	SRR617733		NA	United Kingdom	Clinical	Clade III	>8	4			0	0	0	0	0	0	0	0	0	0	0	0	0	0	K427E	E255D	Y46F	0
F16134	SRR617735		NA	Canada	Clinical	Clade II	>8	4			0	0	0	0	0	0	0	0	0	0	0	0	0	0	K427E	E255D	Y46F	0
F16216	SRR617736		NA	United Kingdom	Clinical	Clade III	>8	8			0	0	0	0	0	0	0	0	0	0	0	L98H	0	0	K427E	E255D	Y46F	0
F16311	SRR617737		NA	United Kingdom	Clinical	Clade II	>8	8			0	0	I412T	0	0	0	0	0	0	0	0	0	0	0	K427E	E255D	Y46F	0
F7763	SRR617744		NA	United Kingdom	Clinical	Clade II	>8	2			0	0	0	0	0	0	0	0	0	0	0	0	0	0	0	0	0	0
F17764	SRR617745		NA	Canada	Clinical	Clade II	0.25	2			0	0	0	0	0	0	0	0	0	0	0	0	0	0	K427E	E255D	Y46F	0
F17582	SRR617738		NA	United Kingdom	Clinical	Clade III	>8	1	https://www.escholar.manchester.ac.uk/api/datastream?publicationPid=uk-ac-man-scw:164264&datastreamId=FULL-TEXT.PDF	EUCAST	0	0	0	0	0	0	0	0	0	0	0	0	0	0	K427E	E255D	Y46F	0
F18085	SRR617742		NA	United Kingdom	Clinical	Clade II	>8	4			0	0	I412T	0	0	0	0	0	0	0	0	0	0	0	K427E	E255D	Y46F	0
T8015994	SRR10997241	PRJNA575185	2015	United States, Pittsburgh, PA	NA	Clade II	NA	NA	NA	NA	0	0	0	0	0	0	0	0	0	0	0	0	0	0	K427E	E255D	Y46F	0
H7810724	SRR10997243		2015	United States, Pittsburgh, PA	NA	Clade II	NA	NA			0	0	0	0	0	0	0	0	0	0	0	0	0	0	K427E	E255D	Y46F	0
925	SRR10997260		2015	United States, Pittsburgh, PA	NA	Clade II	NA	NA			0	0	0	0	0	0	0	0	0	0	0	0	0	0	K427E	E255D	Y46F	0
VPCI 1155/P/13	SRR9265315	PRJNA548244	2017	India	Clinical	Clade II	16	0.25	https://doi.org/10.1016/j.fgb.2019.103265	CLSI M38-A2	0	0	0	0	0	0	0	0	0	0	0	0	G54V	0	K427E	E255D	Y46F	0
VPCI 1882/14	SRR9265316		2017	India	Clinical	Clade II	16	8			0	0	0	0	0	0	0	0	0	0	0	0	0	0	K427E	E255D	Y46F	0
VPCI 40/Ei/13/3/b	SRR9265317		2017	India	Environmental	Clade II	16	0.25			0	0	0	0	0	0	0	0	0	0	0	0	G54V	0	K427E	E255D	Y46F	0
VPCI 497/Ei/12/3	SRR9265318		2017	India	Environmental	Clade II	>16	8			0	0	0	0	0	0	0	0	0	0	0	0	0	0	K427E	E255D	Y46F	0
SGAir0713	SRR9067511	PRJNA388547	2016	Singapore	Environmental	Clade II	NA	NA	NA	NA	0	0	0	0	0	0	0	0	0	0	0	0	0	0	0	0	0	0
V130-54	SRR8759697	PRJNA528395	2011	Netherlands	Clinical	Clade II	>16	1	https://doi.org/10.1016/j.fgb.2018.02.003	EUCAST	0	0	0	0	0	0	0	0	0	0	0	0	0	0	K427E	E255D	Y46F	0
V130-18	SRR8759698		2011	Netherlands	Clinical	Clade II	4	4			0	0	0	0	0	0	0	0	0	0	0	0	0	0	K427E	E255D	Y46F	0
V130-14	SRR8759699		2011	Netherlands	Clinical	Clade II	1	1			0	0	0	0	0	0	0	0	0	0	0	0	0	0	K427E	E255D	Y46F	0
V130-15	SRR8759700		2011	Netherlands	Clinical	Clade II	1	1			0	0	0	0	0	0	0	0	0	0	0	0	0	0	K427E	E255D	Y46F	0
V157-48	SRR8759701		2013	Netherlands	Clinical	Clade II	>16	2			0	0	0	0	0	0	0	0	0	0	0	0	0	0	K427E	E255D	Y46F	0
V157-40	SRR8759702		2013	Netherlands	Clinical	Clade II	>16	1			0	0	0	0	0	0	0	0	0	0	0	0	G54E	0	K427E	E255D	Y46F	0
V157-39	SRR8759703		2013	Netherlands	Clinical	Clade II	>16	1			0	0	0	0	0	0	0	0	0	0	0	0	0	G54W	K427E	E255D	Y46F	0
V157-59	SRR8759704		2013	Netherlands	Clinical	Clade II	>16	4			0	0	0	0	0	0	0	0	0	0	0	0	0	0	K427E	E255D	Y46F	0
V157-47	SRR8759705		2013	Netherlands	Clinical	Clade II	>16	2			0	0	NA	NA	0	0	0	0	P216L	0	NA	0	0	0	NA	E255D	Y46F	0
V157-62	SRR8759706		2013	Netherlands	Clinical	Clade II	>16	8			0	0	0	0	0	0	0	0	0	0	0	0	0	0	K427E	E255D	Y46F	L167*
V157-61	SRR8759707		2013	Netherlands	Clinical	Clade II	>16	4			0	0	0	0	0	0	0	0	0	0	0	0	0	0	K427E	E255D	Y46F	0
V157-60	SRR8759708		2013	Netherlands	Clinical	Clade II	>16	4			0	0	0	0	0	0	0	0	0	0	0	0	0	0	K427E	E255D	Y46F	0
V157-80	SRR8759709		2013	Netherlands	Clinical	Clade II	>16	1			0	0	0	0	0	0	0	0	P216L	0	0	0	0	0	K427E	E255D	Y46F	0
AfA1	DRR237582	PRJDB10244	2016	Japan, Nagasaki, Sakamoto	Clinical	Clade II	NA	NA	NA	NA	0	0	0	0	0	0	0	0	0	0	0	0	0	0	K427E	E255D	Y46F	0
AfA2	DRR237583		2016	Japan, Nagasaki, Sakamoto	Clinical	Clade II	NA	NA			0	0	0	0	0	0	0	0	0	0	0	0	0	0	K427E	E255D	Y46F	0
CON4	SRR12894204	PRJNA671765	2020	Hamilton, Canada	Environmental	Clade II	1	1	DOI: 10.3390/microorganisms8111673	CLSI M38-A2	0	0	0	0	0	0	0	0	0	0	0	0	0	0	K427E	E255D	Y46F	0
CM21	SRR12894203		2020	Hamilton, Canada	Environmental	Clade III	1	0.125			0	0	0	0	0	0	0	0	0	0	0	0	0	0	K427E	E255D	Y46F	0
CM65	SRR12894200		2020	Hamilton, Canada	Environmental	Clade II	1	1			0	0	0	0	0	0	0	0	0	0	0	0	0	0	K427E	E255D	Y46F	0
P80	SRR12894199		2020	Hamilton, Canada	Environmental	Clade II	1	0.5			0	0	0	0	0	0	0	0	0	0	0	0	0	0	K427E	E255D	Y46F	0
15_1	SRR12894198		2020	Hamilton, Canada	Clinical	Clade II	1	0.5			0	0	0	0	0	0	0	0	0	0	0	0	0	0	K427E	E255D	Y46F	0
AV88	SRR12894197		2020	Hamilton, Canada	Environmental	Clade II	1	0.5			0	0	0	0	0	0	0	0	0	0	0	0	0	0	K427E	E255D	Y46F	0
15_33	SRR12894196		2020	Hamilton, Canada	Clinical	Clade II	1	0.125			0	0	0	0	0	0	0	0	0	0	0	0	0	0	K427E	E255D	Y46F	0
P20	SRR12894195		2020	Hamilton, Canada	Environmental	Clade II	1	0.5			0	0	0	0	0	0	0	0	0	0	0	0	0	0	K427E	E255D	Y46F	0
CM38	SRR12894194		2020	Hamilton, Canada	Environmental	Clade II	1	0.25			0	0	0	0	0	0	0	0	0	0	0	0	0	0	K427E	E255D	Y46F	0
CM11	SRR12894193		2020	Hamilton, Canada	Environmental	Clade II	0.5	0.5			0	0	0	0	0	0	0	0	0	0	0	0	0	0	K427E	E255D	Y46F	0
AFB62-1	SRR12894202		2020	San Antonio, United States	Clinical	Clade II	NA	NA	NA	NA	0	0	0	0	0	0	0	0	0	0	0	0	0	0	K427E	E255D	Y46F	0
AFIR928	SRR12894201		2020	Dublin, Ireland	Environmental	Clade II	NA	NA			0	0	0	0	0	0	0	0	0	0	0	0	0	0	K427E	E255D	Y46F	0

NA means not available.
0 in mutation panels indicates the absence of the mutation.

Table S2.2. Overexpressed genes with itraconazole and voriconazole exposure determined through previous RT-qPCR and RNA-seq analyses.

Strain	Overexpressed Gene(s)	Encoded Protein(s)	Function and/or Associated Pathway	Fold Change	Experimental Conditions	Reference
Af293 (wildtype)	*AFUA_2G11580*	MFS Multidrug Transporter, putative	Membrane transport activity	14.20	Exposure to 1 mg/L itraconazole in Vogel's 1% glucose minimal media for 4 hours.	[25]
	abcA-1 (AFUA_1G17440)	ABC Multidrug Transporter	Membrane transport activity	7.10		
	mdr1 (AFUA_5G06070)	ABC Multidrug Transporter	Membrane transport activity	~5.00		
	abcB (AFUA_1G10390)	ABC Multidrug Transporter	Membrane transport activity	~4.50		
	abcC (AFUA_1G14330)	ABC Multidrug Transporter	Membrane transport activity	~5.50		
	abcD (AFUA_6G03470)	ABC Multidrug Transporter	Membrane transport activity	~4.50		
	abcE (AFUA_7G00480)	ABC Multidrug Transporter	Membrane transport activity	~1.00		
	mdr4 (AFUA_1G12690)	ABC Multidrug Transporter	Membrane transport activity	~4.70		
	mfsA (AFUA_8G05710)	MFS Multidrug Transporter	Membrane transport activity	~4.70		
	mfsC (AFUA_1G03200)	MFS Multidrug Transporter	Membrane transport activity	~7.90		
	AFUA_5G02260	ABC multidrug transporter, putative	Membrane transport activity	~4.90		
	abcA-2 (AFUA_2G15130)	ABC Multidrug Transporter	Membrane transport activity	~6.50		
	mfs56 (AFUA_1G05010)	MFS Multidrug Transporter, putative	Membrane transport activity	~4.50		
F20140 (non-cyp51A mutant and itraconazole-resistant)	*abcC (AFUA_1G14330)*	ABC Multidrug Transporter	Membrane transport activity	>25.00*	Growth in Vogel's 1% glucose minimal media with DMSO added in place of itraconzaole.	
F18304 (non-cyp51A mutant and itraconazole-resistant)				>70.00*		
F17727 (non-cyp51A mutant and posoconazole, voriconazole and itraconazole-resistant)				>25.00*		
F19980 (non-cyp51A mutant and voriconazole and itraconazole-resistant)				7.20*		
F20063 (non-cyp51A mutant and itraconazole-resitant)				6.50*		
F20451 (non-cyp51A mutant and itraconazole-resistant)				3.60*		
F18454 (non-cyp51A mutant and voriconazole-resistant only)				5.10*		
F15483 (azole-susceptibe)				2.10*		
F15483 (azole-susceptible)	*mfs56 (AFUA_1G05010)*	MFS Multidrug Transporter, putative	Membrane transport activity	~7.00	Exposure to 1 mg/L itraconazole in Vogel's 1% glucose minimal media for 4 hours.	
F18329 (non-cyp51A mutant and voriconazole-resistant)				~7.00		
F18304 (non-cyp51A mutant and itraconazole-resistant)				~5.00		
F18149 (non-cyp51A mutant and posoconazole, voriconazole and itraconazole-resistant)				~110.00		
F20063 (non-cyp51A mutant and itraconazole-resistant)				~550.00		
F18085 (cyp51A mutation A248T and itraconazole-resistant)				~500.00*		
F17999 (cyp51A mutations G448S and H147Y and voriconazole and itraconazole-resistant)				~700.00*		
F19980 (non-cyp51A voriconazole and itaconazole-resistant)				27.80*		
F20140 (non-cyp51A itraconazole-resistant)				35.60*		
F20451 (non-cyp51A itaconazole-resistant)				17.70*		
F17999 (cyp51A mutations G448S and H147Y and voriconazole and itaconazole-resistant)	*atrF (AFUA_6G04360)*	ABC Multidrug Transporter	Membrane transport activity	31.70*		
F18304 (non-cyp51A mutant and itraconazole-resistant)	*cyp51A (AFUA_4G06890)*	Sterol 14-alpha demethylase	Ergosterol Biosynthesis	550.90*		
F19980 (non-cyp51A mutant and voriconazole and itraconazole-resistant)				21.00*		
ATCC 46645 (wildtype)	*mdr1 (AFUA_5G06070)*	ABC Multidrug Transporter	Membrane transport activity	~2.00	Exposure to 0.5 µg/mL voriconazole for 120 minutes during growth at 37°C.	[38]
				~5.00	Exposure to 0.5 µg/mL voriconazole for 240 minutes during growth at 37°C.	
	abcB (AFUA_1G10390)	ABC Multidrug Transporter	Membrane transport activity	~7.00	Exposure to 0.5 µg/mL voriconazole for 30 minutes during growth at 37°C.	
				~7.00	Exposure to 0.5 µg/mL voriconazole for 60 minutes during growth at 37°C.	
				~13.00	Exposure to 0.5 µg/mL voriconazole for 120 minutes during growth at 37°C.	
				~5.00	Exposure to 0.5 µg/mL voriconazole for 240 minutes during growth at 37°C.	
	abcC (AFUA_1G14330)	ABC Multidrug Transporter	Membrane transport activity	~5.00	Exposure to 0.5 µg/mL voriconazole for 60 minutes during growth at 37°C.	
				~10.00	Exposure to 0.5 µg/mL voriconazole for 120 minutes during growth at 37°C.	
				>20.00	Exposure to 0.5 µg/mL voriconazole for 240 minutes during growth at 37°C.	
	abcD (AFUA_6G03470)	ABC Multidrug Transporter	Membrane transport activity	~2.00	Exposure to 0.5 µg/mL voriconazole for 60 minutes during growth at 37°C.	
				>2.00	Exposure to 0.5 µg/mL voriconazole for 120 minutes during growth at 37°C.	
				>20.00	Exposure to 0.5 µg/mL voriconazole for 240 minutes during growth at 37°C.	
	abcE (AFUA_7G00480)	ABC Multidrug Transporter	Membrane transport activity	~2.00	Exposure to 0.5 µg/mL voriconazole for 30 minutes during growth at 37°C.	
				~7.5	Exposure to 0.5 µg/mL voriconazole for 60 minutes during growth at 37°C.	
				>10.00	Exposure to 0.5 µg/mL voriconazole for 120 minutes during growth at 37°C.	
				>20.00	Exposure to 0.5 µg/mL voriconazole for 240 minutes during growth at 37°C.	
	mfsA (AFUA_8G05710)	MFS Multidrug Transporter	Membrane transport activity	~11.00	Exposure to 0.5 µg/mL voriconazole for 30 minutes during growth at 37°C.	
				~5.00	Exposure to 0.5 µg/mL voriconazole for 60 minutes during growth at 37°C.	
				~1.50	Exposure to 0.5 µg/mL voriconazole for 120 minutes during growth at 37°C.	
				~2.00	Exposure to 0.5 µg/mL voriconazole for 240 minutes during growth at 37°C.	
	mfsB (AFUA_1G15490)	MFS Multidrug Transporter	Membrane transport activity	~4.00	Exposure to 0.5 µg/mL voriconazole for 60 minutes during growth at 37°C.	
				~10.00	Exposure to 0.5 µg/mL voriconazole for 120 minutes during growth at 37°C.	
				~18.00	Exposure to 0.5 µg/mL voriconazole for 240 minutes during growth at 37°C.	
	mfsC (AFUA_1G03200)	MFS Multidrug Transporter	Membrane transport activity	~2.50	Exposure to 0.5 µg/mL voriconazole for 60 minutes during growth at 37°C.	
				>15.00	Exposure to 0.5 µg/mL voriconazole for 120 minutes during growth at 37°C.	
				~30.00	Exposure to 0.5 µg/mL voriconazole for 240 minutes during growth at 37°C.	
	fbpA (AFUA_1G14050)	F-box domain protein	NA	>50.00	Exposure to 0.5 µg/mL voriconazole for 120 minutes during growth at 37°C.	
				~600.00	Exposure to 0.5 µg/mL voriconazole for 240 minutes during growth at 37°C.	

	aaaA (AFUA_7G06680)	AAA-family ATPase, putative	NA	~5.00	Exposure to 0.5 μg/mL voriconazole for 60 minutes during growth at 37°C.	
				~2.00	Exposure to 0.5 μg/mL voriconazole for 120 minutes during growth at 37°C.	
				~90.00	Exposure to 0.5 μg/mL voriconazole for 240 minutes during growth at 37°C.	
	finA (AFUA_8G05800)	C6 zinc finger domain protein	NA	~4.00	Exposure to 0.5 μg/mL voriconazole for 30 minutes during growth at 37°C.	
				~5.00	Exposure to 0.5 μg/mL voriconazole for 60 minutes during growth at 37°C.	
				>5.00	Exposure to 0.5 μg/mL voriconazole for 120 minutes during growth at 37°C.	
				~40.00	Exposure to 0.5 μg/mL voriconazole for 240 minutes during growth at 37°C.	
	cpcA (AFUA_4G12470)	BZIP transcription factor	NA	>1.50	Exposure to 0.5 μg/mL voriconazole for 30 minutes during growth at 37°C.	
				~3.00	Exposure to 0.5 μg/mL voriconazole for 120 minutes during growth at 37°C.	
				~5.50	Exposure to 0.5 μg/mL voriconazole for 240 minutes during growth at 37°C.	
	zfpA (AFUA_8G05010)	C2H2 zinc-finger transcription factor, putative	NA	~2.00	Exposure to 0.5 μg/mL voriconazole for 30 minutes during growth at 37°C.	
				~1.50	Exposure to 0.5 μg/mL voriconazole for 60 minutes during growth at 37°C.	
				~5.00	Exposure to 0.5 μg/mL voriconazole for 120 minutes during growth at 37°C.	
				~60.00	Exposure to 0.5 μg/mL voriconazole for 240 minutes during growth at 37°C.	
A1160C" (wildtype)	*fumR (AFUB_086150)* (Systematic name in other strains: *AFUA_8G00420*)	C6 zinc finger transcription factor	NA	4.70 with RNA-seq	Exposure to 0.5 μg/mL itraconazole for 120 minutes during growth at 37°C.	[39]
				4.00 with qRT-PCR		
	AFUB_063290 (Systematic name in other strains: *AFUA_4G06170*)	Predicted DNA-binding transcription factor	NA	3.89 with RNA-seq		
				3.79 with qRT-PCR		
	AFUB_051190 (Systematic name in other strains: *AFUA_5G02655*)	Predicted DNA-binding transcription factor	NA	3.84 with RNA-seq		
				2.75 with qRT-PCR		
	AFUB_055060 (Systematic name in other strains: *AFUA_5G07510*)	C6 transcription factor	NA	3.50 with RNA-seq		
				2.39 with qRT-PCR		
	AFUB_004490 (Systematic name in other strains: *AFUA_1G04140*)	C6 finger domain protein, putative	NA	2.94 with RNA-seq		
				2.04 with qRT-PCR		
	AFUB_089440 (Systematic name in other strains: *AFUA_7G03910*)	C2H2 zinc finger protein	NA	2.86 with RNA-seq		
				2.50 with qRT-PCR		
	AFUB_094860 (Systematic name in other strains: *AFUA_6G03430*)	C6 finger domain protein, putative	NA	2.78 with RNA-seq		
				2.93 with qRT-PCR		
	AFUB_003250 (Systematic name in other strains: *AFUA_1G02870*)	Transcription factor involved in oxidative stress response, putative	NA	2.48 with RNA-seq		
				2.61 with qRT-PCR		
	AFUB_070520 (Systematic name in other strains: *AFUA_4G13600*)	C2H2 finger domain protein, putative	NA	2.30 with RNA-seq		
				2.71 with qRT-PCR		
	AFUB_018270 (Systematic name in other strains: *AFUA_2G01190*)	Cu-dependent DNA-binding protein, putative	NA	2.10 with RNA-seq		
				1.30 with qRT-PCR		
	ada (AFUB_053880) (Systematic name in other strains: *AFUA_5G06350*)	DNA repair and transcription factor, putative	NA	2.05 with RNA-seq		
				1.23 with qRT-PCR		
	AFUB_096380 (Systematic name in other strains: *AFUA_6G01960*)	C6 finger domain protein, putative	NA	2.01 with RNA-seq		
				3.02 with qRT-PCR		
	AFUB_080380 (Systematic name in other strains: *AFUA_8G07360*)	C6 transcription factor, putative	NA	1.90 with RNA-seq		
				1.92 with qRT-PCR		
	AFUB_015800 (Systematic name in other strains: *AFUA_1G16460*)	BZIP transcription factor (LziP), putative	NA	1.75 with RNA-seq		
				2.12 with qRT-PCR		
	AFUB_040000 (Systematic name in other strains: *AFUA_3G09130*)	C6 transcription factor, putative	NA	1.73 with RNA-seq		
				2.22 with qRT-PCR		
	ace1 (AFUB_041100) (Systematic name in other strains: *AFUA_3G08010*)	C2H2 transcription factor, putative	NA	1.66 with RNA-seq		
				2.32 with qRT-PCR		

*fold-change relative to wildtype

Table S2.3. Significant single-nucleotide polymorphisms located in or near genes overexpressed with triazole exposure.

Overexpressed Gene	Region	Position (bp)	Predicted Effect (Amino Acid Substitution)	Using 122 strains				Using 101 strains				Using 58 strains			
				Fisher's Exact Test (p-values), MIC ≥ 2 mg/L		Fisher's Exact Test (p-values), MIC ≥ 4 mg/L		Fisher's Exact Test (p-values), MIC ≥ 2 mg/L		Fisher's Exact Test (p-values), MIC ≥ 4 mg/L		Fisher's Exact Test (p-values), MIC ≥ 2 mg/L		Fisher's Exact Test (p-values), MIC ≥ 4 mg/L	
				Itraconazole	Pan-azole	Itraconazole	Pan-azole	Itraconazole	Pan-azole	Itraconazole	Pan-azole	Itraconazole	Pan-azole	Itraconazole	Pan-azole
abcA (AFUA_1G17440)	Upstream Intergenic Region	4771080	Intergenic Variant	8.33E-03	2.39E-02	8.33E-03	3.30E-02	1.70E-04	5.82E-04	1.70E-04	3.33E-03	4.85E-05	8.71E-06	4.85E-05	4.20E-05
abcC (AFUA_1G14330)	Upstream Intergenic Region	3830296	Intergenic Variant	1.24E-05	1.75E-04	1.24E-05	6.43E-04	1.10E-04	2.10E-03	1.10E-04	5.21E-03	1.00E+00	1.00E+00	1.00E+00	1.00E+00
		3830605	Intergenic Variant	4.03E-06	7.33E-05	4.03E-06	2.93E-04	4.38E-05	1.02E-03	4.38E-05	2.58E-03	5.13E-01	5.43E-01	5.13E-01	1.00E+00
		3831146	Intergenic Variant	1.44E-06	3.05E-05	1.44E-06	1.96E-04	1.77E-05	7.48E-04	1.77E-05	1.13E-03	4.99E-01	5.21E-01	4.99E-01	5.36E-01
		3831171	Intergenic Variant	1.44E-06	3.05E-05	1.44E-06	1.96E-04	1.77E-05	7.48E-04	1.77E-05	1.13E-03	4.99E-01	5.21E-01	4.99E-01	5.36E-01
		3831268	Intergenic Variant	2.73E-06	5.26E-05	2.73E-06	2.40E-04	3.11E-05	8.71E-04	3.11E-05	2.33E-03	5.07E-01	5.34E-01	5.07E-01	5.51E-01
		3831281	Intergenic Variant	3.32E-06	6.23E-05	3.32E-06	2.64E-04	3.70E-05	9.41E-04	3.70E-05	2.44E-03	5.10E-01	5.38E-01	5.10E-01	1.00E+00
	Gene	3835967	Synonymous Variant (Ser1157Ser)	9.63E-06	1.47E-04	9.63E-06	5.44E-04	9.06E-05	1.97E-03	9.06E-05	4.95E-03	1.00E+00	1.00E+00	1.00E+00	1.00E+00
	Downstream Intergenic Region	3837214	Intergenic Variant	1.24E-05	1.75E-04	1.24E-05	6.43E-04	1.10E-04	2.10E-03	1.10E-04	5.21E-03	1.00E+00	1.00E+00	1.00E+00	1.00E+00
		3837626	Intergenic Variant	1.36E-05	1.75E-04	1.36E-05	6.43E-04	1.23E-04	2.10E-03	1.23E-04	5.21E-03	1.00E+00	1.00E+00	1.00E+00	1.00E+00
abcD (AFUA_6G03470)	Gene	744904	Synonymous Variant (Gly424Gly)	1.36E-05	1.97E-04	1.36E-05	6.43E-04	1.23E-04	2.28E-03	1.23E-04	5.21E-03	1.00E+00	1.00E+00	1.00E+00	1.00E+00
	Downstream Intergenic Region	748394	Intergenic Variant	2.36E-02	1.28E-02	2.36E-02	9.62E-03	1.21E-03	1.82E-04	1.21E-03	2.64E-04	4.23E-04	4.56E-05	4.23E-04	4.20E-05
abcE (AFUA_7G00480)	Gene	126254	Synonymous Variant (Asn316Asn)	3.32E-06	6.23E-05	3.32E-06	2.64E-04	3.70E-05	9.41E-04	3.70E-05	2.44E-03	1.00E+00	1.00E+00	1.00E+00	1.00E+00
		126699	Missense Variant (Val445Ala)	4.03E-06	7.33E-05	4.03E-06	2.93E-04	4.38E-05	1.02E-03	4.38E-05	2.58E-03	1.00E+00	1.00E+00	1.00E+00	1.00E+00
		126930	Intron Variant	4.03E-06	7.33E-05	4.03E-06	2.93E-04	4.38E-05	1.02E-03	4.38E-05	2.58E-03	1.00E+00	1.00E+00	1.00E+00	1.00E+00
		126943	Non-coding Transcript Variant	4.03E-06	7.33E-05	4.03E-06	2.93E-04	4.38E-05	1.02E-03	4.38E-05	2.58E-03	1.00E+00	1.00E+00	1.00E+00	1.00E+00
		126975	Synonymous Variant (Ala522Ala)	4.03E-06	7.33E-05	4.03E-06	2.93E-04	4.38E-05	1.02E-03	4.38E-05	2.58E-03	1.00E+00	1.00E+00	1.00E+00	1.00E+00
		127059	Synonymous Variant (Pro550Pro)	4.03E-06	7.33E-05	4.03E-06	2.93E-04	4.38E-05	1.02E-03	4.38E-05	2.58E-03	1.00E+00	1.00E+00	1.00E+00	1.00E+00
		127437	Synonymous Variant (Arg676Arg)	3.69E-06	7.12E-05	3.69E-06	2.64E-04	4.21E-05	1.04E-03	4.21E-05	2.44E-03	1.00E+00	1.00E+00	1.00E+00	1.00E+00
		127777	Non-coding Transcript Variant	3.32E-06	6.23E-05	3.32E-06	2.64E-04	3.70E-05	9.41E-04	3.70E-05	2.44E-03	1.00E+00	1.00E+00	1.00E+00	1.00E+00
fbpA (AFUA_1G14050)	Front Intergenic Region	3753452	Intergenic Variant	8.22E-06	9.39E-05	8.22E-06	9.87E-05	3.27E-04	1.20E-02	3.27E-04	4.21E-03	1.75E-01	5.62E-01	1.75E-01	3.84E-01
mfsA (AFUA_8G05710)	Gene	1357703	Missense Variant (Ile236Leu)	1.97E-05	1.00E-05	1.97E-05	5.09E-05	2.92E-04	2.15E-04	2.92E-04	5.99E-04	5.10E-01	5.38E-01	5.10E-01	1.00E+00
	Back Intergenic Region	1360714	Intergenic Variant	1.24E-05	1.75E-04	1.24E-05	6.43E-04	1.10E-04	2.10E-03	1.10E-04	5.21E-03	1.00E+00	1.00E+00	1.00E+00	1.00E+00
		1360749	Intergenic Variant	1.24E-05	1.75E-04	1.24E-05	6.43E-04	1.10E-04	2.10E-03	1.10E-04	5.21E-03	1.00E+00	1.00E+00	1.00E+00	1.00E+00
		1360948	Intergenic Variant	1.24E-05	1.75E-04	1.24E-05	6.43E-04	1.10E-04	2.10E-03	1.10E-04	5.21E-03	1.00E+00	1.00E+00	1.00E+00	1.00E+00
		1361307	Intergenic Variant	1.04E-05	1.51E-04	1.04E-05	5.89E-04	9.42E-05	1.97E-03	9.42E-05	5.05E-03	1.00E+00	1.00E+00	1.00E+00	1.00E+00
		1361336	Intergenic Variant	1.04E-05	1.51E-04	1.04E-05	5.89E-04	9.42E-05	1.97E-03	9.42E-05	5.05E-03	1.00E+00	1.00E+00	1.00E+00	1.00E+00
mfsB (AFUA_1G15490)	Front Intergenic Region	4182180	Intergenic Variant	3.58E-07	1.17E-05	3.58E-07	5.09E-05	6.31E-06	4.79E-04	6.31E-06	5.99E-04	1.40E-01	2.85E-01	1.40E-01	2.92E-01
mfsC (AFUA_1G03200)	Back Intergenic Region	923962	Intergenic Variant	4.46E-06	8.36E-05	4.46E-06	3.26E-04	4.97E-05	1.14E-03	4.97E-05	2.83E-03	1.00E+00	1.00E+00	1.00E+00	1.00E+00

fumR (AFUA_8G00420)	Gene	94618	Synonymous Variant (Ser462Ser)	1.24E-05	1.75E-04	1.24E-05	6.43E-04	1.10E-04	2.10E-03	1.10E-04	5.21E-03	1.00E+00	1.00E+00	1.00E+00	1.00E+00
AFUA_4G06170	Back Intergenic Region	1586706	Intergenic Variant	8.85E-05	7.94E-06	8.85E-05	2.26E-06	4.86E-02	2.26E-02	4.86E-02	6.87E-03	1.00E+00	1.00E+00	1.00E+00	1.00E+00
AFUA_5G02655	Front Intergenic Region	693982	Intergenic Variant	1.27E-05	2.97E-04	1.27E-05	1.32E-04	2.18E-04	5.66E-03	2.18E-04	1.31E-03	1.00E+00	1.00E+00	1.00E+00	1.00E+00
		694342	Intergenic Variant	1.27E-05	2.97E-04	1.27E-05	1.32E-04	2.18E-04	5.66E-03	2.18E-04	1.31E-03	1.00E+00	1.00E+00	1.00E+00	1.00E+00
		694623	Intergenic Variant	1.27E-05	2.97E-04	1.27E-05	1.32E-04	2.18E-04	5.66E-03	2.18E-04	1.31E-03	1.00E+00	1.00E+00	1.00E+00	1.00E+00
		695087	Intergenic Variant	1.04E-05	2.62E-04	1.04E-05	1.17E-04	2.03E-04	5.57E-03	2.03E-04	1.20E-03	1.00E+00	1.00E+00	1.00E+00	1.00E+00
	Gene	695661	Synonymous Variant (Ser163Ser)	1.04E-05	2.62E-04	1.04E-05	1.17E-04	2.03E-04	5.57E-03	2.03E-04	1.20E-03	1.00E+00	1.00E+00	1.00E+00	1.00E+00
AFUA_1G04140	Gene	1188593	Synonymous Variant (Arg14Arg)	7.06E-04	1.85E-05	7.06E-04	6.08E-06	8.15E-02	2.26E-02	8.15E-02	6.87E-03	2.70E-01	5.43E-01	2.70E-01	5.43E-01
AFUA_6G03430	Front Intergenic Region	732850	Intergenic Variant	7.53E-06	6.68E-07	7.53E-06	4.29E-06	6.64E-03	1.85E-03	6.64E-03	2.48E-03	5.41E-02	7.54E-02	5.41E-02	2.07E-01
		732931	Intergenic Variant	1.51E-05	1.52E-06	1.51E-05	5.03E-06	1.13E-02	3.56E-03	1.13E-02	2.75E-03	5.59E-02	7.99E-02	5.59E-02	2.11E-01
		732978	Intergenic Variant	1.51E-05	1.52E-06	1.51E-05	5.03E-06	1.13E-02	3.56E-03	1.13E-02	2.75E-03	5.59E-02	7.99E-02	5.59E-02	2.11E-01
		733672	Intergenic Variant	1.51E-05	1.52E-06	1.51E-05	5.03E-06	1.13E-02	3.56E-03	1.13E-02	2.75E-03	5.59E-02	7.99E-02	5.59E-02	2.11E-01
		734459	Intergenic Variant	1.15E-05	1.71E-04	1.15E-05	5.89E-04	1.06E-04	2.11E-03	1.06E-04	5.05E-03	1.00E+00	1.00E+00	1.00E+00	1.00E+00
		734710	Intergenic Variant	1.36E-05	1.97E-04	1.36E-05	6.43E-04	1.23E-04	2.28E-03	1.23E-04	5.21E-03	1.00E+00	1.00E+00	1.00E+00	1.00E+00
AFUA_4G13600	Front Intergenic Region	3552063	Intergenic Variant	1.24E-05	1.75E-04	1.24E-05	6.43E-04	1.10E-04	2.10E-03	1.10E-04	5.21E-03	1.00E+00	1.00E+00	1.00E+00	1.00E+00
		3553292	Intergenic Variant	1.21E-06	4.28E-06	1.21E-06	7.42E-06	2.95E-05	6.01E-05	2.95E-05	5.74E-05	4.09E-03	1.08E-02	4.09E-03	2.09E-02
	Back Intergenic Region	3554500	Intergenic Variant	5.50E-07	8.07E-07	5.50E-07	1.07E-06	3.20E-05	1.19E-04	3.20E-05	5.74E-05	4.09E-03	1.08E-02	4.09E-03	2.09E-02
		3556761	Intergenic Variant	3.60E-05	2.52E-06	3.60E-05	1.45E-05	1.38E-02	4.39E-03	1.38E-02	6.02E-03	2.53E-01	3.67E-01	2.53E-01	5.14E-01
AFUA_2G01190	Front Intergenic Region	277946	Intergenic Variant	1.76E-07	1.92E-06	1.76E-07	1.55E-06	1.15E-04	1.34E-03	1.15E-04	3.66E-04	6.17E-02	2.54E-01	6.17E-02	2.37E-01
AFUA_6G01960	Front Intergenic Region	291654	Intergenic Variant	1.99E-04	1.49E-03	1.99E-04	1.05E-03	1.41E-05	9.89E-04	1.41E-05	1.30E-03	5.12E-01	5.46E-01	5.12E-01	1.00E+00
	Back Intergenic Region	298044	Intergenic Variant	1.04E-05	1.51E-04	1.04E-05	5.89E-04	9.42E-05	1.97E-03	9.42E-05	5.05E-03	1.00E+00	1.00E+00	1.00E+00	1.00E+00
		300286	Intergenic Variant	1.24E-05	1.75E-04	1.24E-05	6.43E-04	1.10E-04	2.10E-03	1.10E-04	5.21E-03	1.00E+00	1.00E+00	1.00E+00	1.00E+00
		300438	Intergenic Variant	1.15E-05	1.71E-04	1.15E-05	5.89E-04	1.06E-04	2.11E-03	1.06E-04	5.05E-03	1.00E+00	1.00E+00	1.00E+00	1.00E+00
		300697	Intergenic Variant	1.36E-05	1.97E-04	1.36E-05	6.43E-04	1.23E-04	2.28E-03	1.23E-04	5.21E-03	1.00E+00	1.00E+00	1.00E+00	1.00E+00
		300966	Intergenic Variant	1.36E-05	1.97E-04	1.36E-05	6.43E-04	1.23E-04	2.28E-03	1.23E-04	5.21E-03	1.00E+00	1.00E+00	1.00E+00	1.00E+00
		301005	Intergenic Variant	1.36E-05	1.97E-04	1.36E-05	6.43E-04	1.23E-04	2.28E-03	1.23E-04	5.21E-03	1.00E+00	1.00E+00	1.00E+00	1.00E+00
		301043	Intergenic Variant	1.36E-05	1.97E-04	1.36E-05	6.43E-04	1.23E-04	2.28E-03	1.23E-04	5.21E-03	1.00E+00	1.00E+00	1.00E+00	1.00E+00
		301157	Intergenic Variant	1.24E-05	1.75E-04	1.24E-05	6.43E-04	1.10E-04	2.10E-03	1.10E-04	5.21E-03	1.00E+00	1.00E+00	1.00E+00	1.00E+00
		301174	Intergenic Variant	1.36E-05	1.97E-04	1.36E-05	6.43E-04	1.23E-04	2.28E-03	1.23E-04	5.21E-03	1.00E+00	1.00E+00	1.00E+00	1.00E+00
AFUA_1G16460	Front Intergenic Region	4463383	Intergenic Variant	3.69E-06	6.23E-05	3.69E-06	2.64E-04	4.21E-05	9.41E-04	4.21E-05	2.44E-03	1.00E+00	1.00E+00	1.00E+00	1.00E+00
		4464005	Intergenic Variant	3.69E-06	7.12E-05	3.69E-06	2.64E-04	4.21E-05	1.04E-03	4.21E-05	2.44E-03	1.00E+00	1.00E+00	1.00E+00	1.00E+00
		4464180	Intergenic Variant	3.32E-06	6.23E-05	3.32E-06	2.64E-04	3.70E-05	9.41E-04	3.70E-05	2.44E-03	1.00E+00	1.00E+00	1.00E+00	1.00E+00
		4464188	Intergenic Variant	3.32E-06	6.23E-05	3.32E-06	2.64E-04	3.70E-05	9.41E-04	3.70E-05	2.44E-03	1.00E+00	1.00E+00	1.00E+00	1.00E+00
		4464359	Intergenic Variant	3.32E-06	6.23E-05	3.32E-06	2.64E-04	3.70E-05	9.41E-04	3.70E-05	2.44E-03	1.00E+00	1.00E+00	1.00E+00	1.00E+00
		4464729	Intergenic Variant	4.03E-06	7.33E-05	4.03E-06	2.93E-04	4.38E-05	1.02E-03	4.38E-05	2.58E-03	1.00E+00	1.00E+00	1.00E+00	1.00E+00
	Back Intergenic Region	4467112	Intergenic Variant	5.57E-05	2.62E-04	5.57E-05	9.72E-04	1.43E-05	4.50E-04	1.43E-05	1.20E-03	1.00E+00	1.00E+00	1.00E+00	1.00E+00

** Statistically significant association between SNP and antifungal resistance are highlighted in red*

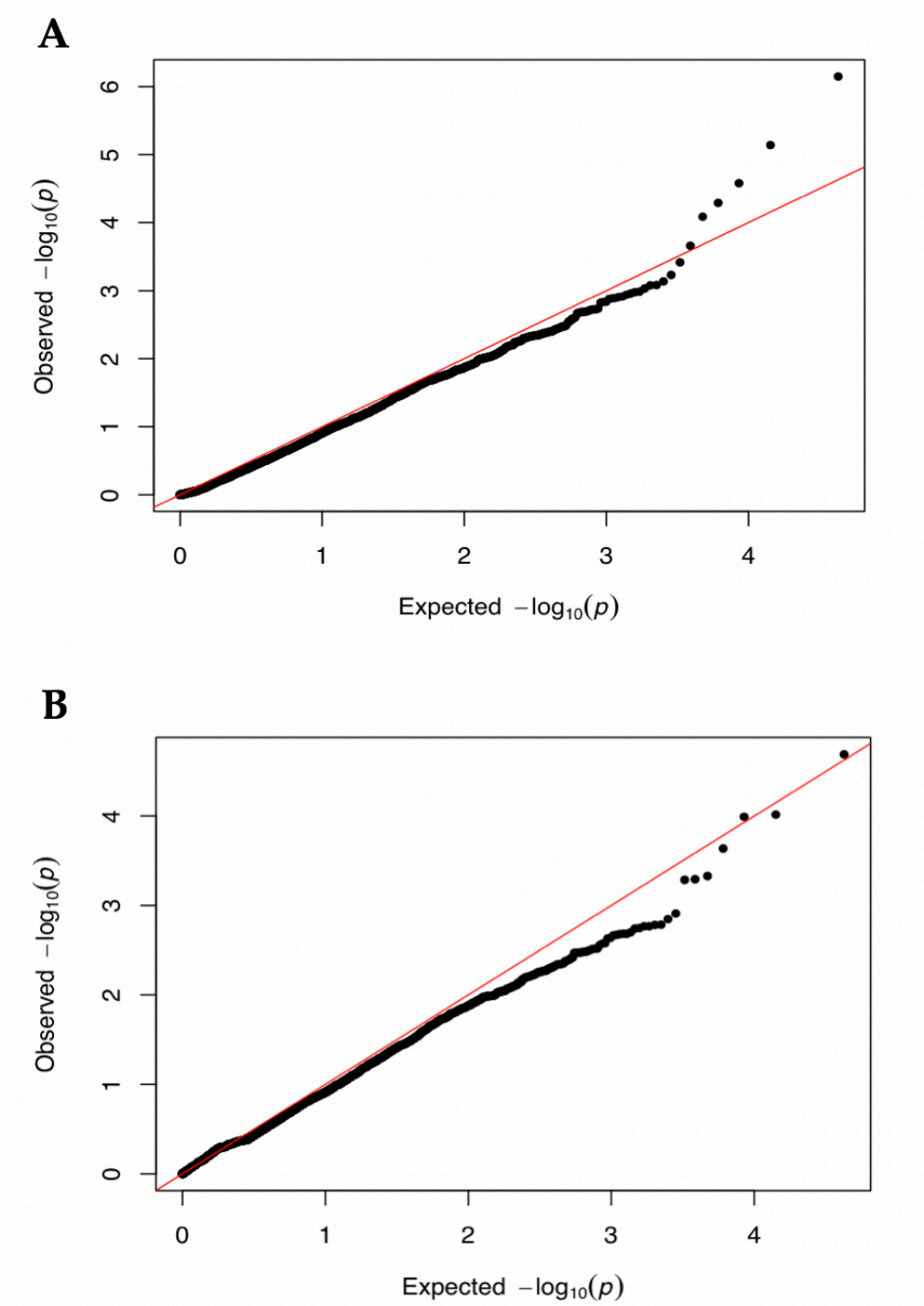

Figure S2.1. Quantile–quantile (Q-Q) plots from the GWAS for **(A)** itraconazole and **(B)** voriconazole.

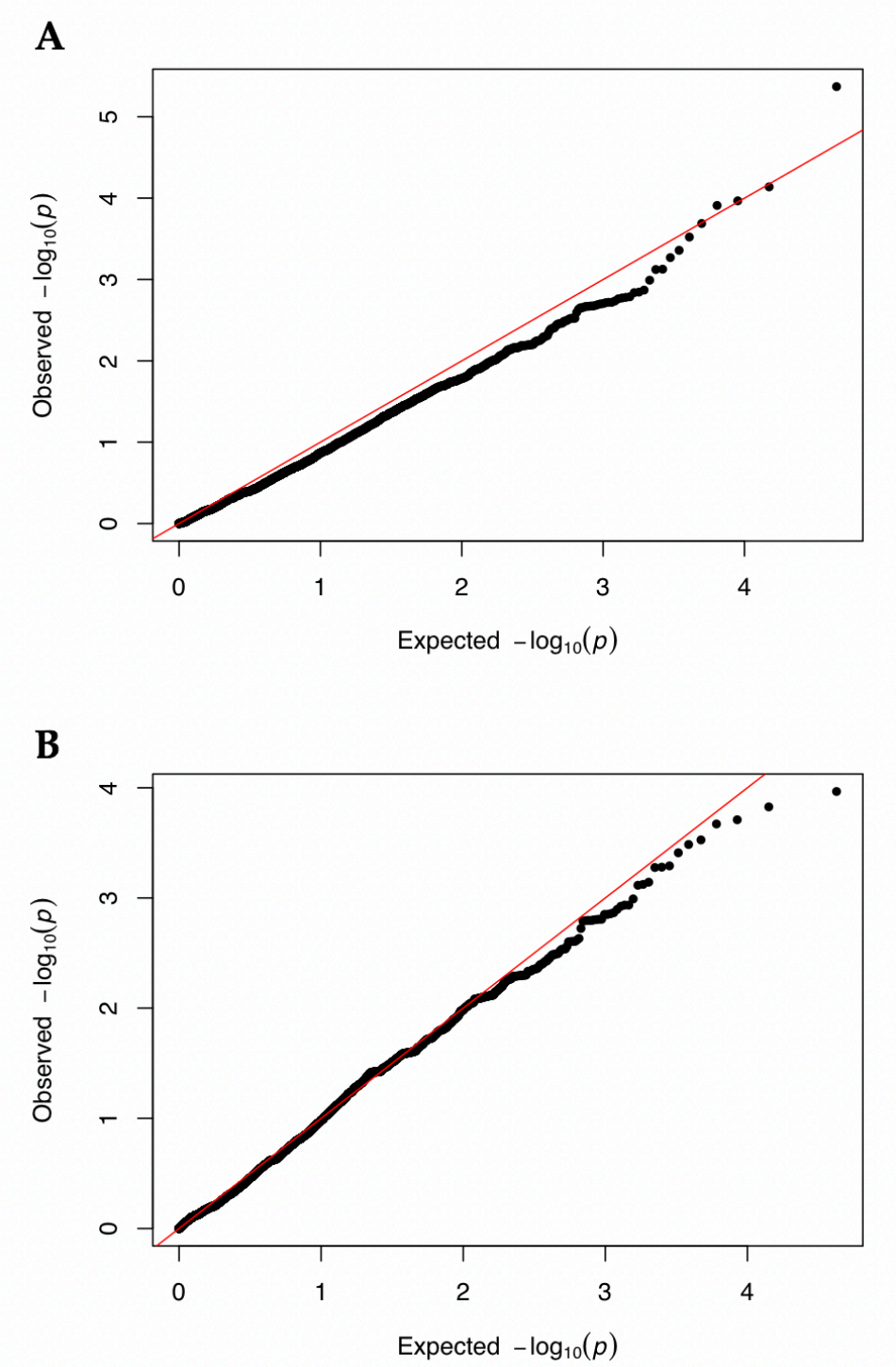

Figure S2.2. Quantile–quantile (Q-Q) plots from the second GWAS analysis, after removal of the 21 strains containing the L98H mutation in *cyp51A*, for **(A)** itraconazole and **(B)** voriconazole.

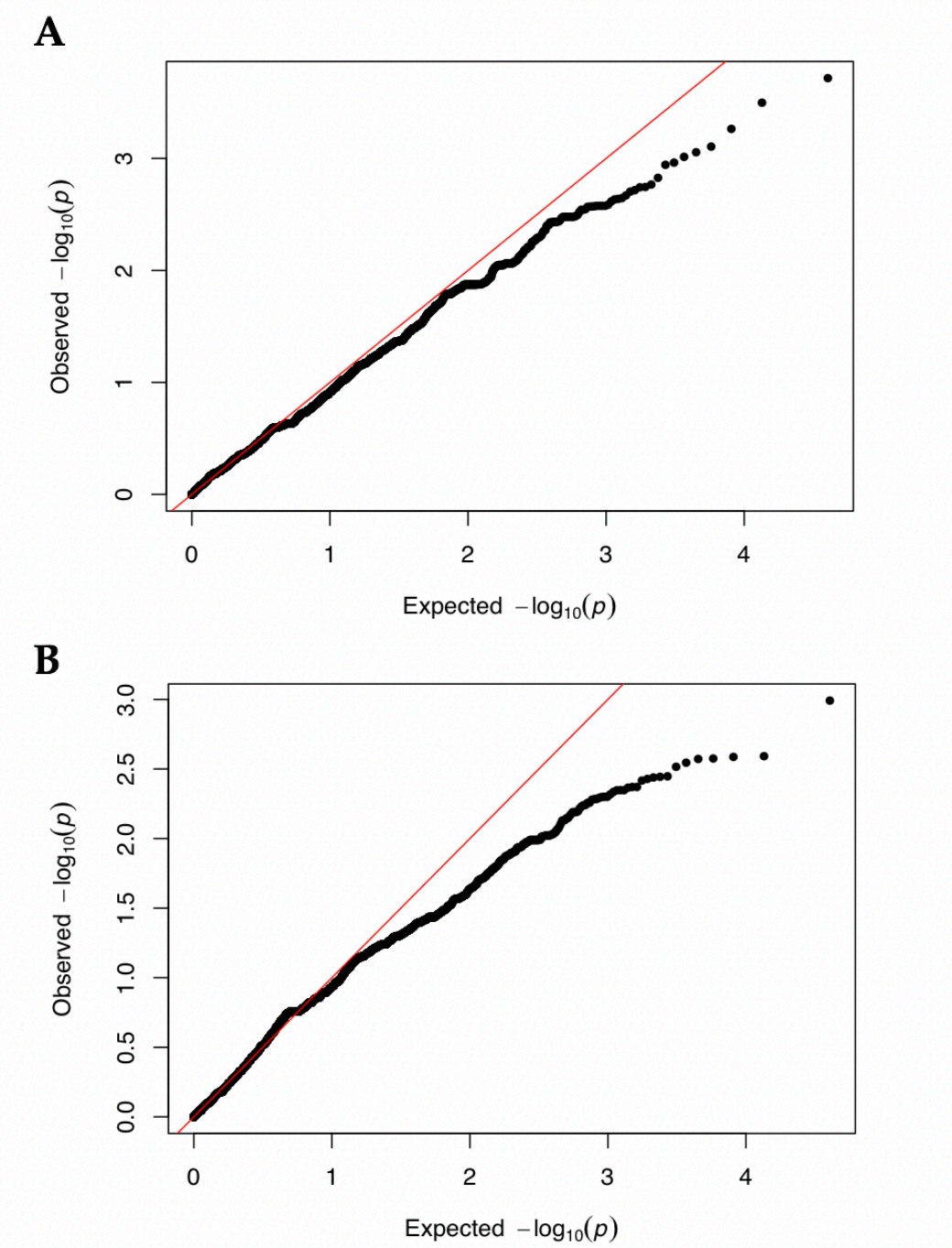

Figure S2.3. Quantile–quantile (Q-Q) plots from the third GWAS analysis, after removal of the 64 strains containing the well-known mutations in *cyp51A*, for **(A)** itraconazole and **(B)** voriconazole

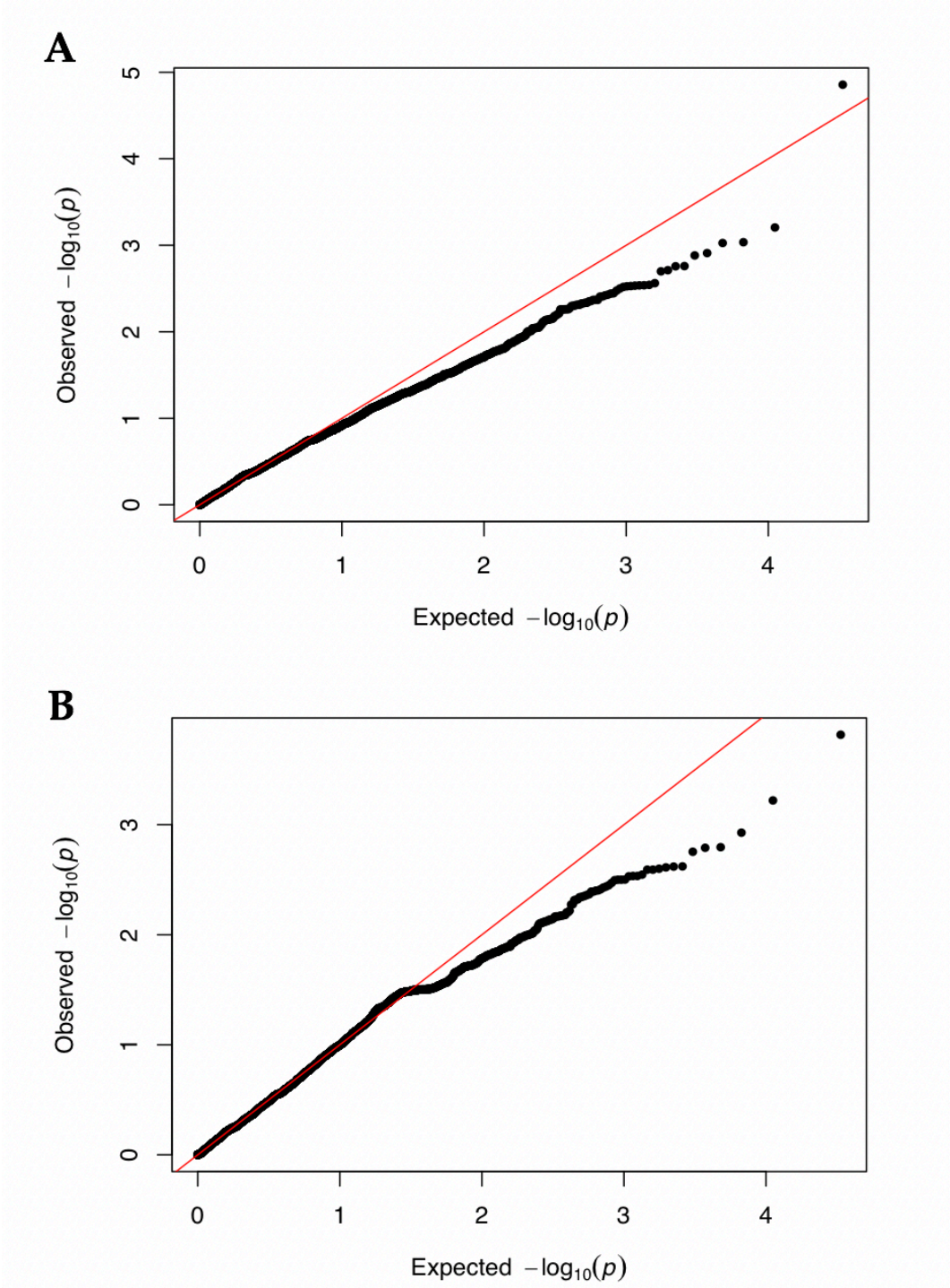

Figure S2.4. Quantile–quantile (Q-Q) plots from the fourth GWAS analysis, focusing on strains from Clade II, for **(A)** itraconazole and **(B)** voriconazole

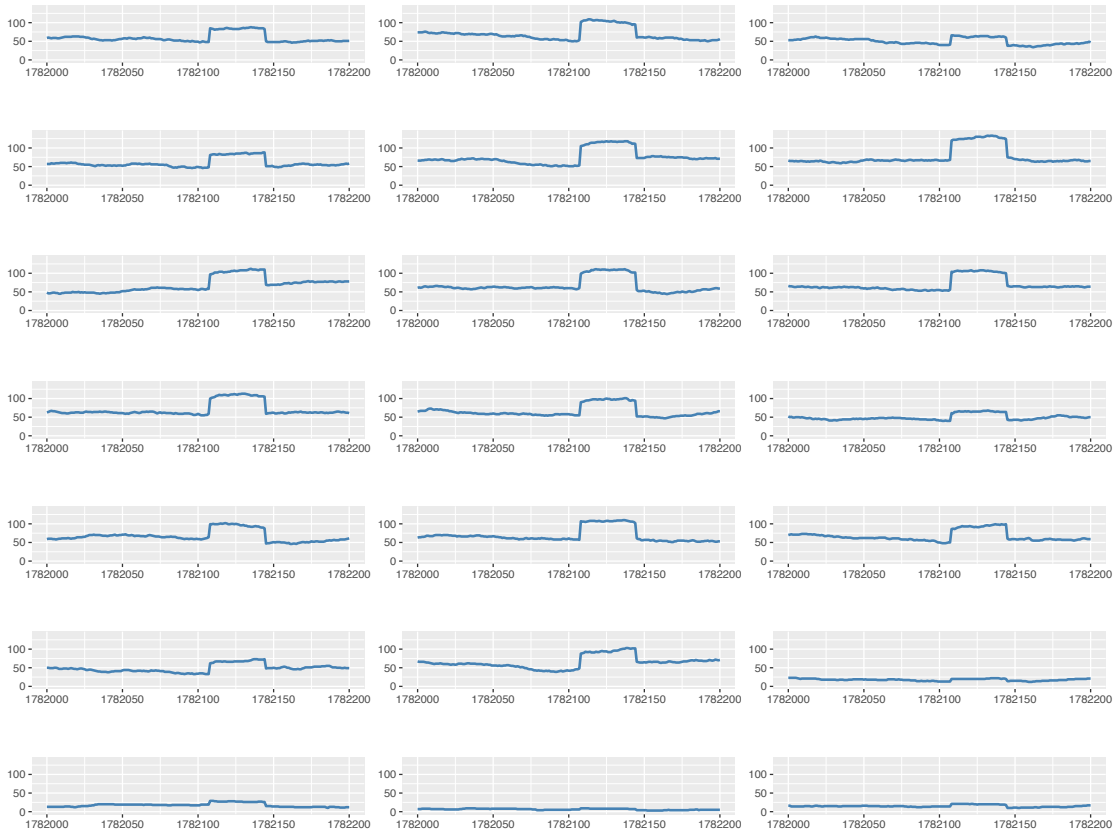

Figure S2.5. Coverage at promoter region of *cyp51A* from position 1,782,000 to 1,782,200 bp for the 21 strains with L98H mutation and known triazole MIC values.

Chapter 3

Analyses of single nucleotide polymorphisms associated with amphotericin B resistance in *Aspergillus fumigatus*

3.1. Preface

This study has been submitted to the journal "Frontiers in Fungal Biology" on July 15, 2021. The authors of this paper are: YuYing Fan, Gregory Korfanty, and Jianping Xu.
I am the primary contributor of this work. The genome-wide association analysis and lab experiments were conducted by me. Gregory Korfanty helped in the harvesting of the 143 progeny strains. Analyses and writing of the manuscript were predominantly completed by me, with great help from Jianping Xu and Gregory Korfanty. Jianping Xu also designed the experiments, supervised the work, and edited the manuscript.

3.2. Abstract

Aspergillus fumigatus is a ubiquitous saprophytic mold that can cause a range of clinical syndromes, from allergic reactions to invasive infections, and is commonly implicated in invasive aspergillosis. Amphotericin B (AMB) is a polyene antifungal drug that has been used to treat a broad range of systemic mycoses since 1958, including as a primary treatment option against invasive aspergillosis in regions with high rates (≥10%) of environmental triazole resistance. However, cases of AMB-resistant *A. fumigatus* strains have been increasingly documented over the years and high resistance rates were recently reported in Brazil and Canada. The objective of this study is to identify candidate mutations associated with AMB tolerance using a combination of approaches that included a genome-wide association analysis of natural strains and an analysis of progeny from a laboratory genetic

cross. The genome-wide association study (GWAS) included a total of 98 *A. fumigatus* strains from 9 countries with reported MIC values ranging from 0.06 to 8 mg/L. The laboratory cross included 143 progeny that were analyzed for five candidate SNPs identified from GWAS. Together, our results identified a total of 34 candidate SNPs associated with AMB tolerance – comprised of 18 intergenic variants, 14 missense variants, 1 synonymous variant, and 1 non-coding transcript variant. Importantly, progeny from the genetic cross allowed us to identify putative SNP-SNP interactions impacting progeny growth at different AMB concentrations. Our analyses expand on previously identified candidate SNPs for AMB tolerance and resistance. We discuss the implications of these results, including the managements of aspergillosis.

3.3. Introduction

The fungal genus *Aspergillus* is one of the most well-studied fungal genera due to their medical, environmental, commercial, and industrial importance. *Aspergillus* species are ubiquitous in nature and can survive in a broad range of environmental conditions. Although there are over 350 identified *Aspergillus* species, only a few are pathogenic to humans (Amchentsev et al., 2008). Among these species, *Aspergillus fumigatus* is the most common cause of human *Aspergillus* infections, responsible for more than 90% of infections (Amchentsev et al., 2008). However, the frequency of aspergillosis caused by *A. fumigatus* varies among countries and patient groups (Paulussen et al., 2016). Multiple physical characteristics of *A. fumigatus* allows the mold to be an efficient and widespread pathogen. The ubiquitous presence of high *A. fumigatus* conidial atmospheric concentrations (both indoors and outdoors) of up to tens of thousands conidia/m^3 results in an average human inhaling ~100 conidia daily. *A. fumigatus* can also tolerate temperature ranges of 12°C to 65°C and pH from 2.1 to 8.8 (Kwon-Chung and Sugui, 2013). Their hydrophobic cell wall facilitates high dispersibility of conidia via wind and these conidia are small enough (2.0 to 3.0 μm in diameter) to reach the lower respiratory tract (Kwon-Chung and Sugui, 2013).

Inhalation of these conidia can develop into aspergillosis, a fungal infection caused by inhalation of *A. fumigatus* spores. Although these spores can cause disease in healthy hosts, for the vast majority of immunocompetent individuals, they are quickly cleared by the innate

immune system (Latgé, 1999). In hosts with a suppressed immune system, however, *A. fumigatus* can germinate, invade tissues through filamentous growth, and disseminate inside the host; resulting in the most severe presentation of aspergillosis, invasive aspergillosis (Paulussen et al., 2016). It is estimated that over 300,000 cases of invasive aspergillosis occur annually with ~10 million at risk (Bongomin et al., 2017). The mortality rates associated with invasive aspergillosis range from 30 to 95% based on the patient population and underlying medical conditions (Brown et al., 2012). However, the global burden of invasive aspergillosis is most likely underestimated due to several reasons including lack of surveillance measures and standardization as well as low sensitivity of current diagnostic assays (Vazquez et al., 2016; Arastehfar et al., 2021).

For treatment of aspergillosis, triazole drugs are recommended as first-line therapy. However, extensive and long-term use of these antifungals, in both clinical and agricultural settings, has led to widespread triazole resistance (Garcia-Rubio et al., 2017). Triazole resistance has become an emerging problem over the last two decades and resistant *A. fumigatus* strains have been identified in six of the seven continents (Nywening et al., 2020; Arastehfar et al., 2021). Previous studies have reported varying triazole resistance prevalence rates worldwide such as 5 to 10% in the Netherlands (reaching 30% in high-risk medical wards) (Lestrade et al., 2016), 5.5% in Belgium (Vermeulen et al., 2015), 4.13% in Poland (Resendiz Sharpe et al., 2018), 5.3% in Germany (Seufert et al., 2018), 8.2% in Italy (Prigitano et al., 2017), 1.8% in France (Choukri et al., 2015), 7.9% in Taiwan (Wu et al., 2015), 6.6% in Pakistan (Chowdhary et al., 2017), 11.2% in Japan (Chowdhary et al., 2017), 3.2 to 4.2% in Iran (Chowdhary et al., 2017), 3.5% in Brazil (Chowdhary et al., 2017), 0 to 80% in China (Deng et al., 2017; Zhou et al., 2021), 2% in Australia (Talbot et al., 2018), 6.6 to 27.8% in the United Kingdom (Resendiz Sharpe et al., 2018), 0.3 to 4.2% in Spain (Resendiz Sharpe et al., 2018), 4 to 6% in Denmark (Resendiz Sharpe et al., 2018), 2.7% in Greece (Resendiz Sharpe et al., 2018), 10.2% in Turkey (Resendiz Sharpe et al., 2018), 1.7% in India (Resendiz Sharpe et al., 2018), 3.2% in Thailand (Resendiz Sharpe et al., 2018), 0.6 to 11.8% in the United States (Resendiz Sharpe et al., 2018), and 20% in Tanzania (Chowdhary et al., 2014). However, it should be noted that reported prevalence rates will vary based on factors such as source (environmental or clinical), underlying patient conditions, and total number of isolates (the

denominator) (Verweij et al., 2016; Resendiz Sharpe et al., 2018). Over the years, increased resistance rates have also been observed: 3.3% (2013) to 6.6% (2015) in Iran (Nabili et al., 2016), 7.6% (2013) to 14.7% (2018) in the Netherlands (Lestrade et al., 2020), and 0.43% (1998-2011) to 2.2% (2015-2017) in the United Kingdom (Abdolrasouli et al., 2018). The prevalence and the observed increasing trend of triazole resistance worldwide is a problem in treatment. Patients with invasive aspergillosis caused by triazole-resistant *A. fumigatus* isolates also have a mortality rate of 88% (Seyedmousavi et al., 2013). In cases of infection by triazole resistant isolates, amphotericin B (AMB) formulations have been recommended as the follow-up treatment of choice and in cases of salvage therapy, particularly for refractory aspergillosis. In addition, AMB is suggested as the primary treatment in regions with ≥ 10% environmental triazole resistance rates (Verweij et al., 2015; Arastehfar et al., 2021).

AMB is a polyene drug that was introduced in the late 1950s and was the first antifungal agent used for treatment against invasive mycoses (Chang et al., 2017; Cavassin et al., 2021). Despite 70 years of investigation and use, AMB's mechanism(s) of action have not been fully elucidated and multiple models of action have been suggested. The majority of these models include the involvement of ergosterol, a major lipid component and most abundant sterol found in fungal cell membranes (Alcazar-Fuoli and Mellado, 2013). The oldest and most accepted mechanism of action is the ion-channel model, where AMB binds to ergosterol and aggregates to form barrel-type pores in the fungal lipid bilayer (Kamiński, 2014). These pores increase the permeability of the fungal cell membrane to K^+ ions and other small cations, thereby allowing for the rapid depletion of intracellular ions that are vital for cell function (Kamiński, 2014). The second model focuses on AMB's ability to generate oxidative stress in cells by inducing intracellular formation of reactive oxygen species (ROS) (Kamiński, 2014). The accumulation of ROS causes oxidative damage to different macromolecules (lipids, proteins, and DNA). Although ROS is known to have a detrimental effect on fungal cells, their specific role in the fungicidal activity of AMB remains unknown. The third model involves surface absorption in which AMB orients parallel to the membrane and sequesters ergosterol to the membrane surface thus destabilizing the membrane (Kamiński, 2014). The final model is known as the sterol sponge model in which AMB primarily exists in the form of large extra-membranous aggregates that extract ergosterol from the lipid bilayer (Kamiński, 2014).

AMB is still frequently and widely used in medical therapy due to its broad spectrum of activity (Chang et al., 2017). Furthermore, resistance to AMB, a fungicidal agent, is less common than resistance to fungistatic agents such as triazoles (Zavrel et al., 2017). However, recent studies have identified high rates of AMB resistance in two geographic populations of *A. fumigatus*. A study in Campinas, Brazil reported AMB resistance (MIC ≥ 2 mg/L) prevalence rates of 27% for *A. fumigatus* isolates and 43% in patients (Reichert-Lima et al., 2018). A high resistance rate of 96.4% was also reported in Hamilton, Canada and is the highest reported rate to date (Ashu et al., 2018). At present, the reasons behind the emergence of high AMB resistance rates in these two geographic populations are unknown. Moreover, the proposed mechanisms for AMB resistance in *A. fumigatus* have mostly come from studies on human pathogenic and non-pathogenic yeasts. In studies of drug resistance among human fungal pathogens, species often differ in their intrinsic drug susceptibility patterns and possess species-specific mechanisms for drug resistance. Thus, it's important to understand the mechanisms of resistance for individual species. Currently, there is little information about the mechanism(s) of AMB resistance in *A. fumigatus* and mutations that confer resistance remain largely unexplored. In our recent investigation, we conducted a genome-wide association study (GWAS) using 71 isolates and identified over 60 candidate SNPs associated with AMB susceptibility (Fan et al., 2020). The objective of this paper is to further investigate genetic variations associated with AMB tolerance in *A. fumigatus* using a combination of GWAS of a larger sample set and the analysis of progeny from a genetic cross. Specifically, genetic variants of interest were first determined by GWAS based on 98 *A. fumigatus* strains and their genome sequences. A mating cross was then conducted between two AMB-resistant strains, CM11 (MIC = 8 mg/L) from Hamilton, Ontario, and the supermater AFB62-1 (MIC = 4 mg/L). The resulting 143 progeny strains from this cross were genotyped at SNP sites of interest to determine potential patterns of inheritance for AMB susceptibility between these two strains.

3.4. Materials and Methods

3.4.1. Whole Genome Sequences and Variant Calling

A total of 98 *A. fumigatus* whole-genome sequences were used in this study, of which 86 sequences were downloaded from the National Center for Biotechnology Information (NCBI) Sequence Read Archive and the remaining 12 sequences were obtained from our previous study (Fan et al., 2020). The strain sample set was collected from 9 countries, which consisted of 10 strains from Canada, 5 strains from Germany, 7 strains from India, 1 strain from Ireland, 31 strains from Japan, 10 strains from the Netherlands, 18 strains from Spain, 11 strains from the United Kingdom, and 5 strains from the United States. The geographical location, source, and AMB MIC values for all 98 strains are listed in Table S3.1.

Sequence mapping, assembly and variant calling were done using the pipeline from our previous study (Fan et al., 2021). Briefly, read quality was checked with FastQC v0.11.5 and trimmed using Trimmomatic v0.36 (Bolger et al., 2014). Reads were mapped and aligned using the *A. fumigatus* reference genome Af293 (GenBank accession GCA_000002655.1) via the BWA-MEM algorithm v0.7.17 (Li, 2013). The MarkDuplicates (Picard) tool was used to identify and remove duplicate reads. Variant calling was done using FreeBayes v0.9.21-19 and variant filtering was done using vcftools to remove indels, variants with a quality score below 15, and variants with a call rate less than 0.90 (Danecek et al., 2011; Garrison and Marth, 2012). A second filtering step was done using vcftools to remove multiallelic sites. This resulting filtered VCF file was denoted as the "soft-filtered" file and contained 277,669 SNP sites. Variant annotation and functional effect predictions were done using SnpEff v5.0 and the reference genome Af293 (Cingolani et al., 2012). Variant pruning was conducted using PLINK 1.90 beta to remove highly-linked variants (VIF > 2) (Purcell et al., 2007).

3.4.2. Genome-Wide Association Study and Linkage Disequilibrium

Association analysis was done in TASSEL 5 by implementing the mixed linear model approach, which included a population structure defined by 5 principal component vectors, determined based on the scree plot, and a kinship matrix calculated using the Identity by State (Centered IBS) method (Bradbury et al., 2007). To avoid biases in the association analysis due to imbalanced allele frequencies, a minor allele frequency threshold of 0.05 was set using TASSEL 5. A total of 20,929 SNP sites were used in the AMB association analysis.

Linkage disequilibrium analysis was also conducted on the resulting 20 SNPs with the lowest p-values and all 277,669 SNP sites from the soft-filtered file to identify highly-linked ($R^2 > 0.85$) SNPs of interest.

3.4.3. Mating and Ascospore Collection

Further investigation was performed for progeny from a cross on selected SNP sites of interest, obtained by the GWAS and linkage disequilibrium analysis, to determine their association with AMB tolerance. Mating crosses were conducted between the *A. fumigatus* strains CM11 and AFB62-1. CM11 was selected due to its high AMB MIC of 8 mg/L, while AFB62-1 was selected due to it being a supermater of the opposite mating type (*MAT1-1*) that is highly virulent and able to complete the sexual cycle in a relatively short period of time (Sugui et al., 2011). A total of five SNPs were analyzed for this cross (For details, please see Results). The five SNPs were selected from the top 20 SNPs obtained by the GWAS and from highly-linked SNPs of interest as determined by linkage disequilibrium analysis. In cases where the SNP site did not produce distinct banding patterns using commercially available restriction enzymes, a neighboring SNP within 1,000 bp distance was genotyped instead. This was done for SNP 2 and SNP 5, using a representative SNP site 656 bp downstream and 723 bp downstream, respectively. Furthermore, the parental strains CM11 and AFB62-1 had differing genotypes at these five SNP sites.

Mating and harvesting of *A. fumigatus* cleistothecia was conducted using a modified protocol from Ashton and Dyer (Ashton and Dyer, 2019).The cross was conducted on oatmeal agar medium, sealed with parafilm, wrapped in aluminum foil, and incubated inverted at 30°C. After one month, single ascospore progenies were harvested from the cleistothecium. Underneath a dissecting microscope, single cleistothecia were isolated using a fine-point sterile syringe. The cleistothecia were washed from any adhering conidia by rolling them on a 4% water agar medium. Two washed cleistothecia were then placed in 0.01% TWEEN 20 solution and crushed using a fine-point sterile syringe to release the ascospores. The solution was vortexed to ensure the cleistothecia had been sufficiently broken and all ascospores were released. Using a hemocytometer, the ascospore solutions were adjusted to a concentration of $\sim 2.00 \times 10^3$

CFU/mL using TWEEN 20. The solutions underwent heat treatment at 70°C for 1 hour to kill any remaining conidia. 100 µL of the ascospore suspension were plated on malt agar plates and incubated at 30°C for 2 to 3 days. After incubation, single ascospore-derived colonies were picked using a sterile loop and each was transferred to new medium. In total, 143 ascospore progeny were obtained from the CM11 and AFB62-1 cross.

3.4.4. AMB Susceptibility Testing

The in vitro susceptibility of all 143 ascospore progeny and the two parental strains were determined using the M38-A2 guideline of the Clinical and Laboratory Standards Institute (CLSI) (Rex et al., 2008). Briefly, strains were grown on Sabouraud dextrose agar for 48 hours at 37°C. The asexual spores, conidia, were harvested from each strain and spore suspensions were adjusted to an optical density at 530 nm from 0.09 to 0.13. Using the RPMI-1640 medium, a 1:50 dilution was done to obtain a final concentration of ~0.4×10^5 to 5×10^6 CFU/mL. Spore suspensions were placed into 96-well microtiter plates containing varying concentrations of AMB and incubated at 35°C for 48 hours. The AMB concentrations tested were 0.25 mg/L, 0.5 mg/L, 1 mg/L, 2 mg/L, 4 mg/L, 8 mg/L, and 16 mg/L. *Candida parapsilosis* (ATCC 22019) and *Candida krusei* (ATCC 6258) were used as quality controls. The AMB MIC of the total 145 strains were determined based on the procedures as recommended by M38-A2. In addition, the amount of growths at each drug concentration for each of the 145 strains was measured spectrophotometrically at 530 nm. The ratio of fungal growth for strains at various AMB concentrations was calculated by comparing the OD_{530} value at the start of incubation (0 hr) and at the end of incubation (48 hr). The value difference between the two time points compared to the positive control (0 mg/L AMB) was taken as a rate of fungal growth over this time period. Antifungal susceptibility testing was performed with three replicates. Outliers for absorbance values were assessed and removed using a Dixon's Q-test ($\alpha = 0.1$). The mean value of three technical repeats was taken to determine the rate of fungal growth for each strain at each AMB concentration.

3.4.5. DNA Extraction of the Progeny Strains

DNA extraction of the 143 progeny strains and the two parental strains was done using a modified protocol described by Xu and colleagues (Xu et al., 2000). Conidia were grown in 1 mL of Sabouraud dextrose broth for 48 hours at 37°C. After incubation, the tubes were centrifuged at 13,000 rpm for 10 minutes and the supernatant was discarded. The cells were resuspended in 0.5 mL of protoplasting buffer and incubated at 37°C for 2 hours. The solutions were then centrifuged at 5,000 rpm for 10 minutes. The supernatant was poured out and 0.5 mL of lysing buffer was added in. The mixture was vortexed and incubated at 65°C for 30 minutes. 500 μL of chloroform/isoamyl alcohol (24:1) and 125 μL of 7.5 M ammonium acetate was added to each sample. The tubes were vortexed and centrifuged at 13,000 rpm for 15 minutes, or until the upper layer was clear. 500 μL from this clear layer was added to 550 μL of ice-cold isopropyl alcohol. The tubes were mixed by inversion, centrifuged at 13,000 rpm for 2 minutes, and the remaining supernatant was discarded. DNA pellets were washed using 50 μL of 70% ethanol for 2 minutes, dried overnight, and resuspended in 60 μL of 1X TE buffer.

3.4.6. Polymerase Chain Reaction and Restriction Fragment Length Polymorphism

The genotypes for the 143 progeny strains at five SNP sites were determined through the use of polymerase chain reaction (PCR) and restriction fragment length polymorphism (RFLP). The details for the five SNPs can be found below in the Results section. Among the five SNP sites, four were located on chromosome 5 and one on chromosome 6. Primers for the SNP sites were designed using the whole-genome sequences of CM11 and AFB62-1. PCR amplification was conducted using a SimpliAmp Thermal Cycler and PCR products were checked using 1% agarose gels. Restriction digests that distinguish nucleotide bases at the five SNP sites were performed on the parental and all 143 progeny strains, following the manufacturer's instructions (NEB, UK). The digested products were run on 2% agarose gels at 80 V for 1.5 hours. Information on the primer sequences, PCR amplification conditions, and restriction enzymes can be found in Table 3.1.

Table 3.1. The primers, amplification conditions, and restrictions enzymes used for distinguishing the five SNP sites between strains CM11 and AFB62-1.

SNP Site Number	Chromosome & Position (bp)	Primer Sequence (5′ to 3′)	Amplification Conditions	Restriction Enzyme
1	CHR 5 – 201,094	F: ACAAACGCCCTTGATCGCTA R: TTTGAGCAGGCCGTAGAGTG	95°C for 10 min. 40 cycles: 95°C for 30 s, 56°C for 30 s, 72°C for 1 min. 72°C for 5 min.	FauI
2	CHR 5 – 2,362,267 (represented by CHR 5 - 2,362,923)	F: CCCTAATGGGTCCGCCAAAA R: CCAGGTGGGGAGTATGGGTA	95°C for 10 min. 40 cycles: 95°C for 30 s, 57°C for 30 s, 72°C for 1 min. 72°C for 5 min.	HpyCH4IV
3	CHR 5 – 2,370,937	F: GCCTACAGGGTCTTGCTTGT R: TGTCAGGACCGCCAATGAAA	95°C for 10 min. 40 cycles: 95°C for 30 s, 56°C for 30 s, 72°C for 1 min. 72°C for 5 min.	BbsI
4	CHR 5 – 2,399,121	F: ATGAGGCAAGGGATCGTACC R: TGCCTACCTCAATCGCACTG	95°C for 10 min. 40 cycles: 95°C for 30 s, 56°C for 30 s, 72°C for 1 min. 72°C for 5 min.	HpyCH4III
5	CHR 6 – 1,608,813 (represented by CHR 6 – 1,608,090)	F: AAGACAACTTCCGAGCCGTG R: GCCCCTCTTGGCCTCATTT	95°C for 10 min. 40 cycles: 95°C for 30 s, 57°C for 30 s, 72°C for 1 min. 72°C for 5 min.	BspDI

3.5. Results

3.5.1. Genome-Wide Association Study and Linkage Disequilibrium Analysis

A genome-wide association study (GWAS) was conducted to determine candidate mutations associated with AMB tolerance using a total of 98 *A. fumigatus* whole-genome sequences and their corresponding AMB MIC values. The results of the GWAS are presented in a Manhattan plot (Figure 3.1). The quantile-quantile plot of observed and expected p-values showed no genomic inflation (Figure 3.2).

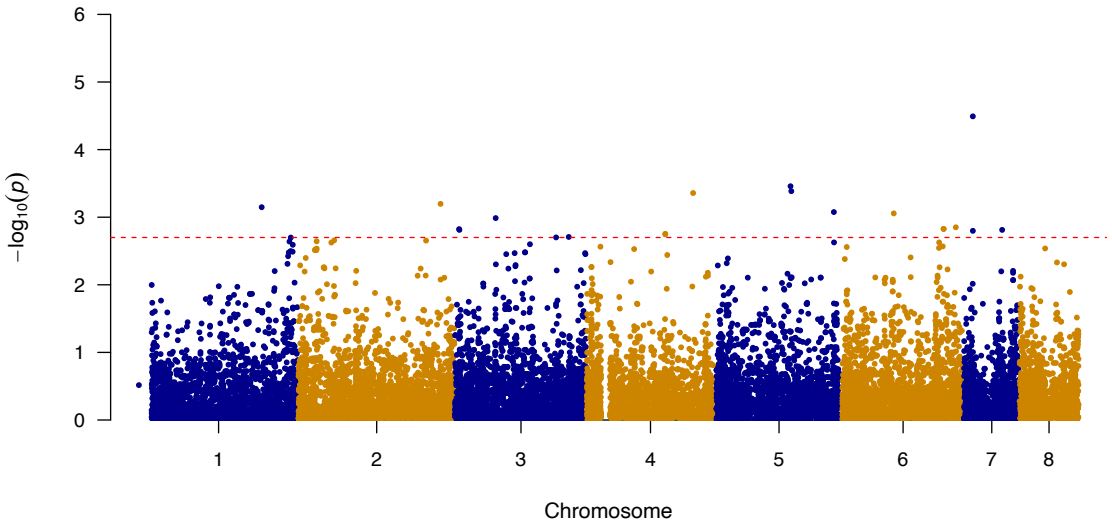

Figure 3.1. Manhattan plot based on the GWAS results for SNPs associated with Amphotericin B sensitivity in *A. fumigatus*. The red dashed line indicates the separation for the top 20 SNPs.

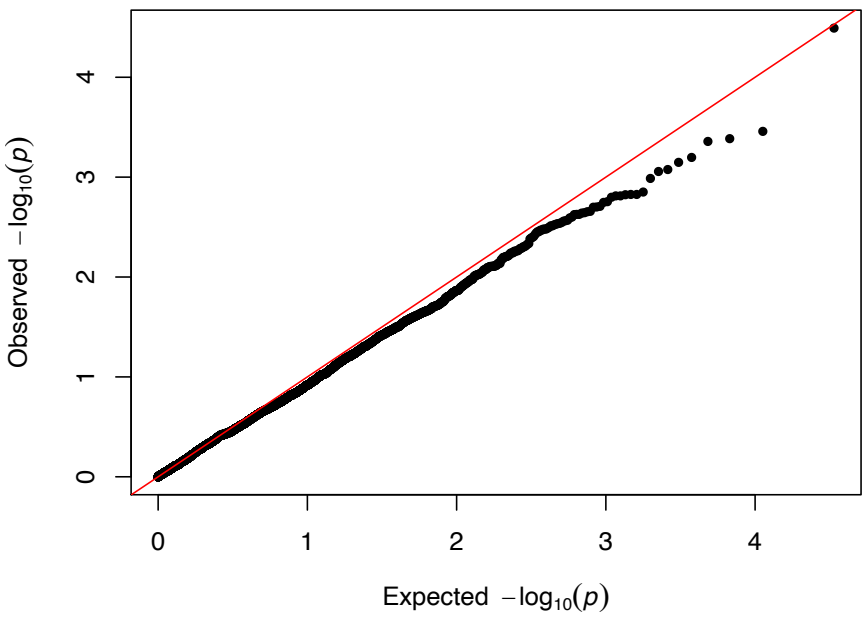

Figure 3.2. Quantile-Quantile (QQ) plot of the Amphotericin B GWAS, which compares observed -$\log_{10}$(p-value) to the expected -$\log_{10}$(p-value).

From the GWAS results, the top 20 significant SNPs with the smallest p-values were further examined. Among these 20 SNPs, 13 (65%) were located in intergenic regions, 6 (30%) were

missense variants and 1 (5%) was a synonymous variant (Table 3.2). In terms of their distribution, one (5%) was located on chromosome 1, one (5%) on chromosome 2, five (25%) on chromosome 3, three (15%) on chromosome 4, three (15%) on chromosome 5, four (20%) on chromosome 6, three (15%) on chromosome 7 and none (0%) were found on chromosome 8 (Table 3.2).

Table 3.2. The top 20 SNPs associated with AMB sensitivity, arranged based on $-\log_{10}$(p-values).

Chromosome	Position (bp)	Change	$-\log_{10}$(*p*-value)	Gene ID	Annotation	Predicted Effect
7	278,099	A to G	4.49	*AFUA_7G01030-AFUA_7G01040*	Calcium-transporting ATPase – Cytidine deaminase, putative	Intergenic Region
5	2,362,267	G to A	3.46	*AFUA_5G09190-AFUA_5G09200*	ABC bile acid transporter, putative – Ubiquitin conjugating enzyme (UbcC), putative	Intergenic Region
5	2,386,509	T to G	3.38	*AFUA_5G09260-AFUA_5G09270*	Phosphatidylinositol transporter, putative – ER membrane protein complex subunit 1	Intergenic Region
4	3,275,045	T to A	3.36	*AFUA_4G12480*	Asparagine synthase related protein	Missense Variant (Ser424Cys)
2	4,385,926	A to G	3.20	*AFUA_2G16500-AFUA_2G16510*	Uncharacterized protein – Uncharacterized protein	Intergenic Region
1	3,787,543	A to G	3.15	*AFUA_1G00400-AFUA_1G00420*	Uncharacterized protein – Carboxypeptidase	Intergenic Region
5	3,698,701	G to T	3.08	*AFUA_5G14160-AFUA_5G14170*	Uncharacterized protein – Uncharacterized protein	Intergenic Region
6	1,608,813	C to T	3.06	*AFUA_6G07160-AFUA_6G07170*	IZH family channel protein (Izh3), putative – Uncharacterized protein	Intergenic Region
3	1,260,557	T to C	2.99	*AFUA_3G04310-AFUA_3G05320*	SnoRNA binding protein, putative – C2H2 finger domain protein, putative	Intergenic Region
6	3,521,360	G to A	2.85	*AFUA_6G13770-AFUA_6G13780*	C6 finger domain protein, putative – MFS multidrug transporter, putative	Intergenic Region
6	3,141,751	G to A	2.83	*AFUA_6G12420*	SprT family metallopeptidase, putative	Missense Variant (Glu245Lys)

6	3,149,653	G to T	2.83	*AFUA_6G12460*	Uncharacterized protein	Missense Variant (Asn213Lys)
3	133,642	T to C	2.82	*AFUA_3G00600*	Uncharacterized protein	Missense Variant (Val519Ala)
3	142,183	A to C	2.81	*AFUA_3G00620*	Zinc-containing alcohol dehydrogenase, putative	Missense Variant (His136Pro)
7	1,182,007	A to C	2.81	*AFUA_7G05020-AFUA_7G05030*	Polysaccharide export protein (Cap59), putative – Pectin lyase B	Intergenic Region
7	279,416	T to C	2.80	*AFUA_7G01050*	Salicylate hydroxylase, putative	Missense Variant (Gln396Arg)
4	2,417,511	A to G	2.75	*AFUA_4G09240-AFUA_4G09250*	Uncharacterized protein – Uncharacterized protein	Intergenic Region
4	2,417,525	T to G	2.75	*AFUA_4G09240-AFUA_4G09250*	Uncharacterized protein – Uncharacterized protein	Intergenic Region
3	3,512,400	T to C	2.71	*AFUA_3G13230*	AT DNA binding protein, putative	Synonymous Variant (Pro380Pro)
3	3,122,663	A to C	2.70	*AFUA_3G11850-AFUA_3G11860*	Uncharacterized protein – Microtubule associated protein EB1, putative	Intergenic Region

Using the top 20 SNPs and all 277,669 variants from the soft-filtered file, linkage disequilibrium analysis was conducted to identify highly-linked ($R^2 > 0.85$) SNPs of interest. From this analysis, 24 highly-linked variants were found (Table 3.3). The additional 24 variants consisted of 17 intergenic variants, 4 missense variants, 1 synonymous variant and 2 non-coding transcript variants (Table 3.3).

Table 3.3. Additional variants found through linkage disequilibrium analysis to be highly-linked with the top 20 SNPs from the AMB GWAS. Fisher's exact test p-values comparing AMB resistant and susceptible strains are listed (n=98).

Chromosome	Position	Gene ID	Predicted Effect (Amino Acid Substitution)	Description	Fisher's Exact Tests (p-value)
1	3,782,532	*AFUA_1G14160*	Missense Variant (Ser65Phe)	Uncharacterized protein	1.96×10^{-1}
1	3,787,813	*AFUA_1G00400-AFUA_1G00420*	Intergenic Region	Uncharacterized protein – Carboxypeptidase	3.42×10^{-1}
1	3,796,235	*AFUA_1G00400-AFUA_1G00420*	Intergenic Region	Uncharacterized protein – Carboxypeptidase	3.43×10^{-1}
1	3,800,222	*AFUA_1G00400-AFUA_1G00420*	Intergenic Region	Uncharacterized protein – Carboxypeptidase	1.90×10^{-1}
1	3,801,124	*AFUA_1G00400-AFUA_1G00420*	Intergenic Region	Uncharacterized protein – Carboxypeptidase	1.96×10^{-1}
1	3,801,488	*AFUA_1G00400-AFUA_1G00420*	Intergenic Region	Uncharacterized protein – Carboxypeptidase	1.96×10^{-1}
1	3,801,524	*AFUA_1G00400-AFUA_1G00420*	Intergenic Region	Uncharacterized protein – Carboxypeptidase	1.96×10^{-1}
1	3,801,974	*AFUA_1G00400-AFUA_1G00420*	Intergenic Region	Uncharacterized protein – Carboxypeptidase	1.96×10^{-1}
1	3,802,717	*AFUA_1G00400-AFUA_1G00420*	Intergenic Region	Uncharacterized protein – Carboxypeptidase	1.88×10^{-1}
1	3,803,746	*AFUA_1G14240*	Missense Variant (Glu467Asp)	Uncharacterized protein	1.99×10^{-1}
3	142,511	*AFUA_3G00620*	Synonymous Variant (Val245Val)	Zinc-containing alcohol dehydrogenase, putative	6.67×10^{-1}

3	3,129,756	*AFUA_3G11890*	Non-coding Transcript Variant	Thermolabile L-asparaginase, putative	1.06×10^{-1}
4	2,416,428	*AFUA_4G09240-AFUA_4G09250*	Intergenic Region	Uncharacterized protein – Uncharacterized protein	3.39×10^{-7} *
4	2,417,416	*AFUA_4G09240-AFUA_4G09250*	Intergenic Region	Uncharacterized protein – Uncharacterized protein	1.28×10^{-6} *
4	2,417,517	*AFUA_4G09240-AFUA_4G09250*	Intergenic Region	Uncharacterized protein – Uncharacterized protein	2.96×10^{-4} *
4	2,417,806	*AFUA_4G09240-AFUA_4G09250*	Intergenic Region	Uncharacterized protein – Uncharacterized protein	2.58×10^{-4} *
5	201,094	*AFUA_5G00700-AFUA_5G00710*	Intergenic Region	Uncharacterized protein – GABA permease, putative	7.12×10^{-4} *
5	201,751	*AFUA_5G00710*	Missense Variant (Arg37Lys)	GABA permease, putative	7.12×10^{-4} *
5	2,370,937	*AFUA_5G09220*	Missense Variant (Leu872Val)	BEACH domain protein	5.15×10^{-4} *
5	2,399,121	*AFUA_5G09320*	Non-coding Transcript Variant	Signal transduction protein (Syg1), putative	7.64×10^{-4} *
6	3,132,855	*AFUA_6G12400-AFUA_6G12410*	Intergenic Region	1,3-beta-D-glucan-UDP glucosyltransferase – 1,3-beta-glucanosyltransferase	7.28×10^{-1}
6	3,136,524	*AFUA_6G12400-AFUA_6G12410*	Intergenic Region	1,3-beta-D-glucan-UDP glucosyltransferase – 1,3-beta-glucanosyltransferase	7.27×10^{-1}

6	3,148,083	*AFUA_6G12440-AFUA_6G12450*	Intergenic Region	Uncharacterized protein – Chaperone/heat shock protein (Hsp12), putative	7.40×10^{-1}
7	1,184,553	*AFUA_7G05030-AFUA_7G05040*	Intergenic Region	Pectin lyase B – Rhamnosidase B, putative	3.18×10^{-1}

* Statistically significant SNPs based on a set threshold of $p < 1.39 \times 10^{-3}$

Fisher's exact tests were further conducted on these 24 highly-linked variants to determine SNPs significantly associated with AMB resistance (Table 3.3). In addition, our previous AMB study, with a total of 71 *A. fumigatus* strains and through the use of Fisher's exact tests, had determined 12 missense variants to be significantly associated with AMB resistance (Fan et al., 2020). The 12 SNPs were located in 6 genes of interest: *erg3* (n=2), *tcsB* (n=4), *mpkC* (n=2), *catA* (n=2), *fos1* (n=1), and *mpkB* (n=1). These SNP sites were also examined in this study using our 98-strain sample set and via Fisher's exact tests (Table 3.4). The European Committee on Antimicrobial Susceptibility Testing (EUCAST) MIC breakpoint of >1 mg/L was used to define AMB resistant *A. fumigatus* strains (Arendrup et al., 2020). From the Fisher's tests and using a Bonferroni-corrected significance threshold of 1.39×10^{-3} (0.05/36), eight of the 24 highly-linked SNPs identified in the current analyses were significantly associated with AMB resistance (Table 3.3). Among these eight SNPs, four were on chromosome 4 and were intergenic variants found between *AFUA_4G09240* and *AFUA_4G09250*. The remaining four SNPs were located on chromosome 5: two were missense variants in *AFUA_5G00710* and in *AFUA_5G09220,* one was a non-coding transcript variant in *AFUA_5G09320*, and the final SNP was found in the intergenic region between *AFUA_5G00700* and *AFUA_5G00710* (Table 3.3). The Fisher's exact tests for the previous 12 missense variants of interest found 6 missense variants significantly associated with AMB resistance in the current sample-set (Table 3.4). These six SNPs comprised of missense variants in three genes *tcsB* (n=3 SNPs), *mpkC* (n=2 SNPs), and *catA* (n=1 SNP) (Table 3.4).

Table 3.4. Fisher's exact tests comparing AMB resistant and susceptible strains on the 12 previously found missense variants associated with AMB resistance (n=98).

Chromosome	Position (bp)	Gene	Amino Acid Substitution	Fisher's Exact Test (p-value)
2	61,543	*AFUA_2G00320* (*erg3*)	Threonine to Isoleucine	3.75×10^{-2}
2	62,002	*AFUA_2G00320* (*erg3*)	Tyrosine to Phenylalanine	3.75×10^{-2}
2	145,934	*AFUA_2G00660* (*tcsB*)	Aspartic acid to Glycine	6.10×10^{-4} *
2	146,469	*AFUA_2G00660* (*tcsB*)	Glycine to Serine	4.27×10^{-3}
2	147,363	*AFUA_2G00660* (*tcsB*)	Arginine to Glycine	1.32×10^{-3} *
2	147,396	*AFUA_2G00660* (*tcsB*)	Alanine to Proline	4.39×10^{-4} *
5	2,342,264	*AFUA_5G09100* (*mpkC*)	Tryptophan to Serine	4.43×10^{-5} *
5	2,342,466	*AFUA_5G09100* (*mpkC*)	Isoleucine to Threonine	4.43×10^{-5} *
6	857,963	*AFUA_6G03890* (*catA*)	Aspartic acid to Asparagine	5.28×10^{-2}
6	858,366	*AFUA_6G03890* (*catA*)	Serine to Asparagine	1.48×10^{-4} *
6	2,533,399	*AFUA_6G10240* (*fos1*)	Alanine to Aspartic acid	8.17×10^{-2}
6	3,232,955	*AFUA_6G12820* (*mpkB*)	Lysine to Arginine	3.23×10^{-2}

* Statistically significant SNPs based on a set threshold of $p < 1.39 \times 10^{-3}$

3.5.2. Mating Cross and AMB Susceptibility of Progeny

We obtained 143 meiotic progenies from the mating cross between CM11 and AFB62-1. The AMB MIC values for the 143 progeny strains and parental strains were listed in Table S3.2. The parental strains CM11 and AFB62-1 had an AMB MIC of 8 mg/L and 4 mg/L,

respectively. Among the 143 progeny strains, 4 (2.80%) strains had an MIC value of 2 mg/L, 120 (83.92%) strains had an MIC of 4 mg/L, and the remaining 19 (13.29%) strains had an MIC of 8 mg/L (Table S3.2).

The amount of fungal growth for the 143 progeny strains and parental strains in the varying concentrations of AMB (0.25 mg/L, 0.50 mg/L, 1.00 mg/L, 2.00 mg/L and 4.00 mg/L) were also measured (Table S3.2). The distribution of growth ratio values for all 145 strains can be found in Figure 3.3. Transgressive phenotypes in the progeny strain were observed in both directions and found at all five AMB concentrations (Figure 3.3).

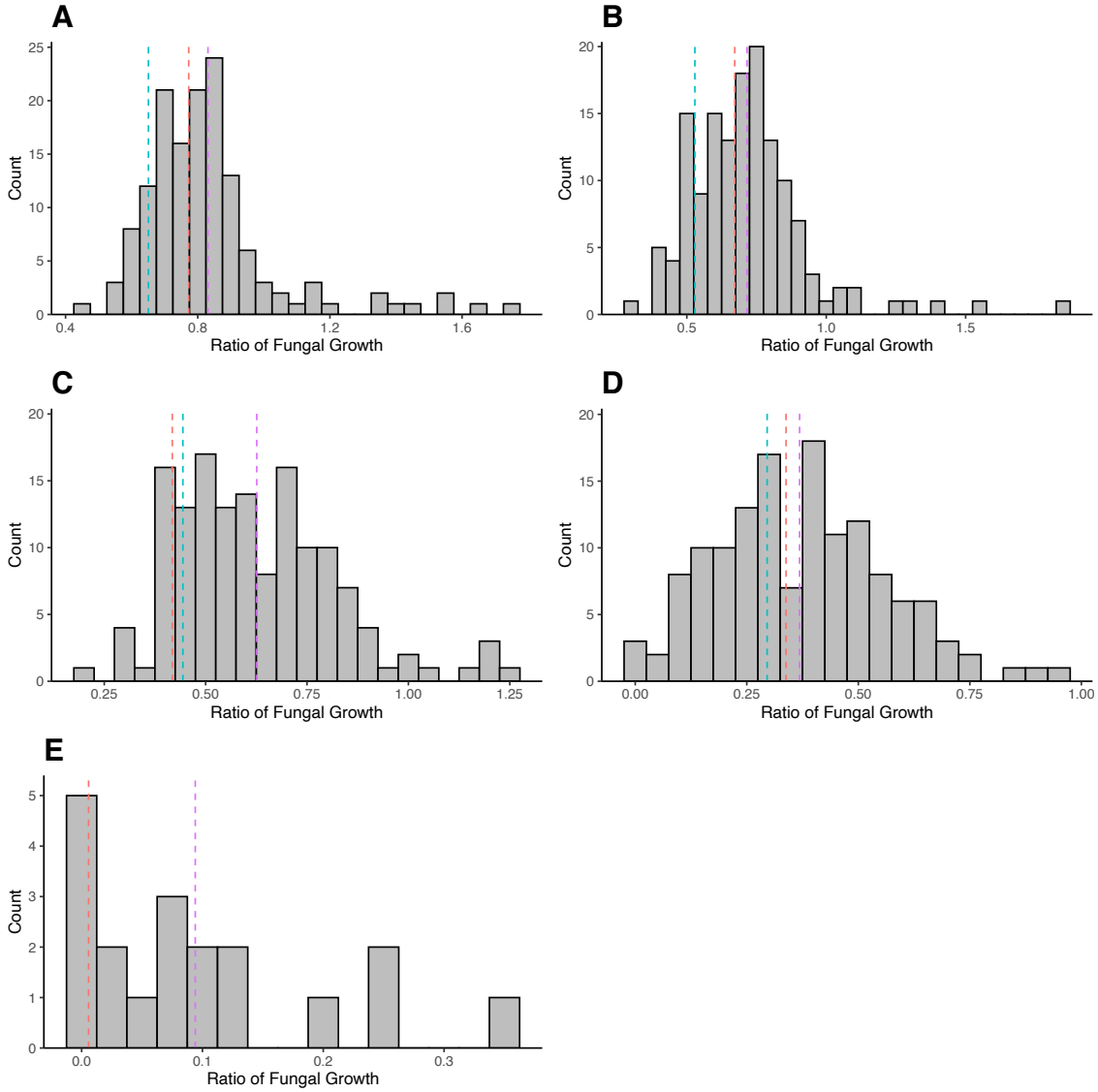

Figure 3.3. Distribution of growth ratio values for the progeny strains measured at Amphotericin B concentrations of **(A)** 0.25 mg/L (n=143), **(B)** 0.50 mg/L (n=143), **(C)** 1.00 mg/L (n=143), **(D)** 2.00 mg/L (n=139), and **(E)** 4.00 mg/L (n=19). Dashed lines represent the values of the two parental strains, CM11 (red) and AFB62-1 (blue), as well as the mean value for the progeny (purple).

At an AMB concentration of 0.25 mg/L, 83 (58.04%) progeny strains had a higher amount of fungal growth than both parents while 16 (11.19%) progeny had lower growths than both parents (Table S3.2). Furthermore, four (2.80%) progeny strains also had growth values more than two-fold higher than the faster parent and no progeny had values two-fold lower than the slower parent. At the 0.50 mg/L concentration, 81 (56.64%) progeny strains had higher

fungal growths than both parents, while 26 (18.18%) progeny had lower growth. Three (2.10%) strains also had growth values more than two-fold higher than the faster parent and no strains had values two-fold lower than the slower parent. At a concentration of 1.00 mg/L, 118 (82.52%) strains had higher growths than both parents while 18 (12.59%) had lower values than both. Twelve (8.39%) strains had values more than two-fold higher than the faster parent and one (0.70%) strain had a growth value more than two-fold lower than the slower parent. At a concentration of 2.00 mg/L, 73 (52.52%) strains had growths higher than the parental strains while 58 (41.73%) had values lower than both parents. In addition, 8 (5.76%) strains had values more than two-fold higher than the faster parent and 17 (12.23%) strains more than two-fold lower than the slower parent. At the final concentration of 4.00 mg/L, 16 (84.21%) strains had growth values higher than the CM11 parent and 3 (15.79%) strains with values lower than CM11. 14 (73.68%) strains had growth values more than two-fold higher than CM11 and no strains had values more than two-fold lower than CM11(Table S3.2). Together, these results indicate substantial difference between the two parental strains in the genetic mechanisms of AMB MIC.

At each AMB concentration, Welch's t-tests were also conducted on the progeny strains to compare ratio of fungal growth and AMB MIC values (Figure 3.4). The results of these tests were that statistically significant differences between MIC groups were present at AMB concentrations of 0.25 mg/L, 1.00 mg/L and 2.00 mg/L (Figure 3.4A, 3.4C, 3.4D). No statistically significant differences were present at a concentration of 0.50 mg/L (Figure 3.4B). At 0.25 mg/L, fungal growths were statistically significantly higher in the 4.00 mg/L MIC progeny group compared to the 2 mg/L MIC progeny group ($p = 0.017$; Figure 3.4A). At the concentration of 1.00 mg/L, the mean growth of the 2 mg/L MIC progeny group was significantly lower than that of both the 4 mg/L and 8 mg/L MIC progeny groups, at $p=0.0059$ and $p=0.00065$, respectively (Figure 3.4C). Lastly, at the 2.00 mg/L concentration, the mean growth of the 8 mg/L MIC progeny group was statistically significantly higher than those of the 4 mg/L MIC progeny group; $p=0.00022$ (Figure 3.4D). These results suggest that strains with higher AMB MICs typically grow faster than those with low AMB MICs at lower AMB concentrations.

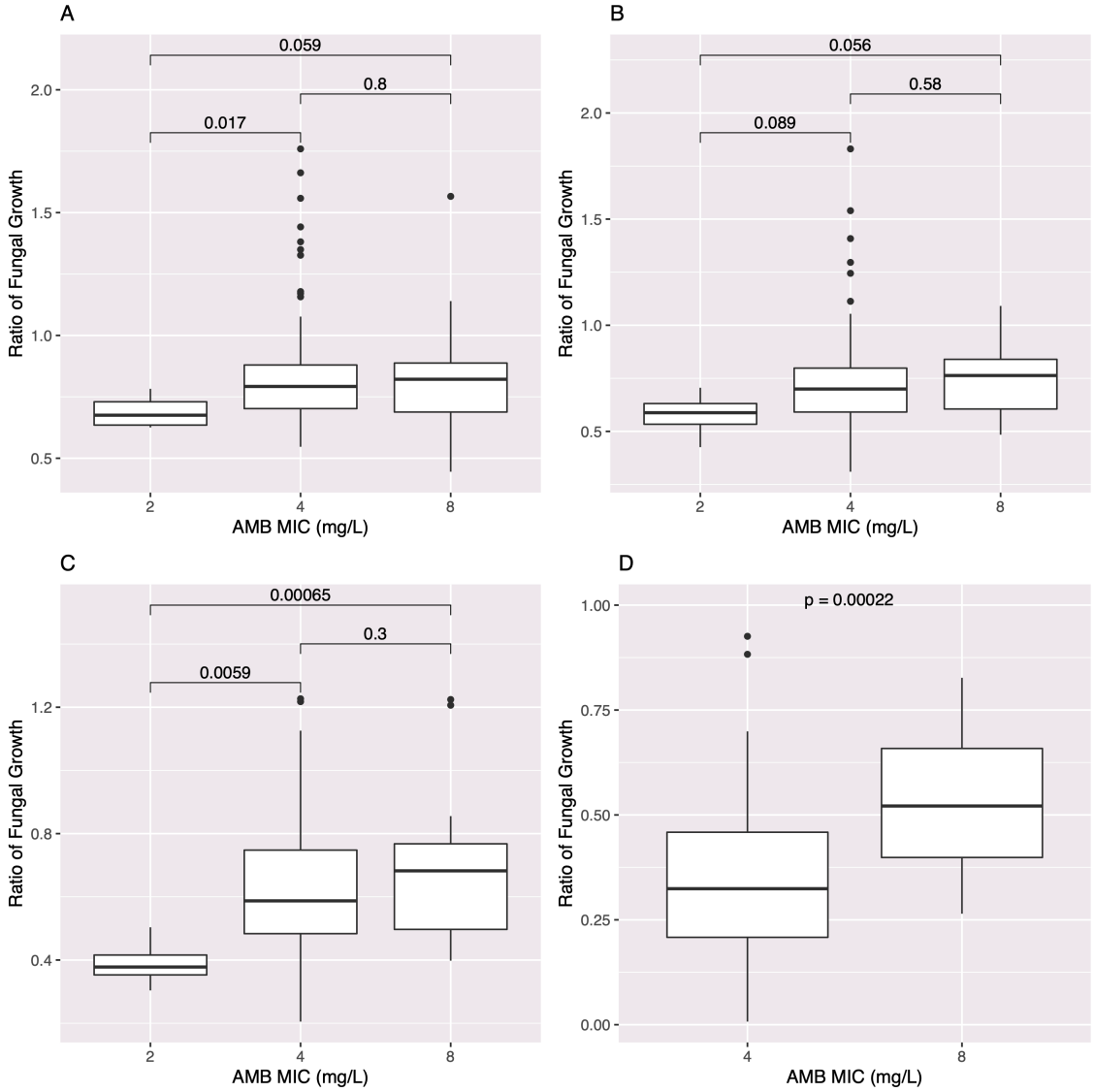

Figure 3.4. Ratio of fungal growth for the 143 progeny strains in Amphotericin B concentrations of **(A)** 0.25 mg/L, **(B)** 0.50 mg/L, **(C)** 1.00 mg/L, and **(D)** 2.00 mg/L. Welch's t-test p-values are also denoted to compare the AMB MIC groups of 2 mg/L (n=4), 4 mg/L (n=120), and 8 mg/L (n=19).

3.5.3. Variant Genotyping

From our final 20,929 SNP sites and using a pairwise SNP comparison, 3,960 SNPs were found between the two parental strains AFB62-1 and CM11. We focused on the 28 SNP sites obtained from the AMB GWAS and the linkage disequilibrium analysis. From the 28 SNPs, 5 SNP sites were selected for further investigation in the 143 progeny strains. The five

SNP sites comprised of three intergenic variants, one missense variant and one non-coding transcript variant (Table 3.5).

Table 3.5. Information about the five SNP sites that were genotyped in the progeny strains using PCR-RFLP.

SNP ID	Chromosome	Position (bp)	Gene ID	Annotation	Predicted Effect
1	5	201,094	*AFUA_5G00700-AFUA_5G00710*	Uncharacterized protein – GABA permease, putative	Intergenic Region
2	5	2,362,267	*AFUA_5G09190-AFUA_5G09200*	ABC bile acid transporter, putative – Ubiquitin conjugating enzyme (UbcC), putative	Intergenic Region
3	5	2,370,937	*AFUA_5G09220*	BEACH domain protein	Missense Variant (Leu872Val)
4	5	2,399,121	*AFUA_5G09320*	Signal transduction protein (Syg1), putative	Non-coding Transcript Variant
5	6	1,608,813	*AFUA_6G07160-AFUA_6G07170*	IZH family channel protein (Izh3), putative – Uncharacterized protein	Intergenic Region

The progeny genotypes at these five SNP sites were determined using PCR-RFLP analysis and are described in Table S3.2. In terms of genotype distribution: for SNP 1, 71 (49.65%) progeny strains had the variant genotype of AB62-1 and 72 (50.35%) had the CM11 variant genotype; for SNP 2, 67 (46.85%) strains had the AFB62-1 genotype while 76 (53.15%) had that of CM11; for SNP 3, 69 (48.25%) strains had the AFB62-1 genotype while 74 (51.75%) had that of CM11; for SNP 4, 73 (51.05%) strains had the AFB62-1 genotype while 70 (48.95%) had that of CM11; for SNP 5, 64 (44.76%) strains had the AFB62-1 genotype while 79 (55.24%) had that of CM11 (Table 3.6).

Table 3.6. Distribution of variant allele frequencies at five SNP sites among the 143 progeny strains. The variant alleles are separated into two AMB MIC groups (MIC ≤ 4 mg/L and MIC of 8 mg/L). Chi-square tests were conducted between MIC groups and the inherited parental allele, with the two-tailed p-values listed.

	MIC ≤ 4 mg/L		MIC = 8 mg/L		p-value
	Allele 1	Allele 2	Allele 1	Allele 2	
SNP 1	64 (51.60%)	60 (48.40%)	7 (36.80%)	12 (63.20%)	0.230
SNP 2	60 (48.40%)	64 (51.60%)	7 (36.80%)	12 (63.20%)	0.348
SNP 3	61 (49.20%)	63 (50.80%)	8 (42.10%)	11 (57.90%)	0.565
SNP 4	64 (48.40%)	60 (51.60%)	9 (52.60%)	10 (47.40%)	0.730
SNP 5	56 (45.20%)	68 (54.80%)	8 (42.10%)	11 (57.90%)	0.803

Allele 1 = AFB62-1, Allele 2 = CM11

3.5.4. Association between Variant SNPs and AMB MIC and Growths at Different AMB Concentrations

Analyses based on individual SNPs: For each of the five SNP sites, a Chi-square test was conducted between the progeny AMB MIC and the inherited parental allele (Table 3.6). The strains with a MIC of 2 mg/L and 4 mg/L were combined into a single group of MIC ≤ 4 mg/L due to the small sample size in the 2 mg/L MIC group. No statistically significant differences were observed between the two MIC groups in their frequencies of alleles at any of the five SNPs (Table 3.6).

In addition to MIC values, the progeny strains' ability to grow in varying AMB concentrations were examined through OD_{530} measurements. For each of the five SNP sites, Welch's t-tests were conducted to compare ratio of fungal growth in varying AMB concentrations between the genotypes inherited in the progeny (Figure 3.5). Based on these tests, a statistically significant difference ($p=0.047$) was found at an AMB concentration of 0.25 mg/L for SNP site 5. Specifically, progeny that inherited the CM11 allele at SNP 5 has statistically significantly higher fungal growth that progeny that inherited the AFB62-1 allele (Figure 3.5).

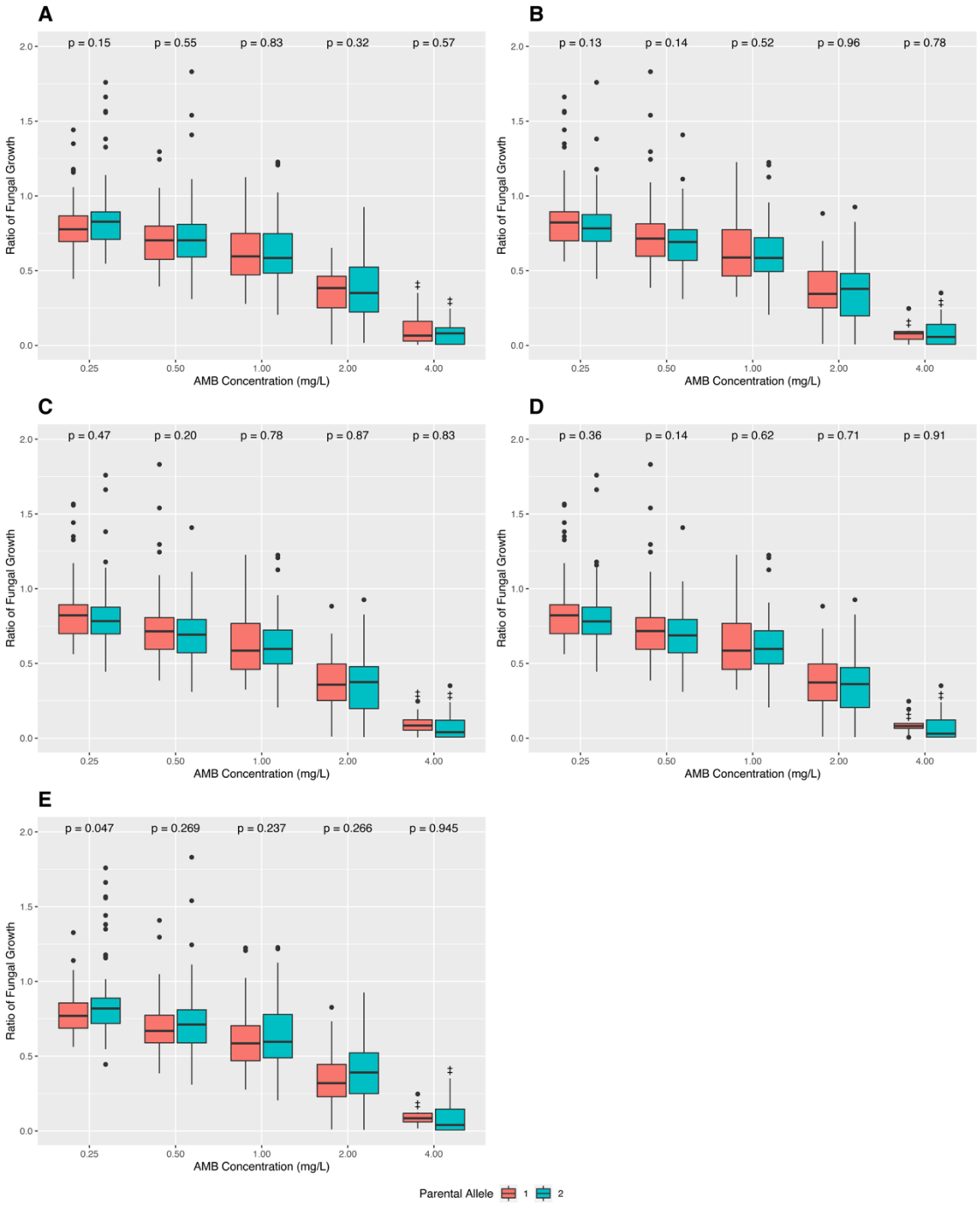

Figure 3.5. Growths of the 143 progeny strains in varying Amphotericin B concentrations, grouped based on the variant genotype at the sites **(A)** SNP 1, **(B)** SNP 2, **(C)** SNP 3, **(D)** SNP 4, and **(E)** SNP 5. Welch's t-test p-values are listed to compare variant genotype. Parental allele 1 denotes the AFB62-1 genotype and parental allele 2 denotes the CM11 genotype. "‡" indicates bar groups with n ≤ 12.

Analyses based on pairs of SNP combinations: To analyze the role of SNP-SNP interactions, all possible pairwise SNP combinations between these five sites were also assessed. In terms of MIC values, Fisher's exact tests were conducted using the two previous MIC groups (MIC ≤ 4 mg/L and MIC = 8 mg/L) and the pairwise SNP combinations (Table S3.3). No statistically significant differences were found between groups (Table S3.3).

In addition to examining MIC values, Welch's t-tests were again conducted using the pairwise genotype combinations to compare ratio of fungal growth in varying AMB concentrations (Figure 3.6). The p-values for all conducted Welch's t-tests of the 10 pairwise SNP combinations can be found in Figure S3.1. The results of this analysis showed statistically significant differences in fungal growth ratio for six of the 10 pairwise combinations: SNP 5 & 1, SNP 5 & 2, SNP 5 & 3, SNP 5 & 4, SNP 4 & 1, and SNP 2 & 1 (Figure 3.6).

For the pairwise combination of SNP 5 & 1, statistically significant differences were found at an AMB concentration of 0.25 mg/L. Progeny strains that inherited the variant alleles from CM11 at both SNP sites had a higher mean fungal growth ratio than progeny strains that inherited both variant genotypes from AFB61-2 (Figure 3.6A).

For SNP 5 & 2, statistically significant differences were found at AMB concentrations of 0.25 mg/L, 0.50 mg/L, and 1.00 mg/L (Figure 3.6B). At a concentration of 0.25 mg/L, progeny that inherited the CM11 genotype at SNP 5 and the AFB62-1 genotype at SNP 2 had higher mean fungal growth ratios than progeny that inherited the AFB62-1 genotype at both SNP sites, progeny that inherited the AFB62-1 genotype at SNP 5 and CM11 genotype at SNP 2, and progeny that inherited the CM11 genotype at both SNP sites. At a concentration of 0.50 mg/L, progeny that inherited the CM11 genotype at SNP 5 and the AFB62-1 genotype at the SNP 2 had higher mean fungal growths than progeny that inherited the AFB62-1 genotype at both SNP sites, and progeny that inherited the CM11 genotype at both SNP sites. Lastly, at an AMB concentration of 1.00 mg/L, progeny that inherited the CM11 genotype at SNP 5 and the AFB62-1 genotype at the SNP 2 had higher mean fungal growth ratios than progeny that inherited the AFB62-1 genotype at both SNP sites (Figure 3.6B). For the pairwise combination of SNP 5 & 3, statistically significant differences were found at AMB concentrations of 0.25 mg/L and 1.00 mg/L (Figure 3.6C). At both AMB concentrations of 0.25 mg/L and 1.00

mg/L, progeny that inherited the CM11 genotype at SNP 5 and the AFB62-1 genotype at SNP 3 had higher mean fungal growths than progeny that inherited the AFB62-1 genotype at both SNP sites (Figure 3.6C). For SNP 5 & 4, statistically significant differences were found at AMB concentrations of 0.25 mg/L, 0.50 mg/L, and 1.00 mg/L (Figure 3.6D). At 0.25 mg/L, progeny that inherited the CM11 genotype at SNP 5 and the AFB62-1 genotype at the SNP 4 had higher mean fungal growths than progeny that inherited the AFB62-1 genotype at both SNP sites, and progeny that inherited the AFB62-1 genotype at SNP 5 and CM11 genotype at SNP 4. At an AMB concentration of 0.50 mg/L, progeny that inherited the CM11 genotype at SNP 5 and the AFB62-1 genotype at the SNP 4 had higher mean fungal growths than progeny that inherited the CM11 genotype at both SNP sites. Lastly, at an AMB concentration of 1.00 mg/L, progeny that inherited the CM11 genotype at SNP 5 and the AFB62-1 genotype at SNP 4 had higher mean fungal growth ratios than progeny that inherited the AFB62-1 genotype at both SNP sites (Figure 3.6D).

For the pairwise combination of SNP 4 & 1, statistically significant differences were found at the AMB concentration of 2.00 mg/L (Figure 3.6E). Progeny strains that had the AFB62-1 genotype at SNP 4 and the CM11 genotype at SNP 1 had a higher mean fungal growth than progeny strains that inherited both variant genotypes from CM11 (Figure 3.6E). For SNP 2 & 1, statistically significant differences were found at the AMB concentration of 0.25 mg/L (Figure 3.6F). Progeny strains with the AFB62-1 genotype at SNP 2 and the CM11 genotype at SNP 1 had a higher mean fungal growth than those with the CM11 genotype at SNP 2 and AFB62-1 at SNP 1 (Figure 3.6F).

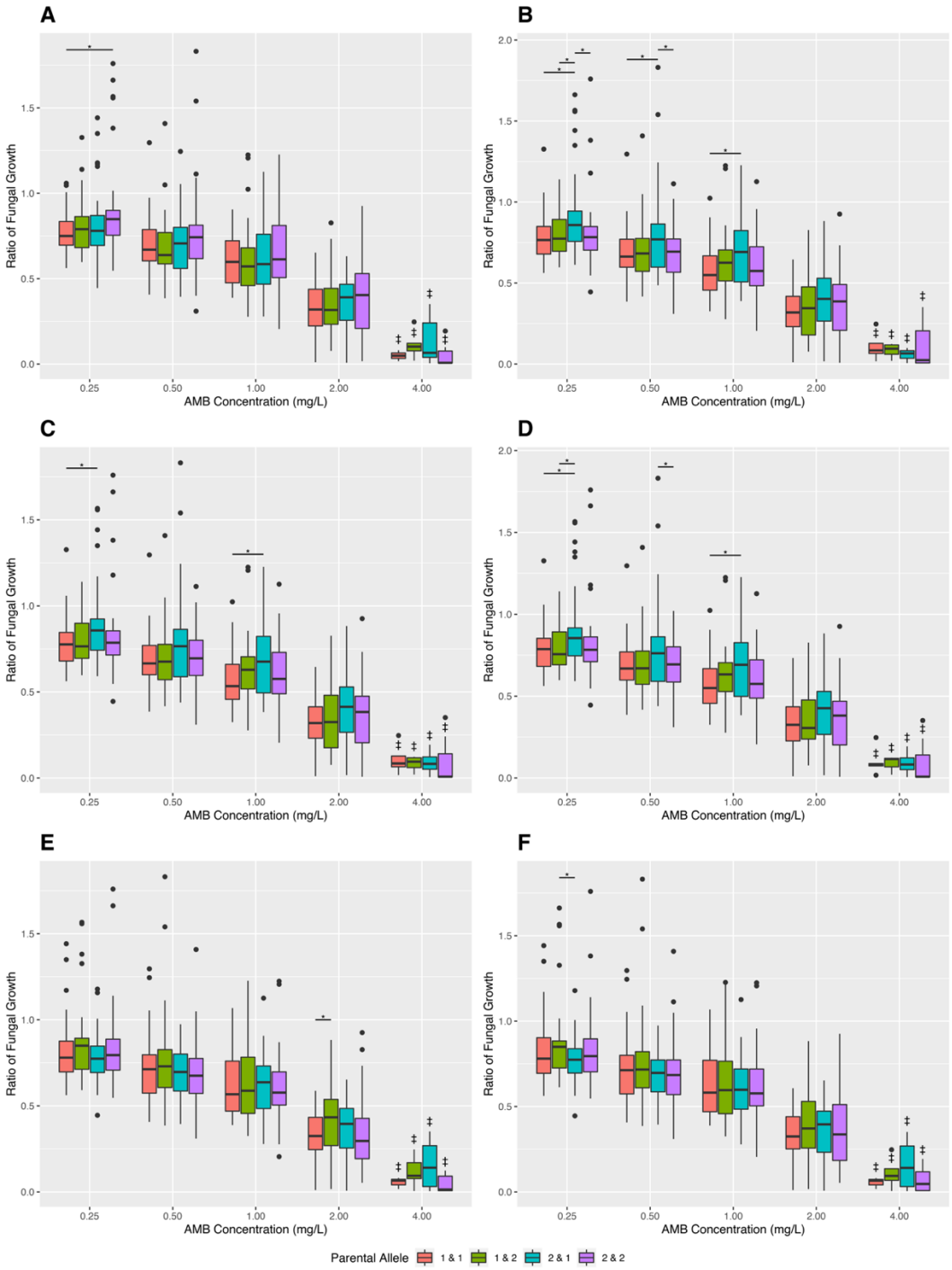

Figure 3.6. Growths of the 143 progeny strains in varying Amphotericin B concentrations, grouped based on pairwise variant genotype at **(A)** SNP 5 & 1, **(B)** SNP 5 & 2, **(C)** SNP 5 & 3, **(D)** SNP 5 & 4, **(E)** SNP 4 & 1, and **(F)** SNP 2 & 1. Parental allele of 1 denotes the AFB62-1 genotype and parental allele 2 denotes the CM11 genotype. "*" denotes statistically significant differences (Welch's t-test p-values < 0.05) and "‡" indicates bar groups with n ≤ 12.

Analyses based on linked SNPs: Additionally, a group of SNP sites showed low rates of recombination in the progeny. The group, denoted as Group A, consisted of SNP 2, SNP 3, and SNP 4. Among the 143 progeny strains, 64 (44.76%) strains inherited all three genotypes from AFB62-1, 67 (46.85%) strains inherited all three genotypes from CM11, and 12 (8.39%) strains had recombination present at these three sites (Table S3.2). Using this additional grouping, Welch's t-tests were done for the additional combinations of SNP 5 & Group A, and SNP 1 & Group A (Figure 3.7).

The additional analyses of SNP 5 & Group A found statistically significant differences present at AMB concentrations of 0.25 mg/L, 0.50 mg/L and 1.00 mg/L (Figure 3.7A). At the AMB concentration of 0.25 mg/L, progeny that inherited the CM11 genotype at SNP 5 and AFB62-1 genotype for all Group A SNP sites had a statistically higher mean fungal growth than progeny with the AFB62-1 genotype at all four SNP sites, and progeny with the AFB62-1 genotype at SNP 5 and recombination present in Group A. At 0.50 mg/L, progeny with the CM11 genotype at SNP 5 and the AFB62-1 genotype for all Group A sites had a higher mean fungal growth than progeny with the CM11 genotype at all four SNP sites. Lastly, at the AMB concentration of 1.00 mg/L, progeny with the CM11 genotype at SNP 5 and AFB62-1 genotype for Group A SNP sites had a higher mean fungal growth than progeny with the AFB62-1 genotype at all four SNP sites (Figure 3.7A). For the SNP 1 & Group A combination, no statistically significant differences were present at any AMB concentration (Figure 3.7B).

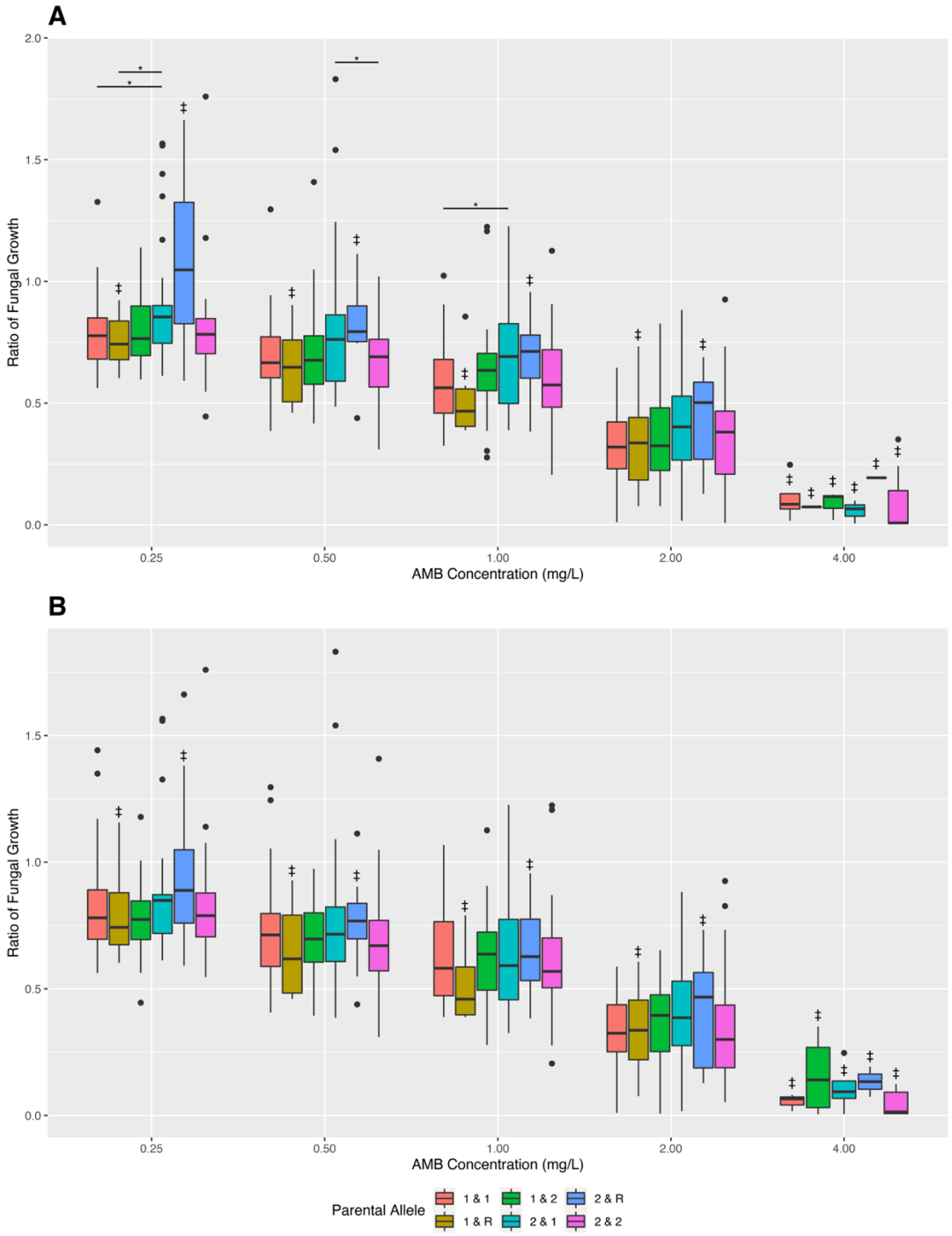

Figure 3.7. Growths of the 143 progeny strains in varying Amphotericin B concentrations, grouped based on the variant genotype combination at the sites **(A)** SNP 5 & Group A and **(B)** SNP 1 & Group A. Parental allele of 1 denotes the AFB62-1 genotype, parental allele 2 denotes the CM11 genotype, and R denotes recombination in the SNP group. "*" denotes statistically significant differences (Welch's t-test p-values < 0.05) and "‡" indicates bar groups with n ≤ 12.

3.6. Discussion

In this study, a GWAS was conducted using 98 *A. fumigatus* whole-genome sequences from strains across 9 countries with reported AMB MIC values ranging from 0.06 to 8 mg/L. From the GWAS analysis, we focused on six missense variants. The six missense variants were located in six genes. The highest scoring missense variant was found in *AFUA_4G12480*, which encodes for an asparagine synthase related protein. Asparagine synthetase is involved with asparagine biosynthesis and converts aspartate to asparagine in an ATP-dependent reaction (Loureiro et al., 2013). The second highest scoring missense variant was in *AFUA_6G12420*, a putative SprT family metallopeptidase. The next two missense variants were found in the uncharacterized proteins, *AFUA_6G12460* and *AFUA_3G00600*. The remaining two variants were found in putative oxidoreductases: a missense variant in *AFUA_3G00620,* encoding a putative zinc-containing alcohol dehydrogenase, and in *AFUA_7G01050*, encoding for a putative salicylate hydroxylase. These two enzymes are involved in the oxidation-reduction process, a process relevant to AMB resistance in *A. fumigatus*. For example, AMB exposure has been reported to induce production and accumulation of intracellular reactive oxygen species (ROS) in *A. fumigatus,* thereby resulting in oxidative damage (Shekhova et al., 2017). Alcohol dehydrogenases catalyze the interconversion between alcohols and aldehydes or ketones (Ying and Ma, 2011). Alcohol fermentation is carried out by many microorganisms in hypoxic environments to allow for regeneration of NAD^+, ensuring an adequate supply for the continuation of glycolysis (Grahl et al., 2011). However, increased production of intracellular ROS is also seen in *A. fumigatus* when exposed to oxygen limiting environments, which then triggers the oxidative stress response (Shekhova et al., 2019). In addition, alcohol dehydrogenase can influence hypoxic fungal growth in invasive aspergillosis infections (Grahl et al., 2011). Meanwhile, salicylate hydroxylase is a flavin-dependent monooxygenase that catalyzes the conversion of salicylate into catechol (Costa et al., 2019). Overexpression of salicylate hydroxylase in *Aspergillus nidulans* is associated with terbinafine resistance, through a putative mechanism of degrading the naphthalene ring in the antifungal, and the enzyme has not been previously linked to AMB tolerance (Graminha et al., 2004). However, terbinafine also induces intracellular ROS

accumulation in *A. fumigatus* (Shekhova et al., 2019). For both antifungal agents, exposure to terbinafine and AMB caused significantly higher levels of mitochondrial lipid oxidation than in unstressed mycelia (Shekhova et al., 2019). Therefore, in addition to naphthalene degradation, salicylate hydroxylase could potentially play a role in antifungal drug resistance through oxidative stress protection.

In comparison to our previous AMB GWAS study, there was no overlap seen between the top 20 SNPs of the two studies (Fan et al., 2020). The difference in results is most likely attributed to changes in sample size and selection criteria; our previous study focused on a clade-level (specifically Cluster 2) comprised of 33 strains, while our current study has expanded this sample-set to a total of 98 strains. Additionally, the software used for association analysis differed between our two studies, PLINK and TASSEL. Different GWAS software often produce dissimilar results, even when using the same input. This was seen in a recent *A. fumigatus* study, which followed up their GWAS analysis by focusing on overlapping SNPs between the two softwares (TASSEL and RoadTrips) as well as validation using knock-out mutants (Zhao et al., 2021). Therefore, confirmation of our resulting 20 SNPs putatively associated with AMB resistance, via additional experiments such as genetic crosses and gene replacements, is still needed.

Linkage disequilibrium analysis, conducted on the top 20 SNPs and the 277,669 SNPs of the soft-filtered VCF file, identified an additional 24 highly-linked ($R^2 > 0.85$) variants among the 98 strains. Fisher's exact tests identified eight SNPs to be significantly associated with AMB resistance (Table 3.3). Five of the SNPs were intergenic variants and comprised of four SNPs in the intergenic region between *AFUA_4G09240* and *AFUA_4G09250*, which both encode for uncharacterized proteins, and one intergenic variant between *AFUA_5G00700* and *AFUA_5G00710*, encoding for an uncharacterized protein and a putative gamma-aminobutyric acid (GABA) permease, respectively. These intergenic variants could impact gene expressions of the surrounding genes and targeted RT-qPCR analyses could help confirm their effects. Two of the eight significantly associated SNPs were missense variants. The first missense variant is in *AFUA_5G00710* that encodes for a putative GABA permease and the second was found in *AFUA_5G09220*, encoding a BEACH (Beige and Chediak-Higashi) domain protein. The final SNP was a non-coding transcript variant in

AFUA_5G09320, which encodes for a putative signal transduction protein (Syg1) with plasma membrane localization. The non-coding mutation can also impact gene expression or function if located in elements such as enhancers, silencers, promoters or other regulatory roles.

Fisher's exact tests were also done on the 12 missense variants that were found in our previous study to be significantly associated with AMB resistance (Fan et al., 2020). Among these 12 SNPs, 6 were found to be significantly associated with AMB resistance using our current 98-strain sample set and a Bonferroni-corrected p-value threshold of 1.39×10^{-3} (0.05/36). These missense variants were in three genes *tcsB* (n=3), *mpkC* (n=2), and *catA* (n=1). As mentioned in the previous study, genes *tcsB* and *mpkC* are involved in the high-osmolarity glycerol (HOG) mitogen-activated protein kinase (MAPK) signaling pathway; encoding for a sensor histidine kinase and mitogen-activated protein kinase, respectively (Fan et al., 2020). The third gene *catA*, which encodes for a catalase, was also included due to its role in the ROS-detoxifying system (Fan et al., 2020). Missense variants in these genes were examined because of their involvement in oxidative stress response pathways and thus being potentially involved in AMB resistance through protection against oxidative stress. However, the molecular roles of these specific genes in AMB resistance remain unknown.

In this study, we used a genetic cross to validate the association between five significantly associated SNPs against AMB resistance and growth under various AMB concentrations. Interestingly, using the 143 progeny strains, Chi-square tests found no statistically significant differences between the MIC groups in their parental allele distributions (Table 3.6). However, Welch's t-tests revealed a significant difference in fungal growths at an AMB concentration of 0.25 mg/L between alleles at SNP site 5. In addition, we found significant interactions between SNP sites influencing progeny growths at various AMB concentrations. Specifically, six of the 10 SNP combinations showed significant interaction effects for growths in at least one of the AMB concentrations (Figure 3.6). In several instances, progeny with allele combinations from one parent showed more robust growth than those from a different parent. This can be seen in the combination of SNP 5 & 1, where progeny that inherited the CM11 genotype at both SNP sites had a higher mean fungal growth ratio at 0.25 mg/L than progeny that inherited both genotypes from AFB61-2 (Figure 3.6A). In other combinations, progeny with recombinant genotypes showed more growths than those with parental genotypes (Figures

3.6B – 3.6D). Examples of this type include combinations of SNP 5 & 2, SNP 5 & 3, and SNP 5 & 4, where progeny that inherited the CM11 allele at SNP 5 and the AFB62-1 allele at the second SNP site (SNP 2, SNP 3, and SNP 4, respectively) had a higher fungal growth than others (Figure 3.6B – 3.6D). This interaction pattern was also seen after combining SNP sites showing significant linkage disequilibrium (Figures 3.7A). Together, these results revealed that progeny growths in various AMB concentrations were influenced by different but sometimes overlapping SNP combinations. Furthermore, both parental and recombinant genotypes showed positive associations with growths at different AMB concentrations. The results are consistent with the two parental strains being genetically very different and with complementary alleles at different SNP loci related to growths at different AMB concentrations.

Among these five SNP sites, SNP 1 was an intergenic variant between *AFUA_5G00700* and *AFUA_5G00710*, which encodes for an uncharacterized protein and a putative GABA permease, respectively. GABA permeases serves as gamma-aminobutyrate transporter proteins and are involved in the utilization of GABA as a nitrogen and carbon source (Kumar and Punekar, 1997). SNP 2 was an intergenic variant found between *AFUA_5G09190* and *AFUA_5G09200*. The gene *AFUA_5G09190* encodes a putative ABC bile acid transporter, part of the ABC transporter superfamily with many members involved in antifungal drug resistance, while *AFUA_5G09200* encodes a putative ubiquitin conjugating enzyme, UbcC. Ubiquitin conjugating enzymes are responsible for ubiquitination or ubiquitin-like modifications of proteins, which play a role in many biological processes (Michelle et al., 2009). The next variant, SNP 3, was a missense mutation in *AFUA_5G09220*, a BEACH domain protein sequence. Their exact biological function remains largely unknown, however, BEACH domain proteins have been implicated in membrane dynamics, vesicular transport, and receptor signaling (Jogl et al., 2002). SNP 4 was a missense variant in *AFUA_5G09320*, encoding a putative signal transduction protein (Syg1) with plasma membrane localization. Although the protein's function is not clear, Syg1 is predicted to be involved in phosphate homeostasis and mediate phosphate export due to its similarity to the mammalian phosphate exporter Xpr1 (Lev et al., 2019). The final variant site, SNP 5, was an intergenic variant located between *AFUA_6G07160* and *AFUA_6G07170*, encoding for a putative IZH family channel

protein (Izh3) and an uncharacterized protein, respectively. The IZH family consists of membrane proteins with involvement in zinc homeostasis (Lyons et al., 2004). These genes are regulated by exogenous fatty acids, suggesting a role in lipid metabolism, and have been proposed to affect zinc homeostasis by altering sterol metabolism (Lyons et al., 2004). Interestingly, in a previous study on *Saccharomyces cerevisiae*, *izh3* deletion mutants were more resistant to AMB than the wild-type strain (Serhan et al., 2014). Furthermore, AMB had no significant effect on ROS production in the deletion mutants but was significantly induced in the wild-type strain (Serhan et al., 2014).

In recent years, the advancement in medical technology and increased usage of immunosuppressive agents has led to an expanding population of immunocompromised as well as a rising incidence of invasive mycoses like aspergillosis. With the recommendation for a shift to AMB use in first-line invasive aspergillosis treatment where triazole resistance rates exceed 10%, the emerging problem of widespread AMB resistance and reports of high resistance rates – 27% in Campinas, Brazil and 96.4% in Hamilton, Canada – is becoming a major public health concern (Verweij et al., 2015; Ashu et al., 2018; Reichert-Lima et al., 2018). This study has identified a total of 34 SNP candidates putatively associated with AMB susceptibility and has highlighted the importance of SNP-SNP interactions in AMB tolerance for 5 of these SNPs. The variants and genomic regions we have identified in this study provide promising candidates for future studies exploring molecular mechanisms for AMB resistance in *A. fumigatus* and for further functional analysis. Furthermore, these candidates can help to accelerate the selection of prospective gene markers for AMB resistance screening to prevent treatment failure.

3.7. References

Abdolrasouli, A., Petrou, M. A., Park, H., Rhodes, J. L., Rawson, T. M., Moore, L. S. P., et al. (2018). Surveillance for azole-resistant *Aspergillus fumigatus* in a centralized diagnostic mycology service, London, United Kingdom, 1998–2017. *Front. Microbiol.* 9. doi:10.3389/fmicb.2018.02234

Alcazar-Fuoli, L., and Mellado, E. (2013). Ergosterol biosynthesis in *Aspergillus fumigatus:* its relevance as an antifungal target and role in antifungal drug resistance. *Front. Microbiol.* 3. doi:10.3389/fmicb.2012.00439

Amchentsev, A., Kurugundla, N., and Saleh, A. G. (2008). *Aspergillus*-related lung disease. *Respir. Med. CME* 1, 205–215. doi:10.1016/j.rmedc.2008.08.008

Arastehfar, A., Carvalho, A., Houbraken, J., Lombardi, L., Garcia-Rubio, R., Jenks, J. D., et al. (2021). *Aspergillus fumigatus* and aspergillosis: From basics to clinics. *Stud. Mycol.* 100, 100115. doi:10.1016/j.simyco.2021.100115

Arendrup, M. C., Friberg, N., Mares, M., Kahlmeter, G., Meletiadis, J., Guinea, J., et al. (2020). How to interpret MICs of antifungal compounds according to the revised clinical breakpoints v. 10.0 European committee on antimicrobial susceptibility testing (EUCAST). *Clin. Microbiol. Infect.* 26, 1464–1472. doi:10.1016/j.cmi.2020.06.007

Ashu, E. E., Korfanty, G. A., Samarasinghe, H., Pum, N., You, M., Yamamura, D., et al. (2018). Widespread amphotericin B-resistant strains of *Aspergillus fumigatus* in Hamilton, Canada. *Infect. Drug Resist.* 11, 1549–1555. doi:10.2147/IDR.S170952

Bolger, A. M., Lohse, M., and Usadel, B. (2014). Trimmomatic: a flexible trimmer for Illumina sequence data. *Bioinformatics* 30, 2114–2120. doi:10.1093/bioinformatics/btu170

Bongomin, F., Gago, S., Oladele, R. O., and Denning, D. W. (2017). Global and multi-national prevalence of fungal diseases—estimate precision. *J Fungi* 3, 57. doi:10.3390/jof3040057

Bradbury, P. J., Zhang, Z., Kroon, D. E., Casstevens, T. M., Ramdoss, Y., and Buckler, E. S. (2007). TASSEL: software for association mapping of complex traits in diverse samples. *Bioinformatics* 23, 2633–2635. doi:10.1093/bioinformatics/btm308

Brown, G. D., Denning, D. W., Gow, N. A. R., Levitz, S. M., Netea, M. G., and White, T. C. (2012). Hidden killers: human fungal infections. *Sci. Transl. Med.* 4, 165rv13. doi:10.1126/scitranslmed.3004404

Cavassin, F. B., Baú-Carneiro, J. L., Vilas-Boas, R. R., and Queiroz-Telles, F. (2021). Sixty years of amphotericin B: an overview of the main antifungal agent used to treat invasive fungal infections. *Infect. Dis. Ther.* 10, 115–147. doi:10.1007/s40121-020-00382-7

Chang, Y. L., Yu, S. J., Heitman, J., Wellington, M., and Chen, Y. L. (2017). New facets of antifungal therapy. *Virulence* 8, 222–236. doi:10.1080/21505594.2016.1257457

Choukri, F., Botterel, F., Sitterlé, E., Bassinet, L., Foulet, F., Guillot, J., et al. (2015). Prospective evaluation of azole resistance in *Aspergillus fumigatus* clinical isolates in France. *Med. Mycol.* 53, 593–596. doi:10.1093/mmy/myv029

Chowdhary, A., Sharma, C., and Meis, J. F. (2017). Azole-resistant aspergillosis: epidemiology, molecular mechanisms, and treatment. *J. Infect. Dis.* 216, S436–S444. doi:10.1093/infdis/jix210

Chowdhary, A., Sharma, C., van den Boom, M., Yntema, J. B., Hagen, F., Verweij, P. E., et al. (2014). Multi-azole-resistant *Aspergillus fumigatus* in the environment in Tanzania. *J. Antimicrob. Chemother.* 69, 2979–2983. doi:10.1093/jac/dku259

Cingolani, P., Platts, A., Wang, L. L., Coon, M., Nguyen, T., Wang, L., et al. (2012). A program for annotating and predicting the effects of single nucleotide polymorphisms, SnpEff: SNPs in the genome of *Drosophila melanogaster* strain w1118; iso-2; iso-3. *Fly (Austin)* 6, 80–92. doi:10.4161/fly.19695

Costa, D. M. A., Gómez, S. V., de Araújo, S. S., Pereira, M. S., Alves, R. B., Favaro, D. C., et al. (2019). Catalytic mechanism for the conversion of salicylate into catechol by the flavin-dependent monooxygenase salicylate hydroxylase. *Int. J. Biol. Macromol.* 129, 588–600. doi:10.1016/j.ijbiomac.2019.01.135

Danecek, P., Auton, A., Abecasis, G., Albers, C. A., Banks, E., DePristo, M. A., et al. (2011). The variant call format and VCFtools. *Bioinformatics* 27, 2156–2158. doi:10.1093/bioinformatics/btr330

Deng, S., Zhang, L., Ji, Y., Verweij, P. E., Tsui, K. M., Hagen, F., et al. (2017). Triazole phenotypes and genotypic characterization of clinical *Aspergillus fumigatus* isolates in China. *Emerg. Microbes Infect.* 6, 1–6. doi:10.1038/emi.2017.97

Fan, Y., Wang, Y., Korfanty, G. A., Archer, M., and Xu, J. (2021). Genome-wide association analysis for triazole resistance in *Aspergillus fumigatus*. *Pathogens* 10, 701. doi:10.3390/pathogens10060701

Fan, Y., Wang, Y., and Xu, J. (2020). Comparative genome sequence analyses of geographic samples of *Aspergillus fumigatus*-relevance for amphotericin B resistance. *Microorganisms* 8, E1673. doi:10.3390/microorganisms8111673

Garcia-Rubio, R., Cuenca-Estrella, M., and Mellado, E. (2017). Triazole resistance in *Aspergillus* species: an emerging problem. *Drugs* 77, 599–613. doi:10.1007/s40265-017-0714-4

Garrison, E., and Marth, G. (2012). Haplotype-based variant detection from short-read sequencing. *arXiv:1207.3907* [Preprint]. Available at: http://arxiv.org/abs/1207.3907 [Accessed April 30, 2021].

Grahl, N., Puttikamonkul, S., Macdonald, J. M., Gamcsik, M. P., Ngo, L. Y., Hohl, T. M., et al. (2011). In vivo hypoxia and a fungal alcohol dehydrogenase influence the pathogenesis of invasive pulmonary aspergillosis. *PLoS Pathog.* 7, e1002145. doi:10.1371/journal.ppat.1002145

Graminha, M. A. S., Rocha, E. M. F., Prade, R. A., and Martinez-Rossi, N. M. (2004). Terbinafine resistance mediated by salicylate 1-monooxygenase in *Aspergillus nidulans*. *Antimicrob. Agents Chemother.* 48, 3530–3535. doi:10.1128/AAC.48.9.3530-3535.2004

Jogl, G., Shen, Y., Gebauer, D., Li, J., Wiegmann, K., Kashkar, H., et al. (2002). Crystal structure of the BEACH domain reveals an unusual fold and extensive association with a novel PH domain. *EMBO J.* 21, 4785–4795. doi:10.1093/emboj/cdf502

Kamiński, D. M. (2014). Recent progress in the study of the interactions of amphotericin B with cholesterol and ergosterol in lipid environments. *Eur. Biophys. J.* 43, 453–467. doi:10.1007/s00249-014-0983-8

Kumar, S., and Punekar, N. S. (1997). The metabolism of 4-aminobutyrate (GABA) in fungi. *Mycol. Res.* 101, 403–409. doi:10.1017/S0953756296002742

Kwon-Chung, K. J., and Sugui, J. A. (2013). *Aspergillus fumigatus*—what makes the species a ubiquitous human fungal pathogen? *PLoS Pathog.* 9, e1003743. doi:10.1371/journal.ppat.1003743

Latgé, J. P. (1999). *Aspergillus fumigatus* and aspergillosis. *Clin. Microbiol. Rev.* 12, 310–350. doi: 10.1128/CMR.12.2.310

Lestrade, P., Buil, J., Beek, M., Kuijper, E., Dijk, K., Kampinga, G., et al. (2020). Paradoxal trends in azole-resistant *Aspergillus fumigatus* in a national multicenter surveillance program, the Netherlands, 2013–2018. *Emerg. Infect. Dis.* 26, 1447–1455. doi:10.3201/eid2607.200088

Lestrade, P. P. A., Meis, J. F., Arends, J. P., Beek, M. T. van der, Brauwer, E. de, Dijk, K. van, et al. (2016). Diagnosis and management of aspergillosis in the Netherlands: a national survey. *Mycoses* 59, 101–107. doi:10.1111/myc.12440

Lev, S., Li, C., Desmarini, D., Sorrell, T. C., Saiardi, A., and Djordjevic, J. T. (2019). Fungal kinases with a sweet tooth: pleiotropic roles of their phosphorylated inositol sugar products in the pathogenicity of *Cryptococcus neoformans* present novel drug targeting ppportunities. *Front. Cell. Infect. Microbiol.* 9, 248. doi:10.3389/fcimb.2019.00248

Li, H. (2013). Aligning sequence reads, clone sequences and assembly contigs with BWA-MEM. *arXiv:1303.3997* [Preprint]. Available at: http://arxiv.org/abs/1303.3997 [Accessed April 30, 2021].

Loureiro, I., Faria, J., Clayton, C., Ribeiro, S. M., Roy, N., Santarém, N., et al. (2013). Knockdown of asparagine synthetase A renders *Trypanosoma brucei* auxotrophic to asparagine. *PLoS Negl. Trop. Dis.* 7, e2578. doi:10.1371/journal.pntd.0002578

Lyons, T. J., Villa, N. Y., Regalla, L. M., Kupchak, B. R., Vagstad, A., and Eide, D. J. (2004). Metalloregulation of yeast membrane steroid receptor homologs. *Proc. Natl. Acad. Sci. U.S.A.* 101, 5506–5511. doi:10.1073/pnas.0306324101

Michelle, C., Vourc'h, P., Mignon, L., and Andres, C. R. (2009). What was the set of ubiquitin and ubiquitin-like conjugating enzymes in the eukaryote common ancestor? *J. Mol. Evol.* 68, 616–628. doi:10.1007/s00239-009-9225-6

Nabili, M., Shokohi, T., Moazeni, M., Khodavaisy, S., Aliyali, M., Badiee, P., et al. (2016). High prevalence of clinical and environmental triazole-resistant *Aspergillus fumigatus* in Iran: is it a challenging issue? *J. Med. Microbiol.* 65, 468–475. doi:10.1099/jmm.0.000255

Nywening, A. V., Rybak, J. M., Rogers, P. D., and Fortwendel, J. R. (2020). Mechanisms of triazole resistance in *Aspergillus fumigatus*. *Environ. Microbiol.* 22, 4934–4952. doi:10.1111/1462-2920.15274

Paulussen, C., Hallsworth, J. E., Álvarez-Pérez, S., Nierman, W. C., Hamill, P. G., Blain, D., et al. (2016). Ecology of aspergillosis: insights into the pathogenic potency of A*spergillus fumigatus* and some other *Aspergillus* species. *Microb. Biotechnol.* 10, 296–322. doi:10.1111/1751-7915.12367

Prigitano, A., Esposto, M. C., Biffi, A., De Lorenzis, G., Favuzzi, V., Koncan, R., et al. (2017). Triazole resistance in *Aspergillus fumigatus* isolates from patients with cystic fibrosis in Italy. *J. Cyst. Fibros.* 16, 64–69. doi:10.1016/j.jcf.2016.06.006

Purcell, S., Neale, B., Todd-Brown, K., Thomas, L., Ferreira, M. A. R., Bender, D., et al. (2007). PLINK: a tool set for whole-genome association and population-based linkage analyses. *Am. J. Hum. Genet.* 81, 559–575. doi:10.1086/519795

Rex, J. H., Ghannoum, M. A., Alexander, B. D., Knapp, C. C., Andes, D., Motyl, M. R., et al. (2008). Reference method for broth dilution antifungal susceptibility testing of filamentous fungi. approved standard—second edition. M38-A2. *Clin. Lab. Stand. Inst.* 28, 1–35.

Reichert-Lima, F., Lyra, L., Pontes, L., Moretti, M. L., Pham, C. D., Lockhart, S. R., et al. (2018). Surveillance for azoles resistance in *Aspergillus* spp. highlights a high number of amphotericin B-resistant isolates. *Mycoses* 61, 360–365. doi:10.1111/myc.12759

Resendiz Sharpe, A., Lagrou, K., Meis, J. F., Chowdhary, A., Lockhart, S. R., Verweij, P. E., et al. (2018). Triazole resistance surveillance in *Aspergillus fumigatus*. *Med. Mycol. J.* 56, S83–S92. doi:10.1093/mmy/myx144

Serhan, G., Stack, C. M., Perrone, G. G., and Morton, C. O. (2014). The polyene antifungals, amphotericin B and nystatin, cause cell death in *Saccharomyces cerevisiae* by a distinct mechanism to amphibian-derived antimicrobial peptides. *Ann. Clin. Microbiol. Antimicrob.* 13, 18. doi:10.1186/1476-0711-13-18

Seufert, R., Sedlacek, L., Kahl, B., Hogardt, M., Hamprecht, A., Haase, G., et al. (2018). Prevalence and characterization of azole-resistant *Aspergillus fumigatus* in patients with cystic fibrosis: a prospective multicentre study in Germany. *J. Antimicrob. Chemother.* 73, 2047–2053. doi:10.1093/jac/dky147

Seyedmousavi, S., Melchers, W. J. G., Mouton, J. W., and Verweij, P. E. (2013). Pharmacodynamics and dose-response relationships of liposomal amphotericin B against different azole-resistant *Aspergillus fumigatus* isolates in a murine model of disseminated aspergillosis. *Antimicrob. Agents Chemother.* 57, 1866–1871. doi:10.1128/AAC.02226-12

Shekhova, E., Ivanova, L., Krüger, T., Stroe, M. C., Macheleidt, J., Kniemeyer, O., et al. (2019). Redox proteomic analysis reveals oxidative modifications of proteins by increased levels of intracellular reactive oxygen species during hypoxia adaptation of *Aspergillus fumigatus*. *Proteomics* 19, 1800339. doi:10.1002/pmic.201800339

Shekhova, E., Kniemeyer, O., and Brakhage, A. A. (2017). Induction of mitochondrial reactive oxygen species production by itraconazole, terbinafine, and amphotericin B as a mode of action against *Aspergillus fumigatu*s. *Antimicrob. Agents Chemother.* 61, e00978-17. doi:10.1128/AAC.00978-17

Sugui, J. A., Losada, L., Wang, W., Varga, J., Ngamskulrungroj, P., Abu-Asab, M., et al. (2011). Identification and characterization of an *Aspergillus fumigatus* "supermater" pair. *mBio* 2, e00234-11. doi:10.1128/mBio.00234-11

Talbot, J. J., Subedi, S., Halliday, C. L., Hibbs, D. E., Lai, F., Lopez-Ruiz, F. J., et al. (2018). Surveillance for azole resistance in clinical and environmental isolates of *Aspergillus fumigatus* in Australia and cyp51A homology modelling of azole-resistant isolates. *J. Antimicrob. Chemother.* 73, 2347–2351. doi:10.1093/jac/dky187

Vazquez, J., Tovar-Torres, M., Hingwe, A., Cheema, F., Welch, V., and Ford, K. (2016). The changing epidemiology of invasive aspergillosis in the non-traditional host: risk factors and outcomes. *Steroids* 25, 5. doi:10.15761/PCCM.1000114

Vermeulen, E., Maertens, J., De Bel, A., Nulens, E., Boelens, J., Surmont, I., et al. (2015). Nationwide surveillance of azole resistance in *Aspergillus* diseases. *Antimicrob. Agents Chemother.* 59, 4569–4576. doi:10.1128/AAC.00233-15

Verweij, P. E., Ananda-Rajah, M., Andes, D., Arendrup, M. C., Brüggemann, R. J., Chowdhary, A., et al. (2015). International expert opinion on the management of infection caused by azole-resistant *Aspergillus fumigatus*. *Drug Resist. Updat.* 21, 30–40. doi:10.1016/j.drup.2015.08.001

Verweij, P. E., Lestrade, P. P. A., Melchers, W. J. G., and Meis, J. F. (2016). Azole resistance surveillance in *Aspergillus fumigatus*: beneficial or biased? *J. Antimicrob. Chemother.* 71, 2079–2082. doi:10.1093/jac/dkw259

Wu, C. J., Wang, H. C., Lee, J. C., Lo, H. J., Dai, C. T., Chou, P. H., et al. (2015). Azole-resistant *Aspergillus fumigatus* isolates carrying TR34/L98H mutations in Taiwan. *Mycoses* 58, 544–549. doi:10.1111/myc.12354

Xu, J., Ramos, A. R., Vilgalys, R., and Mitchell, T. G. (2000). Clonal and spontaneous origins of fluconazole resistance in *Candida albicans*. *J. Clin. Microbiol.* 38, 1214–1220. doi:10.1128/JCM.38.3.1214-1220.2000

Ying, X., and Ma, K. (2011). Characterization of a zinc-containing alcohol dehydrogenase with stereoselectivity from the hyperthermophilic archaeon *Thermococcus guaymasensis*. *J. Bacteriol.* 193, 3009–3019. doi:10.1128/JB.01433-10

Zavrel, M., Esquivel, B. D., and White, T. C. (2017). "The Ins and Outs of Azole Antifungal Drug Resistance: Molecular Mechanisms of Transport," in *Handbook of Antimicrobial Resistance*, eds. A. Berghuis, G. Matlashewski, M. A. Wainberg, and D. Sheppard (New York, NY: Springer New York), 423–452. doi:10.1007/978-1-4939-0694-9_29

Zhao, S., Ge, W., Watanabe, A., Fortwendel, J. R., and Gibbons, J. G. (2021). Genome-wide association for itraconazole sensitivity in non-resistant clinical isolates of *Aspergillus fumigatus*. *Front. Fungal Biol.* 1. doi:10.3389/ffunb.2020.617338

Zhou, D. Y., Korfanty, G., Mo, M. Z., Wang, R. R., Li, X., Li, H. X., Li, S. S., Wu, J. Y., Zhang, K. Q., Zhang, Y., and Xu, J. (2021). Extensive genetic diversity and widespread azole resistance in greenhouse populations of *Aspergillus fumigatus* in Yunnan, China. *mSphere* 6, e00066-21. doi:10.1128/mSphere.00066-21

3.8. Supplemental Materials

Table S3.1. Information on the 98 *A. fumigatus* strains analyzed in this study. These 98 strains have whole-genome sequences and Amphotericin B MIC values.

Strain name	Run	Accession	Project Number	Country	Source	AMB MIC (mg/L)	Reference DOI
Afs35	DRR146814	DRS075098	PRJDB7240	Germany	Clinical	1	10.1371/journal.ppat.1006096
B5233	ERR2863830	ERS2867139	PRJEB28819	United States	Clinical	0.5	10.3201/eid1508.090251
Af65	ERR769499	ERS663171	PRJEB8623	United Kingdom	Clinical	0.5	10.1128/mBio.00536-15
12-7505446	ERR769500	ERS663164		United Kingdom	Clinical	0.25	
12-7505220	ERR769501	ERS663165		United Kingdom	Clinical	0.5	
09-7500806	ERR769502	ERS663166		United Kingdom	Clinical	0.5	
12-7504652	ERR769503	ERS663167		United Kingdom	Clinical	0.25	
12-7504462	ERR769504	ERS663168		United Kingdom	Clinical	0.5	
12-7505054	ERR769505	ERS663169		United Kingdom	Clinical	0.5	
08-12-12-13	ERR769506	ERS663172		Netherlands	Clinical	0.25	
08-36-03-25	ERR769507	ERS663173		Netherlands	Clinical	0.5	
08-31-08-91	ERR769508	ERS663174		Netherlands	Clinical	0.5	
08-19-02-61	ERR769509	ERS663175		Netherlands	Environmental	0.25	
08-19-02-30	ERR769510	ERS663176		Netherlands	Environmental	0.5	
10-01-02-27	ERR769511	ERS663177		Netherlands	Clinical	0.5	
08-19-02-46	ERR769512	ERS663178		Netherlands	Environmental	0.5	
08-19-02-10	ERR769513	ERS663179		Netherlands	Environmental	0.25	
Afu 942/09	ERR769514	ERS663180		India	Clinical	0.25	
Afu 1042/09	ERR769515	ERS663181		India	Clinical	0.25	
Afu 343/P/11	ERR769516	ERS663182		India	Clinical	0.125	
Afu 591/12	ERR769517	ERS663183		India	Clinical	0.5	
Afu 124/E11	ERR769518	ERS663184		India	Environmental	0.125	
Afu 257/E11	ERR769520	ERS663186		India	Environmental	0.125	
Afu 218/E11	ERR769521	ERS663187		India	Environmental	0.125	
CM3262	SRR7418922	SRS3453382	PRJNA477519	Spain	Clinical	0.125 to 0.25 *	10.1128/AAC.00241-18
CM2733	SRR7418923	SRS3453380		Spain	Clinical	0.125 to 0.25 *	
CM2730	SRR7418924	SRS3453381		Spain	Clinical	0.125 to 0.25 *	
CM7560	SRR7418925	SRS3453379		Spain	Clinical	0.125 to 0.25 *	
CM3249	SRR7418926	SRS3453378		Spain	Clinical	0.125 to 0.25 *	
CM4602	SRR7418928	SRS3453376		Spain	Clinical	0.125 to 0.25 *	
CM2495	SRR7418930	SRS3453373		Spain	Clinical	0.125 to 0.25 *	
akuBKU80	SRR7418932	SRS3453372		Spain	Clinical	0.125 to 0.25 *	

CM7570	SRR7418933	SRS3453371		Spain	Clinical	0.125 to 0.25 *	
TP12	SRR7418940	SRS3453364		Spain	Clinical	0.125 to 0.25 *	
CM7632	SRR7418941	SRS3453363		Spain	Clinical	0.125 to 0.25 *	
TP32	SRR7418946	SRS3453358		Spain	Clinical	0.125 to 0.25 *	
CM4946	SRR7418948	SRS3453357		Spain	Clinical	0.125 to 0.25 *	
IFM 59355-1	DRR022916	DRS016460	PRJDB3064	Japan	Clinical	2	10.1128/JCM.01105-14
IFM 59355-2	DRR022917	DRS016461		Japan	Clinical	2	
IFM 59356-1	DRR022919	DRS016462		Japan	Clinical	2	
IFM 59356-2	DRR022922	DRS016463		Japan	Clinical	1	
IFM 59356-3	DRR022924	DRS016464		Japan	Clinical	2	
IFM 59361-1	DRR022925	DRS016465		Japan	Clinical	1	
IFM 59361-2	DRR022926	DRS016466		Japan	Clinical	1	
IFM 60237	DRR022927	DRS016467		Japan	Clinical	2	
IFM 55369	DRR015087	DRS013318	PRJDB1541	Japan	Clinical	1	10.1016/j.jiac.2015.01.005
IFM 59056	DRR015093	DRS013319		Japan	Clinical	2	
IFM 59359	DRR015096	DRS013320		Japan	Clinical	2	
IFM 59361	DRR015099	DRS013321		Japan	Clinical	2	
IFM 59073	DRR015106	DRS013323		Japan	Clinical	2	
IFM 58029	DRR017540	DRS015320		Japan	Clinical	0.5	
IFM 58401	DRR017543	DRS015321		Japan	Clinical	1	
IFM 59777	DRR017549	DRS015323		Japan	Clinical	0.5	
CNM-CM8689	SRR10592629	SRS5766627	PRJNA592352	Spain	Clinical	1	10.3389/fgene.2020.00459
CNM-CM8686	SRR10592630	SRS5766626		Spain	Clinical	0.5	
CNM-CM8812	SRR10592631	SRS5766625		Spain	Clinical	0.25	
CNM-CM8714	SRR10592632	SRS5766624		Spain	Clinical	0.25	
CNM-CM8057	SRR10592633	SRS5766623		Spain	Clinical	0.25	
DI 15-105	SRR7841980	SRS3786101	PRJNA491253	United States	Clinical	0.125	10.1128/mBio.00437-19
F11628	SRR343149	SRS260927	PRJNA67101	United Kingdom	Clinical	0.06	
F12865	SRR343150	SRS260928		United Kingdom	Clinical	0.125	
F12041	SRR617723	SRS375794		United Kingdom	Clinical	0.25	
F13535	SRR617726	SRS375797		United Kingdom	Clinical	0.125	
AF72 (NCPF 7099)	SRR617721	SRS375792		United States	Clinical	0.25 (by M38-A)	10.1093/jac/dkg384
AF90 (NCPF 7100)	SRR617722	SRS375793		United States	Clinical	0.5 (by M38-A)	
V130-15	SRR8759700	SRS4515816	PRJNA528395	Netherlands	Clinical	0.5	10.1016/j.fgb.2019.05.005
V157-62	SRR8759706	SRS4515810		Netherlands	Clinical	0.25	
CON4	SRR12894204	SRS7582162	PRJNA671765	Canada	Environmental	1	10.3390/microorganisms8111673

CM21	SRR12894203	SRS7582164		Canada	Environmental	2	
CM65	SRR12894200	SRS7582166		Canada	Environmental	4	
P80	SRR12894199	SRS7582167		Canada	Environmental	4	
15-1	SRR12894198	SRS7582170		Canada	Clinical	4	
AV88	SRR12894197	SRS7582168		Canada	Environmental	4	
15-33	SRR12894196	SRS7582169		Canada	Clinical	4	
P20	SRR12894195	SRS7582171		Canada	Environmental	4	
CM38	SRR12894194	SRS7582173		Canada	Environmental	4	
CM11	SRR12894193	SRS7582172		Canada	Environmental	8	
AFB62-1	SRR12894202	SRS7582163		United States	Clinical	4	
AFIR928	SRR12894201	SRS7582165		Ireland	Environmental	4	
IFM 46074	SRR11977812	SRS6816741	PRJNA638646	Japan	Clinical	0.5	10.1016/j.jiac.2015.01.005
IFM 48051	SRR11977855	SRS6816698		Japan	Clinical	1	
IFM 49896	SRR11977853	SRS6816700		Japan	Clinical	1	
IFM 50230	SRR11977852	SRS6816701		Japan	Clinical	1	
IFM 50916	SRR11977849	SRS6816704		Japan	Clinical	1	
IFM 50997	SRR11977847	SRS6816706		Japan	Clinical	1	
IFM 50999	SRR11977846	SRS6816707		Japan	Clinical	2	
IFM 51357	SRR11977844	SRS6816709		Japan	Clinical	2	
IFM 51505	SRR11977842	SRS6816711		Japan	Clinical	0.5	
IFM 51746	SRR11977841	SRS6816712		Japan	Clinical	2	
IFM 51977	SRR11977839	SRS6816714		Japan	Clinical	1	
IFM 51978	SRR11977838	SRS6816715		Japan	Clinical	0.5	
IFM 55369	SRR11977835	SRS6816718		Japan	Clinical	1	
IFM 59073	SRR11977828	SRS6816725		Japan	Clinical	2	
IFM 59359	SRR11977826	SRS6816727		Japan	Clinical	2	
CAPA-A	SRR12949929	SRS7620879	PRJNA673120	Germany	Clinical	2 to 4 *	10.1128/Spectrum.00010-21
CAPA-B	SRR12949928	SRS7620880		Germany	Clinical	2	
CAPA-C	SRR12949927	SRS7620882		Germany	Clinical	2	
CAPA-D	SRR12949926	SRS7620881		Germany	Clinical	2	

* The lower numeric value of a reported MIC range was used in the GWAS

Table S3.2. Amphotericin B susceptibility and genotype information for the two parental and their 143 progeny strains.

Strain ID	AMB MIC (mg/L)	Mean Ratio of Fungal Growth in varying AMB Concentrations					Genotype at five SNP sites (AFB62-1 = 1, CM11 = 2)				
		0.25 mg/L	0.50 mg/L	1.00 mg/L	2.00 mg/L	4.00 mg/L	SNP 1	SNP 2	SNP 3	SNP 4	SNP 5
AFB62-1	4	0.651	0.529	0.444	0.296	NA	1	1	1	1	1
CM11	8	0.773	0.672	0.418	0.338	0.006	2	2	2	2	2
1	4	0.752	0.605	0.494	0.007	NA	1	2	2	2	2
2	4	0.975	1.296	0.585	0.216	NA	1	1	1	1	1
3	4	0.799	0.681	0.668	0.187	NA	2	1	1	1	1
4	4	0.597	0.575	0.549	0.300	NA	2	2	2	2	1
5	4	0.591	0.439	0.383	0.127	NA	2	2	1	1	2
6	4	0.612	0.646	0.613	0.086	NA	1	1	1	1	1
7	8	0.938	0.772	0.578	0.523	0.193	2	2	1	1	2
8	4	0.893	0.770	0.714	0.559	NA	2	1	1	1	1
9	4	0.956	0.791	0.825	0.588	NA	1	1	1	1	2
10	4	0.777	0.705	0.575	0.212	NA	1	2	2	2	2
11	4	0.836	0.714	0.637	0.192	NA	1	1	1	1	1
12	4	0.835	0.586	0.584	0.106	NA	2	2	2	2	1
13	4	0.781	0.501	0.389	0.485	NA	1	1	1	1	2
14	4	1.059	0.943	0.878	0.507	NA	1	1	1	1	1
15	2	0.712	0.606	0.369	NA	NA	2	1	1	1	1
16	4	0.719	0.617	0.561	0.119	NA	2	2	2	2	2
17	8	1.140	1.049	1.206	0.684	0.020	2	2	2	2	1
18	4	0.859	0.531	0.422	0.188	NA	2	1	1	1	2
19	4	0.916	0.807	0.780	0.432	NA	1	1	1	1	1
20	4	0.779	0.800	0.827	0.583	NA	1	2	2	2	2
21	4	0.874	0.742	0.821	0.699	NA	2	1	1	1	2
22	4	0.821	0.602	0.559	0.362	NA	2	2	2	2	1
23	4	0.849	0.500	0.441	0.286	NA	2	1	1	1	2
24	4	1.327	0.836	1.024	0.295	NA	2	1	1	1	1
25	4	0.847	0.912	1.126	0.148	NA	1	2	2	2	2
26	4	0.782	0.811	1.227	0.085	NA	2	1	1	1	2
27	4	0.828	0.598	0.905	0.011	NA	1	1	1	1	1
28	4	1.381	1.113	0.956	0.689	NA	2	2	2	1	2
29	4	0.780	0.712	1.004	0.166	NA	1	1	1	1	2
30	2	0.783	0.706	0.504	NA	NA	2	2	2	2	2
31	2	0.626	0.426	0.304	NA	NA	2	2	2	2	1

32	4	0.898	0.766	1.068	0.414	NA	1	1	1	1	2
33	4	0.616	0.386	0.378	0.193	NA	2	1	1	1	1
34	4	0.547	0.310	0.205	0.053	NA	2	2	2	2	2
35	4	0.755	0.666	0.483	0.124	NA	2	2	2	2	2
36	4	0.660	0.730	0.832	0.530	NA	2	1	1	1	2
37	4	0.977	0.826	0.740	0.557	NA	1	2	2	2	1
38	4	0.795	0.400	0.383	0.250	NA	2	2	2	2	2
39	4	0.833	0.810	0.577	0.087	NA	2	2	2	2	2
40	4	1.006	0.731	0.637	0.427	NA	1	2	2	2	1
41	4	0.868	0.797	0.676	0.252	NA	1	1	1	1	2
42	4	0.788	0.612	0.484	0.357	NA	2	1	1	1	1
43	4	0.750	0.663	0.577	0.319	NA	1	1	1	1	1
44	8	0.896	0.810	0.809	0.733	0.008	2	2	2	2	2
45	4	0.678	0.417	0.277	0.179	NA	2	2	2	2	1
46	4	0.712	0.636	0.505	0.286	NA	2	2	2	2	1
47	4	0.838	0.778	0.625	0.292	NA	2	2	2	2	1
48	4	0.718	0.537	0.423	0.415	NA	1	2	2	2	2
49	4	0.652	0.394	0.278	0.170	NA	1	2	2	2	2
50	4	0.698	0.461	0.401	0.077	NA	1	2	2	1	1
51	8	0.864	0.842	0.783	0.645	0.247	2	1	1	1	1
52	8	0.682	0.715	0.586	0.616	0.088	2	1	1	1	1
53	8	0.445	0.484	0.398	0.459	0.040	1	2	2	2	2
54	4	0.741	0.487	0.484	0.238	NA	2	2	2	2	1
55	8	0.831	0.837	0.753	0.566	0.005	1	2	2	2	2
56	4	0.736	0.744	0.746	0.359	NA	1	1	1	1	2
57	4	0.910	0.758	0.444	0.276	NA	2	1	1	1	2
58	4	1.077	0.719	0.767	0.128	NA	2	2	2	2	1
59	4	0.851	0.592	0.573	0.495	NA	2	1	1	1	2
60	4	1.046	0.866	0.470	0.229	NA	1	1	1	1	1
61	8	0.923	0.903	0.855	0.733	0.074	2	2	2	1	1
62	4	0.692	0.703	0.682	0.469	NA	1	2	2	2	2
63	4	0.906	0.488	0.598	0.476	NA	1	2	2	2	1
64	4	0.739	0.594	0.460	0.287	NA	2	1	1	1	1
65	8	1.566	1.091	0.722	0.672	0.099	2	1	1	1	2
66	4	1.558	1.540	1.218	0.528	NA	2	1	1	1	2
67	4	0.844	0.861	0.837	0.653	NA	2	1	1	1	2
68	4	0.789	0.746	0.748	0.481	NA	2	2	2	1	2

69	4	0.955	1.408	0.633	0.077	NA	2	2	2	2	1
70	8	0.618	0.690	0.682	0.419	0.004	2	2	2	2	2
71	4	0.888	0.899	0.907	0.578	NA	1	2	2	2	2
72	4	1.759	0.762	0.822	0.240	NA	2	2	2	2	2
73	4	1.171	1.245	0.758	0.072	NA	1	1	1	1	2
74	4	0.655	0.735	0.724	0.283	NA	1	2	2	2	2
75	4	0.749	0.794	0.707	0.572	NA	1	1	1	1	2
76	4	0.928	0.832	0.814	0.549	NA	2	2	2	2	2
77	4	0.612	0.698	0.567	0.017	NA	2	1	1	1	2
78	8	0.594	0.645	0.740	0.307	0.017	1	1	1	1	1
79	4	0.771	0.802	0.474	0.131	NA	1	2	2	2	2
80	2	0.638	0.570	0.387	NA	NA	2	2	2	2	1
81	4	0.690	0.585	0.486	0.455	NA	1	1	1	1	2
82	4	0.877	1.020	0.691	0.389	NA	2	2	2	2	2
83	4	1.179	0.653	0.804	0.384	NA	1	2	2	2	2
84	4	0.765	0.517	0.549	0.317	NA	1	1	1	1	1
85	4	0.753	0.675	0.613	0.198	NA	2	2	2	2	2
86	4	0.672	0.549	0.416	0.156	NA	2	2	2	1	1
87	4	0.737	0.668	0.848	0.330	NA	1	1	1	1	1
88	4	0.833	0.796	0.482	0.291	NA	1	1	1	1	1
89	4	0.819	0.618	0.508	0.375	NA	2	2	2	2	2
90	4	0.697	0.736	0.762	0.305	NA	1	2	2	2	1
91	4	0.816	0.708	0.575	0.252	NA	1	2	2	2	2
92	4	0.563	0.526	0.442	0.171	NA	1	2	2	2	2
93	8	0.847	0.742	0.714	0.378	0.241	1	2	2	2	2
94	8	0.822	0.779	0.446	0.492	0.081	1	1	1	1	1
95	8	0.695	0.486	0.503	0.265	0.066	1	1	1	1	2
96	4	0.862	0.774	0.645	0.250	NA	2	1	1	1	2
97	4	0.808	0.659	0.637	0.166	NA	1	2	2	2	1
98	4	0.896	0.827	0.596	0.496	NA	2	1	1	1	2
99	4	0.695	0.863	0.704	0.125	NA	1	2	2	2	1
100	4	0.718	0.683	0.700	0.494	NA	1	2	2	2	1
101	4	0.790	0.637	0.588	0.231	NA	2	1	1	1	1
102	4	0.774	0.974	0.803	0.562	NA	1	2	2	2	1
103	4	0.854	0.764	0.572	0.453	NA	2	2	2	1	1
104	4	0.739	0.769	0.489	0.409	NA	1	1	1	1	1
105	4	0.965	0.773	0.704	0.406	NA	2	2	2	2	1

106	4	0.849	0.684	0.870	0.453	NA	2	2	2	2	2
107	4	0.603	0.491	0.388	0.268	NA	1	1	1	2	1
108	4	0.903	0.480	0.556	0.659	NA	2	2	2	2	2
109	4	0.732	0.670	0.641	0.653	NA	1	2	2	2	1
110	4	0.783	0.748	0.719	0.926	NA	2	2	2	2	2
111	4	0.787	0.745	0.518	0.405	NA	1	2	1	1	1
112	4	0.822	0.694	0.716	0.392	NA	1	2	2	2	2
113	4	0.699	0.407	0.444	0.251	NA	1	1	1	1	1
114	4	0.703	0.660	0.532	0.329	NA	2	2	2	2	2
115	4	0.875	0.536	0.390	0.257	NA	1	2	2	2	2
116	4	1.157	0.928	0.790	0.607	NA	1	1	1	2	2
117	4	0.822	0.618	0.519	0.391	NA	1	1	1	1	2
118	4	0.669	0.483	0.418	0.217	NA	1	1	1	1	1
119	4	0.742	0.911	0.536	0.288	NA	1	2	2	2	2
120	4	0.865	1.054	0.863	0.588	NA	1	1	1	1	2
121	4	0.857	1.831	0.900	0.883	NA	2	1	1	1	2
122	4	0.679	0.590	0.325	0.333	NA	2	1	1	1	1
123	4	1.350	0.915	0.768	0.282	NA	1	1	1	1	2
124	4	0.684	0.524	0.507	0.287	NA	2	2	2	2	1
125	4	1.015	0.866	0.748	0.498	NA	2	1	1	1	2
126	4	1.662	0.815	0.677	0.198	NA	2	1	2	2	2
127	4	1.442	0.887	0.450	0.266	NA	1	1	1	1	2
128	8	0.879	0.763	0.680	0.345	0.116	2	2	2	2	1
129	8	0.789	0.566	0.422	0.467	0.351	1	2	2	2	2
130	4	0.625	0.638	0.599	0.522	NA	2	1	1	1	1
131	4	0.668	0.697	0.507	0.442	NA	1	2	2	2	2
132	8	0.756	0.889	1.224	0.827	0.124	2	2	2	2	1
133	4	0.849	0.701	0.506	0.414	NA	2	1	1	1	1
134	4	0.562	0.610	0.445	0.445	NA	1	1	1	1	1
135	4	0.694	0.541	0.557	0.391	NA	1	1	1	1	2
136	4	0.688	0.646	0.587	0.400	NA	1	2	2	2	1
137	8	0.643	0.513	0.491	0.521	0.007	2	2	2	2	2
138	8	0.700	0.522	0.414	0.286	0.006	2	1	1	1	2
139	4	0.661	0.517	0.439	0.439	NA	1	1	1	1	2
140	4	0.680	0.435	0.389	0.395	NA	1	2	2	2	2
141	4	0.667	0.513	0.469	0.403	NA	1	1	1	1	1
142	4	0.889	0.611	0.596	0.631	NA	1	2	2	2	2

143	4	0.853	0.716	0.456	0.386	NA	2	1	1	1	1

NA = Not applicable

Table S3.3. Fisher's exact test p-values of the pairwise single nucleotide polymorphism (SNP) combinations and Amphotericin B MIC groups in the progeny strains.

	MIC ≤ 4 mg/L				MIC = 8 mg/L				Fisher's Exact Tests (p-values)					
	Alleles 1 & 1	Alleles 1 & 2	Alleles 2 & 1	Alleles 2 & 2	Alleles 1 & 1	Alleles 1 & 2	Alleles 2 & 1	Alleles 2 & 2	1&1 vs 1&2	1&1 vs 2&1	1&1 vs 2&2	1&2 vs 2&1	1&2 vs 2&2	2&1 vs 2&2
SNP 5 & 4	32	24	32	36	5	3	4	7	1.00	1.00	0.76	1.00	0.73	0.75
SNP 5 & 3	30	26	31	37	4	4	4	7	1.00	1.00	0.75	1.00	1.00	0.75
SNP 5 & 2	29	27	31	37	4	4	3	8	1.00	0.71	0.54	0.70	0.75	0.33
SNP 5 & 1	29	27	35	33	2	6	5	6	0.26	0.46	0.29	0.53	0.76	0.76
SNP 4 & 3	59	5	2	58	8	1	0	10	0.56	1.00	0.80	1.00	1.00	1.00
SNP 4 & 2	57	7	3	57	7	2	0	10	0.31	1.00	0.61	1.00	0.63	1.00
SNP 4 & 1	33	31	31	29	3	6	4	6	0.48	0.71	0.31	0.74	1.00	0.73
SNP 3 & 2	59	2	1	62	7	1	0	11	0.31	1.00	0.46	1.00	0.41	1.00
SNP 3 & 1	34	27	30	33	3	5	4	7	0.46	0.70	0.31	0.73	1.00	0.53
SNP 2 & 1	33	27	31	33	3	4	4	8	0.70	0.71	0.20	1.00	0.54	0.37

Allele 1 = AFB62-1, Allele 2 = CM11

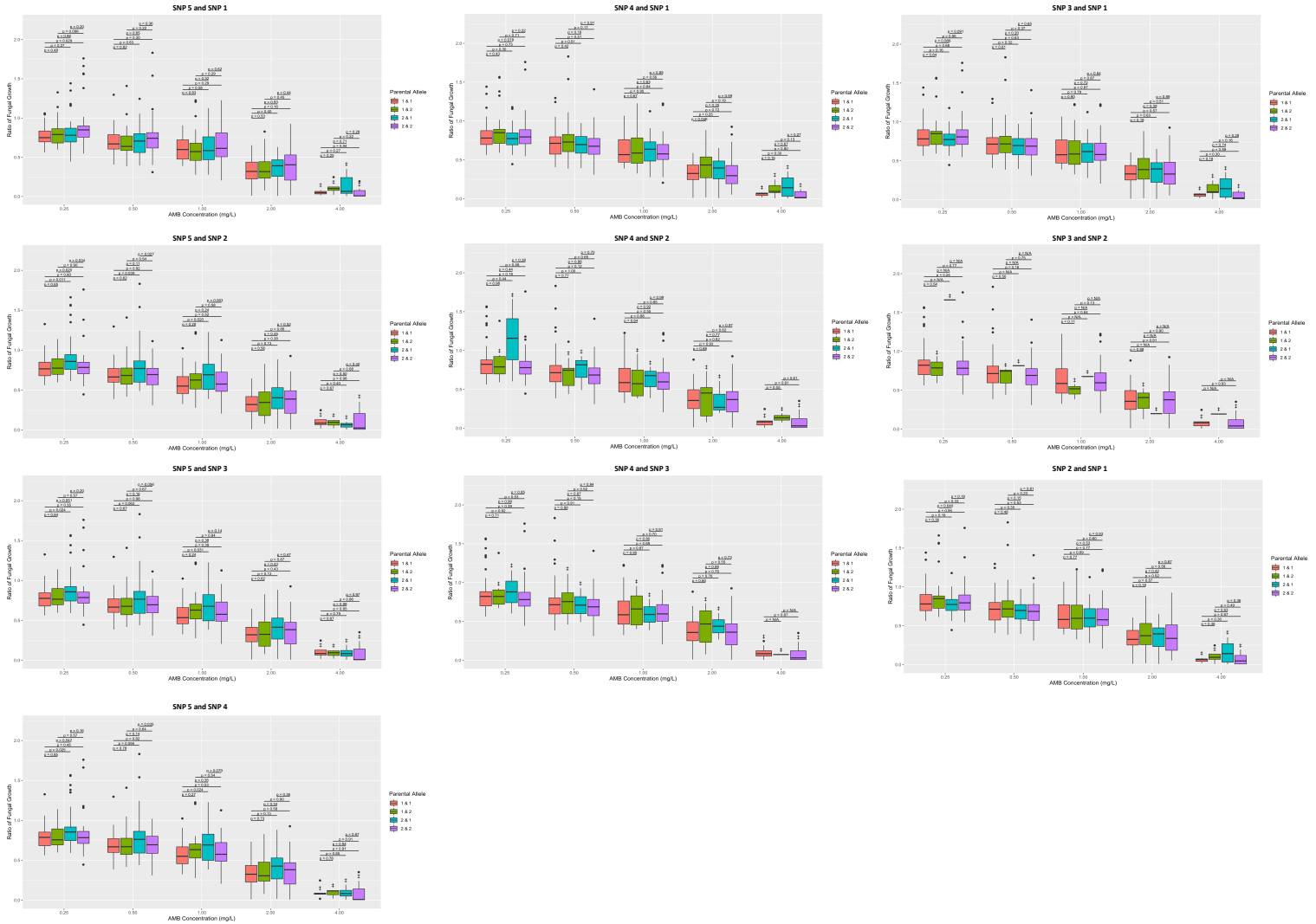

Figure S3.1. Welch's t-test p-values for the 10 pairwise SNP combinations in their associations with fungal growths at different amphotericin B concentrations.

Chapter 4

General Conclusion

4.1. Conclusion

Overall, my thesis work investigated and expanded on the set of putative mutations associated with antifungal resistance in *A. fumigatus*. In Chapter 2, the focus was placed on studying itraconazole and voriconazole resistance. Fisher's exact tests were conducted to examine potential associations between triazole resistance in our sample set with 22 known mutation sites and with SNPs in or near 37 genes overexpressed with triazole exposure. Using both MIC thresholds (2 mg/L and 4 mg/L) as well as sub-sample subsets, a total of 1 known mutation site (L98H) and 64 SNPs in or near the overexpressed genes were found linked to triazole resistance. Stepwise GWAS analyses were also conducted to find novel mutations, which determined that well-characterized and canonical mutation sites did not fully account for the triazole resistance observed in our strain set. The GWAS results found 6 and 18 novel missense variants to be significantly associated with itraconazole and voriconazole resistance, respectively. In addition, linkage disequilibrium analysis was used to identify highly-linked missense variants to the top 20 SNPs obtained from the GWAS analyses, resulting in an additional 26 missense variants of interest. Similar to the previous analyses, a stepwise analysis was then conducted using Fisher's exact tests and sub-sample sets to investigate missense variants significantly associated with itraconazole and pan-azole resistance. The tests found a total of six missense variants to be significantly associated with triazole resistance, of which two were consistently associated with pan-azole resistance in the three sub-sample sets.

In Chapter 3, mutations and SNP-SNP interactions associated with the emerging occurrence of AMB tolerance in *A. fumigatus* was investigated through a GWAS and laboratory cross. The top 20 SNPs were identified from the GWAS results, of which six were missense variants. Linkage disequilibrium was conducted on the top 20 SNPs to identify an

additional 24 highly-linked SNP sites. Furthermore, Fisher's exact tests at these linked SNP sites determined eight variants to be significantly associated with AMB resistance. Fisher's exact tests were also conducted on 12 missense variants that were found in our previous AMB study, which used smaller sample set of 71 strains and focused on a clade-level, to be significantly associated with AMB resistance (Fan et al., 2020). Among these 12 missense variants and using our current expanded sample set, 6 were found to be significantly associated with resistance. Subsequently, a laboratory cross was conducted to generate 143 progeny strains. To validate the association between mutations and AMB resistance, five SNPs were investigated in these progeny strains – two SNPs were chosen out of the top 20 SNPs of GWAS results and three SNPs from the 8 highly-linked SNPs. Using these five SNP sites and the 143 progeny strains, we determined that epistatic interactions were associated with strain growth in various AMB concentrations and emphasized the fact that SNP-SNP interactions can also have a significant effect on AMB tolerance.

In terms of future research and next steps, further experimental validation (e.g., SNP replacement) of the mutations found in our studies to be significantly associated with triazole resistance and with AMB resistance should be conducted. In addition, many of the identified mutations were non-coding. These variants could regulate gene expression via mechanisms such as modification of important regulatory elements (e.g., enhancer and promoter regions) or disrupt binding sites for transcription factors. Therefore, gene expression analyses (e.g., RT-qPCR) of these novel candidate genes as well as neighbouring genes would aid in investigating their effects and determining underlying regulatory events. In Chapter 3, we also determined the potential importance of epistasis effects on fungal growth in various concentrations of AMB between five candidate SNP sites associated with resistance. Therefore, expanding the approach to performing gene set analysis (GSA) of our GWAS data would aid in determining SNP sets impacting AMB tolerance.

In recent years, triazole resistant *A. fumigatus* isolates without mutations in c*yp51A* or in its promoter region have been increasingly prevalent (Camps et al., 2012). A previous study in Manchester, UK had reported that 54% of patients with triazole resistant strains in 2009 did not have Cyp51A-mediated resistance mechanisms (Bueid et al., 2010). Emergence of AMB resistance in *A. fumigatus* has also complicated the problem of medical management

and treatment. The mechanisms of AMB resistance in *A. fumigatus* are also not well understood. With increasing reports of invasive aspergillosis, as demonstrated in a France study that found a 4.4% yearly increase per year from 2001 to 2010, determining the underlying mechanisms for antifungal resistance is becoming more essential for treatment (Bitar et al., 2014). It's been demonstrated that despite other evidence of *A. fumigatus* infection (such as microscopy and the presence of species-specific antigens), the recovery of *A. fumigatus* live culture from infection sites is often low and can vary significantly among patient groups (Zhao et al., 2016). Moreover, invasive procedures are often required to obtain live culture for analyses but that such procedures are not ideal for critically ill patients (Patterson & Donnelly, 2019). Thus, there has been significant interest towards using nonculture-based diagnostics that can help provide an early diagnosis for drug susceptibility and allow for prompt initiation of the appropriate therapy treatment (Patterson & Donnelly, 2019). Our findings will help develop molecular markers for detection of non-Cyp51A associated triazole resistance and of AMB resistance in clinical *A. fumigatus* strains, with the goal of improving patient outcome.

4.2. References

Bitar, D., Lortholary, O., Le Strat, Y., Nicolau, J., Coignard, B., Tattevin, P., ... & Dromer, F. (2014). Population-based analysis of invasive fungal infections, France, 2001–2010. *Emerging Infectious Diseases*, *20*(7), 1149.

Bueid, A., Howard, S. J., Moore, C. B., Richardson, M. D., Harrison, E., Bowyer, P., & Denning, D. W. (2010). Azole antifungal resistance in *Aspergillus fumigatus*: 2008 and 2009. *Journal of Antimicrobial Chemotherapy*, *65*(10), 2116-2118.

Fan, Y., Wang, Y., & Xu, J. (2020). Comparative genome sequence analyses of geographic samples of *Aspergillus fumigatus*—relevance for amphotericin B resistance. *Microorganisms*, *8*(11), 1673.

Camps, S. M., Dutilh, B. E., Arendrup, M. C., Rijs, A. J., Snelders, E., Huynen, M. A., ... & Melchers, W. J. (2012). Discovery of a HapE mutation that causes azole resistance in

Aspergillus fumigatus through whole genome sequencing and sexual crossing. *PloS One*, *7*(11), e50034.

Patterson, T. F., & Donnelly, J. P. (2019). New concepts in diagnostics for invasive mycoses: non-culture-based methodologies. *Journal of Fungi*, *5*(1), 9.

Zhao, Y., Garnaud, C., Brenier-Pinchart, M. P., Thiébaut-Bertrand, A., Saint-Raymond, C., Camara, B., ... & Perlin, D. S. (2016). Direct molecular diagnosis of aspergillosis and CYP51A profiling from respiratory samples of French patients. *Frontiers in Microbiology*, *7*, 1164.